SCT Barrel Module FDR Document

SCT Barrel Module: Final Design Review INTRODUCTION AND OVERVIEW

Abstract

This document provides the introduction and overview to the Final Design Review (FDR) for the ATLAS SCT Barrel Module. It explains the role of the SCT within the ATLAS Inner Detector, gives the structure of the review and comments on relevant areas which are not topics of detailed study for this review but which are documented elsewhere.

Prepared by :	***Checked by :***	***Approved by :***
A. Carter		

Table of Contents

1 SCOPE OF THE DOCUMENT

This document provides the introduction and overview to the Final Design Review (FDR) for the ATLAS SCT Barrel Module. It explains the role of the SCT within the ATLAS Inner Detector and then gives the document agenda of the review. This is followed by a brief account of the Barrel Module, and reference to its integration in to an assembled structure. Status reports are then given for those items of direct association with the Barrel Module implementation, but which are not addressed further in this review. These include : power supplies, detector control system, the cooling system, the readout data-links and off-detector electronics, and the survey and alignment projects.

2 INNER DETECTOR INSTRUMENTATION

The Semiconductor Tracker (SCT) combines with the pixel detector within it, and the gaseous/polypropylene foil transition radiation tracker surrounding it, to form the Inner Detector (ID) tracking scheme of ATLAS. The overall ID is 2.3m in diameter and 7m in length. Its main requirements are:

- the precision tracking of charged particles
- using ionising detection devices that are capable of 40MHz bunch crossing identification
- and that can tolerate large radiation doses, both intrinsically and to their in-situ electronics,
- and that are constructed with minimal material
- within a complete ID that has inclusive capability of electron identification.

The ID has both barrel and endcap regions. This FDR covers only the SCT modules of the barrel region. The SCT endcap modules have, by necessity, a different design, and will be the subject of their own future FDR.

3 THE FINAL DESIGN REVIEW (FDR) DOCUMENTS

Barrel Module Project Plan: SCT-BM-FDR-2

This defines the cluster concept for module production, explains the logistics of component supply, and the responsibilities for assembly on to barrels and assembly at CERN. It emphasises the role of this FDR in the planned execution of the baseboard and hybrid production projects, and discusses site facilities and commissioning, and finally provides the overall production schedule.

The Barrel Module Interfaces: SCT-BM-FDR-3

This validates and documents all the interfaces between the barrel modules and their support brackets, cooling units, electrical harnesses and the overall detector control systems.

Requirements and Specifications of Barrel Modules: SCT-BM-FDR-4

This details the specifications and the general requirements of the barrel modules: electrical, mechanical, thermal, material constraints, and the geometrical envelope, and provides relevant technical drawings and thermal FEA results. The radiation lengths of the separate components and of the whole module are tabulated.

Details of Barrel Module Components: SCT-BM-FDR-5

This document describes all aspects of the Barrel Module components and their quality assurance, discusses the silicon detector and ASIC projects in depth, and pays particular attention to the technical specification, production and QA in the baseboard and hybrid projects, both of which are seeking approval to place production orders.

Module Assembly: SCT-BM-FDR-6

This explains the procedures for module assembly, from initial components through to the final tested module. It also explains the cluster strategy for assembly and appends documentation of the procedures at each cluster site. There is also a section on the boxes needed for safe testing and transport of modules.

Module QA: SCT-BM-FDR-7

This discusses the QA for modules during the full-scale production period. It explains monitoring procedures for mechanical and electrical performance both during the assembly sequence and after construction is complete. It also considers how product sampling tests through irradiation, beam tests and source measurements will ensure the overall high quality throughout the project.

Mechanical and Thermal Performance of Modules: SCT-BM-FDR-8

The metrology and thermal results are presented for modules produced in the current pre-series, including some constructed specially for thermal studies, and these are compared and shown to be satisfactory either by direct comparison with required specifications or finite element calculations.

Electrical Performance of Modules: SCT-BM-FDR-9

This summarises the electrical performance of barrel modules read out by front-end binary ASICs that have come from process runs of ABCD2T, ABCD3T and the current ABCD3T-A versions of the SCT chip. The detailed performance of noise occupancy and extracted noise are shown pre- and post-irradiation as well as tracking efficiency, charge collection and spatial resolution from test beams. Finally, encouraging and successful first results from a 10-module system test are used to demonstrate that the Barrel Module project can expect to now move to the production phase.

4. A BARREL MODULE

The Barrel Module, shown in Figure 1, is the focus of this review, and some of its basic features, properties and specifications are briefly summarised here:

- particle-induced ionization within high-resistivity n-type silicon wafers processed with p-strip implant diodes, provide the signals to on-board ASICs with binary readout functionality.

- the module itself has minimum mass, is radiation hard in its overall functionality, to the levels anticipated after 10 years of ATLAS operation, and is robust and efficient both mechanically and thermally.

- for tracking, the rφ position resolution per SCT layer (i.e. from two measurements per module) is aimed to be around 17μm, with the SCT instrumentation covering a rapidity range of ±2.5 with four cylindrical layers in the barrel and nine layers of disks in each end-cap.

- the total area of such silicon microstrip coverage is 61m^2, where the silicon detectors have implants with 80μm pitch and an effective active strip length of 124mm. In total there are 768 readout strips on each side of a module and each is capacitively coupled to a metal strip through an oxide layer.

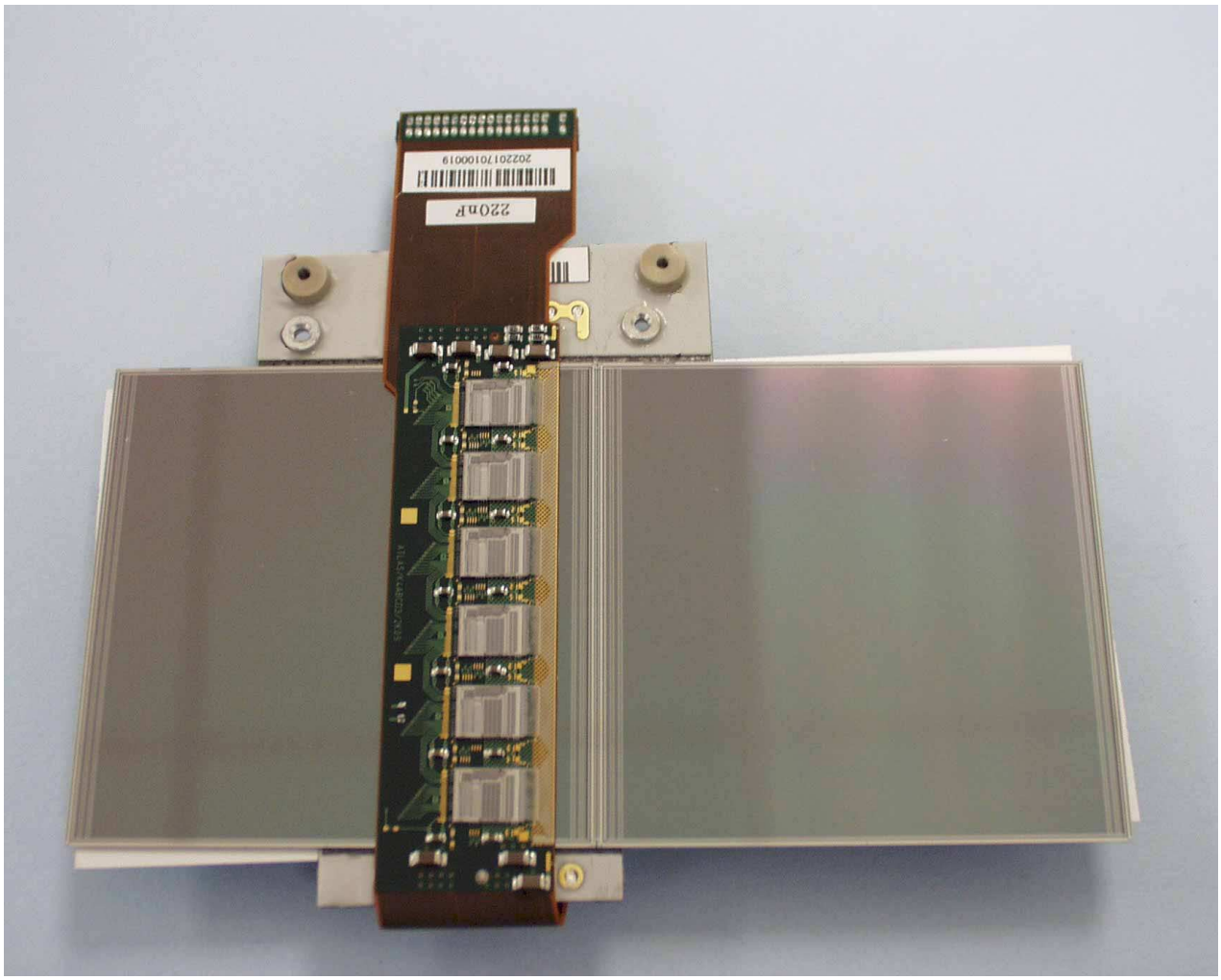

Figure 1: Barrel Module, showing two inter-bonded silicon detectors, with a wrap-around hybrid and 6 of the 12 front-end ASICs, with the hybrid pigtail leaving the module above the region of the beryllia-faced baseboard that interfaces directly to the external cooling pipe.

5. THE BARREL STRUCTURES AND ASSEMBLY

The barrel modules are supported on carbon fibre cylinders through attachment to brackets that are located by precision inserts in the cylinders. The diode implants and readout strips on one side of the module are along the axis of the cylinders, and on the other side at a 40mr stereo angle to provide the longitudinal coordinate. Alternate barrels have stereo u-v orientation (ie ± 40mr). Adjacent modules are overlapped longitudinally each end, requiring that they are staggered in radius by 2.8mm. A tilt angle near 10^0 (different for each of the barrels) allows adjacent rows of modules to be overlapped, hence providing an hermetic detector coverage. More details of the barrels and the assembly procedures are provided in the documentation of their Final Design Reviews, where ATL-IS-AP-0002 is the top-level assembly document, ATL-IS-AP-0032 describes the module mounting procedure, and ATL-IS-AP-0027 gives a description of the assembly facilities.

6. THE POWER SUPPLIES and DETECTOR CONTROL SYSTEM (DCS)

The operation of the module requires low voltage supplies for the ASIC analogue and control functions, and for associated temperature control readout and for components on the opto harness. A high voltage system provides the bias for depleting the silicon strip detectors. All the supplies are interfaced to the ATLAS DCS for the safe operation of the complete SCT. The details and reference documents for the SCT Power Supplies are available in http://www-hep.fzu.cz/Atlas/WorkingGroups/Projects/MSGC.html. The DCS is detailed in the documentation dcsfdr.pdf on EDMS, within the document ATL-IS-ES-0011.

7 THE COOLING SYSTEM

This is an important item for the overall satisfactory operation of the Barrel Module, and was comprehensively reviewed in ATC-IC-MT-0001 in June 2000. Its properties and performance will not be covered further in this review. It is based upon an evaporative fluid cooling scheme developed for this project. This provides fluid that circulates through blocks that interface directly to the barrel modules, at temperatures down to -30^0C. This is sufficient for safe operation of the barrel modules in all expected powering and radiation-damaged conditions at any point over the planned ten year lifetime of the detector. The implications on the thermal management of the SCT and the consequent module performance are given in detail in the appropriate sections of the ATLAS TC review.

8. THE READOUT SYSTEM

The front-end ASICs, the ABCD3T-A chips, are situated directly on the module and their specifications are described in SCT-BM-FDR-5.4. Their electrical output, in the form of binary data, is passed from the module via links to the ReadOut Drivers (ROD)s. There are two streams of 40 Mbits/s data from each module with each link reading out the data from one side of an SCT module. In the event of a link failure, the data can be re-routed through the other link. The 40 MHz bunch crossing (BC) clock and the L1 trigger and all fast and slow commands (TTC data) are also transferred from the RODs to the modules. A BiPhase mark

encoding is used to send a 40 Mbits/s data stream down the same fibre as the 40 MHz BC clock. The system is based on optical links and the initial scheme was described in the Inner Detector TDR, and the LEDs described there have now been replaced by VCSELs. The module is interfaced to the readout chain through the opto harness and this is referenced in SCT-BM-FDR-5.3. The ROD has been through a series of review updates, but its basic requirements are those given in the original specification document: http://www-wisconsin.cern.ch/~atlas/off-detector/ROD/doc/1996-09-OffDet-Requirements.txt.

9. THE ALIGNMENT AND SURVEY

In ATLAS, the SCT will be within a nitrogen environment to ensure that the modules are in the optimum conditions for long-term operation of silicon devices; it is also the environment in which the properties and long-term behaviour of modules have been studied and qualified. There will be an initial comprehensive X-ray survey of the modules on the barrels, and the alignment will subsequently be tracked through a Frequency Scanning Interferometry (FSI) system developed for this purpose, and by particle tracks. The macro-assembly of the modules and their alignment are topics covered by the Final Design Review that precedes this review and details can be found in its documentation, where the alignment and X-ray overviews are given respectively in ATL-IS-ES-0026 and ATL-IS-EN-0004, and the structure is described in ATL-IS-ES-0010.

SCT Barrel Module FDR Document

SCT Barrel Module: Project Plan

Abstract

This document outlines the responsibilities and schedule for the SCT Barrel Module Project.

Prepared by:	***Checked by:***	***Approved by:***
J. Carter		

Distribution List

Table of Contents

1 SCOPE OF THE DOCUMENT

This document outlines briefly the SCT plans and responsibilities for:

- The supply of the components making up the SCT barrel modules;
- The assembly of these components into modules;
- Module QA;
- The assembly of modules to cylinders;
- Procurement.

2 BARREL MODULE CLUSTERS

The responsibility for producing the barrel modules for the SCT is devolved to four *clusters*:

Cluster	**Contact Physicist**	**Cluster Composition**	**Number of Modules to be delivered by cluster to the barrel assembly sites[1]**
Japan	Y. Unno	Hamamatsu Photonics, Hiroshima, KEK, Kyoto-edu, Okayama, Tsukuba	606
Scandinavia	R. Brenner	Bergen, Oslo, Uppsala	404
UK-B	A. Carter	Birmingham, Cambridge, QM, RAL	549
US	C. Haber	LBL, Santa Cruz	663

[1]The numbers given for the modules to be delivered by clusters to the barrel assembly sites are estimated as 5% more than the final number of modules assembled on the SCT barrel.

The overall co-ordinators of the barrel module programme are A. Carter and Y. Unno.

3 BARREL MODULE COMPONENT SUPPLY

The components of the ATLAS SCT barrel modules are described in SCT-BM-FDR-5. They are, for each module,:

- 4 single-sided silicon microstrip detectors.
- 1 VHCPG baseboard with epoxy coating and 4 beryllia facings fused onto the structure.
- 1 hybrid consisting of a flex circuit, with passive components and glass pitch-adaptor mounted, glued to two carbon bridges.
- 12 ABCD3T-A readout ASICs.

- Electrically conducting epoxy (Eotite P-102) for gluing the ASICs to the hybrid and making electrical contact to the back of the detectors.
- Structural epoxy (AW106/HV953U) with a boron nitride additive (PT1045) for gluing the detectors and the hybrid onto either side of the baseboard.

The responsibility for providing the fully tested components to each module assembly site is summarised in Table 1.

Component	Cluster	Responsible for cluster supply	Component Source	Location of SCT QA of component
Silicon Detectors	Japan&US	Y. Unno	Hamamatsu	Hamamatsu, Hiroshima, KEK, Tsukuba
	Scandinavia	B. Stugu	Hamamatsu, Sintef[1]	Bergen
	UK-B	J. Carter	Hamamatsu	Cambridge, RAL
VHCPG Baseboard complete with BeO facings	All	A. Carter	Industry and Baseboard assembly facility at CERN	CERN
Hybrid	All	Y. Unno	Industry	KEK
ASICs	Japan, Scandinavia US	A. Grillo	Atmel	Santa Cruz, CERN
	UK-B	A. Carter	Atmel	RAL
Electrically conducting epoxy	All	Y. Unno	Industry	KEK
Epoxy with boron nitride additive	All	M. Gibson	Industry	RAL

1 Up to 30% of the detectors used by the Nordic cluster may be supplied by Sintef, subject to acceptance of the Sintef Pre-series in 2001.

Table 1: Responsibilities for Module Component Supply

4. ASSEMBLY OF COMPONENTS INTO MODULES

The barrel modules are assembled from their components and tested within the clusters. These tasks are described in SCT-BM-FDR-6 and SCT-BM-FDR-7. For series production, the tasks will be located according to Table 2:

Cluster	ASICs mounted on hybrids and bonded	Full QA of hybrid+ASIC assembly	Module assembled / bonded	Full thermal and mechanical QA of individual modules	Full electrical QA of individual modules
Japan	Industry	KEK	Hamamatsu	KEK	KEK
Scandinavia	Industry	Oslo	Oslo/Uppsala	Uppsala	Bergen, Oslo, Uppsala
UK-B	Birmingham	Birmingham	RAL	RAL	Birmingham, Cambridge, QM, RAL
US	Industry	LBL, Santa Cruz	LBL	LBL	LBL, Santa Cruz

Table 2: Module assembly and test locations during series production

The modules reported at this FDR come from the Japanese, Scandinavian and UK-B clusters, with the industrial steps of Table 2 carried out within the SCT cluster. The modules have been constructed with the full assembly equipment described in SCT-BM-FDR-6, which is commissioned in all four clusters. The full qualification of all the assembly sites for series module production will take place between October 2001 and February 2002 (see Appendix 1).

5. ASSEMBLY OF MODULES ON TO CYLINDERS

The modules from the Scandinavian, UK-B and US clusters will all be sent to Oxford, where they will be assembled on to three of the four SCT cylinders (barrels 3, 4 and 6). The modules for barrel 5 are being made in Japan and will be assembled on to barrel 5 at KEK. The complete and fully tested barrels will be sent individually to CERN. At CERN they will be re-tested and assembled together into the four barrel structure. An X-ray survey will be carried

out on the complete four barrel structure.

References to full descriptions of the assembly to cylinders, commissioning and survey processes are given in SCT-BM-FDR-1.

6 SCHEDULE AND PROCUREMENT RELEASE

The work plan of the SCT is being developed with the aim of delivering the complete sub-detector on the schedule required by ATLAS.

This requires series barrel module production to start in late 2001, with completion in the first half of 2003. The current SCT barrel module schedule is shown in Appendix 1.

The requirement for barrel module production to begin in 2001 is also driven by budgetary issues; in particular the cost of retaining trained staff on the project to carry out the module assembly tasks.

The long (and different) lead times of the major module components have required the procurement phases to begin in advance of the barrel module FDR or PRR. The procurement status is as follows:

- **Silicon microstrip detectors**; contracts are placed for the total supply and the series release has been authorised (SCT-BM-FDR-5.1). The delivery of series production is in progress.
- **Baseboards**; tenders have been sent out for the VHCPG and the BeO facings. These tenders will be opened in May 2001, just before this FDR. The approval for placing the Contracts in early June is requested from this FDR.
- **Hybrids:** tenders are to be sent out immediately following this FDR.
- **ASICs:** it is planned to release the full series production order in July 2001, following both an ASIC PRR and detailed negotiations with Atmel. In the meantime, sufficient ASICs are being purchased to support the start of series barrel module production according to the appended schedule.

Full funding is secured from the SCT institutes for the procurement of the barrel module components, for module assembly and for the barrel engineering and assembly.

Appendix 1: Barrel Module Schedule

ID	Task Name	Duration	Start	Finish
1	**SCT Barrel Modules (A. Carter, Y. Unno)**	**563 days**	**01/05/2001**	**26/06/2003**
2	SCT Barrel Module FDR	0 days	25/05/2001	25/05/2001
3				
4	Delivery of Tested Silicon Detectors	429 days	01/05/2001	20/12/2002
5				
6	Order VHCPG & BeO	0 days	30/05/2001	30/05/2001
7	Delivery of Tested Baseboards	320 days	01/10/2001	20/12/2002
8				
9	Order Hybrids	0 days	30/05/2001	30/05/2001
10	Delivery of Tested Hybrids	220 days	15/10/2001	16/08/2002
11				
12	Order ASICs	0 days	30/05/2001	30/05/2001
13	Delivery of Tested ASICs	285 days	01/10/2001	01/11/2002
14				
15	**SCT Barrel Module Site Qualification**	**80 days**	**15/10/2001**	**01/02/2002**
16	Japan	1 day	15/10/2001	15/10/2001
17	Scandinavean	1 day	30/11/2001	30/11/2001
18	UK-B	1 day	15/10/2001	15/10/2001
19	US	1 day	01/02/2002	01/02/2002
20				
21	**SCT Barrel Module production**	**431 days**	**01/11/2001**	**26/06/2003**
22	Japan	350 days	01/11/2001	05/03/2003
23	Nordic	350 days	03/12/2001	04/04/2003
24	UK-B	350 days	01/11/2001	05/03/2003
25	US	350 days	22/02/2002	26/06/2003

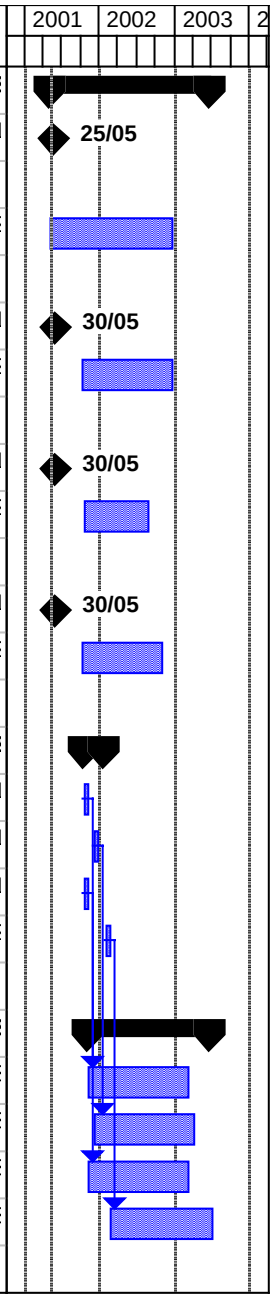

SCT Barrel Module FDR Document

SCT Barrel Module : Interfaces

Abstract

This document defines and documents the interfaces and relationships between the SCT barrel modules and other SCT barrel components.

Prepared by :	*Checked by :*	*Approved by :*
R. Apsimon, G. Barbier, **D. Greenfield, T. Hayler,** **E. Perrin, Y. Unno**		

Distribution List

Table of Contents

1 SCOPE OF THE DOCUMENT

The document defines and documents the interfaces and relationships between the Barrel detector modules and the following items:

- Barrel module support brackets
- Barrel cooling units
- Barrel electrical harnesses
- Barrel DCS components

2 MECHANICAL INTERFACES TO THE BARRELS

The design of the four SCT barrels is described in the Final Design Report on ATLAS SCT Barrel Cylinder FDR / 2000-1.

The mechanical interfaces and the Z position of the modules are described in the detail drawings:

For cylinder 3: ATLISBB30012

For cylinder 4: ATLISBB40010

For cylinder 5: ATLISBB50008

For cylinder 6: ATLISBB60008

(These drawings are the machining drawings of the 4 cylinders that were prepared for the Invitation to tender for the SCT cylinders).

The R-φ position of the modules are defined in the Geometry drawings:

For Barrel 3: Geneva 252205P3C ATLISBB30001

For Barrel 4: Geneva 252210P3B ATLISBB40001

For Barrel 5: Geneva 252207P3B ATLISBB50001

For Barrel 6: Geneva 252212P3B ATLISBB60001

(These drawings have an earlier module separation of 2mm, which will soon be updated to the current value of 2.8mm).

2.1 SCT BARREL CYLINDERS

The overall SCT barrel envelope is defined in drawing RAL A1-TB-0049-158-01-F. However each of the four SCT barrels has also to be built within its own radial envelope, which are defined by:

	Inner radius (mm)	Outer radius (mm)	Overall outer radius (mm)
Barrel 3	260	284	323
Barrel 4	327	355	393
Barrel 5	397	427	464
Barrel 6	468	498	534
Thermal enclosure	540		549

2.2 SUPPORT BRACKETS

The CFRP support cylinders are equipped with small glued pads that are machined afterwards (see, for example, drawing ATLISBB30012). There are 32, 40, 48 or 56 rows of 12 pairs of pads spaced around and along the cylinder. The 'z' separation of the module physics centres is the same for all 4 barrels (see, for example, drawing ATLISBC0001). A barrel module will be mounted on a low-mass bracket which is screwed into the cylinder pads. The principles of the bracket can be seen in drawing Geneva 252575P1 (which is not up-to-date). Each barrel type requires 2 types of bracket shells for lower and upper modules, make a total of 8 different types for the whole SCT Barrel.

The positions of the support brackets are calculated to ensure sufficient clearance between modules. The layout is designed to result in a minimum separation of 1mm between the sensor surfaces of overlapping modules after all tolerances have been allowed for. This minimum separation is used for both mechanical and electrical reasons, as described in SCT-BM-FDR-4, section 4. The radial 'centre to centre' module separation is 2.8mm, nominal. The module thickness in this region is nominally 1.15mm (see section 1.3 below). Subtracting the required 1mm separation between sensor surfaces leaves a radial distance of 650 μm to accommodate the module tolerances and module non-planarity, and the bracket tilt tolerance (which gives movement at the end of a module amplified by a lever-arm effect). The division of the 650 μm is 250 μm for the bracket tolerance and 400 μm for the module tolerance and non-planarity.

2.3 MODULES

The module envelope is given in drawing RAL 1-TB-0059-522-00. The module parameters (without tolerance) are:

Thickness of module:

Region	*thickness [mm]*
Sensor	1.15
BeO facings	0.92
Hybrid surface	3.28
Highest component	6.28
ASICs	4.48
Wire-bonds	5.08
Stay-clear wire-bonds	7.08

The wrap-around part of the hybrid interconnect cable (SCT-BM-FDR-5.3) extends to reach a distance of between 40.0 mm from the module centre (for a perfect round shape at the wrap-around) and 41.22 mm maximum (for a perfect wedge shape at the wrap-around). The hybrid placement error of order 50 μm will add to these number.

The front edge of the wrap-around is at x=4.2 mm, and the back edge at x=27.2 mm in the module coordinate system, which has its origin at the geometrical centre of the four sensors. The hybrid placement error of order 50 μm will add to the numbers.

The location of the hybrid connector can be specified by the location of pins number 1 and 35, which are at (x,y) = (3.612, -69.451) mm and (25.197, -69.883) mm, respectively, in the module coordinate system.

The error in the pigtail connector position is introduced by the error in the hybrid placement, connector (pin) play, and the soldering error, which are of order of 100 μm, 100 μm, and 200 μm, respectively, thus of order 500 μm in total. Note that the pigtail cable part is flexible and can absorb the errors as long as the mating connector is shorter.

Each module is fastened by 2 points on the bracket, screwed on pads, and by a third mounting point situated on one pad of the adjacent row of pads (see drawing Geneva 252552P0). The position of the modules on each barrel is defined according to geometry drawings (section 2).

Drawing ATLISBB0011 shows the details of the module mounting on the bracket and the 3rd mounting point on an opposing bracket. The lower-face contact with the cooling block is also shown. The module mounting accuracy is achieved by the use of precision set screws locating on the internal bore of a circular and a slotted aluminium washer, both mounted on the upper, cooled facing of the baseboard. Both the diameters of the screws and the holes in the washers are controlled to better than 10 μm. To ensure consistency, all drawings show this assembly method. Prototyping work has revealed that the same precision can be achieved by machining precision holes and slots directly into the epoxy in-fill of the baseboard assembly. These precision holes have been shown to be stable with temperature and they offer a cost reduction and also a small material reduction. An upgrade to this alternative scheme will therefore be followed. The conceptual drawing of a hand-held mounting/handling tool to be available for handling modules without washers is shown in http://atlas.kek.jp/~unno/si_mod/Jigs/ModulePicker2frame.pdf.

The mounting of modules to the cylinder brackets is accomplished using a robot. Document ATL-IS-ES-0022 “ATLAS SCT – Barrel Module Mounting Robot Specification” describes the mechanical specification of the Barrel module mounting robot and the procedure and equipment to be used to mount and remove modules.

The document, ATL-IS-AP-0032 “ATLAS SCT – Module Mounting/Removal Procedure” describes the procedure and equipment to be used to mount the module on the barrels. It also provides an overview of the complete system and contains references to further more detailed documentation.

The Barrel module dimensions are detailed in the ‘500 series’ drawings 107761. The interfaces to the brackets are formed by the four beryllium oxide (beryllia) facings that are epoxy-fused to the VHCPG thermal substrate to form the Barrel module baseboard. This item is detailed in SCT-BM-FDR-5.2.

2.4 COOLING SYSTEM

Cooling tubes run along the axis of the cylinders and are held by clips against the modules. By arrangement, four adjacent cooling tubes become known as a cooling unit. The four tubes in each cooling unit are split into pairs, in each pair the two adjacent tubes connect together in series. Fine bore capillary tubes deliver the evaporative fluid to each pair of tubes. An exhaust manifold connects the two pairs together to make a cooling unit, see drawing RAL TD-1006-610 and TD-1006-990. The required precision of assembly is also defined in this drawing.

Cooling units are relatively decoupled from the CFRP cylinder in the sense that they are fixed to it via removable brackets bolted in the castellated flanges at either end of each barrel. The fixed end is on the inlet/outlet side of the cooling unit, the other end being allowed to slide to avoid stresses induced by CTE mismatches to be transmitted to the support structure.

The cooling pipes form the critical thermal interface between coolant and module. This interface is formed, by Dow Corning 340 thermal grease, between the cooling block and the cooled, lower beryllia facing of the baseboard. The choice of this thermal grease has been motivated by past experience and by laboratory tests. Further details are contained in the following documents:

- ATLAS Internal Note INDET-NO-177 Radiation hardness of thermal compound
- ATLAS Internal Note INDET-NO-166 Status report on modules cooling and mechanics.
- CMS-TN/94-248 Testing of radiation effects on thermal conductivity of a thermal grease.
- MEE-12-92-289 (LANL) Evaluation of available thermal greases

2.5 ELECTRICAL HARNESSES

The interface between the modules and the opto-harness is fully described in SCT-BM-FDR-3-Appendix 1.

2.6 DCS COMPONENTS

An SCT barrel module will contain two thermal sensors on the electrical hybrid, to monitor the temperature at one point on each 6-chip side of each module during operation.

3 THERMAL INTERFACES

The cooling of the modules is provided by the upper face of a cooling pipe running underneath the beryllia cooling facings of the modules. Thermal contact between the modules and cooling tubes takes place over an area of about 420mm^2. The cooling block entirely encapsulates the tube, so making use of the entire diameter. This is achieved by having the block in two halves, the block having a split line along the axis of the diameter. The block is joined to the tube by copper-plating the aluminium block making it possible to use conventional solder and non corrosive flux. The lower face of the tube provides cooling for the opto-package. Two spring clips compress the module, cooling tube and opto-package together. A thermal grease layer between each component enhances the thermal contact. The grease to be used is Dow Corning 340 which has demonstrated both good thermal conduction and high radiation tolerance.

There are twelve modules in each row. Every second module has an increased radial dimension of 2.8 mm to allow the overlap between adjacent modules. This will be achieved through use of a stepped CuNi cooling tube. The aluminium cooling block will be joined to the surface of the tube by solder. The aluminium block is copper plated to make possible the use of conventional solder.

4 ELECTRICAL INTERFACES

The three module mounting points are made of insulating material. The cooling tubes are made of electrically conductive material. They are isolated from the modules and opto-packages whose parts, in contact with the tubes, are made of insulating material. The option of two alternative grounding schemes is kept open, as it cannot be confirmed that the baseline scheme will work satisfactorily until it is are tested in a practical situation. Until such time as this practical test takes place, the cooling block design must be able to cater for both possibilities.

The baseline design has a shunt shield that exists in the form of a glue layer and aluminium foil on top of the cooling block. This scheme incorporates a wire that connects the foil to the dogleg making the module isolated from the cooling system but grounded to the electrical harness. If this scheme should fail then the foil will be employed to connect back to the cooling block making the shunt shield (glue layer and foil) redundant

The foil in the shunt shield will be no thicker than 200 μm. The thickness of the glue layer is yet to be determined.

The cylinder is equipped with patches of conductive material near each module to allow for a connection of each module to the CFRP structure and for pipe grounding connections.

The cable harness has an insulating kapton cover layer over its conductive tracks. No further insulation is required for the harness between itself and the CFRP cylinders or harness clamps.

5 ASSEMBLY

The overall procedure for assembly of the cooling units, harnesses, other services and detector modules is described in the barrel assembly procedure, RAL ATL-IS-AP-0002.

The main electronic parts of a module are four silicon detectors and a hybrid that interfaces to ASICs and provides the electrical readout. It is essential that the module connector, found at the end of the hybrid, mates with the dog-leg connector. The position of the connector on the module is defined in drawing A1-TB-0059-520-01 (the precision of this positioning is to be such that connection and disconnection can be made without damage to either a module or connector). The adopted scheme locates each dog-leg connector with reference to the hybrid connector on an individual basis. This is achieved by a jig that references the position of the module connector to the mounting points on the module baseboard. Once set, the jig is then offered to the mounting points on the bracket and the dog-leg connector is then located by the jig. A feature in the dog-leg allows two screws to pass through it, tightening these screws onto the bracket sets its final position.

It is proposed that the connection at patch-panel PPB1 is made by soldering six low mass tapes to a printed circuit board having a MOLEX 240 pin board-to-board connector. This assembly must first be routed underneath cooling manifolds and past further structures at the end of the cylinders. The assembly has a cross section of 26mm by 6mm and details of the low mass cables can be found at; http://www-f9.ijs.si/~cindro/low_mass.html.

The cooling unit is a fragile and precise assembly and must be supported at all times. A temporary structure will span between each of the brackets that will eventually support the cooling unit on the cylinder. The temporary structure can then be removed once the cooling unit is set in its final position. At the time of mounting the cooling units to the cylinder there will be no modules in place, dummy modules and spring clips will support the cooling tube along its axis.

SCT-BM-FDR-3_Appendix 1

SCT BARREL MODULE : ELECTRICAL HARNESS INTERFACE

A. Weidberg

Table of Contents

1. Scope of the document

This document describes the interface of the SCT barrel modules to the opto-harness. An overview of the SCT links system is given in Section 2. The electrical specification of the SCT links for the barrel harness is given in Section 3 and the mechanical specification is given in Section 4.

2. SCT Links system overview

Optical links will be used in the SCT to transmit data from the silicon strip detector modules to the RODs and to distribute the Timing, Trigger and Control (TTC) data from the RODs to the ABCD ASICs. The SCT optical links are based on VCSELs and epitaxial silicon PIN diodes operating at a wavelength of 850 nm. There will be one opto-package for each of the 4088 SCT detector modules. Each of these opto-packages will contain two VCSELs for the data links and one PIN diode for the TTC link (see Figure 1).

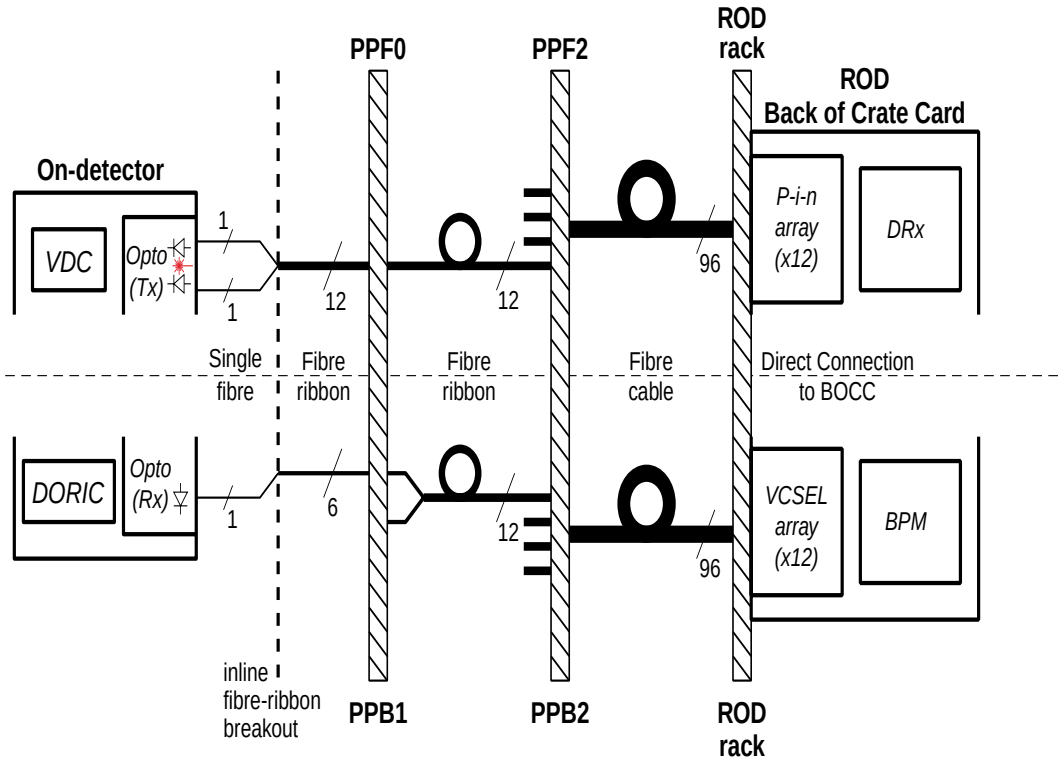

Figure 1 SCT Links architecture. PPB1, PPF0, PPB2, PPF2 refer to fibre and cable patch panels.

The opto-packages are pig-tailed with multi-mode radiation-hard fibres. The data from the SCT front end modules are read out serially via the VDC ASIC. The data link uses an NRZ data format and the minimum fibre coupled power will be 300 μW. The off-detector opto-electronics for the data links consists of 12 way arrays of silicon PIN diodes to receive the optical signals and the DRX-12 ASIC to amplify and discriminate the resulting electrical signals.

The TTC links use BiPhase Mark encoding to send the 40 MHz bunch crossing (BC) signal and the 40 Mbits/s control data stream for each module down the same fibre. For the TTC links, the off-detector opto-electronics consists of the BPM12 ASICs and 12 way VCSEL arrays. The BPM12 performs the BiPhase Mark encoding and drives the VCSELs. The TTC optical signal is converted to an electrical signal by the PIN diode in the on-detector opto-package and the resulting electrical signal is decoded by the DORIC4A ASIC to produce the recovered BC clock and control data signals.

Redundancy is provided for in the data links by having two independent data channels per module. If one link fails or a master ABCD fails, then the data can be routed via the other data link of the same module. Redundancy is built into the TTC system in that if a TTC link fails, then the TTC data can be taken from a neighbouring module.
This redundancy links the modules along one half row. Two neighbouring rows in φ are joined together to produce a redundancy loop covering 12 modules.

3. ELECTRICAL SPECIFICATIONS

The opto-electronic components (opto-package and DORIC4A and VDC ASICs) for the barrel SCT will be mounted on opto-flex cables. The opto-flex cables will be produced as a four layer flexible copper/kapton circuit. There will be two signal/ground layers and one ground screen plane so that the tracks for the high speed signals can be laid out as strip lines. There will be one thermal layer, which will be used to transfer heat from the opto-electronics to the cooling pipe.

The schematic diagrams, layouts and details of the connectors used for the opto-flex cables are available on the web at http://webnt.physics.ox.ac.uk/wastie/dogleg.htm
The pin-out of the connectors on the opto-flex cable is defined in the schematic.
The module connector is used to contact the opto-flex cable to the module pig-tail. The pin-out of the interface PCB connector is available on the web at
http://webnt.physics.ox.ac.uk/wastie/dogleg.htm

The connector at the opposite end of the opto-flex cable is used to connect to an interface PCB. The low mass Al tapes will be thermode soldered to the opposite side of this interface PCB. The Samtec horizontal mating connectors on the opto-flex and the interface PCB are also defined at http://webnt.physics.ox.ac.uk/wastie/dogleg.htm
The low mass cables are made from single sided aluminium/kapton cables. Two pairs of tapes are glued together to form a pair with each pair supplying one SCT module. The schematic diagrams of the low mass Al tapes are available on the web at http://www-f9.ijs.si/~cindro/cables/cable2001_barrel.pdf

The specifications for the DORIC4A and VDC ASICs are available on the web at
http://www-pnp.physics.ox.ac.uk/~weidberg/doric_specs.pdf
http://www-pnp.physics.ox.ac.uk/~weidberg/vdc_specs.pdf

In order to have the possibility of implementing two different grounding schemes there will be a 50 μm thick aluminum foil below each barrel harness. Two different grounding schemes can be implemented:

1. **Shunt Shield Configuration**. In this option the foils are unconnected to the modules or thermal shield. Another 50 μm thick aluminum foil, 5mm wide makes an electrical connection from the cooling pipe to the digital ground on the opto-flex near the module connector.
2. **Solid Ground Configuration**. In this option arms of the foils are unfolded so as to connect to the opto-flex digital ground. The other ends of the foils are connected to the thermal shield. The digital ground near the module connector is then connected to the cooling pipe by a 50 μm thick aluminum foil, 5mm wide.

4. MECHANICAL SPECIFICATIONS

The opto-flex cable should have a minimum bend radius of 4.5mm. There are 16 different flavours of the opto-flex cables to take into account the following factors:

1. left handed or right handed opto-flex;
2. left or right redundancy flow;
3. opto-flexes for barrels 3 and 5 are different to 4 and 6 because of the different stereo angles (uφ compared to vφ stereo).
4. High and low modules have different opto-flex cables to allow for the extra length and the need to respect the minimum bend radius.

The mechanical drawing for one of the 16 flavours of the opto-flex cable is on the web at http://webnt.physics.ox.ac.uk/wastie/dogleg.htm
The opto-package dimensions are 5.5*5.5*1.6 mm^3. The wire bonds from the opto-package to the ASICS and the wire bonds from the ASICs to the opto-flex will be protected by a plastic u-profile lid. Allowing for this lid, the space envelope for the opto-package plus ASICs is 1.6*9*11 mm^3. The clearances for the opto-package to the silicon is 1.27 mm. The total height of the Al tapes plus interface PCB, plus opto-flex and connector is 5.6mm. This leaves a minimum of 2.4mm clearance (6 pairs low mass tapes and worst case barrel radii and eccentricity variations). The positions of the opto-package, opto-flex and SCT modules on the barrels is illustrated in the CDD drawings number 252683P0, 252684P0, 252685P0 and 252686P0.

Six SCT barrel modules are supplied by low mass tapes and optical fibres that come in from the +Z side of the barrel and the other six in the same row from the –Z side. Each set of six tapes (called an opto-harness) will be assembled and mounted onto the barrel together (see drawing RAL-A0-TB-0045-742-00-A). The 12 data fibres for one opto-harness will be fusion spliced to a 12 way fibre ribbon and the 6 TTC fibres for one opto-harness will be fusion spliced onto a six way ribbon fibre. The location of the splices will be after the fibres have left the barrel surface. The lengths of bare fibre near the modules will be protected by 900 micron furcation tubing which will allow the fibre to be strain relieved at the back of the opto-package. The individual fibres run in parallel with the low mass tapes along the surface of the barrel. The fibres are routed from the barrel to the opto-flex so as to respect the minimum bend radius of 20mm. The tapes are held on the surface of the barrel by a clamp to isolate them from mechanical strain. The clamp will allow movement of the tapes on thermal cycling. The opto-flex leaves the barrel at the location of the clamp and is fastened to the bracket by two screws. The bend of the opto-flex will respect the minimum bend radius of 4.5 mm. The screws used will be smaller than the 3.5mm diameter of the holes (see the CDD drawings number 252683P0, 252684P0, 252685P0 and 252686P0). This tolerance will be used to accommodate the actual module dimensions in order to ensure that the connector at the end of the opto-flex can mate with the connector on the end of the module pig-tail. The opto-flex is routed underneath the cooling pipe and is held against the tube by two spring clips. The opto-electronics are all on the upper side of the opto-flex. A heat sink layer is used to transfer the heat from the opto-electronics to the area under the cooling pipe. Thermal calculations are being performed to optimise the heat transfer as to allow the VCSELs and PIN diodes to operate around 0^0C.

The SCT barrel opto harnesses will be fully tested at RAL before mounting on the barrel. The tests that will be performed are defined in the document
http://www-pnp.physics.ox.ac.uk/~weidberg/assembly_and_test_procedures.doc
The opto-harnesses will be mounted on the barrels and simple functionality tests will be performed.

SCT Barrel Module FDR Document

SCT Barrel Module : Requirements and Specification of Barrel Modules

Abstract

This document details the requirements and specifications of the SCT barrel modules with reference to the chosen module design.

Prepared by :	*Checked by :*	*Approved by :*
A. Carter, J. Carter, J. Morin, Y. Unno		

Distribution List

Table of Contents

1 SCOPE OF THE DOCUMENT

The document describes the requirements and specifications of the SCT barrel module, and how these relate to the final module design.

2 REQUIREMENTS OF THE BARREL MODULES

For the SCT barrel, the required tracking precision is obtained by modules with an intrinsic point resolution of 23 μm in the r-φ coordinate per single side measurement. The precision is obtained for the binary readout scheme (on-off readout) using silicon microstrip sensors with 80 μm readout pitch. A back-to-back sensor pair with a stereo rotation angle of 40 mrad gives a precision of 17 μm in the r-φ coordinate and 500 μm in the z coordinate from the correlations obtained through fitting. The mechanical tolerance for positioning sensors within the back-to-back pair must be ~ 5 μm lateral to the strip direction.

The severity and consequences of the high accumulated radiation levels for silicon detector operation, causing increased leakage current and type inversion, give rise to the need to operate the sensors at about -7 ^{o}C. The maximum expected fluence after 10 years of operation in the SCT is $2x10^{14}$ 1 MeV-neutron-equivalent/cm^2 (at the upper limit of uncertainty of 50% in the total cross section). The corresponding detector bias voltage required for high charge collection efficiency will be in the range 350-450 volts, depending upon SCT warm-up scenarios. This will result in a total leakage current of ~ 0.5 mA for a barrel detector operated at -7 ^{o}C at a bias voltage of 450 V. The leakage current is strongly dependent on temperature, roughly doubling every 7 ^{o}C. The detector heat generation is therefore a strong function of the temperature of the sensors in the module.

Thermal considerations, and especially concerns of thermal run-away, lead to a module design where the effective in-plane thermal conductivity must be increased beyond that of silicon. In practice this will be achieved by the use of high-thermal conductivity material in a baseboard which is laminated as part of the detector sandwich. The power consumption of the front-end ASICs is expected to be 6.0 W nominal and 8.1 W maximum. The thermal design of the module must allow for this.

The SCT will undergo temperature cycling over the range -20 ^{o}C to +25 ^{o}C in a controlled sequence, and it must be safe, in the event of cooling or local power fluctuations, up to temperatures of 100 ^{o}C. This requires the module design to have minimal CTE, and to be capable of elastic deformation. The precision of the tracking measurement depends on the modules having a stable profile after changes of the operating conditions.

The SCT modules are in the tracking volume and required to have as little mass as possible. With the use of carbon and organic materials, the goal for the amount of material is 1.2% X_o (radiation length) per module, averaged over the sensor area.

After considering the combined electrical, thermal and mechanical requirements, the optimised design of the barrel modules has a hybrid placed near the centre of the module, above the detectors, and connected to the strips near the middle of their total length.

3 SPECIFICATION OF THE MODULE DESIGN

In the barrel region, one module is made of four 63.96 mm x 63.56 mm (cut-edge to cut-edge) single-sided silicon microstrip sensors. Geometrical dimensions are shown in Figure 1 for the two sensors aligned to form a 128 mm long unit. Strips of the two sensors are wire-bonded to form 126 mm long strips. The pitch of the strips is 80 μm and there are 770 strips physically with the first and the last being connected to the strip bias potential for the electric field shaping and defining the strip boundary.

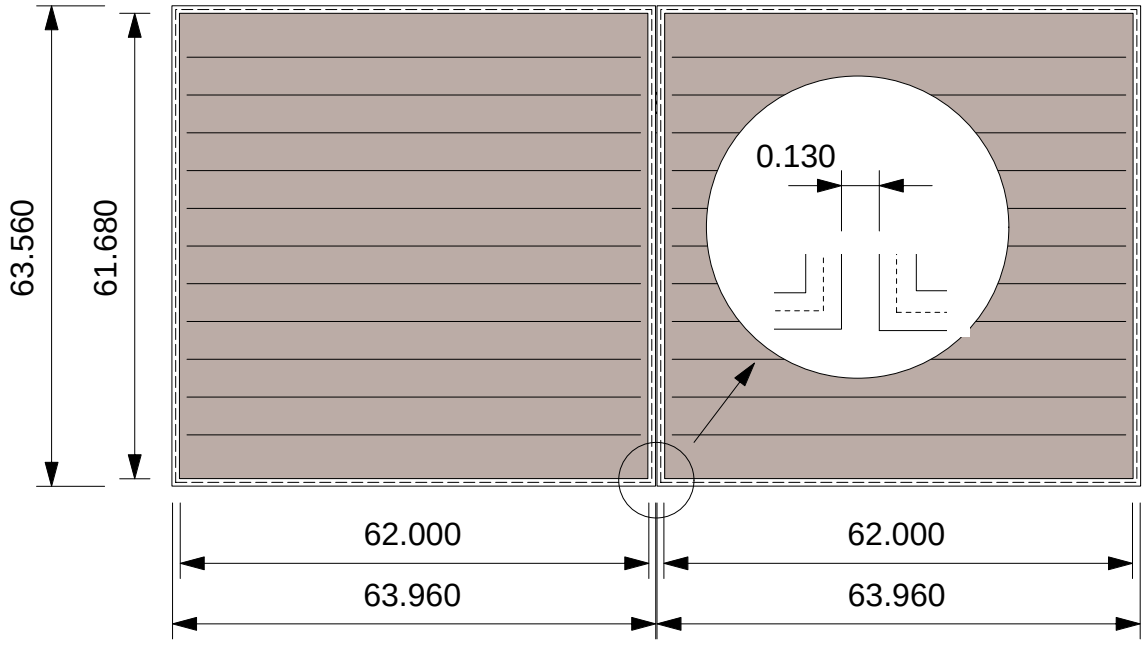

Figure 1 A pair of the barrel microstrip sensors forming a 128 mm strip unit. The active areas of the sensors are shaded and the gap between the sensors is shown in the inset.

Figure 2 shows a 3D view of the barrel module and the key features of the design. In order to form a double-sided readout module, a pair of 128 mm long units are back-to-back aligned and glued with a stereo angle of 40 mrad. Figure 3 shows an expanded view of all the components. The measuring planes, each formed of a pair of wafers, are glued to a central VHCPG baseboard of thermal conductivity up to 1700 W/m/K. As shown in the figure, the baseboard extends outwards, with BeO facings fused to the VHCPG surfaces, on both lateral sides of the module. These exposed facings are the places at which the readout hybrids are attached, and the larger facing contacts the cooling pipe. The contact BeO facing includes dowel holes to locate the module on the support structure accurately. The hybrids form mechanical bridges across the silicon, in a design that reduces the thermal coupling between the front end chips and the silicon by avoiding contact with the silicon surface. This also has the advantage of avoiding gluing to the active surface, which would carry the potential for damage and also the uncertainties associated with long term ageing and radiation effects.

The module parameters are summarised in Table 1.

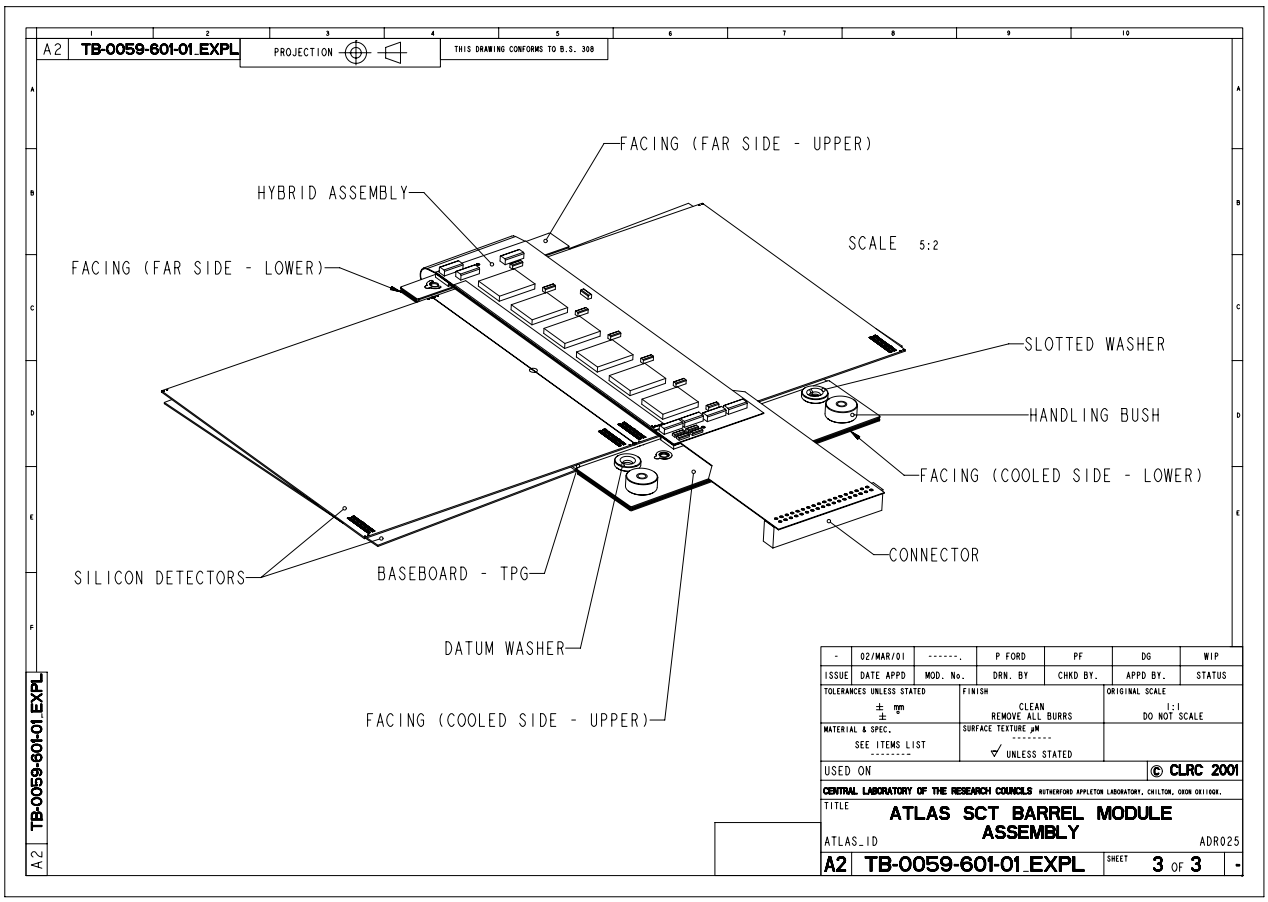

Figure 2 Layout drawing of barrel module

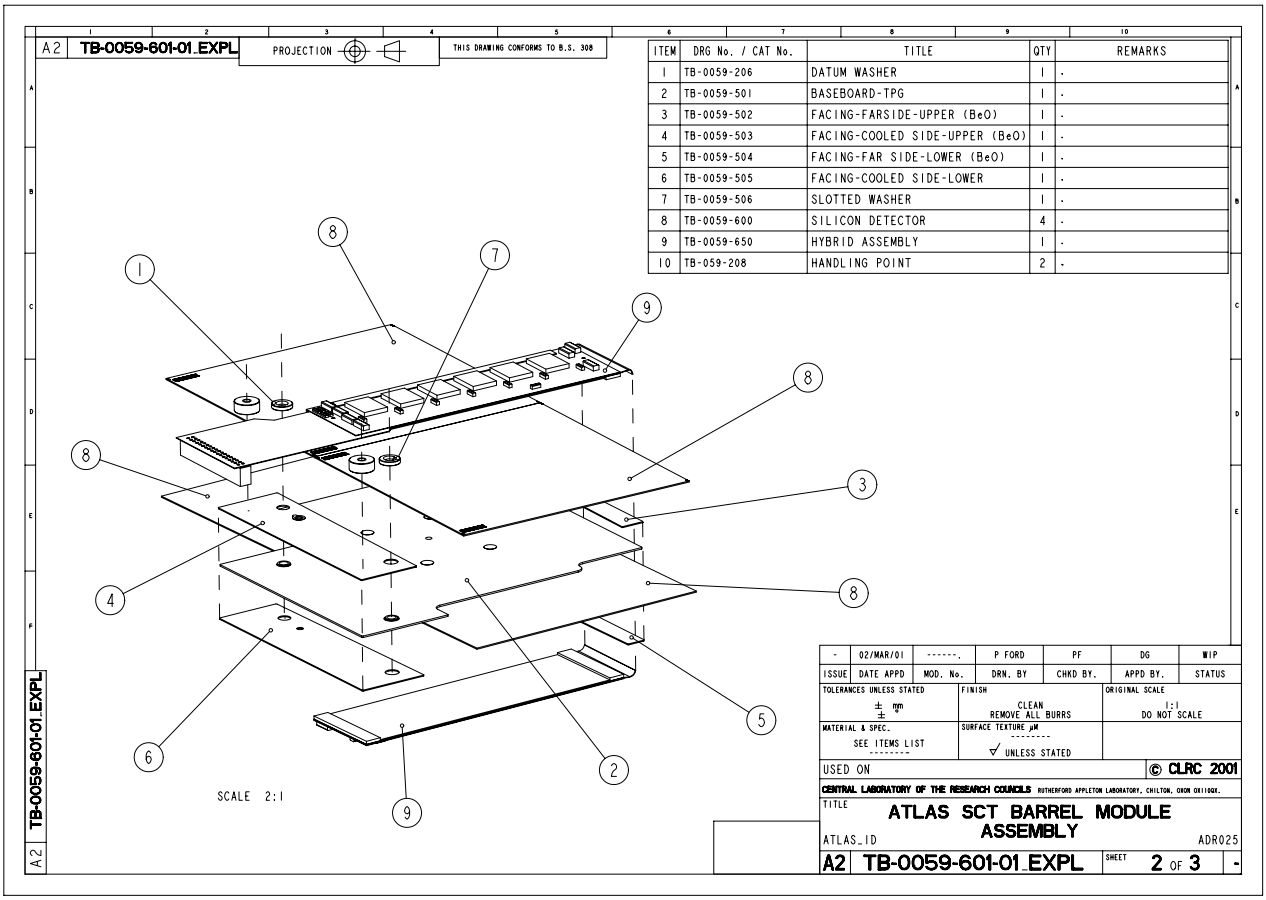

Figure 3 Exploded view of barrel module

Silicon outer dimension	63.56 mm x 128.05 mm (cut-edge)
Construction	Four 63.56 mm x 63.96 mm p-in-n single sided sensors to form back-to-back glued sensors
Mechanical tolerance	back-to-back: <5 μm (in-plane lateral), <10 μm (in-plane longitudinal), <50 μm (out-of-plane, deviation from the average profile) Fixation point: <30 μm (in-plane lateral), <30 μm (in-plane longitudinal)
Strip length	126.09 mm (2.090 mm dead in the middle)
Strip directions	±20 mrad (0, ±40 mrad on support structure)
Number of readout strips	768 per side, 1536 total
Strip pitch	80 μm
Hybrid	two single-sided hybrids bridged over the detector
Hybrid power consumption	6.0 W nominal, 8.1 W maximum
Maximum detector bias voltage	460 V (on the detector), up to 500 V in the module
Operating temperature of detector	-7 ^{o}C (average)
Uniformity of silicon temperature	<5 ^{o}C
Detector power consumption	1 W total at -7 ^{o}C, Heat flux (285 μm): 120 μW/mm^2 at 0^{o}C
Thermal runaway	Heat flux: >240 μW/mm^2 at 0 ^{o}C
Radiation length	<1.2% X_o

Table 1: Barrel module parameters

4 MODULE ENVELOPE AND ELECTRICAL STAY-CLEAR REQUIREMENTS

Figure 4 shows the barrel module envelope. The thicknesses of the modules are 1.15 mm in the sensor area, 0.92 mm in the BeO facing area, 3.28 mm in the blank hybrid area, 6.28 mm in the highest component area, 4.48 mm in the ASIC area, and 5.08 mm in the highest wire-bond area. Since wire-bonds have height variations, at least a 1 mm stay clear distance is required in elevation, and so the module stay-clear thickness in the highest wire-bond area is 7.08 mm.

The wrap-around part of the interconnect cable extends to reach a distance of between 40.0 mm from the module centre (for a perfect round shape at the wrap-around) and 41.22 mm maximum (for a perfect wedge shape at the wrap-around). The hybrid placement error of order 50 μm is then to be added to these number.

The error in the pigtail connector position comes from the error in the hybrid placement, the connector pin-hole play, and the soldering error, which are of order of 100 μm, 100 μm, and 200 μm, respectively, and thus of order 500 μm in total. The pigtail cable, which is flexible, connects to the less flexible opto-harness. The flexible pigtail cable is therefore made sufficiently long so that its route can adjusted to achieve the correct mating between the two connectors.

The cut edge of the sensor is conductive and at the backplane bias high voltage; conducting debris between the cut edge and ground could cause high voltage shorts. An electrical stay clear distance of at least 1 mm has been defined. This assures a high voltage breakdown of 3 kV to ground at sea level in air[1]. The distance between the centres of the modules is specified to be 2.8 mm in height in the overlap region of adjacent modules on the barrel cylinder, which leaves a nominal stay clear distance of 1.65 mm between the cut edge and the opposing sensor surface. Of this, 400 μm is allocated to accommodate thickness tolerances and non-planarity of overlapping modules (see SCT-BM-FDR-3. Section 2.2). A maximum deviation of 200 μm of the module surface from the nominal can thus be accommodated.

5 MODULE THERMAL PERFORMANCE

A thermal FEA simulation has been carried out for the barrel module design (see Figure 5). Figure 6 and Figure 7 shows the maximum (T_{si} max) temperature of the silicon sensors in the module as a function of the bulk heat generation normalized at 0 ^{o}C, for hybrid power consumption of both 6.0 W and 8.1 W and three coolant temperatures. The simulation shows that the thermal runaway of the silicon detector occurs at 220 μW/mm^2 for the maximum 8.1 W chip power at -14 ^{o}C coolant temperature. The bulk heat generation after 10 years of operation at LHC is estimated to be 120 μW/mm^2 in the worst case. The 6W power at –17^{o}C has a factor 3 in the thermal runaway safety margin, and for 8.1W, -14^{o}C gives nearly the required factor of 2, and –20^{o}C more than a factor of 3.

Thus the barrel module design is expected to provide the necessary thermal environment for normal operation of the silicon detectors and the ASICs, and to be safe against thermal runaway.

[1] Spark gap voltages, based on results of the American Institute of Electrical Engineers, Air at 760 mmHg, 25 oC

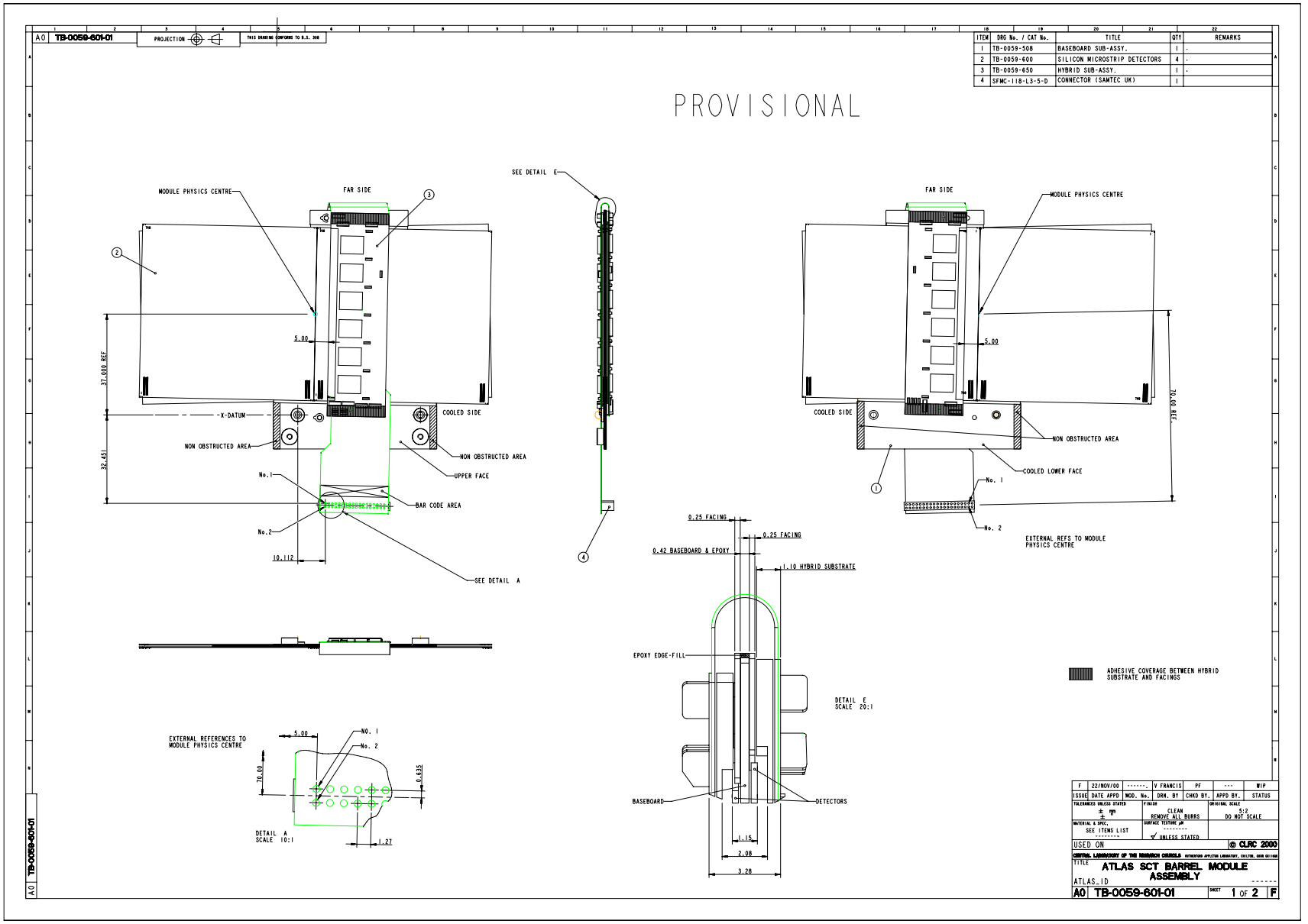

Figure 4 Barrel module envelope

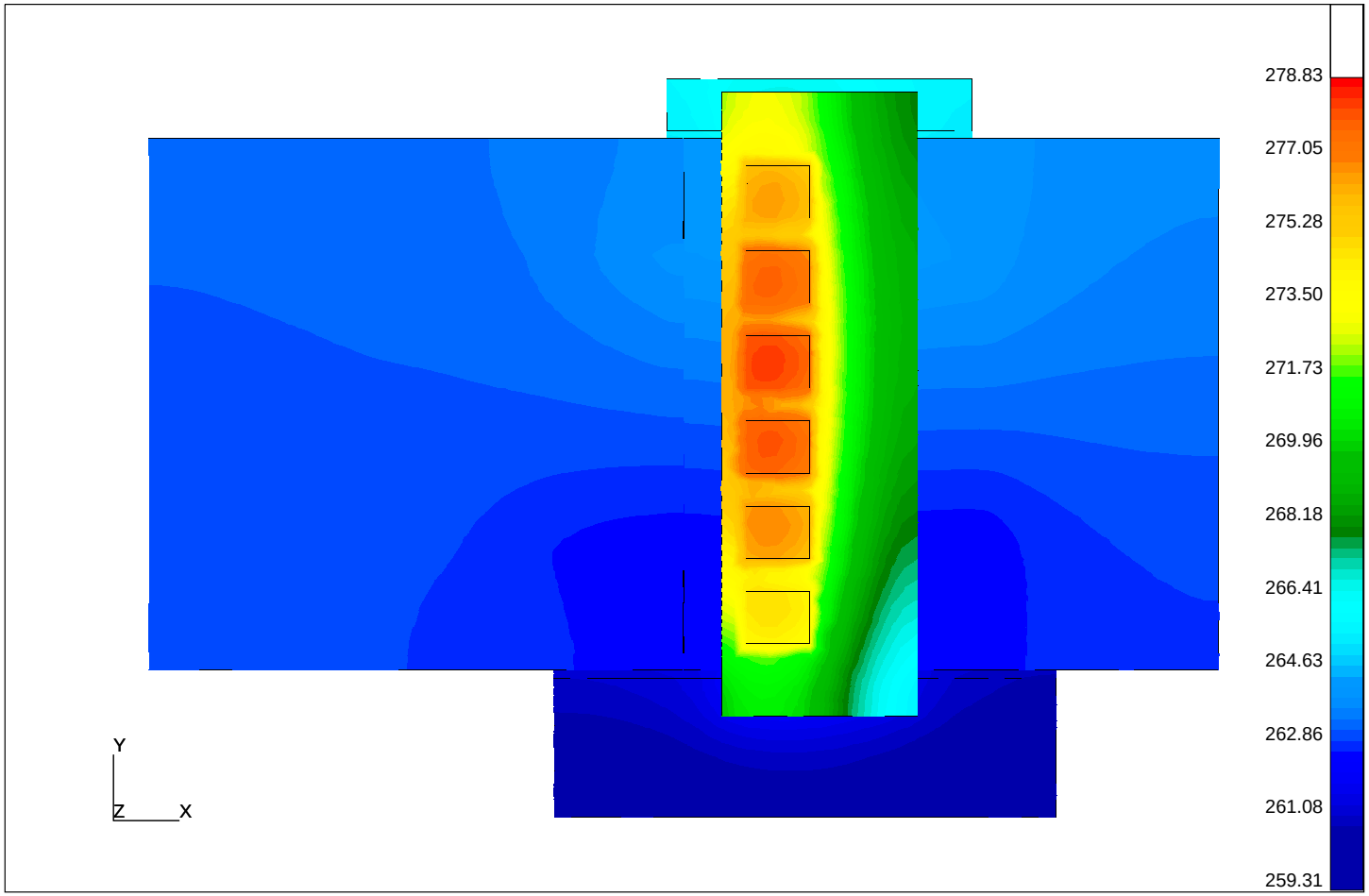

Figure 5 Thermo profile of the module with nominal heat generation in the silicon sensors and a hybrid power of 6.0 W

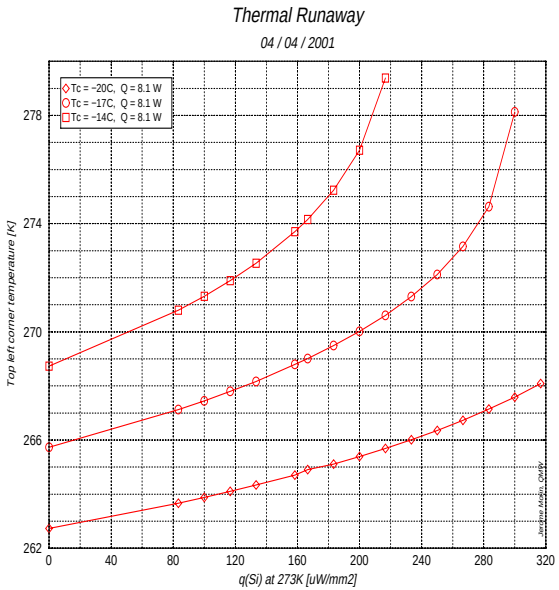

Figure 7: Temperature of the hottest point in the sensors as a function of heat flux, with various coolant temperatures, for the hybrid power at 8.1 W

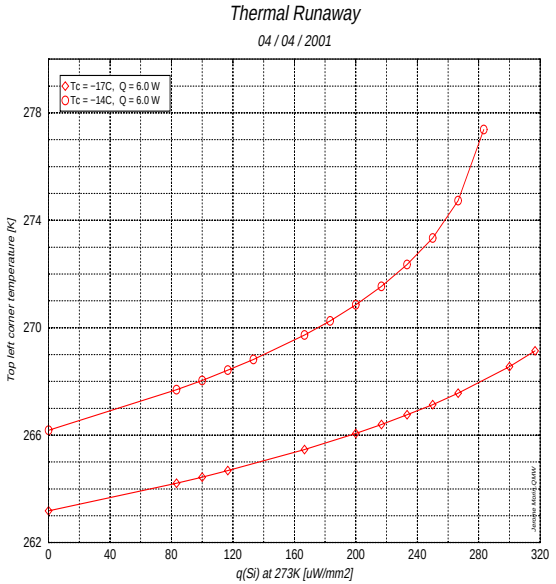

Figure 6 Temperature of the hottest point in the sensors as a function of heat flux, with various coolant temperatures, for the hybrid power at 6.0 W

6 RADIATION LENGTH OF THE MODULE

Table 2. summarises the estimated radiation length and weight of the module components. The weight of each item has been measured and the results match to within a few percent of the estimated value. The matching in weight ensures the validity of the estimation of the radiation length of the module in the table. The overall weight of the module is 25 gm and the radiation length averaged over the silicon sensor area is 1.17 $\%X_o$, which satisfies the specified <1.2 $\%X_o$.

Component	**Radiation length [% X_o]**	**Weight [gm]**
(a) Silicon sensors and adhesive	0.612	10.9
(b) Baseboard and BeO facings	0.194	6.7
(c) ASICs and adhesive	0.063	1.0
(d) Cu/Polyimide hybrid	0.221	4.7
(e) Passive components	0.076	1.6
Summed material	**1.17**	**24.9**

Table 2: Radiation length and weight of the module

SCT Barrel Module FDR Document

SCT Barrel Module Components Section 5.1: Silicon Microstrip Detectors

Abstract

This document describes the technical status and procurement of the silicon microstrip detectors for the SCT barrel modules.

Prepared by :	***Checked by :***	***Approved by :***
J. Carter		

Distribution List

Table of Contents

1 SCOPE OF THE DOCUMENT

This document describes the silicon microstrip detectors that form part of the ATLAS SCT barrel module. It covers their Technical Specification; results from the detector Pre-series; procurement status, QA procedures in place and status of the Series deliveries.

2 INTRODUCTION

Each barrel module contains four silicon microstrip detectors, with two on each side glued back-to-back on the barrel baseboard, as described in SCT-BM-FDR-4. A total of approximately 10,600 barrel detectors will be required for construction of the SCT, the exact number depending of the actual loss factors in series module construction and in the assembly of modules to barrels. Because the lead time is long for the delivery and acceptance of such a large number of detectors, the procurement phase for this component was begun in 1999.

The ATLAS detector FDR was held in May 1999, and contracts for the Pre-series and Series production of detectors were placed in autumn 1999. The Pre-series detectors were delivered in the spring of 2000 and thoroughly evaluated by the ATLAS Institutes. The detector PRR was held in August 2000. The barrel detector Series production was released with Hamamatsu Photonics, who will supply at least 94% of the barrel SCT silicon detectors. The remaining detectors will be supplied either by SINTEF or by Hamamatsu, depending on the quality of a second Pre-series being produced by SINTEF in summer 2001.

The documents presented at the silicon detector PRR are located on EDMS. They are:

ATLAS SCT/Detector PRR/00-1	Contractual documentation, including Technical Specification, Delivery Schedule, Provisional Acceptance, Quality Assurance
ATLAS SCT/Detector PRR/00-2	Detector Procurement Arrangements
ATLAS SCT/Detector PRR/00-3	Database for Detectors
ATLAS SCT/Detector PRR/00-4	Quality Assurance at the Institutes
ATLAS SCT/Detector PRR/00-5	Reports on the Pre-series Detectors
ATLAS SCT/Detector PRR/00-6	Detectors in Modules.

3 DETECTOR TECHNICAL SPECIFICATION

The full contractual Technical Specification of the detectors is located on EDMS, as are the detector engineering drawings. They are also appended to this document for completeness. (The Technical Specification covers also the detectors of the Forward SCT, which is not part of this FDR).

Following evaluation of both oxygenated and thin (260 μm thick) detectors for the innermost of the four barrels, where the radiation levels are highest, the decision has been made to use 285 μm thick detectors on a standard silicon substrate for all layers of the SCT. These are the *B2* detectors in the Technical specification. The detectors have a rectangular geometry, with 768 ac-coupled readout strips at a pitch of 80 μm.

After 10 years of LHC operation, the detectors in the innermost regions are expected to be operated at about 400V bias, with over 90% charge collection efficiency.

4 PRE-SERIES AND SERIES PRODUCTION RELEASE

The results of the pre- and post-irradiation evaluation of the Hamamatsu barrel Pre-series production are summarised in ATLAS SCT/Detector PRR/00-5. The Pre-series detectors were in general of excellent quality with on average more than 99.9% of good readout strips per detector and a pre-irradiation average leakage current of only 140nA at 350V bias at 20^{o}C. The post-irradiation characteristics, after exposure to $3x10^{14}$ pcm^{-2} 24 GeV/c protons, were as measured in the prototype R&D phase of the project, and fully satisfied the post-irradiation requirements of the Technical Specification.

There were five areas to be followed up with Hamamatsu from the Pre-series results, before Series production release:

(a) *The quality of the cut edge of the detector*. It is important that the detector edges are clean, with no loose or rough pieces of silicon or aluminium present. This is because the edge is at the full post-irradiation bias potential, and so any danger of shorting to the grounded bond wires or to exposed grounded areas of neighbouring modules on the barrel structure must be avoided. The detector edge quality of the Pre-series was variable. As a result, new visual inspection procedures have been agreed and instituted at Hamamatsu for the Series production, and these are being carefully checked during the QA of the Institutes. To-date, the edge quality of the delivered Series detectors has been satisfactory.

(b) *The detector passivation mask*. The prototype and Pre-series Hamamatsu detectors had openings in the passivation mask that were used by the Company for QA purposes. These again presented some risk of shorts developing to bond wires or to neighbouring modules. A new passivation mask, without these openings, has been made and is being used for the Series detectors to eliminate this particular risk.

(c) *Strip quality tests*. There were some discrepancies between the identification of bad strips between the QA at Hamamatsu and at the Institutes in the Pre-series detectors. This is now fully understood and resolved.

(d) *Orientation of silicon substrate.* Detectors have been processed on both <111> and <100> silicon substrates by Hamamatsu and fully tested both pre- and post-irradiation by the SCT. No significant differences in performance were found. The final choice of substrate was in the end dictated by the availability of supply; <111> silicon is being used for the Series production.

(e) *Series delivery schedule*. The schedule agreed with Hamamatsu for the basic supply is shown in Table 1. Additional detectors will be ordered as required for delivery in 2002 through contract purchase options.

All details of the Series production release were agreed with Hamamatsu in autumn 2000, and the Series detectors are now being delivered.

Hamamatsu Delivery Schedule for B2 Detectors				
Year/month	Number to be delivered to Japan	Number to be delivered to UK	Number to be delivered to Norway	**Total monthly delivery**
01/01		10		**10**
01/02	230	135		**365**
01/03	230	135		**365**
01/04	230	120	100	**450**
01/05	230	120	100	**450**
01/06	230	120	100	**450**
01/07	230	120	100	**450**
01/08	230	120	100	**450**
01/09	230	120	100	**450**
01/10	230	120	100	**450**
01/11	230	120	100	**450**
01/12	230	120	100	**450**
02/01	230	120	100	**450**
02/02	230	120	100	**450**
02/03	230	120	100	**450**
02/04	230	120		**350**
02/05	230	120		**350**
02/06	230	120		**350**
02/07	230	120		**350**
02/08	260	100		**360**
02/09	350			**350**
02/10	350			**350**

Table 1: Delivery Schedule for the basic supply of Hamamatsu barrel detectors

5 DETECTOR QA AT THE INSTITUTES

The detector acceptance QA carried out at the SCT Institutes is detailed in Appendix 1 of the Technical Specification. This is now in operation for the Series detector deliveries. The Institute responsibilities are shown in Table 1 of SCT-BM-FDR-2.

6 DATABASE

The use of the SCT database is well developed for detectors. The Contractors enter their tests and agreed data directly into the database and ship the detectors electronically at delivery. The Institutes receive the detectors in the database and enter their acceptance test data. Detectors are shipped to the module building cluster after their provisional acceptance.

7 SUMMARY

The silicon detector procurement for the barrel modules is so far proceeding to plan. The start of series barrel module production in autumn 2001 will allow build yields to be assessed within the contractual timeframe of the detector purchase options.

Appendix to SCT-BM-FDR-5.1:

Detector Technical Specification

Supply of Silicon Microstrip Detectors for the ATLAS SemiConductor Tracker (SCT)

Extracted from the 1999 Tender and Contract Documents, using the example of CERN being the Contract partner.

1 Technical Description

Unless stated explicitly otherwise, all dimensions quoted are those to be found in the processed devices, not the dimensions on the mask designs which may vary between suppliers. The technical description is separated into four sections. The first (article 3.1 below) gives the specifications that are in common for all the 6 detector shapes and the 2 different detector thicknesses that make up the total ATLAS requirement of 20,000 detectors. The second (article 3.2) defines the geometrical details of the barrel detectors, and the third (article 3.3) those of the forward detectors. The fourth (article 3.4) specifies the performance required of detectors after irradiation.

1.1 Specifications Applying to all Detector Shapes and Thicknesses

1.1.1 Mask Requirements

The Contractor shall be responsible for the final mask designs and shall produce engineering drawings or mask designs to be submitted to CERN for approval in writing before the start of Pre-series and Series production.

- *Number of metallised implanted strips*: 768+2 (the edge strip on each side may be coupled to the bias ring either directly or via a bias resistor).
- *Number read out*: 768.
- *Read-out implant strip width*: in the range 16µm to 20µm wide, high doped *p*-implants. (As stated above, these are the dimensions in the device).
- *Read-out strips*: Aluminium, capacitively coupled (see below) over the *p*-implant strips; width in the range 16µm to 22µm.
- *Polysilicon*[#] *bias resistors*: Either overlapping the implanted strips or running beside the implanted strips.
- *Reach-through protection*: Strip to low bias voltage difference to be limited by a reach-through protection structure (5µm - 10µm gap as processed from end of implanted strip to grounded implant).
- *Sensitive region to cut edge distance*: 1mm.
- *Outermost edge termination structure to cut edge*: >300µm.
- *High Voltage Contact*: Large metalised contactable *n*-layer on back.
- *Read-out*: 200×56µm bond pads, ≥ two rows, daisy-chainable. See articles 3.2 and 3.3 for their geometrical positioning for barrel and forward detectors.

[#] (Footnote added August 2000: Implant resistors for detectors manufactured by CiS)

- *p-bias contacts*: Available at each corner. See articles 3.2 and 3.3 for their geometrical definitions for barrel and forward detectors.

- *Probe pad contacts*: Provided to every read-out strip implant at contact point to bias resistor. Probe pad contact to inner guard also provided. See articles 3.2 and 3.3 for their geometrical definitions for barrel and forward detectors.

- *Passivation*: Detectors to be passivated on the strip side and un-passivated on the backplane.

- *Identification*: Every 10^{th} strip to be clearly numbered, starting at **1** for the first read out strip. Identification pads to be used for detector labelling and agreed alignment marks required for module optical metrology. See articles 3.2 and 3.3 for details for the barrel and forward detectors. The detector labelling is to be marked on the identification pads by the Contractor (see article 5.1.3).

1.1.2 Wafer Test Structures

***(a) Miniature detector*:**

A percentage of the main detectors in every processed batch are to be accompanied at delivery by a fully-diced miniature detector test structure from the same wafer. These fully-diced miniature detectors will be used by ATLAS Institutes for routine quality control of post-irradiation performance during the delivery period (see article 5.2). The percentage of main detectors to be accompanied by fully-diced miniature detectors is expected to be in the region of 5-10%, the exact figure being established by CERN during the Pre-series and Series production phases. The dicing of the miniature detectors is included as a purchase option in article 5.2 of the Tender Form.

The miniature detector shall have a similar design to the main detector apart from the differences consequential on a reduced sensitive area and, in the case of forward detectors, on a rectangular geometry. The miniature detector has outer dimensions of 10mm×10mm, with 98 readout strips, 8mm long and at 80μm pitch. The miniature detector mask design is to be approved in writing by CERN before the start of the Pre-series and Series production.

(b) Further Test Structures (subject to negotiation):

CERN requests access to further (undiced) miniature detectors and other monitoring test structures, if these can be made available without additional cost. They are to be delivered to the ATLAS Institutes with the main detector from the same wafer (see article 6). They will be used to help in the rapid identification of any processing changes, and to provide diagnostic capability should problems arise. Detailed designs of a large diode, large capacitor, MOS capacitors, test resistors (polysilicon, implants, aluminium) will be supplied to the Contractor.

If these further test structures are not delivered to the ATLAS Institutes, the Contractor is asked to retain the undiced miniature detectors and his own, or the ATLAS, processing test structures at his premises at the disposal of CERN for a period to be determined by CERN and which shall not be less than two years following completion of the contract.

1.1.3 Detector Mechanical/Optical Properties

- *Quality of cut edges*: Edge chipping to be avoided and all cut edges to be clean and smooth. No chips or cracks should extend inwards by more than 50μm.

- *Thickness:* 285±15μm for detectors for barrels 2,3 & 4 and forward detectors to be mounted on the middle and outer disk regions.
  260±10μm for detectors for barrel 1 and forward detectors to be mounted on the inner disk regions.

- *Uniformity of thickness within one detector*: 10μm.

- *Mask alignment tolerances*: ≤3μm misalignment with respect to any other mask. Specific values are the responsibility of the Contractor.

- *Damage and defects:* Device free from scratches and other defects that ATLAS Institutes judge could compromise the detector performance during the lifetime of the experiment. The criteria are to be established in collaboration with the Contractor during the Pre-series production.

- *Bond Pads*: Metal quality, adhesion and bond pad strength to be such as to allow successful uniform bonding to all readout strips of the detector using standard microstrip detector bonding techniques, and without causing a degradation in strip quality.

- *Alignment Fiducials*: All fiducial marks situated between the cut edges and the bias line (see articles 3.2 and 3.3) to be fully visible.

- *Flatness*: The detectors should be flat (when unstressed) to within 200μm.

1.1.4 Detector Electrical Properties

- *Strips*: *p*-implant <200KΩ/cm.

- *Read-out strips*: Aluminium <15Ω/cm.

- R_{BIAS} *(Polysilicon):* 1.25±0.75MΩ resistor bias.

- $R_{inter\text{-}strip}$: >2×R_{BIAS} at operating voltage after correcting for bias connection.

- *Interstrip Capacitance*: Capacitance between a strip and its nearest neighbour on both sides <1.1pF/cm at 150V bias measured at 100 kHz.

- $C_{coupling}$: ≥20pF/cm, measured at 1 kHz.

- *Processing reproducibility*: ***To be monitored by Contractor*** on test structures (V_{FB}, t_{ox}, polysilicon resistivity, aluminium sheet resistance, etching uniformity, dielectric strength). A sample of the miniature detectors supplied will be irradiated by ATLAS Institutes to check that gross characteristics are unaltered.

- *Initial Depletion voltage*: $V_{depletion}$< 150V.

- *Total initial leakage, including guard, normalised to 20°C*: <6μA at 150V and <20μA at 350V ***to be verified by Contractor*** (see article 5).

- *Leakage current stability*: Current to increase by no more than 2μA during 24 hours in dry air at 150V ***to be verified by ATLAS Institutes*** (see article 5).

- *Percentage of good strips (i.e. those conforming to the Technical Specification)*: A mean of ≥99% good readout strips per detector required in each delivery batch, with no detector having less than 98% of good strips.

  Definition of bad strips (i.e. those not conforming to the Technical Specification):

  Any of the following 4 types of fault will cause a strip to be counted as bad:

  1. *Coupling dielectric*: Shorts through dielectric with 100V applied between the metal and the substrate.
     Measured by Contractor, see article 5.

  2. *Defective metal strips*: Metal breaks or shorts to neighbours.
     Measured by Contractor, see article 5.

  3. *Defective implant strips*: Implant breaks or shorts to neighbours.
     Monitored by ATLAS Institutes on a sample of detectors, see article 5.

  4. *Resistor connection*: Implant strip connection via resistor to bias rail broken.
     Monitored by ATLAS Institutes on a sample of detectors, see article 5**.**

1.2 Geometrical Specifications for the Barrel Detectors

The barrel detectors all have the same geometrical specification apart from thickness. Detectors for the innermost barrel (called B1 detectors) are 260±10μm thick. All the remaining (called B2) barrel detectors are 285±15μm thick.

1.2.1 External Cut Dimensions for Barrel Detectors

- *Length:* 63960±25μm, distances of cut edges to fiducial marks to be within ±25μm of specified values (see appended drawing).

- *Width*: 63560±25μm, cut symmetric about the centre line of the detector to ±25μm.

- *Thickness*: 260±10μm for B1 detectors; 285±15μm for B2 detectors.

1.2.2 Mask Requirements for Barrel Detectors

- *Length*: 64mm *nominal* centre cutting line of scribe to centre cutting line of scribe. The exact value determined to give the cut mechanical dimension specified in article 3.2.1 above.

- *Width*: 63.6mm *nominal* centre cutting line of scribe to centre cutting line of scribe. The exact value determined to give the cut mechanical dimension specified in article 3.2.1 above.

- *Read-out implant strip dimensions*: 16μm - 20μm wide, 62mm long, 80μm pitch, high doped *p*-implants. (As stated above, these are the dimensions in the device).

- *Locations* of bias contacts, bond pads, probe points, alignment features, identification marks, *etc* are indicated in the appended drawing.

1.3 Geometrical Specifications for the Forward Detectors

There are 5 different types of forward wedge detector. They are referred to as W12, W21, W22, W31, W32. Their geometrical specifications are shown in the appended drawings. W21 + W22 are used together to make one type of module, and W31 + W32 form a pair for a second type of module. W12 is used by itself for a third module type. The W12 detectors are 260±10μm thick. All the remaining forward detectors are 285±15μm thick.

1.3.1 External Cut Dimensions for Forward Detectors

The dimensions of the forward detectors are such as to allow the processing of any of the following combinations together on a 6″ wafer: W21+W22; W31+W32, two W12 detectors.

- *Lengths and Widths:* The external cut dimensions of the 5 detector shapes are given in Table 1.

  The tolerance on all cut lengths and widths is ±25μm.

  The detectors must be cut symmetrically, to within ±25μm, about the centre lines of the sensitive region of the detector. Along their lengths, distances of detector cut edges to fiducial marks must be within ±25μm of the specified values.

Detector Type	Cut Length (mm)	Outer Width (mm)	Inner Width (mm)
W12	74.060	55.488	43.659
W21	65.085	66.130	55.734
W22	54.435	74.847	66.152
W31	65.540	64.635	56.475
W32	57.515	71.814	64.653

Table 1: *External Cut dimensions of the 5 forward detector shapes*

- *Thickness:* 260±10μm for W12, 285±15μm for W21, W22, W31, W32.

1.3.2 Mask Requirements for Forward Detectors

The mask requirements for the five wafers are summarised in the appended drawings.

1.4 Required Detector Performance During and After Irradiation

All delivered detectors must meet both the pre-irradiation specifications and the post-irradiation requirements up to a fluence equivalent to ~ 3×10^{14} cm^{-2} 24 GeV/c protons. The pre-irradiation properties will be measured by the Contractor and the ATLAS Institutes as described in article 5. The post-irradiation requirements cannot be tested on a device by device basis, but will be monitored by ATLAS Institutes during production. This is foreseen as the regular irradiation (approximately monthly) of miniature detectors to check bulk properties, and the irradiation of approximately 1% of the main detectors, sampled through the production, for full performance characterisation (see article 5.2).

No main detector is suitable that does not satisfy the requirements listed below during and after irradiation. During the irradiation the detectors are maintained at a temperature of about -8ºC and biased to 100V, with their implant strips biased to 0V and their aluminium readout strips grounded. Their total leakage current is monitored throughout the irradiation.

Performance during the irradiation:

- The detector leakage current should increase in a stable and monotonic fashion during the irradiation.

Post-irradiation Performance:

The figures below assume an annealing period of 7 days at 25ºC after completion of the irradiation:

- *Maximum operating voltage required for >90% of maximum achievable charge collection efficiency***:** 350V. (Checked after connection to readout electronics with an effective peaking time of 25ns).

- R_{BIAS} *(Polysilicon):* to remain within the pre-irradiation acceptance limits.

- $R_{inter\text{-}strip}$: $>2\times R_{BIAS}$ at 350V after correcting for bias connection.

- *Interstrip Capacitance***:** Capacitance between a strip and its 2 nearest neighbours on both sides <1.5pF/cm at 350V bias, measured at 100 kHz.

- *Total Leakage Current***:** <250μA at -18ºC up to 450V bias.

- *Leakage current stability*: Current to vary by no more than 3% during 24 hours at 350V and –10ºC (after correction for any temperature fluctuations).

- *Micro-discharge***:** There must be <5% increase in the measured noise of any channel due to this effect on raising the detector bias from 300V to 400V. (Checked after connection to readout electronics with an effective peaking time of 25ns).

- *Bad strips***:** After irradiation, the number of strips failing the pre-irradiation criteria (article 3.1.4) should remain within the pre-irradiation acceptances at 350V bias.

2 Qualified Prototypes and Consistency of Substrate Material and Processing

2.1 Qualified Prototypes

One of the Qualification Criteria of the CERN Market Survey MS-2612/EP/ATL is that several prototype detectors already supplied by a Bidder have been proven by ATLAS Institutes to be satisfactory for use in the experiment both before and after irradiation up to fluences of ~3×10^{14} cm^{-2} 24 GeV/c protons.

These are the *Qualified Prototypes* of the Bidder and their serial numbers are listed in the Tender documents.

2.2 Consistency of Substrate Material and Processing during Production

The objective of the Contractor shall be to maintain the same processing, passivation and substrate material properties as those used to produce the Qualified Prototypes throughout the Pre-series and Series production. The conditions applying if this objective is not met are set out in article 10 of the Tender Form.

3 Quality Control, Inspection, Acceptance Tests and Data Sheets

3.1 Quality Control, Inspections, Acceptance Tests to be performed by the Contractor

3.1.1 General

The Contractor is required to perform sufficient checks to ensure consistency of processing and to maintain all electrical parameters within the ATLAS specifications defined in article 3. The properties of the polished silicon substrate material used must be tightly controlled to ensure uniformity over the production. Adequate evidence of this must be provided in the Technical Questionnaire and, prior to manufacturing, in the Production and Quality Plan. Different detector batches must be easily identified with particular silicon substrate batches.

The Contractor shall set up a Production and Quality Plan, to be supplied to CERN for approval within four weeks of the notification of contract, specifically including:

- definition, size and identification of production and delivery batches ensuring traceability;
- raw material control;
- acceptance testing, measuring methods;
- labelling;
- format of data supplied with delivered detectors.

Any proposed changes with respect to the approved Production and Quality Plan incurred during production must be subject to prior approval by CERN in writing.

3.1.2 Acceptance Test Measurements

The Contractor is required to perform the following test measurements on every detector, and to supply the measurement results to ATLAS Institutes with the delivered detector:

1. Detector IV up to 350V bias, measuring the current in 10V steps as the voltage is raised from 0V up to 350V, with a maximum of a 10 second delay time between steps.

2. Strip dielectric shorts for all strips with 100V across the strip dielectric. Immediately after this test the strip metal is to be returned to the ground potential in order to remove residual charge.

3. Strip metal breaks for all strips.

4. Strip metal shorts to neighbours for all strips.

If possible the Contractor should use Row C of the strip pads and bias contacts for probing tests for Barrel detectors and Row B for Forward detectors (see appended drawings), as these pads are not used during any stage in the module construction. However, if this is too inconvenient due to standard procedures, the standard probing pattern is acceptable.

3.1.3 Special Labelling

1. A unique binary-coded decimal ATLAS identification number (1 to 99999) for each detector is to be marked on the detector identification pads by the Contractor. This will require in most cases a simple modification to the strip test prober software. The details of this labelling process and the identification numbers to be used are to be agreed by CERN and the Contractor before the manufacture of the Pre-series.

2. Any test structures being delivered in addition to the fully-diced miniature detector (article 3.1.2), should be supplied undiced as a test structure quadrant with the Contractor's serial number of the associated detector clearly marked on the surface on an unused part of the quadrant. The packaging of the diced miniature detector must be clearly marked with the associated detector serial number.

3.1.4 Data Supplied by the Contractor

The following data are required from the Contractor for each detector:

1. The detector serial number, which should identify the processed batch, and the ATLAS identification number.

2. Detector type (B1, B2, W12, W21, W22, W31 or W32).

3. Detector thickness.

4. Substrate description (ie origin, orientation, approximate resistivity and any special comments, which should include information, coded if necessary, to ensure traceability of the substrate and polishing).

5. IV data up to 350V bias, including the value of the current at 150V and 350V.

6. Temperature of IV measurement.

7. List of strip numbers of oxide pinholes with 100V across the oxide.

8. List of strip numbers with strip metal discontinuities.

9. List of strip numbers with strip metal shorts to neighbours.

10. Depletion voltage (usually measured by the Contractor using a diode).

11. Typical polysilicon bias resistance value(s) for the detector, or range for the processed batch.

The data are to be provided both on paper and on a PC-formatted disk to a pre-agreed format for uploading into the ATLAS database by the ATLAS Institute. The database entries to be provided by the Contractor are summarised in Appendix 2.

3.2 Tests carried out by the ATLAS Institutes

The ATLAS Institutes will carry out tests on the detectors. The test procedures to be used throughout the Series production will be finalised and agreed with the Contractor during the Pre-series production phase.

When a batch is delivered to an ATLAS Institute the detector packages will be inspected for damage and stored in an inert atmosphere.

A visual inspection and an electrical IV measurement will be carried out on all detectors by the ATLAS Institutes.

The ATLAS Institutes will carry out more detailed measurements on a representative sample of delivered detectors using the procedures outlined in Appendix 1, both to verify the Contractor's measurements and to measure additional properties, as indicated in article 3.

The measurements of current made by the Contractor and the ATLAS Institutes on a given detector and the bad strips identified must agree to within defined tolerances. The tolerances for the initial Pre-series measurements will require that the measured currents agree to within 2μA at 150V bias and 4μA at 350V bias, and that a maximum of 2 bad strips are differently identified. The values for these tolerances to be used throughout the Series production will be agreed with the Contractor during the Pre-series measurements.

The post-irradiation detector performance will be monitored by the ATLAS Institutes by irradiating samples of both detectors and miniature detectors and carrying out the test measurements detailed in Appendix 1, article 2.

CERN will notify the Contractor in writing of any delivered detectors failing the specifications or performance requirements in ATLAS Institute measurements, or where results differ by more than the agreed tolerances (refer to article 10).

4 Packing and Transportation of Delivery Batches

Packing and the method of delivery must ensure adequate protection against damage (including theft, loss etc) during handling and transportation.

The detectors are to be individually packed, with their surfaces protected, in envelopes and/or boxes, which are sealed and packed within boxes for transportation. Each individual detector package must be clearly labelled with the Contractor's serial number and the ATLAS identification number (article 5.1.3) of the detector. Labelling in bar code format in addition to alphanumerical form is preferred.

The miniature detectors that are fully-diced are also to be individually packed, and each package clearly labelled with the serial number and ATLAS identification number of the associated main detector. The undiced miniature detectors and additional test structures, if supplied, are to be packaged on a per-wafer basis and clearly labelled with the serial number and ATLAS identification number of the associated main detector.

The transportation boxes are to be externally labelled with the Packing List showing the delivery batch number and quantities it contains, and clearly identified as fragile.

The batches for both the Pre-series and Series production are to be delivered directly to ATLAS Institutes listed in Annex B. The particular destination for each detector shape will be notified to the Contractor before delivery of the Pre-series.

The Contractor shall carry out whichever customs and other formalities may be necessary for the importation of the detectors into the country of the premises of the ATLAS Institute concerned, including any advance requests for the authorisation of temporary importation. CERN shall provide to the Contractor any pro forma invoice and all documentation reasonably required by the Contractor to enable him to carry out the above obligations.

In case the detectors are delivered to another country than the one in which they have been manufactured transport shall be by air, otherwise transport shall be by a recognised courier service.

CERN reserves the right to order detectors on an ex-works basis and to organize the transport itself. This does not a-priori exclude use of the Contractor's sub-contractors.

5 Pre-Series

CERN shall require the Contractor to produce a Pre-series to demonstrate his ability to comply fully with this Technical Specification. This Pre-series shall be produced with the same processing and substrate material properties as for both the Qualified Prototypes and the Series. The Pre-series will consist of approximately 5% of the total contract. Manufacture of this Pre-series is intended for testing:

- the quality of the produced detectors: these will be tested by the Contractor and the ATLAS Institutes (see article 5).
- the inspection and acceptance tests carried out by the Contractor and the supplied documentation and data;
- the production capability of the Contractor;
- the ability of the Contractor to comply with the delivery schedule;
- the effectiveness of the labelling, packing and transportation methods.

CERN's written notification of Provisional Acceptance of the Pre-series is required before the start of the Series production.

6 Delivery Schedule

The required delivery schedule and the conditions attached to late delivery are detailed in articles 7 and 8 of the Tender Form.

7 Provisional Acceptance

The conditions for Provisional Acceptance of detectors are set out in article 11 of the Tender Form.

8 Non-Compliant Detectors

The conditions in case a detector does not comply with the specifications and requirements as set out in these Tender documents are detailed in article 12 of the Tender Form.

11 Documentation

To be supplied with the Invitation to Tender:
Technical Questionnaire IT-2612/EP/ATL dated August 1999, duly filled in.

To be supplied for approval four weeks after notification of contract:
Detector engineering drawings or mask designs for at least one detector shape;
Production and Quality Plan (article 5.1.1) and schedule for delivery of the Pre-series.

To be supplied with each delivered batch during Series production:
Test data defined in article 5.

12 List of Drawings Appended

Drawing of the Barrel Detector http://hepwww.ph.qmw.ac.uk/~beck/picb8a4.ps
Drawing of the Forward W12 Detector http://hepwww.ph.qmw.ac.uk/~beck/w12a4.ps
Drawing of the Forward W21 Detector http://hepwww.ph.qmw.ac.uk/~beck/w21a4.ps
Drawing of the Forward W22 Detector http://hepwww.ph.qmw.ac.uk/~beck/w22a4.ps
Drawing of the Forward W31 Detector http://hepwww.ph.qmw.ac.uk/~beck/w31a4.ps
Drawing of the Forward W32 Detector http://hepwww.ph.qmw.ac.uk/~beck/w32a4.ps
Drawing of Alignment and Identification Marks
http://hepwww.ph.qmw.ac.uk/~beck/alida4.ps

Appendix 1: Acceptance Tests to be carried out by the ATLAS Institutes

1 Tests on Detectors as delivered

The role of the ATLAS Institutes during production testing is mainly that of a visual inspection and of an electrical IV measurement on every detector as a check on the basic quality. However, on a subset of detectors (expected to be 10-20% initially, but reducing to ~5% with experience during production), a thorough evaluation of detector (and test-structure where possible) characteristics will be performed as a check on processing consistency and as a verification of the Contractor's tests.

1.1 Tests on every detector

1.1.1 Visual inspection

Aim: To ensure the detector is free from physical defects and scratches.

Procedure: Place the detector on a probe-station chuck and scan it visually using a microscope.

Acceptance: The detector is free from significant scratches and blemishes. The cut edge is straight, clean and free from chipping. No chips or cracks should extend inwards by more than 50μm.

1.1.2 IV Curve

Aim: To perform a basic check of detector quality, to cross-check with Contractor data and to ensure there has been no transit damage.

Procedure: This test requires a voltage source/picoammeter (SMU). The detector backplane is placed on the chuck of a probe-station and the IV characteristic between the bias rail and the backplane measured using the SMU. The detector bias may be applied via a front edge contact instead of via the detector backplane if appropriate. The current is measured in 10V steps from 0V up to 350V[#], with a 10 second delay between steps. The temperature of the probe-station environment should be recorded.

Acceptance: The detector displays a characteristic at 20°C which is below 6μA at 150V and below 20μA at 350V, and which agrees with the Contractor's data to within the agreed tolerances.

1.2 Tests on a detector subset

These tests are a verification of the measurements performed by the Contractor. If any of these tests fail, this is an indication of either a variation in processing and/or a possible failure in the testing procedures of the Contractor. Further samples from the batch should then be tested and contact made immediately with the Contractor.

[#] Updated February 2000 to the value of 500V

1.2.1 Detector depletion voltage

Aim: To determine the depletion voltage and verify the Contractor's data.

Procedure: This measurement requires a CV meter equipped (if necessary) with an external bias adaptor and a voltage source. Place the detector backplane on the chuck of a probe-station and contact the bias rail with a probe needle. Connect the probe needle to the AC output of the CV meter bias adaptor, and the backplane to the voltage output of the CV meter bias adaptor. Alternatively the capacitance can be measured between the bias rail and the front edge contact if appropriate. Record the capacitance in 10V steps up to 350V, with a 10 second delay between steps. Use 1 kHz with CR in SERIES. Plot the data as $1/C^2$ ($1/nF^2$) vs bias (volts), and extract the depletion voltage.

Acceptance: Depletion < 150V

1.2.2 Strip integrity[#]

Aim: Check each strip for punch-throughs to the oxide, for shorts between strip metals, and for discontinuities in the strip metals as a verification of Contractor supplied data and to check that the strip defects are within specifications.

Procedure: This test requires a volt source / picoammeter (SMU) to check for oxide punch-throughs, a CV meter to measure capacitance, and a switching matrix. The detector is placed on the chuck of an automatic probe-station, and strip metal pads corresponding to Row C for Barrel detectors or Row B for Forward detectors are probed under computer control with the light on. Punch-throughs across the strip oxide are determined by a measurement of current between the strip metal and backplane with -100V on the needle and the detector backplane at ground potential. A series resistor of ~2-5Mohm should be used to limit the current in case of pinholes. The following technique for each strip measurement has been demonstrated to work well without any damage to the detector, and is therefore recommended, though alternative techniques are acceptable:

1.Switch the probe-needle to the high output of the SMU sourcing 0V, and the backplane to grounded low output of the SMU.

2.Step to strip n and raise the chuck

3.Increase the SMU source to -10V, wait 1 second and measure the current to determine electrical continuity across the oxide. If there is electrical continuity (ie a pinhole exists at low volts) skip steps 4 and 5 and go to step 6.

4.If there is no electrical continuity, increase the SMU source to -100V (no ramp), wait 1 second and recheck the electrical continuity.

5.Decrease the SMU source to 0V (no ramp).

6.Switch the probe-needle to ground (ie short the needle to the detector backplane) and wait for 500ms

[#] Updated February 2000, see Annex D

7.Switch the probe-needle to the AC output of the CV meter, and the backplane to the voltage source of the CV meter (with the CV meter sourcing 0V).

8.Wait 1 second and measure the capacitance (at 1kHz, with CR modelled in SERIES)

9.Lower the chuck

10.Repeat the measurement cycle from point 1 above for strip n+1.

The test (as demonstrated on a SUMMIT 10K probe station) takes about 1 hour 10 minutes.

Detector Acceptance: < 2 % bad strips, where a bad strip has electrical continuity between the strip metal and backplane, strip metal short to neighbour or evidence for metal discontinuity.

and agreement with the Contractor on the list of identified bad strip numbers within the agreed tolerance.

Batch Acceptance: The batch is accepted if the mean number of good strips is ≥99% and no detector falls below 98% good strips.

1.2.3 Leakage Current Stability

Aim: To check that any variation in leakage current over a 24 hour period is within specifications.

Procedure: This test requires a voltage source / picoammeter (SMU), a meter for temperature monitoring, an environment chamber, and, if available, a switching matrix. Detector is assembled into a support frame and the backplane and bias rail are bonded to soldable contacts. The backplane and bias rail of the detector are connected to the high and grounded-low outputs of the SMU respectively. The assembly is installed in an environment chamber containing dry air (nitrogen) maintained at 20°C. The bias is ramped to 150V, and after 60 seconds settling time the current is monitored every 15 minutes over a 24 hour period. Several detectors may be measured in parallel by use of a switching matrix.

Acceptance: Maximum increase in leakage current during 24hours is less than 2μA.

1.2.4 Full Strip Test [#]

Aim: To measure the polysilicon bias resistance and coupling capacitance for every strip, and to check for pinholes, strip metal shorts and opens, implant breaks, and electrical contact between the polysilicon resistor and strip implant.

Procedure: This test requires all 768 strips to be probed while the detector is partially depleted via contacts to the bias rail and backplane. The test requires a voltage source to deplete the detector, a voltmeter/picoammeter (SMU) to check for pinholes, a CV meter for a CR calculation, and a switching matrix. Either mount the detector into a frame and bond the bias rail and backplane to

[#] Updated February 2000, see Annex D

soldable contacts or, if a probe needle manipulator can be fixed to the moving chuck, place the detector directly on to the chuck and contact the detector bias rail with the chuck-mounted probe-needle. If the option of mounting the detector into a frame is used, attach the frame to the probe-station chuck using a jig which permits adjustment of the planarity of the detector so that it is flat with respect to the platen of the probe-station. Switch off the light and apply +20V to the detector backplane with the bias rail at ground potential in order partially to deplete the detector. Under computer control, probe all 768 strip pads along row C for Barrel detectors or row B for Forward detectors according to the following instructions:

1.Switch the high output of the SMU (sourcing 0V) to the probe-needle via a 2-5Mohm series resistor, and switch the low output of the SMU to the detector bias rail.

2.Step to strip n and raise the chuck

3.Increase the SMU source to -10V, wait 1 second and measure the current to determine electrical continuity across the oxide. If there is electrical continuity (ie a pinhole exists at low volts) skip steps 4 and 5 and go to step 6.

4.If there is no electrical continuity, increase the SMU source to -100V (no ramp), wait 1 second and recheck the electrical continuity

5.Decrease the SMU source to 0V (no ramp)

6.Switch the probe-needle to ground (ie short the needle to the detector backplane) and wait for 500ms

7.Switch the probe-needle to the AC source output of the CV meter, and the bias rail to the voltage source output of the CV meter, with the CV meter sourcing 0V.

8.Wait 1 second and measure C and R (at 100Hz, with CR modelled in SERIES)

9.Lower the chuck

10.Repeat the measurement cycle from point 1 above for strip n+1.

The test (as demonstrated on a SUMMIT 10K probe-station) takes about 1 hour 10 minutes. The measured values of R and C yield the polysilicon resistor value and coupling capacitance respectively. Deviations imply a strip defect as listed above. Note the test may be performed at 1kHz if measurements at 100Hz are not possible or are unstable; at 1kHz the coupling capacitance is underestimated by 10-20%.

Acceptance: The number of strips with a significant deviation from the mean of the capacitance and resistance distributions must be <2%.

1.3 Diagnostic Tests

This article lists the recommended procedures for a more detailed evaluation of detector electrical parameters should acceptance tests indicate that some variation in processing has occurred. After any diagnostic tests on the detector, the IV measurement listed in article 1.1.2 should be repeated.

1.3.1 Interstrip Capacitance

Aim: To ensure the interstrip capacitance is within specifications.

Procedure: This test requires a CV meter and a voltage source. Place the detector on the chuck of a probe-station, and contact the bias rail by probe-needle. The backplane and the bias rail should be connected to the high and grounded-low sides (respectively) of the voltage source. Contact three adjacent metal strips (pad row C for Barrel detectors or row B for Forward detectors with probe needles. Contact the central strip to the AC output of the CV meter, and the neighbours to the voltage output (with the CV meter soucing 0V). Measure the capacitance between the central strip and its neighbours on both sides as a function of detector bias up to 150V. Use 100 kHz test frequency with CR in parallel.

Acceptance: Interstrip capacitance < 1.1 pF/cm at 150V bias.

1.3.2 Polysilicon Bias Resistance and Interstrip Resistance

Aim: Determine the bias resistor value is within specifications and that the interstrip isolation is sufficient when under bias.

Procedure: This test requires a voltage source and a volt source/picoammeter (SMU). This measurement yields both the polysilicon bias resistance and the interstrip resistance. Place the detector backplane on the chuck of a probe-station and contact the bias rail and a strip implant by probe-needles. The backplane and bias rail should be connected to the high and grounded-low outputs (respectively) of the voltage source. The strip implant and bias rail should be connected to the high and low outputs (respectively) of the SMU. Perform an IV (using the SMU) up to 1V to determine the resistance between the strip implant and bias rail as a function of bias voltage (increase detector bias from 0 V to 5 V in steps of 0.2 V).

Acceptance: Interstrip resistance is sufficient if the measured resistance vs detector bias plateaus. The plateau level resistance is equivalent to the polysilicon bias resistance, and must be within 1.25 ± 0.75 MΩ.

1.3.3 Metal Series Resistance

Aim: To determine that the strip metal resistance is within specifications (deposited metal is sufficiently thick) and to monitor processing consistency.

Procedure: This test requires an ohmmeter or a voltage source / picoammeter (SMU). Apply an ohmmeter (or perform an IV using the SMU) between the two ends of the appropriate metal line test-structure (if available) or to either end of one of the detector metal strips (if no test-structure available).

Acceptance: Series resistance < 15Ω/cm

1.3.4 Coupling Capacitance

Aim: To determine the coupling capacitance between the strip metal and strip implant, to check that the value is within specification and to monitor processing consistency.

Procedure: This test requires a CV meter. Place the detector backplane on the chuck of a probe-station and contact the metal and implant of a strip with probe needles. Connect the strip metal and implant to the AC and voltage outputs

(respectively) of the CV meter, with the CV meter sourcing 0V. Measure the capacitance between the metal and implant at 1 kHz with CR in PARALLEL.

Acceptance: Coupling capacitance ≥ 20 pF/cm

1.3.5 Implant sheet resistance

Aim: Measurement of sheet resistance of p implant, to check that the value is within specifications and to monitor processing consistency.

Procedure: This test requires an ohmmeter or a voltage source / picoammeter (SMU), and requires the use of the appropriate test-structure if available. Contact the ohmmeter (or perform an IV using the SMU) between the two contacts of the sheet resistor test-structure.

Acceptance: Sheet resistance < 200 KΩ/cm

1.3.6 Flat band voltage

Aim: To determine flat band voltage as a monitor of processing consistency.

Procedure: This test requires a voltage source, and a CV meter equipped (if necessary) with an external bias adaptor. The measurement requires a MOS test-structure if available. Place the MOS on a probe-station chuck and contact the MOS with a probe needle. Connect the MOS metal and the backplane to the AC and voltage outputs (respectively) of the CV meter. Measure capacitance across the MOS (at 1kHz with CR in SERIES) as a function of bias up to 50V.

Acceptance: There is no defined acceptance criterion. Flat band voltage is used as a monitor of processing consistency.

2 Post-Irradiation Tests on detectors

A small number (probably around 1%) of full-sized detectors will be selected for irradiation during production, and a thorough evaluation of these detectors will be performed for detailed comparisons with the requirements of the Tender documents and the data from the Qualified Prototypes. It is anticipated that larger numbers of miniature detectors (identical to the full-size detector (of barrel geometry) but only $1cm^2$ in size with 98 strips of 8mm length) will be used for irradiation tests, as their small size means that they can be irradiated more quickly and easily. It is anticipated that the measurement of the post-irradiation IV characteristics of miniature detectors will provide a minimum check of processing consistency.

2.1 Tests before detector irradiation

On delivery the full set of detector measurements described in article 1 of Appendix 1 should be performed to ensure the detector is fully characterised. The detectors are then glued with araldite 2011 to ceramic support cards and bonded to pitch adaptors for compatibility with readout by both binary and analogue readout electronics. During irradiation the strip metals are shorted together (via bonds on the pitch adaptor to a common rail) to simulate the condition of being bonded to readout electronics. The detector bias rail and backplane must be connected to ~3cm long leads (via bonds to the pitch adaptor and/or flexible PCB) terminating in 2-pin SIL connectors for biasing. The IV characteristics should be remeasured after gluing to ensure no deterioration has occurred during assembly.

2.2 Post-Irradiation Tests

Unless otherwise specified, all post-irradiation detector tests are performed cold (-10°C) in a freezer containing dry air, and with the detector ceramics screwed to an aluminium support frame protected by an aluminium cover lid. To ensure good thermal contact, the aluminium support frame should itself be in direct contact with a large thermal mass inside the freezer. Annealing times (when the detector is brought to room temperature for measurements, bonding/soldering work etc) should be recorded in units of days at 25°C equivalent temperature.

2.2.1 Annealing

After irradiation the detectors should undergo a controlled beneficial anneal for 7 days at 25°C, taking them to the minimum region of the depletion voltage.

2.2.2 IV Curve

Aim: To measure the IV characteristic after irradiation.

Procedure: This test requires a voltage source/picoammeter (SMU) to measure the IV characteristic between the bias rail and the backplane. The current is measured at -18°C at every 10V step up to 500V, with a 10 second delay between steps. The temperature of the detector should be recorded (either via a PT100 on the detector ceramic, or a PT100 in contact with the large thermal mass inside the freezer). On a sub-sample of detectors, the IV should be remeasured at -10°C to verify that the current scales in the expected way with temperature.

Acceptance: The detector displays a characteristic at -18°C which is below 250 μA at bias voltages up to 450V.

2.2.3 Strip Integrity

Aim: To check for additional oxide punch-throughs caused by the irradiation.

Procedure: This test requires a volt source/picoammeter (SMU) to check for oxide punch-throughs, and a CV meter to measure capacitance anomalies due to strip metal shorts/opens and pitch adaptor scratches/shorts. The detector is warmed to room temperature and the lid of the aluminium frame is removed. Any bonds still connecting strip metals to the common ground rail of the pitch adaptor must be removed. The frame is attached to a jig on the chuck of an automatic probe-station, and the planarity adjusted such that the pitch adaptor is flat relative to the probe-station platen. All metal pads of the pitch adaptor are then probed (in 4 groups of 128) under computer control with the light on. +10V is supplied continuously by the SMU to the backplane via the voltage output of the CV meter (or the external bias adaptor of the CV meter if applicable), with the needle connected to the AC output of the CV meter. A series resistor may be necessary to limit current if the CV meter external bias adaptor (which usually contains a large series resistance) is not used. The following technique for each strip measurement has been demonstrated to work well without any damage to the detector, and is therefore recommended, though alternative techniques are acceptable:

1. Before the first pitch adaptor pad is probed, source +10V from the SMU and wait several seconds for the SMU current to drop to <1nA (due to the capacitor charging in the CV meter external bias adaptor)
2. Raise the chuck to contact the pad with the probe-needle.
3. Measure the current drawn from the SMU. Currents 1nA indicate an oxide punch-through
4. Measure the capacitance (1kHz, CR in SERIES, 100mV amplitude).

5. In the case of an oxide punch-through, drop the chuck and wait several seconds for the SMU current to resettle to <1nA. If there is not oxide punch-through, no delay is necessary.
6. Move to the next pad, and repeat from Step 2 above.

The test (as demonstrated on a SUMMIT 10K probe-station) takes about 25 minutes.

Acceptance: The number of strip defects (due to oxide punch-throughs and strip metal defects) is < 2%.

2.2.4 Leakage Current Stability

Aim: To check that any variation in leakage current over a 24 hour period is within specifications.

Procedure: This test requires a voltage source / picoammeter (SMU), a meter for temperature monitoring, an environment chamber, and, if available, a switching matrix. The backplane and bias rail of the detector are connected to the high and grounded-low outputs of the SMU respectively. The assembly is installed in freezer containing dry air (nitrogen) maintained at -10^{o}C. The bias is ramped to 350V, and after 60 seconds settling time the current is monitored every 15 minutes over a 24 hour period. Several detectors may be measured in parallel by use of a switching matrix.

Acceptance: Maximum variation in leakage current during 24hours is less than 3%, after correcting for any temperature fluctuations.

2.2.5 Interstrip Capacitance

Aim: To determine that the interstrip capacitance is within specifications.

Procedure: This test requires a CV meter and a voltage source, and requires the detector aluminium support frame to be attached to a jig to allow for bonding from the strip pads on the pitch adaptor to solderable contacts (eg a piece of PCB with appropriate gold tracking). Remove the bonds (if not already removed) connecting the detector strips to the common ground rail on the pitch adaptor. From one of the rows of 128 pads on the pitch adaptor that corresponds to 6cm strips, bond one strip pad out to a solderable contact on the PCB, and bond the two neighbouring strip pad on both sides to the common ground rail of the pitch adaptor. Bond out from the common ground rail to a second solderable contact on the PCB. The central strip should then be connected (via a cable soldered to the PCB) to the AC output of the CV meter, and the two neighbouring strips to the voltage output of the CV meter (sourcing 0V). The backplane and bias rail of the detector should be connected to the high and grounded-low sides (respectively) of the voltage supply. Measure the capacitance between the central strip and its neighbour on both sides as a function of detector bias up to 500V, using 20V steps. Use 100kHz test frequency with CR modelled in parallel. Note: parasitic capacitance arising from the PCB and its cabling to the CV meter needs to be subtracted from the measured capacitance values. The best way to estimate the parasitic capacitance is to remove the bond between the pitch adaptor and PCB that connects the central strip, and remeasure capacitance.

Acceptance: Interstrip capacitance < 1.5 pF/cm at 350V bias.

2.2.6 Polysilicon Bias Resistance and Interstrip Resistance

Aim: Determine the bias resistor value is within specifications and that the interstrip isolation is sufficient when under bias.

Procedure: This test requires a voltage source and a volt source / picoammeter (SMU). This measurement yields both the polysilicon bias resistance and the interstrip resistance, and must be performed cold (-10ºC). The backplane and bias rail should be connected to the high and grounded-low outputs (respectively) of the voltage source. The DC contact to a strip implant and bias rail should be connected to the high and low outputs (respectively) of the SMU (it is necessary to bond from the strip DC contact to a track on the pitch adaptor. Some bonds from the strip metals to the pitch adaptor will need to be removed to provide space for this). Perform an IV (using the SMU) from -5V to +5V to determine the resistance between the strip implant and bias rail as a function of bias voltage (increase detector bias from 0 V to ~300V or until the measured resistance plateaus).

Acceptance: Interstrip resistance is sufficient if the measured resistance vs detector bias plateaus. The plateau level resistance is equivalent to the polysilicon bias resistance, and should be within 1.25 ± 0.75 MΩ.

2.2.7 Charge Collection Efficiency

Aim: To determine the onset of the plateau in charge collection efficiency vs detector bias up to 500V.

Procedure: Bond one group of 6cm 128 channels to an analogue readout chip with an effective peaking time of 25ns and measure the signal collected vs bias triggered using a Ru^{106} beta-source.

Acceptance: The onset of the plateau matches the value observed for the Qualified Prototypes and the operating voltage required for >90% of maximum achievable charge collection efficiency is < 350V.

2.2.8 Strip Quality vs Bias

Aim: To determine the number of strips with excess noise due to microdischarge.

Procedure: Bond all channels of the pitch adaptor to either binary or analogue readout electronics with an effective peaking time of 25ns, and measure the noise per channel vs detector bias at 200V, 300V, 400V and 500V bias.

Acceptance: There is < 5% increase in the measured noise of any channel due to microdischarge on raising the detector bias from 300V to 400V.

Appendix 2: Database entries to be provided by Contractor[#]

The Contractor shall provide the data required below on a PC-formatted disk to a pre-agreed format for uploading into the database by the ATLAS institute. The following table summarises the database entries to be provided by the Contractor. The "Entry Example" column lists typical values only and does not correspond to a particular detector.

Parameter	Type	Units	Entry Example
Contractor's Name	Text	N/A	
Detector Type	Text	N/A	W21

[#] Updated February 2000, see ATLAS SCT/Detector PRR/00-3

Serial Number	Text	N/A	Contractor's S.N.
Identification Number	INTEGER	N/A	ATLAS ID number
Substrate Origin (or code)	Text	N/A	
Substrate Orientation	Text	N/A	111 or 100
Substrate Resistivity	Text (range)	KΩ-cm	3-5
Special Comments	Text	N/A	Substrate batch ID
Thickness	INTEGER	Microns	290
Depletion Volts	FLOAT	Volts	85.0
Polysilicon Bias Resistance	Text (range)	MΩ	1.22-1.67
Oxide pinholes	Text (List)	N/A	23,301,510
Metal Shorts	Text (List)	N/A	610,611,612
Metal Opens	Text (List)	N/A	701
IV Characteristics	Data (List Volts, nA)	N/A	Example
IV Temperature	FLOAT	°C	20.2

Annex D: Updates to Appendix 1, dated February 2000

Exact definitions of PINHOLE and OXIDE-PUNCHTHROUGH defects in the strip tests have been included, modifying sections 1.2.2 and 1.2.4. The changes are shown below in italics:

1.2.2 Strip integrity

Aim: Check each strip for punch-throughs to the oxide, for shorts between strip metals, and for discontinuities in the strip metals as a verification of Contractor supplied data and to check that the strip defects are within specifications.

Procedure: This test requires a volt source / picoammeter (SMU) to check for oxide punch-throughs, a CV meter to measure capacitance, and a switching matrix. The detector is placed on the chuck of an automatic probe-station, and strip metal pads corresponding to Row C for Barrel detectors or Row B for Forward detectors are probed under computer control with the light on. *Pinholes in* the strip oxide are determined by a measurement of current between the strip metal and backplane with *–10V or* -100V on the needle and the detector backplane at ground potential. A series resistor of *~10* Mohm should be used to limit the current in case of pinholes. The following technique for each strip measurement has been demonstrated to work well without any damage to the detector, and is therefore recommended, though alternative techniques are acceptable:

1.Switch the probe-needle to the high output of the SMU sourcing 0V, and the backplane to grounded low output of the SMU.

2.Step to strip n and raise the chuck

3.Increase the SMU source to -10V, wait 1 second and measure the current to determine electrical continuity across the oxide. *If the current exceeds 50nA (which defines the existence of a pinhole at low volts),* skip steps 4 and 5 and go to step 6.

4.*If the measured current is less than 50nA,* increase the SMU source to -100V (no ramp), wait 1 second and recheck the *current*.

5.Decrease the SMU source to 0V (no ramp).

6.Switch the probe-needle to ground (ie short the needle to the detector backplane) and wait for 500ms

7.Switch the probe-needle to the AC output of the CV meter, and the backplane to the voltage source of the CV meter (with the CV meter sourcing 0V).

8.Wait 1 second and measure the capacitance (at 1kHz, with CR modelled in SERIES)

9.Lower the chuck

10.Repeat the measurement cycle from point 1 above for strip n+1.

The test (as demonstrated on a SUMMIT 10K probe station) takes about 1 hour 10 minutes.

Detector Acceptance:

Both:

< 2 % bad strips, *where a bad strip is defined by either of the following:*

- *a current exceeding 50nA is measured when either –10V or –100V is applied between the strip metal and backplane with a 10 Mohm series resistance. The defect is defined as a PINHOLE if observed at –10V, and an OXIDE-PUNCHTHROUGH if observed at –100V.*
- *the measured capacitance indicates a strip metal short to a neighbour or a discontinuity in the strip metal, with the defect defined as a SHORT or OPEN, respectively.*

And:

agreement with the Contractor on the list of identified bad strip numbers within the agreed tolerance.

Batch Acceptance: The batch is accepted if the mean number of good strips is ≥99% and no detector falls below 98% good strips.

1.2.4 Full Strip Test

Aim: To measure the polysilicon bias resistance and coupling capacitance for every strip, and to check for pinholes, strip metal shorts and opens, implant breaks, and electrical contact between the polysilicon resistor and strip implant.

Procedure: This test requires all 768 strips to be probed while the detector is partially depleted via contacts to the bias rail and backplane. The test requires a voltage source to deplete the detector, a voltmeter/picoammeter (SMU) to check for pinholes, a CV meter for a CR calculation, and a switching matrix. Either mount the detector into a frame and bond the bias rail and backplane to soldable contacts or, if a probe needle manipulator can be fixed to the moving chuck, place the detector directly on to the chuck and contact the detector bias rail with the chuck-mounted probe-needle. If the option of mounting the detector into a frame is used, attach the frame to the probe-station chuck using a jig which permits adjustment of the planarity of the detector so that it is flat with respect to the platen of the probe-station. Switch off the light and apply +20V to the detector backplane with the bias rail at ground potential in order partially to deplete the detector. Under computer control, probe all 768 strip pads along row C for Barrel detectors or row B for Forward detectors according to the following instructions:

1.Switch the high output of the SMU (sourcing 0V) to the probe-needle via a *~10* Mohm series resistor, and switch the low output of the SMU to the detector bias rail.

2.Step to strip n and raise the chuck

3.Increase the SMU source to -10V, wait 1 second and measure the current to determine electrical continuity across the oxide. *If the current exceeds 50nA (which defines the existence of a pinhole at low volts),* skip steps 4 and 5 and go to step 6.

4. *If the measured current is less than 50nA,* increase the SMU source to -100V (no ramp), wait 1 second and recheck the *current*

5.Decrease the SMU source to 0V (no ramp)

6.Switch the probe-needle to ground (ie short the needle to the detector backplane) and wait for 500ms

7.Switch the probe-needle to the AC source output of the CV meter, and the bias rail to the voltage source output of the CV meter, with the CV meter sourcing 0V.

8.Wait 1 second and measure C and R (at 100Hz, with CR modelled in SERIES)

9.Lower the chuck

10.Repeat the measurement cycle from point 1 above for strip n+1.

The test (as demonstrated on a SUMMIT 10K probe-station) takes about 1 hour 10 minutes. The measured values of R and C yield the polysilicon resistor value and coupling capacitance respectively. Deviations imply a strip defect as listed above. Note the test may be performed at 1kHz if measurements at 100Hz are not possible or are unstable; at 1kHz the coupling capacitance is underestimated by 10-20%.

Acceptance: < 2 % bad strips, *where a bad strip is defined by any of the following:*

▪ *a current exceeding 50nA is measured when either –10V or –100V is applied between the strip metal and backplane with a 10 Mohm series resistance. The defect is defined as a PINHOLE if observed at –10V, and an OXIDE-PUNCHTHROUGH if observed at –100V.*

▪ *the measured capacitance indicates a strip metal short to a neighbour or a discontinuity in the strip metal, with the defect defined as a SHORT or OPEN, respectively.*

▪ *a significant deviation is seen in the capacitance and/or resistance distributions, indicating either a break in the strip implant or a break in the baissing resistance (defined as either an IMPLANT BREAK or RESISTOR BREAK, respectively).*

SCT BARREL MODULE Document

SCT Barrel Module: Module Components Section 5.2: Baseboards

Abstract

This document describes the requirements and details of the thermo-mechanical baseboard that forms part of the SCT Barrel Module. The assembly processes are explained and reviews given of the components and product specifications. The methods of achieving both component assurance and baseboard quality assurance are described, and finally the production schedule is presented.

Prepared by :	*Checked by :*	*Approved by :*
R. Apsimon, A.Carter, J. Carter		

Table of Contents

1. SCOPE OF THE DOCUMENT

The document :

- describes the barrel module baseboards and their fundamental requirements,
- explains their assembly procedures,
- gives the technical specifications of their components
- reviews the preparations for pre-series and subsequent series production
- discusses the details of quality assurance procedures
- briefly considers the role of the baseboard within the construction and performance of a barrel module
- and summarises the future production plans.

2. THE BARREL MODULE BASEBOARD

The baseboard is the central element, sandwiched between two silicon wafers on each of its sides during the module construction. To minimise the overall material within a module the baseboard must have the lowest possible mass, be mechanically rigid, and provide the interface for the module cooling contact. Intrinsically the baseboard must be highly efficient in its thermal transfer capabilities in order to transmit injected heat from both the attached ASIC-hybrid structure and, after some years of running, the leakage currents of the silicon detectors that will arise from radiation damage. The ability to achieve the latter requirement is know as the safety against thermal runaway, as such leakage currents double every 7^{o}C increase in silicon temperature and hence are a potential source of uncontrolled temperature rise. The results of detailed FEA simulations are shown in the documents SCT-BM-FDR-4, and these are compared with experimental data in SCT-BM-FDR-8. The low mass has been achieved by designing a minimal volume baseboard, constructed from customised graphite sheets of very high thermal conductivity, and the overall thermo-mechanical properties and electrical integrity are achieved through the use of new encapsulation processes and graphite-beryllia (BeO) epoxy-fusing techniques that have been developed for this project.

The baseboard substrate is thermalised pyrolytic graphite and is referred to as VHCPG, (very high thermal conductivity pyrolytic graphite), to which are attached BeO facing plates. The VHCPG is an anisotropic material having both mechanical and thermal properties that are basically constant within the plane of a substrate sheet and are significantly different in the orthogonal direction, due to the planar mosaic ordering of the carbon structures. The main features of the 380 ± 15μm thick sheets of VHCPG are: (a) in-plane thermal conductivity typically in the range 1450 W/mK to 1850 W/mK at temperatures around 20°C, and increasing by 0.4% for each degree lower in temperature it is operated, and (b) a transverse thermal conductivity of typically 6 W/mK. Although the VHCPG material is intrinsically extremely friable, electrically conducting, and easily delaminated the encapsulation techniques developed in this project provide a baseboard with the necessary robustness and one which is easily handled in the module construction process. The attached BeO facings have a thermal conductivity greater than 280 W/mK at 20°C and consist of at least 99.5% beryllium oxide with a minimum density of 2.86 gm/cc. They are 250 ± 10μm thick, having precision holes and edges created by laser machining and with metallised electrical contact pads 13 ± 5μm thick.

Following successful prototyping of complete baseboard assemblies, and the appropriate Market Surveys, the tenders for both the VHCPG substrates and the BeO facings have been issued. The Tender document for VHCPG substrates and the Technical Specifications for both items are included as appendices 1, 2 and 3 to this Section 5.2 of the SCT-BM-FDR

3. BASEBOARD ASSEMBLY

A picture of an assembled baseboard is given in Figure 1 showing the dark profiled epoxy-coated VHCPG substrate and the light-coloured BeO facings of the upper-side. Similar BeO facings exist on the lower-side of the baseboard, and are inclined by 40mr with respect to those on the upper surface. The technical drawings of the VHCPG-BeO assembly are also shown in Figure 2. The baseboard fabrication, which is carried out at CERN with customised equipment and facilities in a dedicated laboratory, consists of the following operations:

- Initially a square plate, 100mm by 100mm, of VHCPG is profiled both externally and internally by laser cutting to the shape specified in the technical drawing. A fine matrix of 120μm diameter holes is also made within the body of the substrate as an integral feature of the encapsulation technique. The hole area amounts to less than 2% of the total baseboard surface.

- The relative positioning of the four BeO facing plates and the profiled VHCPG plate is then provided by a set of precision jigs and templates, with the appropriate quantity of epoxy being applied by screen printing to each side of the substrate board. The whole assembly is then cured under an appropriate cycle of temperature, pressure and surrounding vacuum to achieve a bubble-free epoxy coating and graphite-BeO intra-surface junction. The encapsulation is typically 20μm thick.

- Four small disks of epoxy are removed from each side of each baseboard, in a dedicated machining process with a diamond tipped tool, to provide openings for electrical conducting epoxy contacts to be made to the rear side of the silicon detectors in the subsequent stages of module construction. This complements the drilled and filled holes in the upper BeO cooling facing which provide direct high voltage electrical contact from the metallised pad on the upper cooled facing to the conducting graphite of the baseboard substrate.

- The completed baseboards are then checked visually for mechanical integrity, and thermal performance is monitored by a dedicated thermal imaging testing procedure before devices are individually packaged and dispatched to module construction centres.

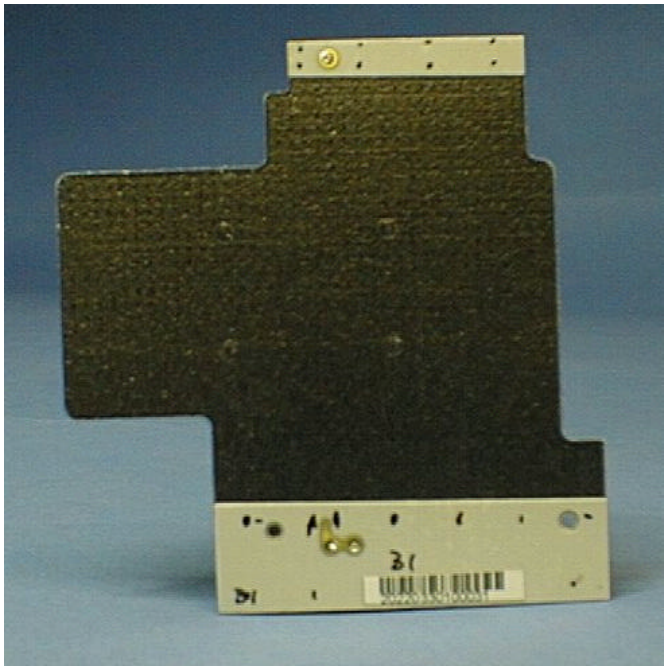

Figure 1. Encapsulated VHCPG baseboard with BeO facing plates

Title:
Converted from HPGL file
Creator:
Designer viewer V5.01
Preview:
This EPS picture was not saved
with a preview included in it.
Comment:
This EPS picture will print to a
PostScript printer, but not to
other types of printers.

Figure 2. Baseboard Assembly Drawing

4. COMPONENT SPECIFICATIONS AND ASSURANCE

The quality assurance requirements and procedures for the component beryllia facings and for the pyrolytic graphite substrates are addressed in detail in the appended documents that have been prepared within the tendering processes.

4.1 The Beryllia Facing Plates

The geometrical specifications are given in Appendix 3. All the BeO facings are inspected visually and samples are checked for their dimensions by direct measurements before use. Trial insertions will also be made in the high precision fabrication templates. Sample testing of bondability to the gold HV contact pads will also be made from each delivered batch. During the series construction phase sets of the four facings necessary for making an individual assembly will be pre-selected and associated with each VHCPG profiled substrate prior to the fabrication step.

4.2 The VHCPG Substrates

The geometrical and thermal specifications are given in Appendix 2. The thermal and mechanical properties of sample substrates have been extensively studied over the last three years, with the necessary dedicated equipment having been designed and built specially for this project. The thermal conductivity has been measured both in-plane and transverse to verify the material properties, and such measurements, with absolute precision of better than ±3%, will be made on sample sheets from each delivered batch during series production. The mechanical moduli have been measured with a customised tensiometer designed for such anisotropic friable materials. During the R&D and prototyping phases a significant database of geometrical measurements has been acquired for initial VHCPG sheets and fabricated baseboards. This has been used to define the specification of the VHCPG material for use in series module construction. The bare substrates will be 380 ± 15μm in mean thickness and the preferred tender option is for none to have internal thickness variations above 20μm within a given plate. If a 30μm variation for some sheets needs to be accepted on cost grounds a well-defined production technique has been demonstrated to cope with it at the screen printing stage(see section 3). The pre-series will give a further 200 sample of correlated component-baseboard measurements to aid the optimisation of production yield for the series production. The silicon detectors themselves are bowed at the level of 60μm to 80μm and predominantly control and intrinsically limit the module flatness. However, as has been shown in baseboard and module prototyping, the flatness of both the board and the module can be adequately controlled using the accepted component specifications. Full metrology will be carried out on each completed module during SCT Barrel Module production to facilitate initial track reconstruction.

5. THE PRODUCTION PROCESS AND QUALITY ASSURANCE

During the prototyping phase all uncut VHCPG sheets have been measured for thickness and flatness at RAL prior to profiling at CERN. As is shown in the tender documents an option is presented for substrate suppliers to carry out all acceptance measurements at their source, and this is our preferred solution for series production. However, if necessary such acceptance measurements will be carried out at CERN by the SCT, where there is production capability for fabricating at least 16 baseboards per day. This will allow the scheduled production target of 200 baseboards per month to be achieved for the 12 to 15 month series production phase.

Each completed baseboard will be subject to a quality assurance of its thermal performance and electrical contact-continuity at CERN. The electrical continuity will be checked by direct measurements between the contact pads on the beryllia facings and the HV openings on both sides of the central baseboard area. Thermal measurements will be provided be injecting known heat sources at well defined points around the board, and having a controlled heat sink attached to the lower cooling face, while measuring the thermal contours of the structure with an infra-red thermal imaging camera. The form of the necessary equipment, that is now being prototyped, is illustrated in Figure 3, and the nature of the recorded thermal contour data that will be stored for each board is shown in Figure 4. Data for each board will be recorded, and stored in a database for comparison with both standard images and with FEA simulations.

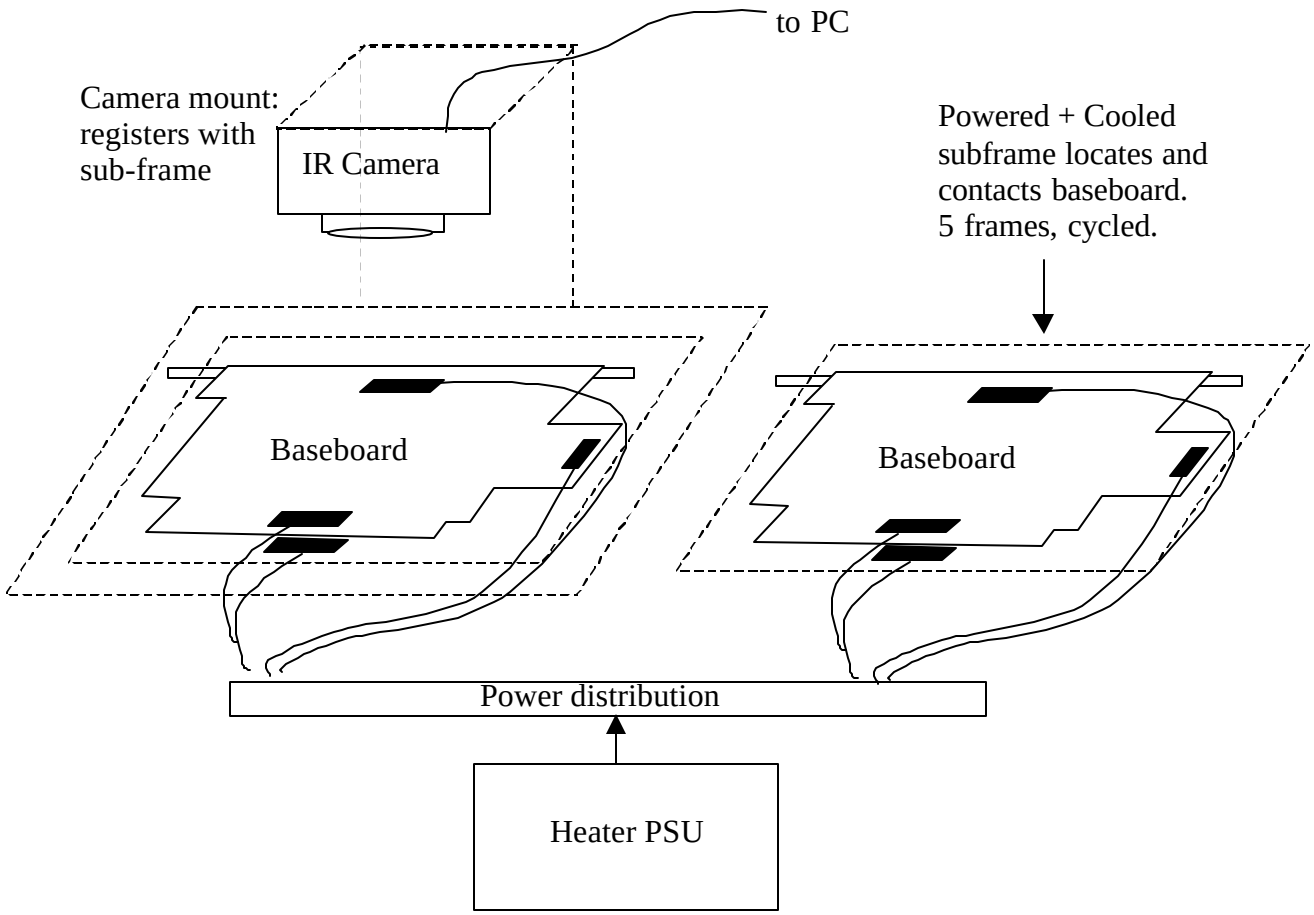

Figure 3. The layout of the IR camera and multi-baseboard support scheme for the thermal QA.

Figure 4. Thermal contour from the IR image of a baseboard.

Each board is given a bar-coded identity from the SCT database and is finally inspected visually before packaging. During the pre-series production each baseboard will be shipped to RAL where a three dimensional profile will be measured with a Smartscope, in order to monitor and record the overall geometrical properties of the baseboards. Figure 5 shows the measured flatness properties of a baseboard that has recently been fabricated.

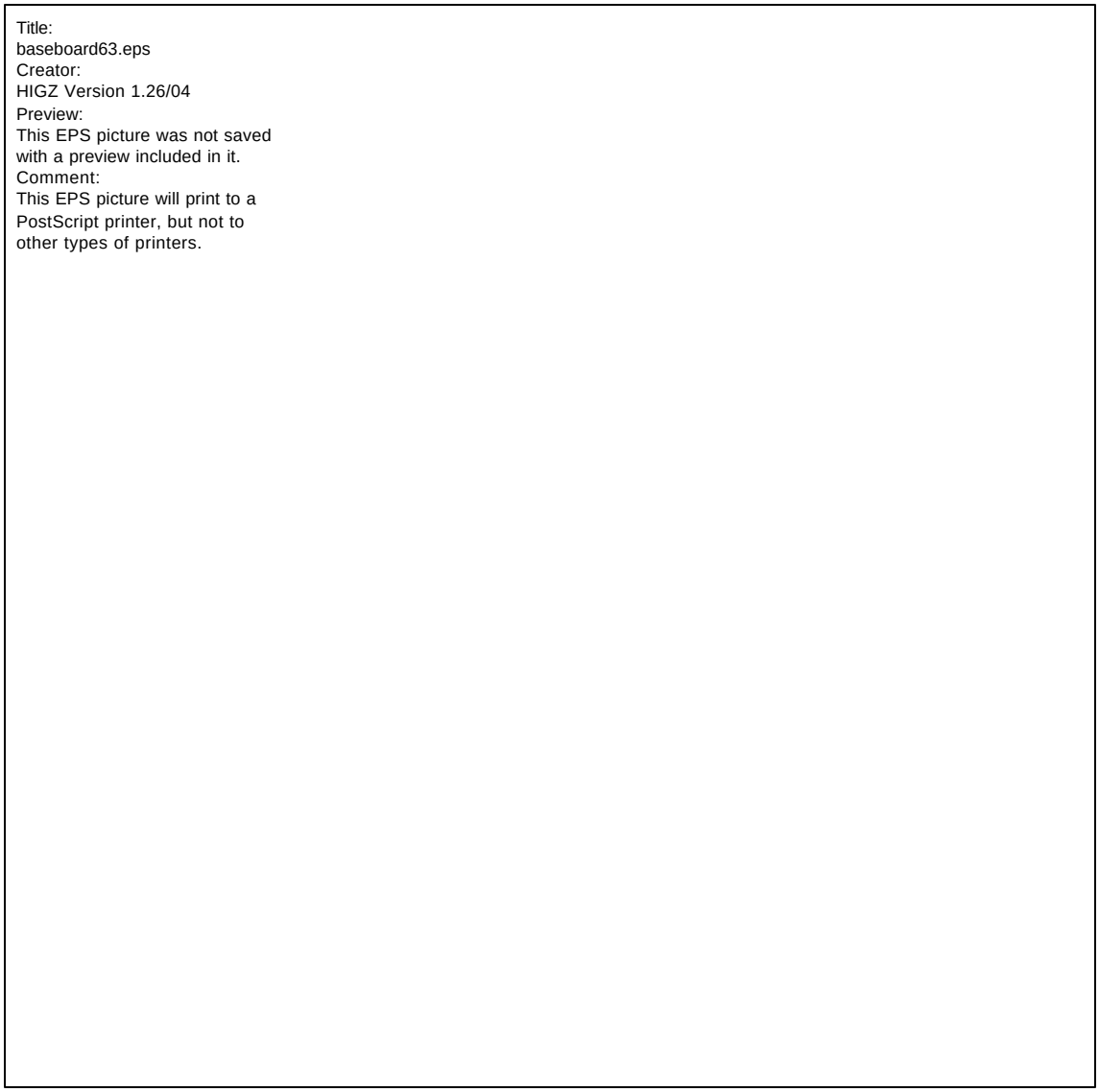

Figure 5 Baseboard flatness profile, contour and orthogonal projections. In-plane dimensions (xy) are cm and out of plane dimensions (z) are mm.

6. THE PRODUCTION SCHEDULE

The fabrication facility is now commissioned and can be brought into full production during the next two months, during which period the final thermal quality assurance instrumentation will be commissioned. The orders for both the beryllia facing plates and the VHCPG substrates are expected to be placed by the beginning of June 2001 and the projected baseboard production schedule is as follows:

- Pre-series fabrication of 200 baseboards begins in August 2001 and following provisional acceptance of the BeO facings and the VHCPG by September 2001 it is aimed to be completed by mid-October 2001
- The initial series batch of 200 baseboards will begin in November 2001 and be completed in December 2001
- The fabrication and dispatch of the 2,400 baseboards will be complete by the end of November 2002.

ATLAS Project Document No.	Institute Document No.	Created:	Page: 1 of 26
SCT-BM-FDR5.3		Modified: 07/05/01	Rev. No.: A

SCT Barrel Module FDR Document

Cu/Polyimide barrel hybrids

abstract

This document outlines the hybrids used in the barrel modules

Prepared by:	Checked by:	Approved by:
Y. Unno, T. Kohriki, T. Kondo, KEK		

Distribution List

SCT

History of Changes

Rev. No.	*Date*	*Pages*	*Description of changes*
A	07/05/01	All	First version

1 Introduction

A hybrid based on copper layers and organic insulator material has been developed for the application to the ATLAS SCT silicon microstrip modules. The technology has been widely used in the industry as a flexible circuit. The basic technology used to use “through-hole”s to connect the traces between layers. As the name “though-hole” indicates, the vertical connection between the layers was made with drilled holes penetrating all the layers. This penetration limited the freedom in laying traces and trace sizes at the “though-hole”s because of the minimum size of the drills. With the advent of micro-via formation, the technology is refined and developed to be “build-up” technology, since a layer can be overlaid over an underneath layer, layer-by-layer, by connecting the two layers with a small diameter of “via”s. The “build-up” flexible circuit is the key technology in industry to make the product small and light [1]. Benefiting from the latest technology, the ATLAS SCT has developed and chosen its hybrids made of the “build-up” Cu/Polyimide flexible circuit [2]. Another benefit of the flexible circuit is to make an one-piece construction of hybrid and cable combination. This eliminates vulnerable connections between the hybrids and cables.

Electrical function is one face of the hybrid. The other is the thermal and mechanical functions. Since the ASICs dissipate a power of 6 W in a module, a good thermal conduction is required in order to draining the heat out to the cooling element. A good mechanical strength is also required. The design of the barrel module is to make the hybrid bridging over the sensors so that the hybrid does not contact the surface of the sensors, other than the wire-bondings between the hybrid and the sensors. The hybrid bridge must be strong enough to make the supersonic wedge bonding of aluminium wire possible. The material of the bridge is required to be low in radiation length.

2 Electrical schematics

The electrical schematics of the hybrid is shown in the Figure 1 and Figure 2, “Circuit Diagram of Barrel Cu/Polyimide Hybrid for ABCD3T chips”. One module requires 12 ASICs; 6 ASICs per side. Two thermistors are equipped to monitor the temperature of hybrid; one per side. The digital and analog ground connection is made on the hybrid, aside of every ASICs.

The components of a hybrid is listed in Table 1.

The pin assignment in the connector at the end of pigtail is listed in Table 2.

Electrical properties of the hybrid is listed in Table 3.

3 Dimensions of the hybrid assembly

Dimensions of the hybrids are shown in Figure 3. The main hybrid sections are made of the area of 74.6 mm (L) x 21.3 mm (W). Two such sections are connected with a 8.4 mm long interconnect, and one end is connected to the pigtail cable of 35.4 mm long. These cable sections are the extension of the layers of the hybrid sections so that the hybrids and cables are made in one-piece, saving additional interconnections between the hybrid and cables. The Cu/Polyimide flexible circuit is reinforced with a substrate for the thermal, mechanical and electrical performance. The substrate has a cut-out in the bottom side in order to bridge over the silicon microstrip sensors.

The thickness of the hybrid from the bottom of the steps is 1.1 mm, including the adhesive layers between the flexible circuit and the bridges. The highest components in the hybrids are the SMD ceramics capacitors, C51~C58 and C71~C75 of the size of 3.2 mm (L) x 1.6 mm (W) x 1.25 mm (H), which height from the bottom is 2.6 mm, including a space between the components and the hybrid. The height of the wire-bonds on the ASICs is about 2.0 mm from the bottom with the ASIC thickness of 0.5 mm and an adhesive layer of 0.1 mm.

4 Specification of components

4.1 Cu/Polyimide flexible circuit

4.1.1 Layer structure

The layer structure of the flexible circuit is shown in Figure 4. The structure is a four Cu layer construction. Two Cu layers are made from a centre core of the double-sided Cu/polyimide sheet and two layers from two single-sided Cu/polyimide sheets glued on the core from top and bottom. The Cu layers of the centre core sheet extend the full length of the circuit from the pigtail connector to the far-end of hybrid. In the cable section the top and the bottom Cu layers are removed to be flexible and the remaining polyimide sheet to be a cover layer. The hybrid section has an extra layer of Cu resulting from the through-hole and via plating and the cover layers for insulation and protection. The Cu/Polyimide sheet is made with “adhesive-less” technology.

Through-holes and via’s are used for inter-connecting the layers: though-holes for the connections between the top (L1) and the bottom (L4) layers; via’s between the top two layers where buses and branches are running. The via’s are formed with a laser.

The layouts of layers are shown in Figure 5. The labels L1 to L4 show the layers from the top to the bottom. The functions of the layers are

- L1 bonding pads, branch traces to the pads from the longitudinal bus lines in the layer L2, and ground and shield planes
- L2 bus lines, and power supply planes in the cable section
- L3 analog and digital ground planes all-through the circuit
- L4 power supply planes, and windows for the ground contact to the bridges

4.1.2 Minimum line and gap widths

There are number of bonding pads in the back-end of the ABCD3T chips. The minimum pitch of the pads are 180 μm. The line/gap of the mating pads on the hybrid are, thus, to be 90 μm/90 μm. The width of the line where the wire bonding is made is better to be wider for ease of bonding. The industry has recommended the minimum gap of 80 μm in the large scale mass production, in order to ensure straight and clean-cut edges and non-existence of metal residues in the gaps. In the etching, the gap width becomes wider. Thus, the tolerance is specified for the minimum line/gap widths to be 100 +0/-20 μm for the line and 80 -0/+20 μm for the gap.

4.1.3 Thermal pillars

There are "thermal through-holes" in the "Front part, i.e., analog circuitry" area of each ASIC, which are vertically connecting the backside of the chips to the surface of the carbon-carbon

bridge thermally. There are 17 such through-holes per chip. The diameter of each through-hole is 300 μm, plated with Cu, and filled with electrically conductive adhesive [ref. the section 5.4] when the flexible circuits are glued on the bridges. The effective thermal conductivity of the "pillar" is estimated to be about 40 W/m/K.

4.2 Carbon-carbon bridge

The bridges reinforcing the Cu/Polyimide flexible circuit is required to have a good thermal conductivity, high young's modulus, and low radiation length. It is shown to improve the electrical performance of the hybrid, specially the stability of the electronics near the zero threshold, by having an electrically conductive bridges and connecting the ground of the hybrid to the bridges.

The hybrids made with a carbon material called carbon-carbon with uni-directional fibres has demonstrated in the prototype modules to suit the requirements with its superb properties of mechanical rigidity, large thermal conductivity, very long radiation length and low electrical resistivity.

The properties of carbon-carbon is summarized in Table 4 for a product available [3]. The product has a thermal conductivity of 700 W/m/K (in the fibre direction), nearly twice of Cu, and a young's modulus of 300 GPa (in the fibre direction), as strong as ceramics.

The specification of the bridge is shown in Figure 6. The bridge is machined, with a milling machine, so that the steps of the bridge are part of the original material in order to maximize the thermal conduction and the easiness of mechanical construction.

The surface of the bridge is coated with a polymer called Parylene of 10 μm thick for insulating the surface and improving reliability in handling. The surface of coating is roughened with a laser where adhesion is required. The coating is removed where an electrical and thermal conduction is required.

4.3 Glass pitch-adaptor

The basic pitch of input pads of the ASIC is 48 μm, while that of the silicon microstrip sensor is 80 μm. In order to make a simple parallel wire-bonding, a pitch-adaptor is used in front of the ASICs. Since a fine pitch of 48 μm is required, the pads and traces are fabricated on a separate piece with a thin-film technology: aluminium deposition on a glass substrate. The barrier metal between the glass and the aluminium is an important factor for the adhesion of the aluminium which is a proprietary knowledge of the vendor.

The specification of the pitch-adaptor is shown in Figure 7. The size of the pitch adaptor is 63 mm (L) x 2.7 mm (W) x 0.2 mm (T). The thickness of aluminium is 1 ~ 1.5 μm.

4.4 Surface mount components

The components of the hybrids are listed in Table 1. The capacitors are of the type X7R for the best temperature characteristics which has a capacitance change of 5% between -20 and +40 °C. The resistors are of metal film precision type.

The thermistors are those of R25 = 10 kΩ ± 1% and B = 3435K±1%. The temperature is readily calculated from the equation,

$$R = R25\exp\left(B\left(\frac{1}{T}+\frac{1}{T25}\right)\right) \quad (1)$$

where T is given in absolute temperature. T25 and R25 are the nominal temperature of 25 °C and the resistance at the temperature, respectively.

Loading of the components is shown in Figure 8.

5 Cu/Polyimide hybrid production and Quality Assurance

The barrel hybrids are delivered to the module assembly clusters as "passive component stuffed" hybrids, i.e., the ASIC stuffing, testing, and mounting the hybrids into modules is the responsibility of the clusters. The "passive component stuff" hybrids are to be fabricated in industry. The total quantity is rounded to be 2,500 pieces. Assuming various yields in fabrication steps, the required numbers of components are estimated and listed in Table 5.

5.1 Production of Cu/Polyimide flexible circuits

The Cu/Polyimide flexible circuits will be produced based on the specification described in the section 4.1. The quantity is 3,200. Along the fabrication of the circuits, a quality assurance (QA) will be carried out by vendor: (1) visual inspection for all products, (2) specimen tests for mechanical tolerance on outer dimensions, bonding pads/gap widths, plating thicknesses, and (3) integrity test of lines: open/short test for all products, and resistance measurement for samples.

5.2 Production of carbon-carbon bridges

The carbon-carbon (CC) bridges are fabricated based on the specification in the section 4.2 and delivered as a finished product. The fabrication quantity of the carbon-carbon bridges is 6,300. QA is made for: (1) mechanical tolerance of outer dimensions, (2) mechanical performance of Young's modulus and tensile strength for samples to be greater than 90% of specified values, (3) thermal performance of thermal conductivity to be greater than 600 W/m/K, and (4) electrical resistivity less than 25 mΩ measured on the two farthest windows.

5.3 Production of glass pitch-adaptors

The glass pitch-adaptor is made according to the drawing in the section 4.3 for the quantity of 5,700. QA is made for: (1) visual inspection of the mechanical finish, tolerance, and open/short of the traces for all products, (2) tape-peel test of the aluminium traces and (3) wire-bond pull test, for samples. The wire-bond pull strength is to be greater than 6 gr for the 30% height/distance ratio (H/L) setting.

5.4 Production of Cu/Polyimide/CC hybrids

This is the gluing process of the Cu/Polyimide flexible circuit and the CC bridges. This process produces "bare" hybrids, i.e., no components on the hybrid, yet. Two epoxy adhesive sheets are used: thermally conductive and electrically conductive. A set of small windows has been cut out on the surface of the bridges in order to improve the thermal and electrical contact between the carbon bridge and the ASICs. The area other than the windows is adhered with the thermally conductive adhesive sheet, ABLEFILM 563K-.002, 50 μm thick, alumina-filler filled, and at the windows with the electrically conductive sheet, ABLEFILM 5025E-.002, 100 μm thick, silver loaded [4]. The electrically conductive film is thicker so that the adhesive will fill up the through-holes in the hybrid.

Both adhesive films require curing at an elevated temperature at 125 deg.C for two hours. During

the curing, the flexible circuit and the bridges are held and pressed together at 4 kg/cm^2 by a press jig.

QA is made for: (1) visual inspection for excess adhesives, residuals on the surface, and mechanical tolerance for the alignment and thickness, and (2) bows of the hybrid section at the room temperature, which are less than 75 μm in the long and the across directions, for all products.

5.5 Production of "Passive component stuffed" hybrids

This is the process soldering the surface-mount components (SMDs) and the connector on the hybrids and adhering two pitch-adaptors. About 50 SMD parts: resistors, capacitors, and thermistors as listed in Table 1, are installed on the hybrid. A component loading diagram is shown in Figure 8. Since a high temperature application, higher than 60 °C, is to be avoided after the adhesion of the flexible circuit and CC bridges, the solder reflow technique is eliminated in soldering the components. A method being used is to place and hold the components with a dot of epoxy, cure, and then apply soldering manually. The detail of the soldering process is being refined further incorporating the process involved in industry.

Two pitch-adaptors are glued on the hybrid by using a room temperature curing epoxy, Araldite 2011. No filler is used. The low viscosity epoxy makes the glue layer thin and without trapping air bubbles. The surface of the hybrid is protected beforehand with a masking tape in order to prevent contamination with the epoxy. The pitch-adaptor is positioned under a microscope to align the edge of the pitch-adaptors to the fiducial marks on the flexible circuit. The width of the line of the fiducial mark is 100 μm and alignment of the edge of the pitch-adaptor within the line width assures the position of the pitch-adaptor to be within ±50 μm.

QA is made for all hybrids: (1) visual inspection of component placement, solder fillet, surface contamination and residuals, (2) electrical measurement from the connector for the termination resistors and the capacitancies of the Vcc-GND and the Vdd-GND, and (3) a wire-bond pull test at the test pads to be greater than 6 gr for the 30% H/L setting.

5.6 Thermal cycling

The passive-component-stuffed hybrids are thermal-cycled between -30 and +60 °C for 5 times. QA is made for: (1) visual inspection for component loss, cracks, (2) mechanical tolerance for thickness and bows, (2) electrical performance of resistance, capacitance, and leakage current in the low and high voltage lines, the latter at 500 V.

6 Hybrid datasheet

A datasheet per hybrid is prepared summarising the QA in the section 5. The datasheet of a hybrid is shown in the appendix 7.1 as an example. An ATLAS parts identification number (atlas id) is given to the hybrid, as registered in the datasheet, and a barcode label is attached on the pigtail section of the hybrid. The datasheet will be uploaded to the database in a similar fashion as the detector datasheet.

7 Appendix

7.1 Hybrid datasheet

An example of the hybrid datasheet is appended in the following pages.

Hybrid datasheet	
ATLAS ID classification (KEK)	20220170100051
Mfr serial number	K4211
Overall Quality	Good
Parts:	
220 nF capacitors/batch	20220170111002
330 nF capacitors/batch	20220170112001
10nF/630V HV capacitors/batch	20220170113001
100 ohm resistors/batch	20220170114001
5.1K ohm resistors/batch	20220170115001
1K ohm resistors/batch	20220170116001
0 ohm resistors/batch	20220170117001
Semitec 103KT1608-1P thermistors/batch	20220170118001
Connector Samtec SFMC-140-L3-S-D/batch	20220170119001
Pitch adaptors/batch	20220170121001
Carbon-carbon bridges/batch	20220170122001
Conductive epoxy glue (Eotite P-102)/batch	20220170131001
Electrically non-conductive epoxy glue for hybrid/batch	20220170132001
Araldite+BN filler/batch	20220170133001
Attaching CC bridges to flex circuit/batch	20220170141001
Stuffing passive components/batch	20220170142001
1 Cu/Polyimide Flex circuits	Good
1.1 Visual inspection by vendor	Good
(1) Design features sizes and structures	Good
(2) Nicks and pin holes on conductor	Good
(3) Protrusions and residual conductor	Good
(4) Entrapped foreign materials	Good
(5) Wrinkles and fold lines	Good
(6) Air bubbles under cover film	Good
(7) Dents and delamination of conductor	Good
(8) Scratches on conductor	Good
(9) Discoloration and corrosion	Good
(10) Adhesive squeeze-out	Good
(11) Adhesive stain	Good
(12) Non-plating	Good
1.2 Integrity test of lines by vendor	Good
2 Cu/Polyimide/Carbon-bridge hybrid	Good
2.1 Visual inspection by vendor	Good
(1) Cracks	Good

(2) Alignment between flex circuit and Carbon-bridge	Good
(3) Fill up electrical conductive adhesive	Good
(4) Adhesive residuals	Good
(5) Adhesive squeeze-out	Good
2.2 Mechanical tolerance	Good
(1) Thickness measurement (microns) (6points)	Good
Link0 (average)	599.830000
Link1 (average)	597.830000
(2-1) Flatness measurement Bow (long)	Good
Link0 (<75)	29.727000
Link1 (<75)	36.600000
(2-2) Flatness measurement Bow (across)	Good
Link0 (<75)	42.705000
Link1 (<75)	40.815000
(2-3) Flatness measurement Twist	Good
Link0 (<100)	44.670000
Link1 (<100)	70.650000
3 Passive-component-stuffed hybrids	Good
3.1 Visual inspection by vendor	Good
(1) Passive-component alignment	Good
(2) Soldering	Good
(3) Residuals and foreign materials on surface	Good
3.2 Wire-bond pull test	
(1) pull strength (>6gr)	
4 Passive-component-stuffed hybrids with pitch adaptor	Good
4.1 Visual inspection by vendor	Good
(1) Pitch adaptor crack	Good
(2) Pitch adaptor alignment	Good
(3) Adhesive residuals	Good
(4) Adhesive squeeze-out	Good
5 temperature cycle tests	Good
5.1 Capacitance and impedance measurement by vendor	Good
Vcc-GND (microF) at 1KHz (4.0<x<4.8)	4.108700
Vdd-GND (microF) at 1KHz (4.0<x<4.8)	4.057000
HV-GND (kOhm) at 100Hz (30<X<36)	34.500000
HV-GND (kOhm) at 1KHz (9<X<11)	10.060000
HV-GND (kOhm) at 10KHz (5.7<X<7.7)	6.737000
HV-GND (kOhm) at 100KHz (5.1<X<7.1)	6.070300
5.2 temperature cycle test by vendor	Good
5.3 Visual inspection by vendor	Good
(1) Component loss	Good
(2) Cracks	Good
(3) Residuals and foreign materials on surface	Good
5.4 Mechanical tolerance	Good
(1) Thickness measurement(microns)(6points)	Good

Link0 (average)	602.830000
Link1 (average)	599.670000
(2-1) Flatness measurement Bow (long)	Good
Link0 (<75)	36.277000
Link1 (<75)	37.700000
(2-2) Flatness measurement Bow (across)	Good
Link0 (<75)	50.430000
Link1 (<75)	38.615000
(2-3) Flatness measurement Twist	Good
Link0 (<100)	57.880000
Link1 (<100)	47.100000
5.5 Resistance and capacitance measurement by vendor	Good
Vcc-GND (microF) at 1KHz (4.0<x<4.8)	4.129000
Vdd-GND (microF) at 1KHz (4.0<x<4.8)	4.081300
HV-GND (kOhm) at 100Hz (30<X<36)	34.400000
HV-GND (kOhm) at 1KHz (9<X<11)	10.060000
HV-GND (kOhm) at 10KHz (5.7<X<7.7)	6.738000
HV-GND (kOhm) at 100KHz (5.1<X<7.1)	6.070000
R27 (Ohm) (99<X<101)	100.060000
R28 (Ohm) (99<X<101)	100.020000
R29 (Ohm) (99<X<101)	99.960000
R30 (Ohm) (99<X<101)	99.980000
TM0 (kOhm) (9.8<X<10.2) at 25 degC	10.097000
TM1 (kOhm) (9.8<X<10.2) at 25 degC	10.150000
ASIC die pad No.1-No.6 (milliOhm) (<4)	3.600000
ASIC die pad No.7-No.12 (milliOhm) (<4)	3.600000
5.6 LV leakage current measurement by vendor	Good
Icc (nA) at 10V (<10)	9.000000
Idd (nA) at 10V (<10)	9.000000
5.7 HV leakage current measurement by vendor	Good
HV current (nA) at 500V (<10)	9.000000
6.Barcode and data sheet entry	Done

7.2 ASICs stuffing and replacing

After the receipt of the passive-component-stuffed hybrids, the module assembly sites attach ASICs on the hybrids. Some cautions and instructions are given here.

7.2.1 ASIC stuffing

The ASICs are glued on the chip pads with electrically conductive epoxy, Eotite p-102, in order to have a good thermal and electrical conduction. Four fiducial marks are prepared at the corner of the chip pad for aligning the ASICs. The bonding pads near the ASICs should be masked for not contaminating the bonding surface. Apply a correct amount of glue such that the glue extends full area of the ASICs and form a smooth fillet to the sides of the ASICs. When curing the epoxy at elevated temperature, e.g., at 50 °C for 2 hrs. or more, hold the hybrids at the steps of

the bridges in order to prevent warping.

7.2.2 ASIC replacing

An ASIC can be replaced on the hybrid. A simple special jig for the ASIC replacement has been developed. It is made of a Cu block on a soldering iron. The Cu block is a 8 mm x 8 mm x 12 mm which has a trench of 6.5 mm wide and 0.3 mm deep where the ASIC can be fit and picked-off with vacuum-chucking. The block is attached on the tip of a conventional soldering iron. Heat the block at 250 °C. Apply the head to the ASIC. The glue underneath becomes soft in about 5 sec. By applying a twist to the ASIC, it can be picked off easily once the ASIC moves. A high power soldering iron (e.g., 20W) is to be used in order to have a heat capacity and heating time as short as possible. A photo of the jig is shown in Figure 10.

References

[1] Y. Unno, “High-density low-mass hybrid and associated technologies”, 6th Workshop on Electronics for LHC Experiments, pp 66-76, CERN 2000-010
[2] M. Tyndel, et al., “Internal Design Review of the SCT Barrel Hybrids”, reference id, 5 July, 2000
[3] A product is available from Nippon Mitsubishi Oil Corporation, catalog no. NCC-AUD28
[4] These adhesive sheets are made by ABLESTICK co. Ltd..

Table 1
List of components

parts No.	# of pieces	dimensions (mm)	specifications	products
U1 ~ U12	12	6.55x8.40x0.5	ABCD3T chip	
C1 ~ C28	28	1.6x0.8x0.8	Ceramic capacitor 220 nF, 10V,	Murata GRM39-X7R-224-K-10
C51 ~ C58	8	3.2x1.6x1.25	Ceramic capacitor 330 nF, 25 V,	Murata GRM42-6-X7R-334-K-25
C71 ~ C75	5	3.2x1.6x1.25	Ceramic capacitor 10 nF, 630 V	Murata GHM1530-B-103-K-630
R27 ~ R30	4	1.6x0.8x0.8	Resistor, 100Ω	
R33, R34	2	1.6x0.8x0.8	Resistor, 5.1 kΩ	
R35	1	1.6x0.8x0.8	Resistor, 1 kΩ	
R36	1		jumper wire	
TM1, TM2	2		Thermistor	Semitec 103KT1608-1P
CON	1		Connector, 2x18pins, 1.27mm pitch,	Samtec SFMC-120-L3-S-D or 0.05”x0.05” 40 square-pins female
PA	2		pitch adaptor	pa4880

Table 2
Pin assignment of the hybrid connector.

1	+bias(HV)	10	analog ground	19	digital ground	28	com0-bar
2	+bias(HV)	11	V_{CC}	20	digital ground	29	clock0
3	NC	12	analog ground	21	V_{DD}	30	clock0-bar
4	NC	13	VCC	22	V_{DD}	31	led
5	-bias(ag)	14	analog ground	23	digital ground	32	led-bar
6	-bias(ag)	15	com1	24	digital ground	33	ledx
7	tempret	16	com1-bar	25	reset	34	ledx-bar
8	analog ground	17	clock1	26	select	34	temp1
9	V_{CC}	18	clock1-bar	27	com0	36	temp2

Table 3
Electrical properties of the Cu/Polyimide barrel hybrid

Trace/Plane	Capacitance [pF]		Resistance [mΩ]	
	bare flex circuit	with bridge	pigtail section	rest of hybrid section
Analog ground (AGND)	--	--	13	24
Digital ground (DGND)	--	--	13	46
Analog power (Vcc)	1.2	1.9	15	46
Digital power (Vdd)	0.9	0.9	15	46
Command bus line	39		500	1700
Data/token longest lines	32		1800	
Data/token short lines	3		100	
Values are based on measurement. Errors are estimated to be about 10%.				

Table 4
Properties of Carbon-carbon

Material	Uni-directional fibres
Thermal conductivity (fibre direction) [W/m/K]	700 ± 20
Thermal conductivity (transverse to fibres) [W/m/K]	35±5
Density [g/cm^3]	1.9
Young's modulus (fibre direction) [GPa]	294
Tensile strength (fibre direction) [MPa]	294
Thermal expansion coefficient (CTE) (fibre direction) [ppm/K]	-0.8
Thermal expansion coefficient (CTE) (transverse to fibres) [ppm/K]	10
Electrical resistivity (fibre direction) [Ωm]	2.5 x 10^{-6}

Table 5
Required numbers of components (numbers rounded to 100)

“passive component stuffed” hybrids	2500
Cu/Polyimide flexible circuits	3200
Carbon-carbon bridges	6300
Pitch-adaptors	5700
SMDs and connector (set)	3000

Figure captions:

Figure 1 Schematic circuit diagram of the barrel hybrid (version 4), connector side

Figure 2 Schematics circuit diagram of the barrel hybrid (version 4), far-end side

Figure 3 Dimensions and profile of the Cu/Polyimide barrel hybrid (version 4)

Figure 4 Layer structure of the Cu/Polyimide flex circuit of the barrel hybrid (version 4)

Figure 5 Layer layouts of: top traces (L1), bus traces (L2), ground planes (L3), and power planes (L4)

Figure 6 Hybrid bridge made of carbon-carbon

Figure 7 Glass pitch adaptor

Figure 8 Component loading diagram

Figure 9 Radiation length and weight of the barrel hybrid (version 4)

Figure 10 An ASIC replacement jig

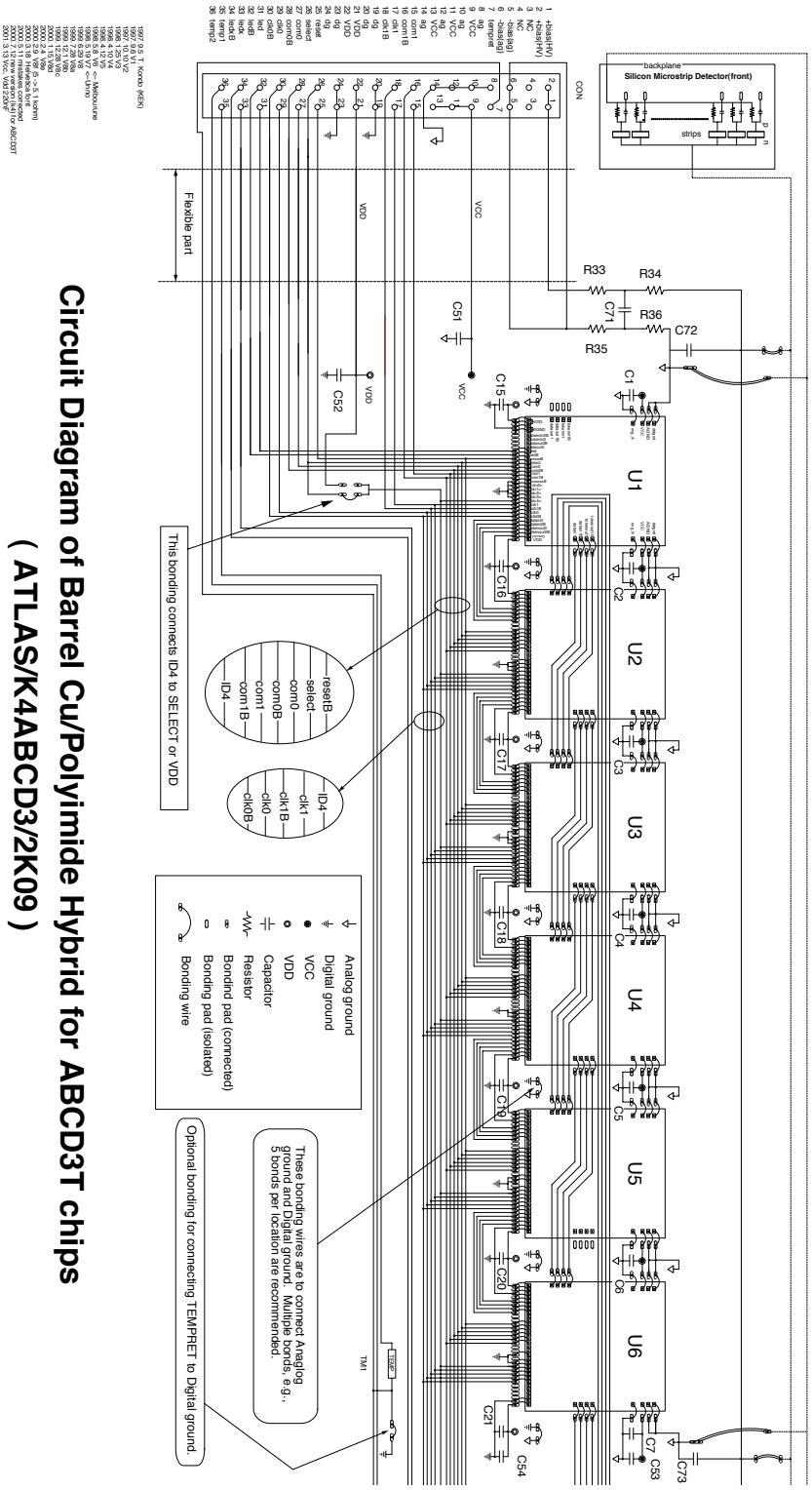

Figure 1 Schematic circuit diagram of the barrel hybrid (version 4), connector side

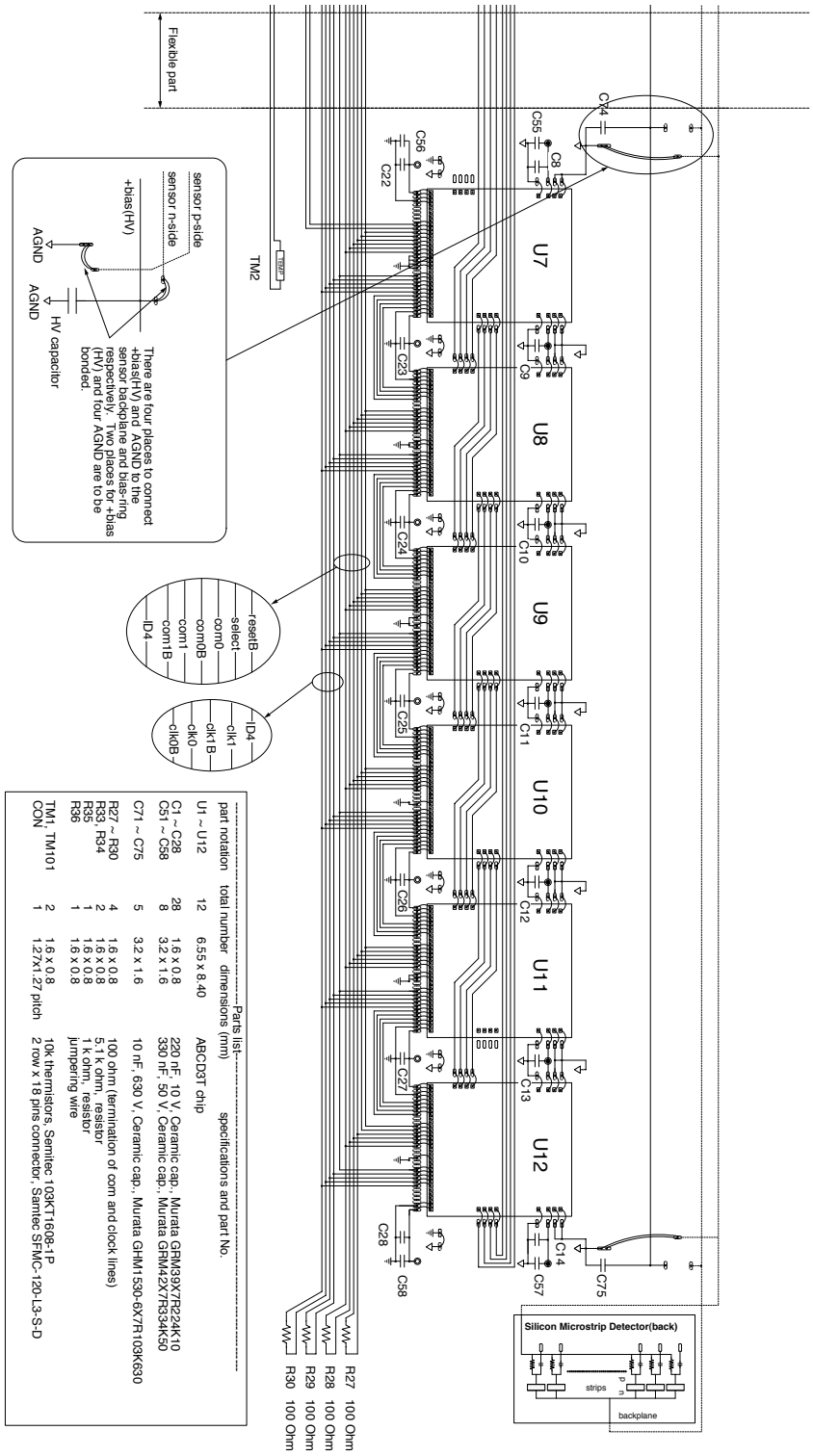

Figure 2 Schematics circuit diagram of the barrel hybrid (version 4), far-end side

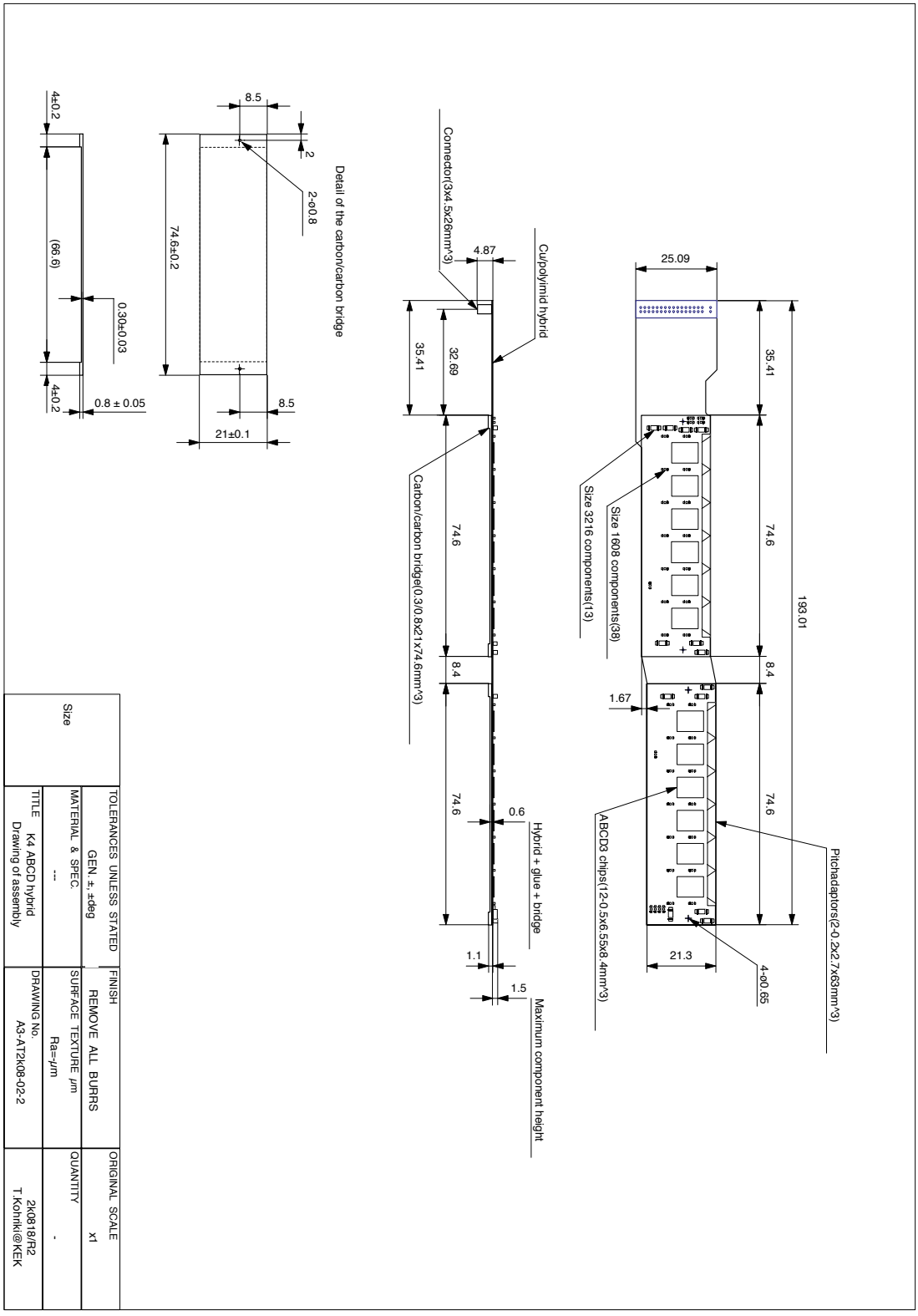

Figure 3 Dimensions and profile of the Cu/Polyimide barrel hybrid (version 4)

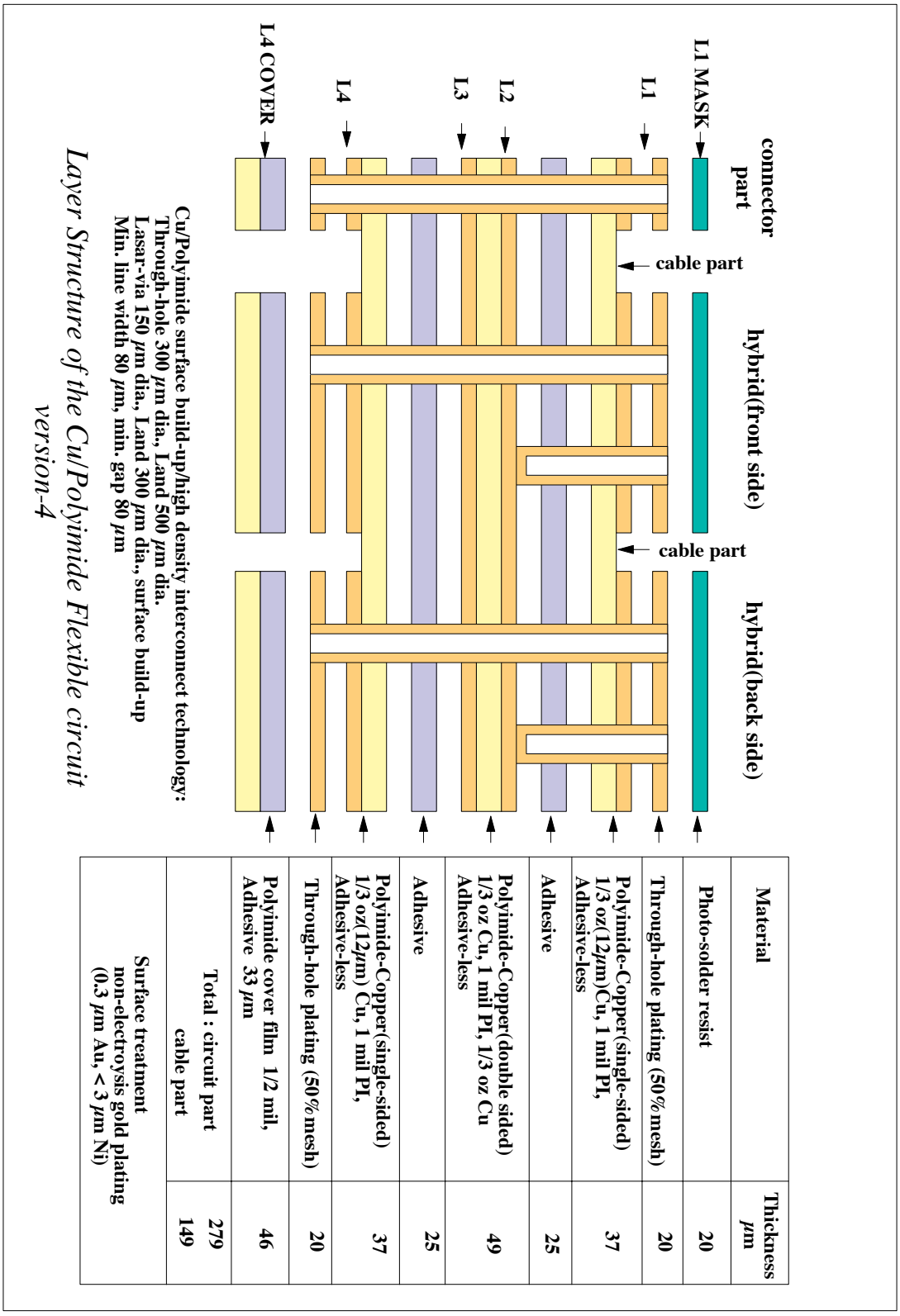

Material	Thickness μm
Photo-solder resist	20
Through-hole plating (50% mesh)	20
Polyimide-Copper(single-sided) 1/3 oz(12μm)Cu, 1 mil PI, Adhesive-less	37
Adhesive	25
Polyimide-Copper(double sided) 1/3 oz Cu, 1 mil PI, 1/3 oz Cu Adhesive-less	49
Adhesive	25
Polyimide-Copper(single-sided) 1/3 oz(12μm) Cu, 1 mil PI, Adhesive-less	37
Through-hole plating (50% mesh)	20
Polyimide cover film 1/2 mil, Adhesive 33 μm	46
Total : circuit part	279
cable part	149
Surface treatment non-electroysis gold plating (0.3 μm Au, < 3 μm Ni)	

Cu/Polyimide surface build-up/high density interconnect technology:
Through-hole 300 μm dia., Land 500 μm dia.
Lasar-via 150 μm dia., Land 300 μm dia., surface build-up
Min. line width 80 μm, min. gap 80 μm

Layer Structure of the Cu/Polyimide Flexible circuit version-4

Figure 4 Layer structure of the Cu/Polyimide flex circuit of the barrel hybrid (version 4)

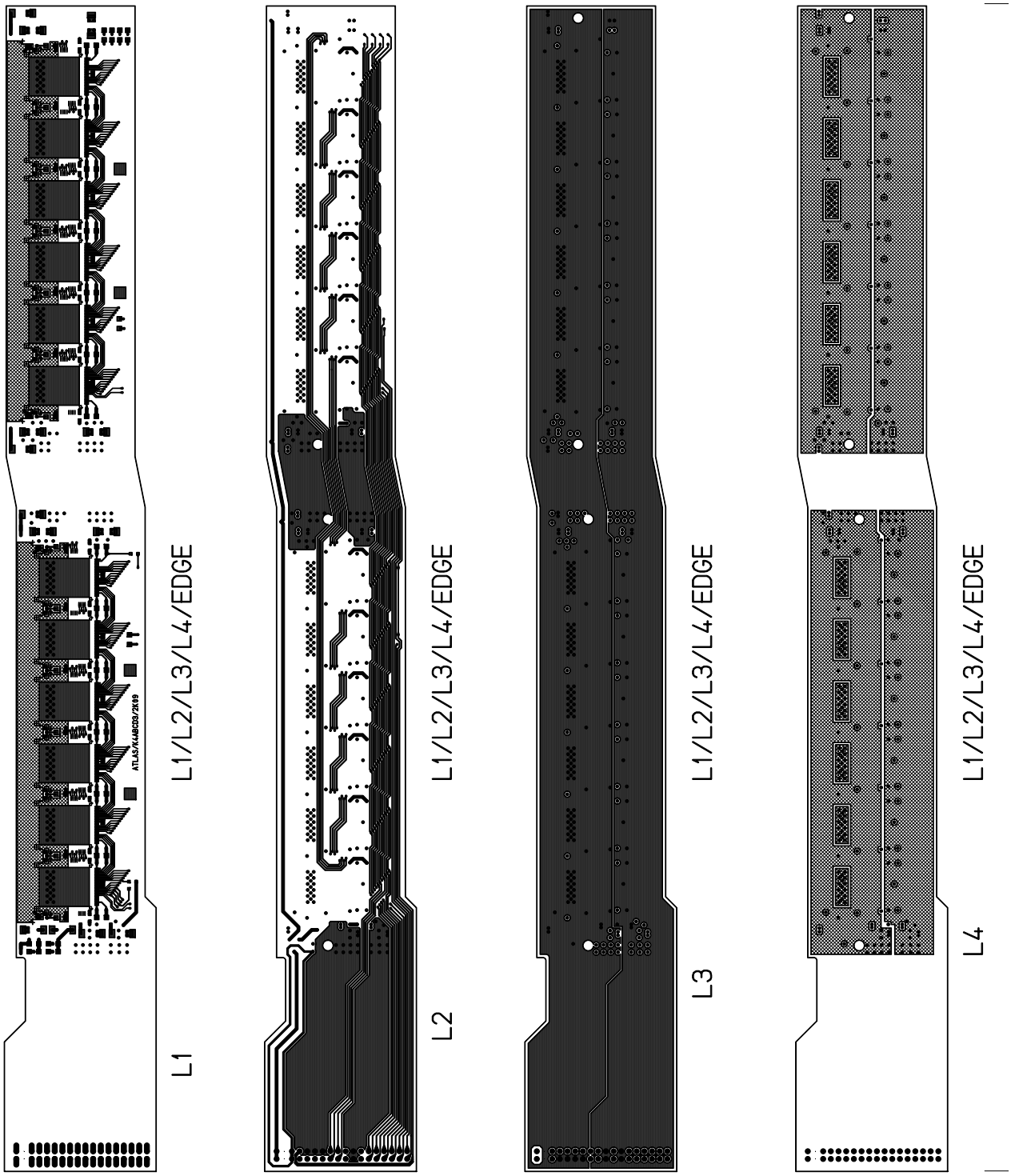

Figure 5 Layer layouts of: top traces (L1), bus traces (L2), ground planes (L3), and power planes (L4)

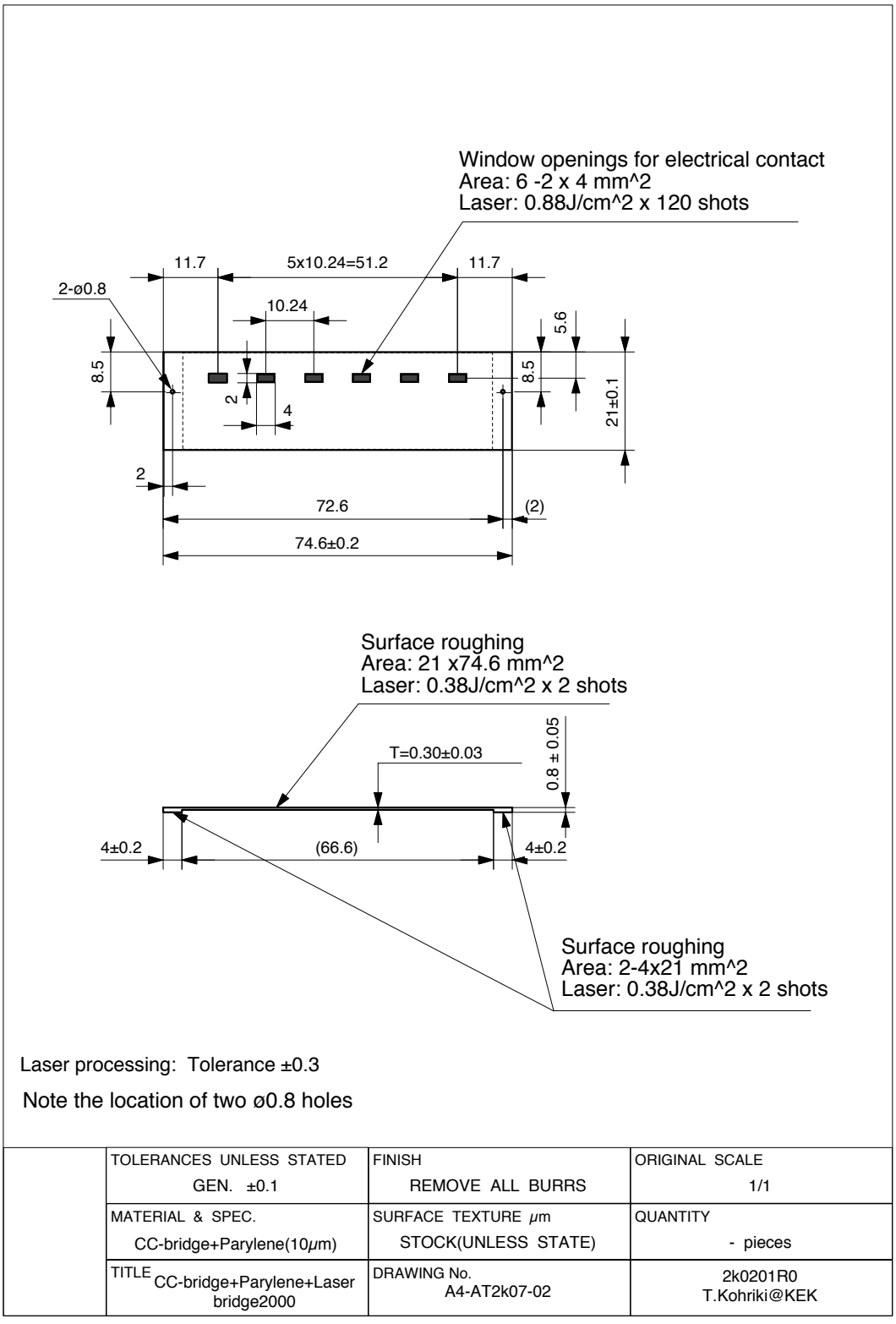

	TOLERANCES UNLESS STATED GEN. ±0.1	FINISH REMOVE ALL BURRS	ORIGINAL SCALE 1/1
	MATERIAL & SPEC. CC-bridge+Parylene(10μm)	SURFACE TEXTURE μm STOCK(UNLESS STATE)	QUANTITY - pieces
	TITLE CC-bridge+Parylene+Laser bridge2000	DRAWING No. A4-AT2k07-02	2k0201R0 T.Kohriki@KEK

Figure 6 Hybrid bridge made of carbon-carbon

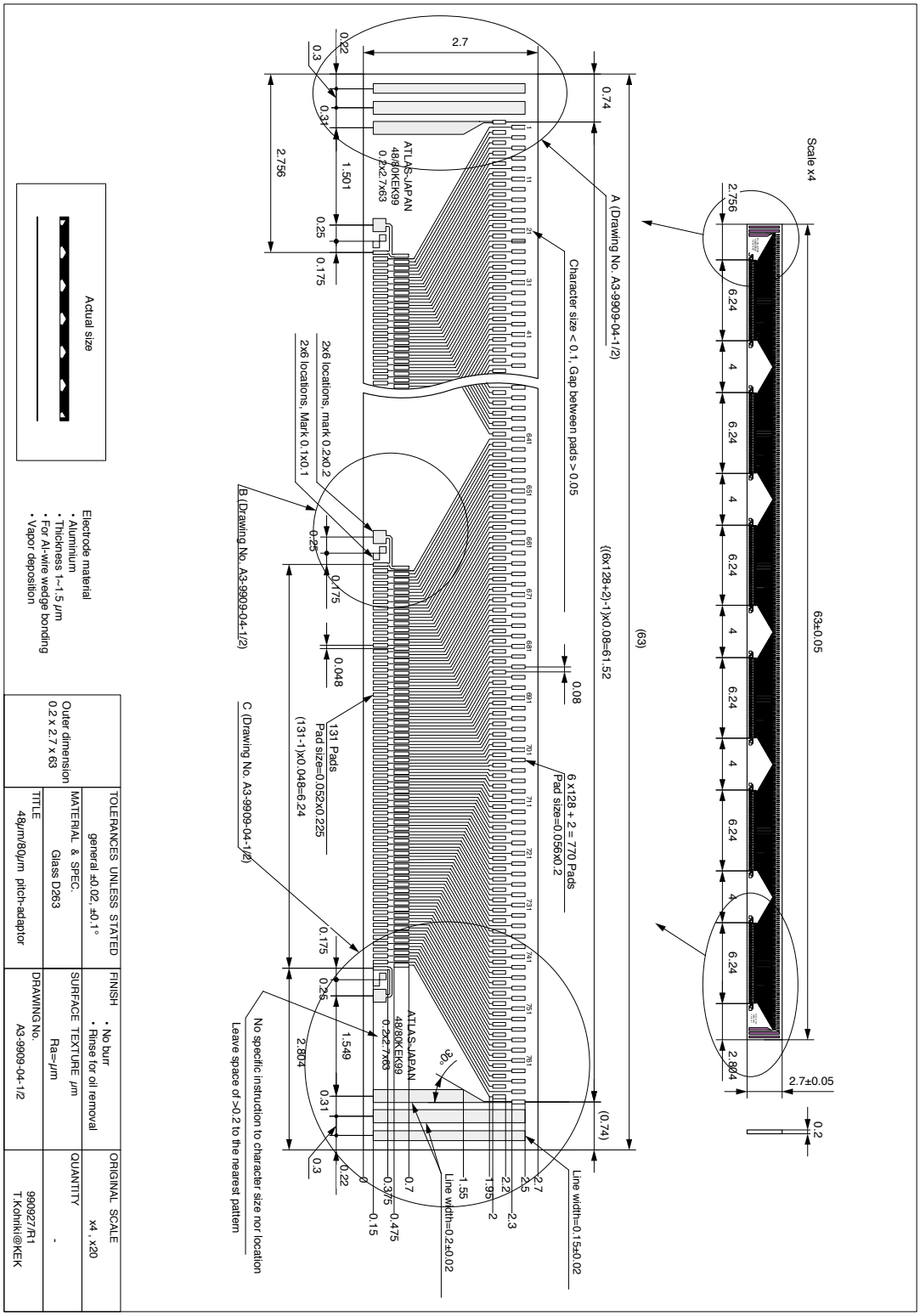

Figure 7 Glass pitch adaptor

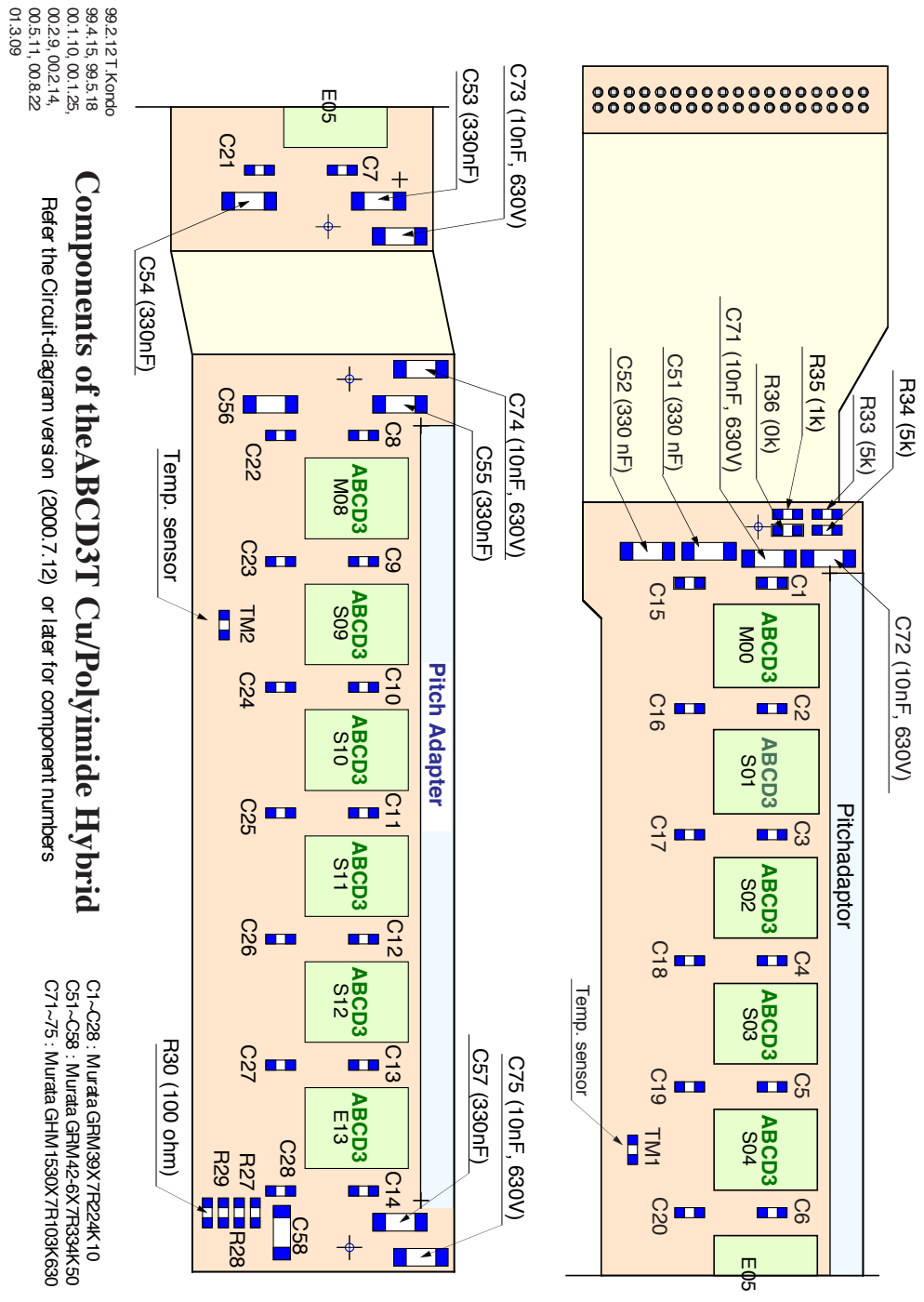

Figure 8 Component loading diagram

KhybridXo01feb26.xls

Cu/Polyimide hybrid 12μm Copper, version4

Normalise to 74.6 x 21 mm^2 =	1566.6															
Item	No. off	Basic x (mm)	Basic y (mm)	Basic area	Less area	Actual area	Scaled area	Thickness (mm)	Thickness mea (mm)	Scaled thickness	X0 (mm)	Rad len (%)	Density (g/cm^3)	Weight (gm)	Summed weight (gm)	Measured weight (gm)
Main hybrids (2-in-1)	2	74.6	21			1566.6		0.267	0.233	0.2203	86.13	0.621		1.681	2.03	2.04
Gold flash(0.4μm)	2	74.6	21	1566.6	881	686	0.438	0.000		0.0002	3.35	0.010	19.3	0.011		
Nickel plating(2μm)	2	74.6	21	1566.6	881	686	0.438	0.002		0.0009	14.7	0.012	8.845	0.024		
Photoresist (20μ) layer	2	74.6	21	1566.6	567	1000	0.638	0.020		0.0128	357.5	0.007	1.136	0.045		
L1:Copper(12μm)+TH-plating(13μm) (60% hash)	2	74.6	21	1566.6	881	686	0.438	0.025		0.0109	14.3	0.153	8.93	0.306		
Polyimide+adhesive (25μ+25μ) layer	2	74.6	21	1566.6	0	1567	1.000	0.050		0.0500	357.5	0.028	1.136	0.178		
L2:Copper tracking(12μm)	2	74.6	21	1566.6	1268	298	0.190	0.012		0.0023	14.3	0.032	8.93	0.064		
Polyimide layer (25μ)	2	74.6	21	1566.6	0	1567	1.000	0.025		0.0250	357.5	0.014	1.136	0.089		
L3:Copper gnd plane(12μm)	2	74.6	21	1566.6	112	1455	0.929	0.012		0.0111	14.3	0.156	8.93	0.312		
Polyimide+adhesive (25μ+25μ) layer	2	74.6	21	1566.6	0	1567	1.000	0.050		0.0500	357.5	0.028	1.136	0.178		
L4:Copper(12μm)+TH-plating(13μm) (60% hash)	2	74.6	21	1566.6	873	694	0.443	0.025		0.0111	14.3	0.155	8.93	0.310		
Polyimide cover+adhesive (13μ+33μ) layer	2	74.6	21	1566.6	0	1567	1.000	0.046		0.0460	357.5	0.026	1.136	0.164		
Interconnect	1	9	21			189		0.149	0.141	0.0173	90.43	0.020		0.058		
Polyimide+adhesive (25μ+25μ) layer	1	9	21	189.0	0	189	0.121	0.050		0.0060	357.5	0.002	1.136	0.011		
Copper tracking	1	9	21	189.0	72	117	0.075	0.012		0.0009	14.3	0.006	8.93	0.013		
Polyimide layer	1	9	21	187.1	0	187	0.119	0.025		0.0030	357.5	0.001	1.136	0.005		
Copper gnd plane	1	9	21	189.0	14	176	0.112	0.012		0.0013	14.3	0.009	8.93	0.019		
Polyimide+adhesive (25μ+25μ) layer	1	9	21	189.0	0	189	0.121	0.050		0.0060	357.5	0.002	1.136	0.011		
Pig tail	1	30	24.5			735		0.149	0.141	0.0658	87.78	0.080		0.228		
Polyimide+adhesive (25μ+25μ) layer	1	30	24.5	735.0	42	693	0.442	0.050		0.0221	357.5	0.006	1.136	0.039		
L2:Copper tracking(12μm)	1	30	24.5	735.0	192	543	0.347	0.012		0.0042	14.3	0.029	8.93	0.058		
Polyimide plane	1	30	24.5	735.0	42	693	0.442	0.025		0.0111	357.5	0.003	1.136	0.020		
L3:Copper gnd plane(12μm)	1	30	24.5	735.0	87	648	0.414	0.012		0.0050	14.3	0.035	8.93	0.069		
Polyimide/adhesive (25μ+25μ) layer	1	30	24.5	735.0	0	735	0.469	0.050		0.0235	357.5	0.007	1.136	0.042		
Connector pad	1	5	25			125		0.267		0.0173	110.15	0.019		0.060		
Gold flash(0.4μm)	1	5	25	125.0	80	45	0.029	0.000		0.0000	3.35	0.000	19.3	0.000		
Nickel plating(2μm)	1	5	25	125.0	80	45	0.029	0.002		0.0001	14.7	0.000	8.845	0.001		
Photoresist (20μ) layer	0	5	25	125.0	0	125	0.080	0.020		0.0016	357.5	0.000	1.136	0.000		
L1:Copper(12μm)+TH plating(13μm)	1	5	25	125.0	80	45	0.029	0.025		0.0007	14.3	0.005	8.93	0.010		
Polyimide/adhesive (25μ+25μ) layer	1	5	25	125.0	0	125	0.080	0.050		0.0040	357.5	0.001	1.136	0.007		
L2:Copper tracking (12μm)	1	5	25	125.0	105	20	0.013	0.012		0.0002	14.3	0.001	8.93	0.002		
Polyimide layer(25μm)	1	5	25	125.0	0	125	0.080	0.025		0.0020	357.5	0.001	1.136	0.004		
L3:Copper gnd plane (12μm)	1	5	25	125.0	75	50	0.032	0.012		0.0004	14.3	0.003	8.93	0.005		
Polyimide/adhesive (25μ+25μ) layer	1	5	25	125.0	0	125	0.080	0.050		0.0040	357.5	0.001	1.136	0.007		
L4:Copper(12μm)+TH plating (13μm)	1	5	25	125.0	80	45	0.029	0.025		0.0007	14.3	0.005	8.93	0.010		
Polyimide cover+adhesive (13μ+33μ) layer	2	5	25	125.0	0	125	0.080	0.046		0.0037	357.5	0.002	1.136	0.013		
Substrate	2	74.6	21			1566.6		0.337		0.3108	199.42	0.338		2.345		2.368
CC	2	74.6	21	1566.6	0	1567	1.000	0.300		0.3000	218.10	0.275	2.0385	1.916		
CC "step"	4	4	21	84.0	0	84	0.054	0.500		0.0268	218.10	0.049	2.0385	0.342		
Parylene top layer (10 μm)	2	74.6	21	1566.6	105	1462	0.933	0.010		0.0093	286	0.007	1.42	0.042		
Parylene bottom layer (10 μm)	2	74.6	21	1566.6	0	1567	1.000	0.010		0.0100	286	0.007	1.42	0.044		
Substrate-hybird adhesive	2	74.6	21			1566.6		0.100		0.0500	277.80	0.072		0.312		
Conductive adhesive (7% area)	2	74.6	21	1566.6	1462	105	0.067	0.050		0.0034	42.77	0.016	3.68	0.039		
Thermal adhesive (93% area)	2	74.6	21	1566.6	105	1462	0.933	0.050		0.0466	165.65	0.056	1.87	0.273		
Total	**1**					**1566.6**				**0.681**	**59.27**	**1.150**		**4.683**		

k4polymer

Figure 9 Radiation length and weight of the barrel hybrid (version 4)

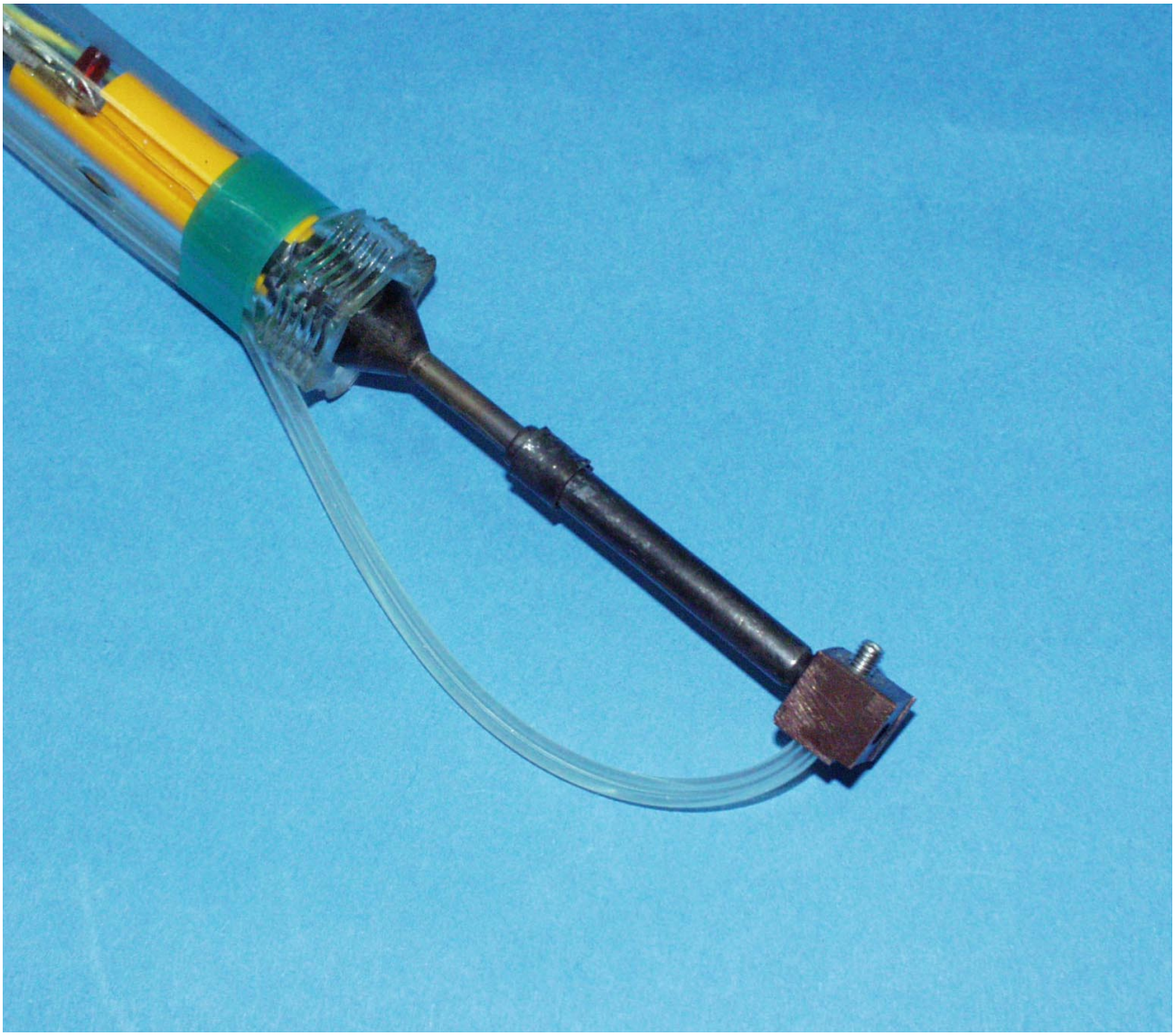

Figure 10 An ASIC replacement jig

SCT Barrel Module FDR Document

SCT Barrel Module : ASICs

Abstract

This document summarises the requirements and target design specifications for the front-end ASIC (ABCD3T), procedures and criteria used for qualification of the ABCD3T chips and parameters of the ABCD3T chips delivered to the SCT Production Database.

Prepared by :	*Checked by :*	*Approved by :*
W. Dabrowski		

History of Changes

Rev. No.	*Date*	*Pages*	*Description of Changes*
1	22/04/01	30	
2	30/04/01	31	Brief description of ABCD2T, ABCD3T and ABCD3TA versions added.

Table of Contents

1 SCOPE OF THE DOCUMENT

In this document we summarise:

- **the requirements and target design specifications for the front-end ASIC (ABCD3T) to be used in the binary readout architecture of silicon strip detectors in the ATLAS Semiconductor Tracker (SCT),**
- **procedures and criteria used for qualification of the ABCD3T chips,**
- **parameters and characteristics of the ABCD3T chips delivered to the SCT Production Database.**

The content of this document is based on two working documents on ASICs, in which more detailed information is available:

1. **ABCD Chip, Project Specification, Version V1.2.**
2. **Testing specification for the wafer screening. Project Name: ABCD3T ASIC. Version: V1.4, 20 April, 2001.**

The ABCD3T design is based upon the ABCD2T prototype chip which was a major step in development of the front-end ASIC. Satisfactory matching of thresholds, a critical parameter for the binary architecture, has been achieved in the ABCD2T design by implementation of individual threshold correction in every channel using 4-bit digital-to-analogue converter (TrimDAC) per channel. The ABCD2T version has met all basic requirements of the ATLAS SCT, however, in the front-end circuit we have identified two points which compromised performance of that prototype, namely: (i) the internal calibration circuitry showed non-linearity for low input charges, (ii) TrimDACs response curves appeared to be non-linear and exhibited large spread from channel-to-channel. Furthermore, extensive radiation tests showed that after proton irradiation up to a fluence of 3×10^{14} cm^{-2} the spread of the threshold offsets increased by a factor of 3 and exceeded the range of the TrimDACs.

The sources of non-linearity of the calibration circuit and of the TrimDAC circuit have been identified and the designs of these two blocks have been corrected in the ABCD3T version. The resolution of the TrimDAC in the ABCD3T design remains 4 bits. In order to not compromise the resolution of the TrimDAC, i.e. achievable uniformity of thresholds for non-irradiated chips, and to guarantee that for fully irradiated chips all the channels can be corrected, 4 selectable ranges of the TrimDAC have been implemented in the ABCD3T design.

Irradiation tests of the ABCD3T chips showed that the circuitry responsible for loading the range of the TrimDAC was not sufficiently robust and in some fraction of chips the required ranges could not be loaded correctly. A minor correction in the design, resulting in the ABCD3TA version, has been implemented after receiving two batches of the pre-production series. In the second part of the pre-production series the ABCD3TA version was manufactured. The correction implemented in the ABCD3TA has absolutely no impact on the chip performance before irradiation and it is not visible for the users at all as long as the basic range of the TrimDAC is used.

2 DESIGN SPECIFICATION OF THE ABCD3T IC.

2.1 REQUIREMENTS

2.1.1 GENERAL

The chip must provide all functions required for processing of signal from 128 strips of a silicon strip detector in the ATLAS experiment employing the binary readout architecture. The simplified block diagram of the chip is shown in Figure 2.1. The main functional blocks are:

front-end, input register, pipeline, derandomizing buffer, command decoder, readout logic, threshold&calibration control.

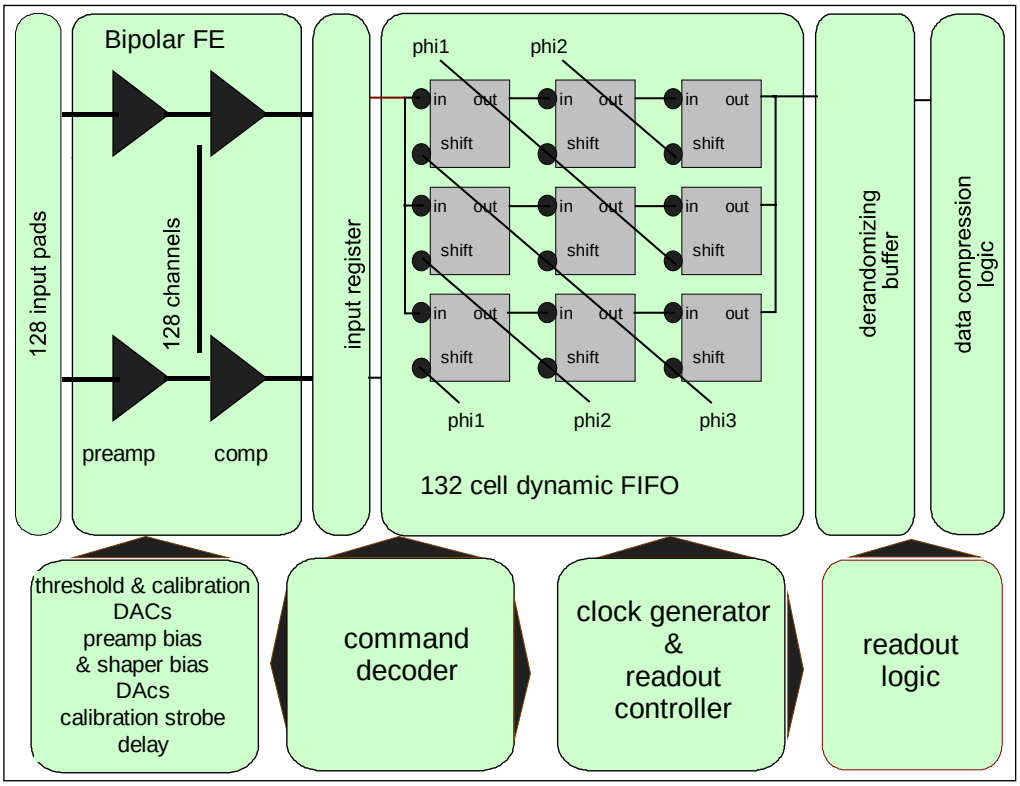

Figure 2.1: Block diagram of the ABCD3T IC.

2.1.2 SIGNAL PROCESSING.

The chip must contain following functions:

- **Charge integration**
- **Pulse shaping**
- **Amplitude discrimination. The threshold value for the amplitude discrimination is provided as a differential voltage either from internal programmable DAC or from an external source.**
- **The outputs of the discriminators must be latched either in the edge sensing mode or in the level sensing mode.**
- **At the start of each clock cycle the chip must sample the outputs from the discriminators and store these values in a pipeline until a decision can be made whether to keep the data.**
- **Upon receipt of a L1 Trigger signal the corresponding set of values together with its neighbours are to be copied into the readout buffer serving as a derandomizing buffer.**
- **The data written into the readout buffer is to be compressed before being transmitted off the chip.**
- **Transmission of data from the chip will be by means of token passing and must be compatible with the ATLAS protocol.**
- **The chip is required to provide reporting of some of the errors that occur:**
- **Attempt to read out data from the chip when no data is available.**
- **Readout Buffer Overflow: The readout buffer is full and data from the oldest event(s) has been overwritten.**
- **Readout Buffer Error: The readout buffer is no longer able to keep track of the data held in it. (Chip reset required).**

- **Configuration error (ChipID sent).**
- **The chip shall incorporate features that will enable the system to continue operating in the event of a single chip failure.**

It is a system requirement that the fraction of data which is lost due to the readout buffer on the chip being full is less than 1%. This assumes that on average only 1% of the silicon strip detectors are hit during any particular beam crossing.

2.1.3 CALIBRATION AND TESTABILITY.

Each channel has an internal Calibration Capacitor connected to its input for purposes of simulating a "hit" strip. The Calibration Capacitors are charged by an internal chopper circuit which is triggered by a command. Every fourth channel can be tested simultaneously with group selection determined by two binary coded Calibration Address inputs (CALD0, CALD1). The strobe and the address signals are delivered from the control circuitry. The voltage applied to the Calibration Capacitors by the chopper is determined by an internal DAC. The four calibration bus lines, each of which connects the calibration capacitors of every fourth channel, are also brought out to pads which can be directly driven with an AC coupled voltage step. This is intended for use during IC testing. A tuneable delay of the calibration strobe with respect to the clock phase covering at least two clock periods must be provided. The chip must incorporate such features that will enable to test and calibrate it either on the wafer level or in situ.

2.2 DESIGN SPECIFICATION

2.2.1 DETECTOR PARAMETERS

The parameters of the analogue front-end part are specified for the electrical parameters of 12.8 cm long p-type silicon strip detector. The assumed detector parameters are listed in Table 1.

Table 2.1: Assumed detector electrical parameters.

	Unirradiated	Irradiated
Coupling type to amplifier	AC	AC
Coupling capacitance to amp Total for 12 cm strips	20 pF/cm 240 pF	20 pF/cm 240 pF
Capacitance of strip to all neighbour strips	1.03 pF/cm	1.40 pF/cm
Capacitance of strip to backplane	0.30 pF/cm	0.30 pF/cm
Metal strip resistance	15 Ω/cm	15 Ω/cm
Bias Resistor	0.75 MΩ	0.75 MΩ
Max leakage current per strip for shot noise	2.0 nA	2.0 μA
Charge collection time	< 10 ns	< 10 ns

2.2.2 FRONT-END

2.2.2.1 ELECTRICAL REQUIREMENTS:

Note that notation convention for currents used in the entire specification is "+" for current going into (sunk by) the chip and "-" for current going out of (sourced from) the chip.

2.2.2.2 INPUT CHARACTERISTICS:

Input Signal Polarity: **Positive signals from p-type strips.**

Crosstalk: **< 5% (via detector interstrip capacitance)**

Input Protection: **Must sustain voltage step of 450 V of either polarity with a cumulative charge of 5 nC in 25 ns.**

Open Inputs: **Any signal input can be open without affecting performance of other channels.**

Max Parasitic Leakage Current: **100 nA DC per channel with < 10 % change in gain at 1 fC input charge.**

2.2.2.3 PREAMPLIFIER-SHAPER CHARACTERISTICS

Gain at the discriminator input: **50 mV/fC for the nominal shaper current of 20 μA and the nominal process parameters**

Linearity: **better than 5% in the range 0 - 4 fC**

Peaking time: **20 ns**

Noise: **Maximum rms noise for nominal components as measured on fully populated modules**

<= 1500 electrons rms for unirradiated module

<= 1800 electrons rms for irradiated module

Gain Sensitivity to VCC for 1 fC signal: **1%/100mV**

2.2.2.4 COMPARATOR STAGE:

A threshold is applied as a differential voltage offset to the comparator stage. This threshold voltage is applied from an internal DAC in the normal operation mode or can be applied from the external pads for test purposes.

Threshold setting range: **0 fC to 12.8 fC , nominal setting at 1 fC**

Threshold setting step: **0.05 fC of input charge around nominal threshold of 1 fC**

Threshold variation at 1 fC: **(1 sigma) channel to channel matching within one chip vs Range Set of TrimDACs by 2 bits in the Configuration Register.**

min (00)	**2.5%**
x2 (01)	**5.0%**
x3 (10)	**7.5%**
x4 (11)	**10%**

2.2.2.5 TIMING REQUIREMENTS:

Timewalk: **<= 16 ns. This specification depends on the precision of the digital acquisition latch edge. Good alignment, 1 or 2 ns over a common clocked array of channels implies a longer timewalk assignment to the rising edge of the shaped signal.**

Timewalk defined: **The maximum time variation in the crossing of the time stamp threshold over a signal range of 1.25 to 10 fC, with the comparator threshold set to 1 fC.**

Double Pulse Resolution: **<= 50 ns for a 3.5 fC signal followed by a 3.5 fC signal**

Max recovery time for a 3.5 fC signal following a 80 fC signal: **1 μs**

2.2.2.6 THRESHOLD GENERATION CIRCUIT

Differential voltage for the discriminator threshold is generated by an internal DAC circuit (Threshold DAC). The threshold voltages generated by the internal circuit are applied to the same pads VTHP and VTHN to which the external threshold is applied. When the external threshold is not applied the internal threshold voltage can be measured at pads VTHP and VTHN.

Range: **0 - 640 mV**

Step value: **2.5 mV**

Absolute accuracy: **1%**

2.2.2.7 CALIBRATION CIRCUIT CHARACTERISTICS

Calibration signal can be applied to one of the four calibration lines via the external pads or from the internal calibration circuit. In the later case the address of the calibration line, the amplitude of the calibration signal and its delay is set via the control logic.

Calibration Capacitors:	**100 fF ±20% (3 sigma) over full production skew ±2% (3 sigma) within one chip.**
Calibration signal:	
amplitude range:	**0 - 160 mV (charge range: 0 - 16 fC)**
amplitude step:	**0.625 mV (charge step: 0.0625 fC)**
Absolute accuracy of amplitude:	**5% (full process skew)**
Relative accuracy of amplitude:	**< 2 % (for known values of calibration capacitors, amplitude range 0.8 to 4 fC, across one chip, including switching pickup, etc.)**
Relative accuracy of amplitude:	**< 10 % (for known values of calibration capacitors, amplitude range 0.8 to 8 fC, across one chip, including switching pickup, etc.)**

Calibration Strobe signal pickup at comparator should be less than 0.1 fC equivalent sensor input.

For test purposes, a voltage step can be applied directly to any one of the four groups of calibration capacitor via the input pads (CAL0, CAL1, CAL2, CAL3). When not used, these four pads must be left floating.

2.2.2.8 THRESHOLD CORRECTION CIRCUIT

In order to compensate channel-to-channel variation of the discriminator offset each channel is provided with a trim DAC of 4-bit resolution. Each channel can be addressed individually and the threshold correction can be applied channel by channel. The range of the trim DAC can be selected with two bits in the configuration register. This is to cover the offset spread which is expected to increase after irradiation. The selectable ranges and corresponding steps of the TrimDAC are:

Trim DAC range	Trim DAC step
0 mV - 60 mV	**4 mV**
0mV -120 mV	**8 mV**
0mV -180 mV	**12 mV**
0mV -240 mV	**16 mV**

2.2.3 DATA READOUT AND REDUNDANCY

The figure below shows the data and token interconnections on a typical silicon detector module. The module has 6-ABCD chips on each side. The datalink outputs of 2 of these chips are connected to a fibre-optic interface and are configured to act as Masters in controlling the readout of data from each side of the module. On the diagrams the Master chips are denoted by a "M" and all the other chips are configured to act as slaves as denoted by a "S" or "E' on the diagram.

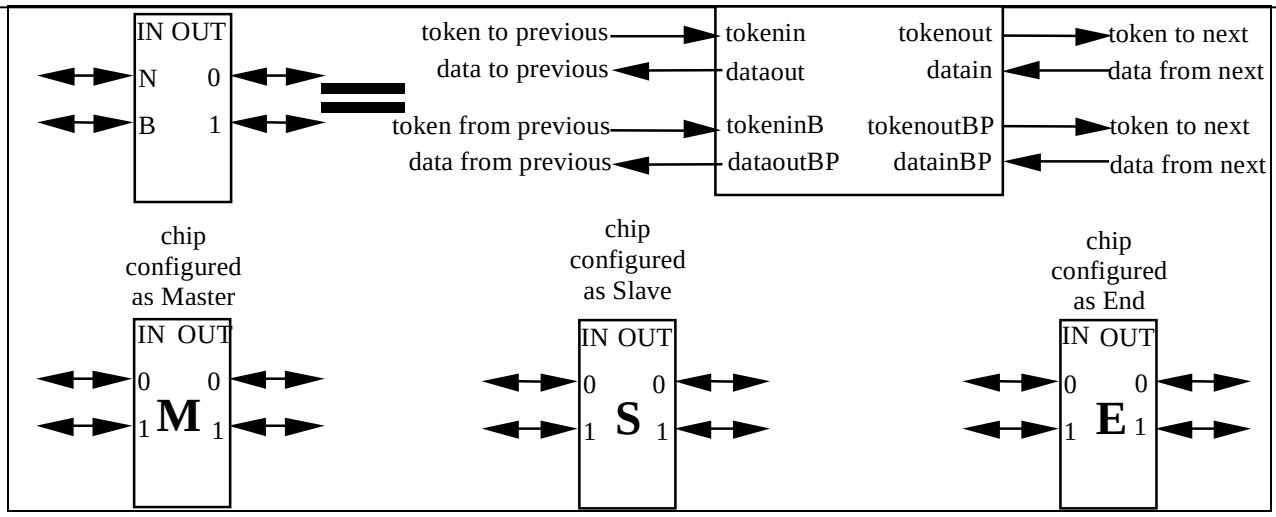

Figure 2.2: Key to symbols used in following Diagrams.

After the receipt of a L1 Trigger, the Master chip initiates a readout cycle by sending the pre-amble bits at the start of each data block to the optical link driver. It then appends its data bits to the output stream sent to the optical link driver. A few clock cycles before the last bit has been sent, it sends a token to the slave chip on it's right. The slave chip on the right responds by sending its data packet to the Master which in turn is appended to the pre-amble and data bits from the Master already sent to the optical link driver.

Once this slave chip has finished sending its data, it also passes on the token to the next chip on the right. The next chip on the right passes its data onto the previous chip on the left which in turn passes it back to the Master chip for transmission to the LED driver. This process continues until the last chip in the chain has sent its data.

A bit is set in the last chip in the chain to inform it that it is the last chip (these chips are shown as 'E' on the diagrams). When this chip has sent its data it appends a trailer to the end of the data stream. While the Master chip is outputting data, it is constantly looking for the trailer pattern which has been carefully chosen to be distinct from the data. Once it finds the trailer pattern, it knows that all the data from the event has been sent and it can start processing the next event.

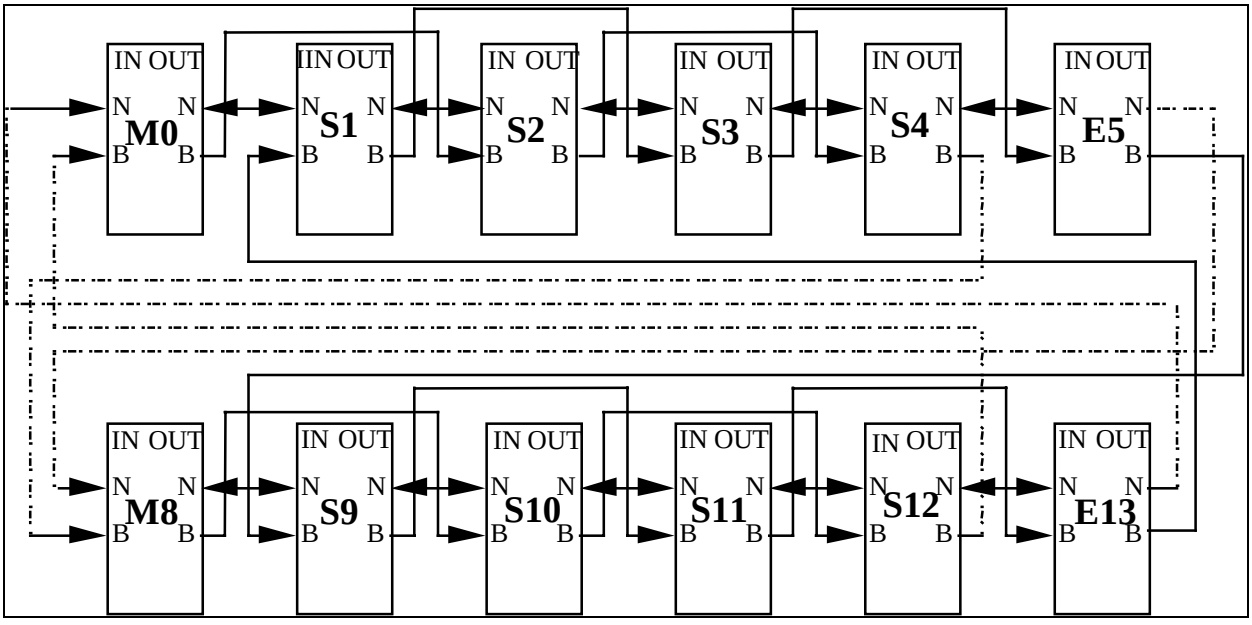

Figure 2.3: Diagram Showing the Interconnection of ABCD chips on a Silicon Detector Module.

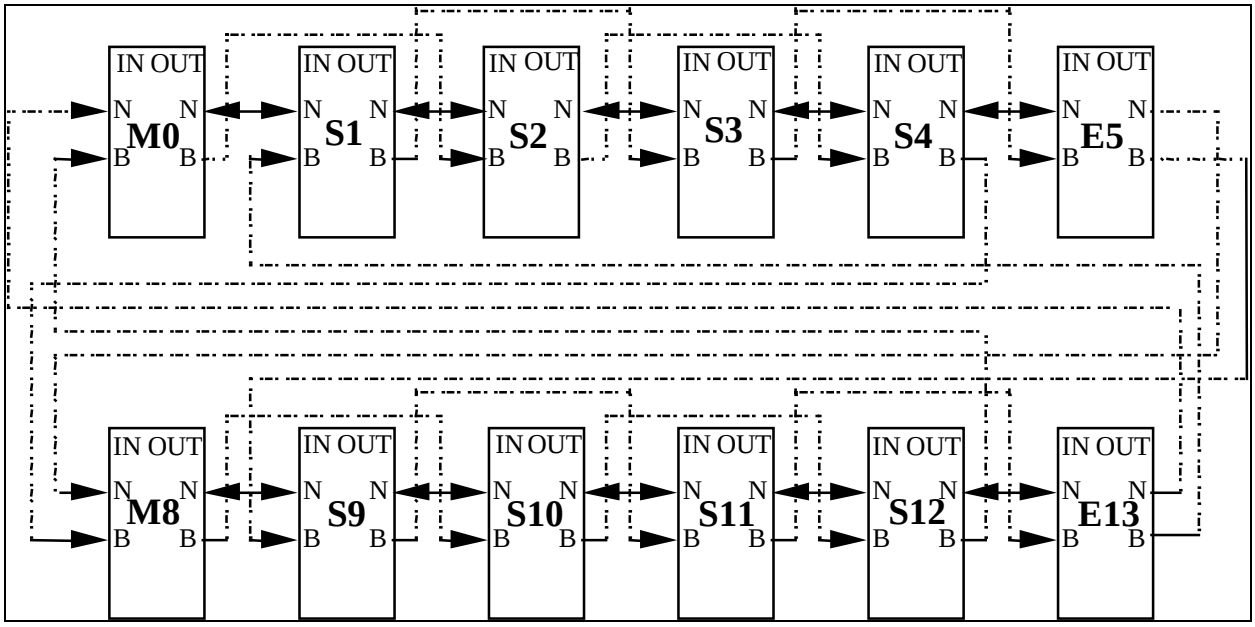

Figure 2.4: Diagram Showing the normal flow of Data and Tokens between chips.
(Active links are highlighted with solid lines.)

In the event of the failure of one of the Slave chips, the previous and next slave chips in the chain are programmed to route their data and tokens around the failed chip. If the last chip in the chain should fail, then the penultimate chip in the chain is programmed to perform the operation of the "End chip".

In the event of the failure of a Master chip in the chain, the data and tokens from the chain with the failed Master chip are routed to the working master chip as shown in the next diagram .

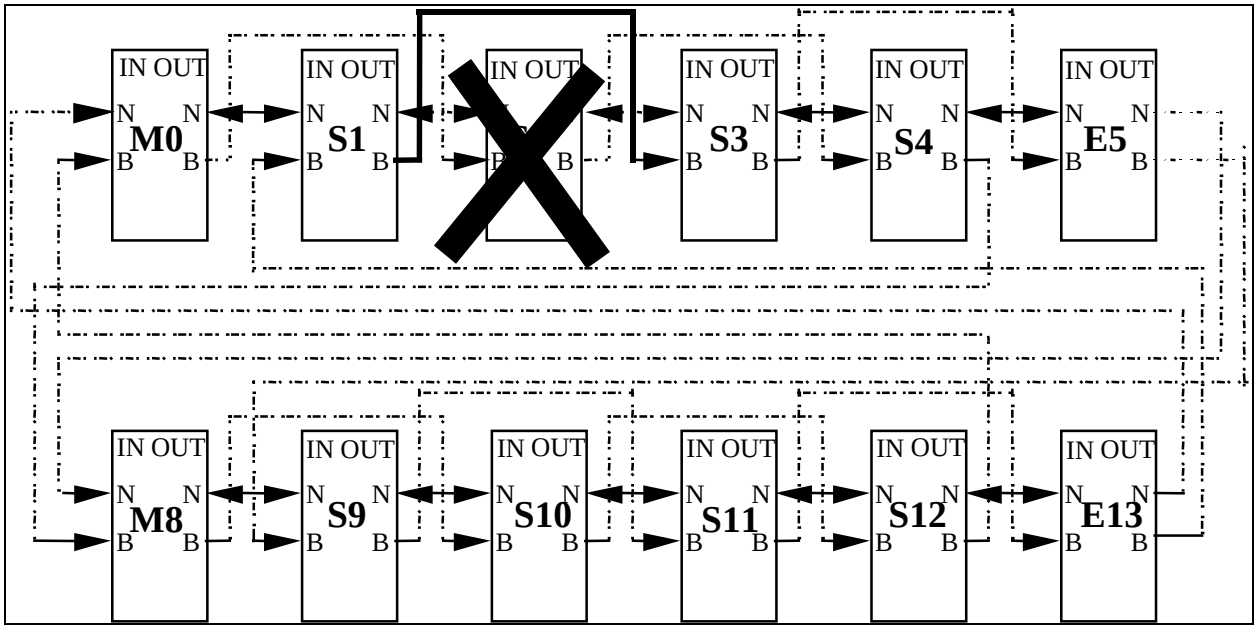

Figure 2.5: Diagram Showing the flow of Tokens and Data in the event of the failure of a Slave ABCD chip.

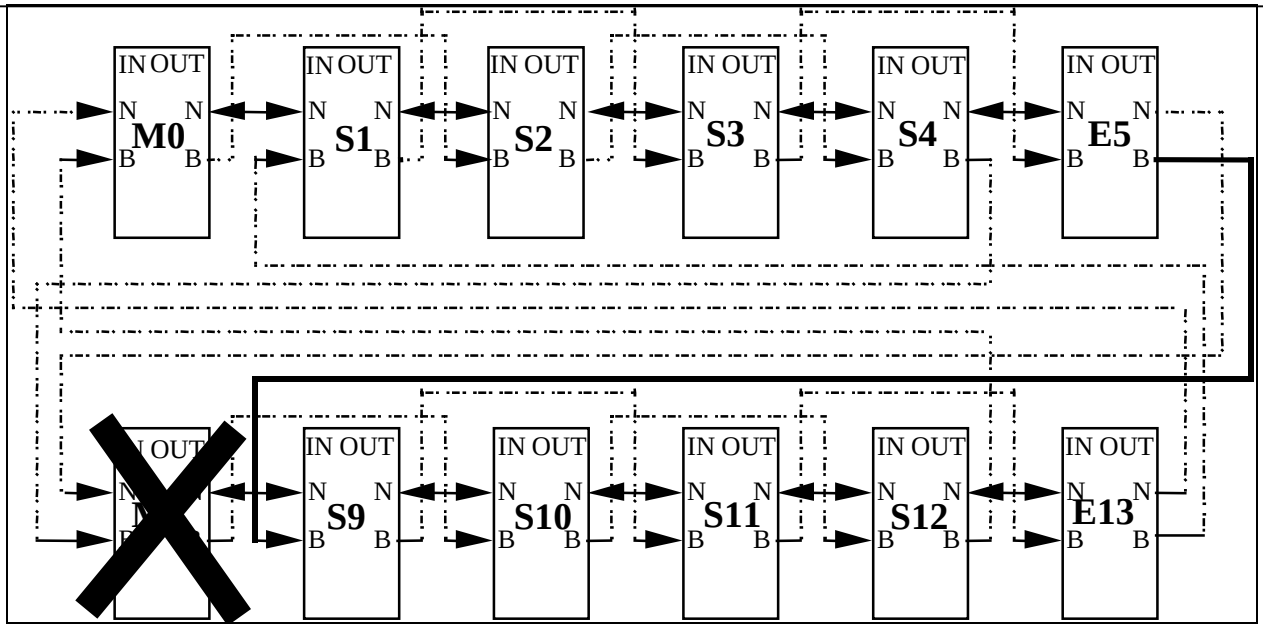

Figure 2.6: Diagram Showing the flow of Tokens and Data in the event of the failure of a Master ABCD chip.

2.2.3.1 MASTER/SLAVE SELECTION

The default state of the chip on power up is determined by the state on the masterB input pin. If this pin has been left unconnected or tied high, the chip will power-up as a Slave. If this pin has been tied to ground, the chip will power up as a Master. If the chip is configured as a Mater on power up it may be re-configured as a slave. However if the chip has been configured as a slave on power up it may not be re configured as a master.

2.2.4 INPUT/OUTPUT CONNECTIONS

The following tables describes the names and function of the various Input/Output connections to the chip.

Table 2.2: Input Signals.

Name	**Function**	**Type**
clk0 & clk1	Clock input	LVDS
clk0B & clk1B	Complement of above signal	LVDS
com0 & com1	Command Input	LVDS
com0B & com1B	Complement of above signal	LVDS
tokenin & tokeninBP	Token Input	Current Mode
tokeninB & tokeninBPB	Complement of above signal	Current Mode
datain & datainBP	Data Input	Current Mode
datainB & datainBPB	Complement of above signal	Current Mode
ID<5:0>	Geographical address of chip	CMOS
masterB	Sets chip default to master	CMOS
select	Selects clock/command inputs	CMOS
resetB	Resets Chip	CMOS

Table 2.3: Default settings of CMOS input signals.

Name	**Function**	**Default setting**
ID<4>	Geographical address of chip	Low, pull-down with 300 kOhm
ID<3:0>	Geographical address of chip	High, pull-up with 100 kOhm
masterB	Sets chip default to master	High, pull-up with 100 kOhm
select	Selects clock/command inputs	Low, pull-down with 300 kOhm
resetB	Resets Chip	High, pull-up with 300 kOhm

Table 2.4: Output Signals.

Name	**Function**	**Type**
tokenout, tokenoutBP	Token Output	Current Mode
tokenoutB, tokenoutBPB	Complement of above	Current Mode
dataout, dataoutBP	Data Output	Current Mode
dataoutB, dataoutBPB	Complement of above	Current Mode
datalink	Data Output to optical link driver	LVDS
datalinkB	Complement of above	LVDS

2.2.5 DC SUPPLY AND CONTROL CHARACTERISTICS:

Table 2.5: DC supply voltages.

	Pad Name	**Absolute Min**	**Min**	**Nominal**	**Max**	**Absolute Max**
Analogue Supply	VCC	0 V	3.3 V	3.5 V	3.7 V	5.5 V
Analogue Ground	GNDA			0 V		
Input transistor current*	Set by internal DAC	0 μA	100 μA	200 μA	300 μA	400 μA
Input transistor current monitor	IP_PR	$V_{ip} = I_p$ x 250 Ω				
Shaper current *	Set by internal DAC	0 μA	10 μA	15 μA	30 μA	50 μA
Shaper current monitor	IS_PR	$V_{is} = I_{sh}$ x 10 kΩ				
Discriminator threshold	VTHP	0 V	3.3 V	3.5 V	3.7 V	VCC
Discriminator threshold	VTHN	0 V	3.25 V	3.45 V	3.65 V	VCC
(VTHP - VTHN)		0 V	0 V	0.05 V	0.5 V	1.0 V
Digital Supply **	VDD	0 V	3.8 V	4.0 V	4.2 V	5.5 V
Digital Ground	DGND			0 V		

*** The Min/Max values define the range of the bias currents for which the front-end circuit will be biased correctly and will amplify the input signal. The absolute Min/Max values are the values which can be delivered from the internal DACs. The absolute Max values cover the worst case combination of corner process parameters and operating conditions.**

**** For the on chip power-up reset to operate correctly the VDD power supply must be ramped up to 90% of its final value in less than 10 ms.**

The current draw at each DC input is as follows.

Table 2.6: DC supply currents for the nominal voltage supplies (VCC=3.5V, VDD=4.0V) and nominal operating conditions.

		Min	**Nominal**	**Max**
Analogue Supply	VCC	50 mA	75 mA	100 mA
Analogue Ground	GNDA	-50 mA	-75 mA	-100 mA
Digital Supply*	VDD	32 mA	36 mA	41 mA
Digital Ground	DGND	-32 mA	-36 mA	-41 mA
Discriminator threshold**	VTHP	0.3 μA	0.5 μA	1.5 μA
Discriminator threshold**	VTHN	0.3 μA	0.5 μA	1.5 μA

***In the Master chip the current draw at VDD power supply will be approximately 20 mA higher compared to the values shown in the table.**

**** If threshold voltages applied from external pads and the TrimDACs are set to zero.**

Table 2.7: Current draws at power supply inputs: nominal and absolute min/max values which may occur in non-standard operating conditions, e.g. all bias DACs set at zero or to full range, clock not supplied to the chips.

		Absolute Min	**Nominal**	**Absolute Max**
Analogue Supply	VCC	2 mA	75 mA	110 mA
Digital Supply	VDD	10 mA (30 mA)*	36 mA (56 mA)*	43 mA[#] (63 mA)* [#]

[#]Maximum current expected for the VDD power supply of 4.2 V

***Current draws by the Master chip**

Table 2.8: Current draws by the fully loaded module: nominal and min/max values are specified for the normal operating conditions and nominal supply voltages, absolute min/max values may occur in non-standard operating conditions, e.g. all bias DACs set at zero or to full range, clock not supplied to the chips.

		Absolute Min	**Min**	**Nominal**	**Max**	**Absolute Max**
Analogue Supply	VCC	24 mA*	600 mA	900 mA	1200 mA	1320 mA
Digital Supply	VDD	140 mA*	360 mA	400 mA	450 mA	470 mA[#]
Total power		0.58 W*	3.54 W	4.75 W	6.0 W	7.0 W

*** For the absolute minimum values it is assumed that all 12 chips on the module are connected to the power lines and none of them is damaged. The power consumption is calculated for the minimum supply voltages: VCC = 3.3V and VDD = 3.8V**

[#]Maximum current expected for the VDD power supply of 4.2 V.

2.2.6 BOND PAD ARRANGEMENT

Table 2.9: Bond Pad Position with respect to the origin at the lower left corner (detgnd pad).

Pad Name	**Pad Centre (x,y)**	**Pad Size (x x y)**	**Pad Name**	**Pad Centre (x,y)**	**Pad Size (x x y)**
INPUT PADS					
detgnd	(65,6266)	120x43	in<127>	(266,6218)	120x43
in<126>	(65,6170)	120x43	in<125>	(266,6122)	120x43
in<124>	(65,6074)	120x43	in<123>	(266,6026)	120x43
in<122>	(65,5978)	120x43	in<121>	(266,5930)	120x43
in<120>	(65,5882)	120x43	in<119>	(266,5834)	120x43
in<118>	(65,5786)	120x43	in<117>	(266,5738)	120x43
in<116>	(65,5690)	120x43	in<115>	(266,5642)	120x43
in<114>	(65,5594)	120x43	in<113>	(266,5546)	120x43
in<112>	(65,5498)	120x43	in<111>	(266,5450)	120x43
in<110>	(65,5402)	120x43	in<109>	(266,5354)	120x43
in<108>	(65,5306)	120x43	in<107>	(266,5258)	120x43
in<106>	(65,5210)	120x43	in<105>	(266,5162)	120x43
in<104>	(65,5114)	120x43	in<103>	(266,5066)	120x43
in<102>	(65,5018)	120x43	in<101>	(266,4970)	120x43

in<100>	(65,4922)	120x43	in<99>	(266,4874)	120x43
in<98>	(65,4826)	120x43	in<97>	(266,4778)	120x43
in<96>	(65,4730)	120x43	in<95>	(266,4682)	120x43
in<94>	(65,4634)	120x43	in<93>	(266,4586)	120x43
in<92>	(65,4538)	120x43	in<91>	(266,4490)	120x43
in<90>	(65,4442)	120x43	in<89>	(266,4394)	120x43
in<88>	(65,4346)	120x43	in<87>	(266,4298)	120x43
in<86>	(65,4250)	120x43	in<85>	(266,4202)	120x43
in<84>	(65,4154)	120x43	in<83>	(266,4106)	120x43
in<82>	(65,4058)	120x43	in<81>	(266,4010)	120x43
in<80>	(65,3962)	120x43	in<79>	(266,3914)	120x43
in<78>	(65,3866)	120x43	in<77>	(266,3818)	120x43
in<76>	(65,3770)	120x43	in<75>	(266,3722)	120x43
in<74>	(65,3674)	120x43	in<73>	(266,3626)	120x43
in<72>	(65,3578)	120x43	in<71>	(266,3530)	120x43
in<70>	(65,3482)	120x43	in<69>	(266,3434)	120x43
in<68>	(65,3386)	120x43	in<67>	(266,3338)	120x43
in<96>	(65,3290)	120x43	in<65>	(266,3242)	120x43
in<64>	(65,3194)	120x43	in<63>	(266,3146)	120x43
in<62>	(65,3098)	120x43	in<61>	(266,3050)	120x43
in<60>	(65,3002)	120x43	in<59>	(266,2954)	120x43
in<58>	(65,2986)	120x43	in<57>	(266,2858)	120x43
in<56>	(65,2810)	120x43	in<55>	(266,2762)	120x43
in<54>	(65,2714)	120x43	in<53>	(266,2666)	120x43
in<52>	(65,2618)	120x43	in<51>	(266,2570)	120x43
in<50>	(65,2522)	120x43	in<49>	(266,2474)	120x43
in<48>	(65,2426)	120x43	in<47>	(266,2378)	120x43
in<46>	(65,2330)	120x43	in<45>	(266,2282)	120x43
in<44>	(65,2234)	120x43	in<43>	(266,2186)	120x43
in<42>	(65,2138)	120x43	in<41>	(266,2090)	120x43
in<40>	(65,2042)	120x43	in<39>	(266,1994)	120x43
in<38>	(65,1946)	120x43	in<37>	(266,1898)	120x43
in<36>	(65,1850)	120x43	in<35>	(266,1802)	120x43
in<34>	(65,1754)	120x43	in<33>	(266,1706)	120x43
in<32>	(65,1658)	120x43	in<31>	(266,1610)	120x43
in<30>	(65,1562)	120x43	in<29>	(266,1514)	120x43
in<28>	(65,1466)	120x43	in<27>	(266,1418)	120x43
in<26>	(65,1370)	120x43	in<25>	(266,1322)	120x43

in<24>	(65,1274)	120x43	in<23>	(266,1226)	120x43
in<22>	(65,1178)	120x43	in<21>	(266,1130)	120x43
in<20>	(65,1082)	120x43	in<19>	(266,1034)	120x43
in<18>	(65,986)	120x43	in<17>	(266,938)	120x43
in<16>	(65,890)	120x43	in<15>	(266,842)	120x43
in<14>	(65,794)	120x43	in<13>	(266,746)	120x43
in<12>	(65,698)	120x43	in<11>	(266,650)	120x43
in<10>	(65,602)	120x43	in<9>	(266,554)	120x43
in<8>	(65,506)	120x43	in<7>	(266,458)	120x43
in<6>	(65,410)	120x43	in<5>	(266,362)	120x43
in<4>	(65,314)	120x43	in<3>	(266,266)	120x43
in<2>	(65,218)	120x43	in<1>	(266,170)	120x43
in<0>	(65,122)	120x43	detgnd	(266,74)	120x43
detgnd	(65,26)	120x43			
FRONT-END SERVICE PADS					
detgnd	(596,74)	200x140	detgnd	(596,6221)	200x140
GNDA	(896,74)	200x140	GNDA	(896,6221)	200x140
VCC	(1196,74)	200x140	VCC	(1196,6221)	200x140
VTHN	(1446,74)	100x140	VTHN	(1446,6221)	100x140
VTHP	(1646,74)	100x140	VTHP	(1646,6221)	100x140
ring_a	(1846,74)	100x140	ring_a	(1846,6221)	100x140
D_ISH	(2046,74)	100x140	cal0	(2046,6221)	100x140
IP_PROBE	(2246,74)	100x140	cal1	(2246,6221)	100x140
IS_PROBE	(2446,74)	100x140	cal2	(2446,6221)	100x140
			cal3	(2646,6221)	100x140
BYPASS PADS					
			tokenoutBPB	(5211,6211)	100x160
			tokenoutBP	(5543,6211)	100x160
			datainBPB	(5875,6211)	100x160
			datainBP	(6207,6211)	100x160
tokeninBPB	(6522,84)	100x160	**Spare digital bias pads**		
tokeninBP	(6854,84)	100x160	DGND	(6540,6211)	100x160
dataoutBPB	(7186,84)	100x160	VDD	(6872,6211)	100x160
dataoutBP	(7518,84)	100x160			
OUTPUT PADS					
VDD	(8069,6187)	160x180			
DGND	(8069,5914)	160x180			

tokenoutB	(8069,5688)	160x100			
tokenout	(8069,5508)	160x100			
datainB	(8069,5328)	160x100			
datain	(8069,5148)	160x100			
clk0B	(8069,4968)	160x100			
clk0	(8069,4788)	160x100			
clk1B	(8069,4608)	160x100			
clk1	(8069,4428)	160x100			
ID<4>	(8069,4238)	160x140			
ID<3>	(8069,4038)	160x140			
ID<2>	(8069,3838)	160x140			
ID<1>	(8069,3638)	160x140			
ID<0>	(8069,3438)	160x140			
masterB	(8069,3238)	160x140			
com1B	(8069,3048)	160x100			
com1	(8069,2868)	160x100			
com0B	(8069,2688)	160x100			
com0	(8069,2508)	160x100			
select	(8069,2318)	160x140			
resetB	(8069,2118)	160x140			
datalinkB	(8069,1928)	160x100			
datalink	(8069,1748)	160x100			
dataout	(8069,1568)	160x100			
dataoutB	(8069,1388)	160x100			
tokenin	(8069,1208)	160x100			
tokeninB	(8069,1028)	160x100			
DGNG	(8069,848)	160x100			
DGND	(8069,621)	160x180			
VDD	(8069,395)	160x100			
VDD	(8069,169)	160x180			

2.2.7 PHYSICAL REQUIREMENTS

The die size of the ABCD3T chip is 6550 µm x 8400 µm.

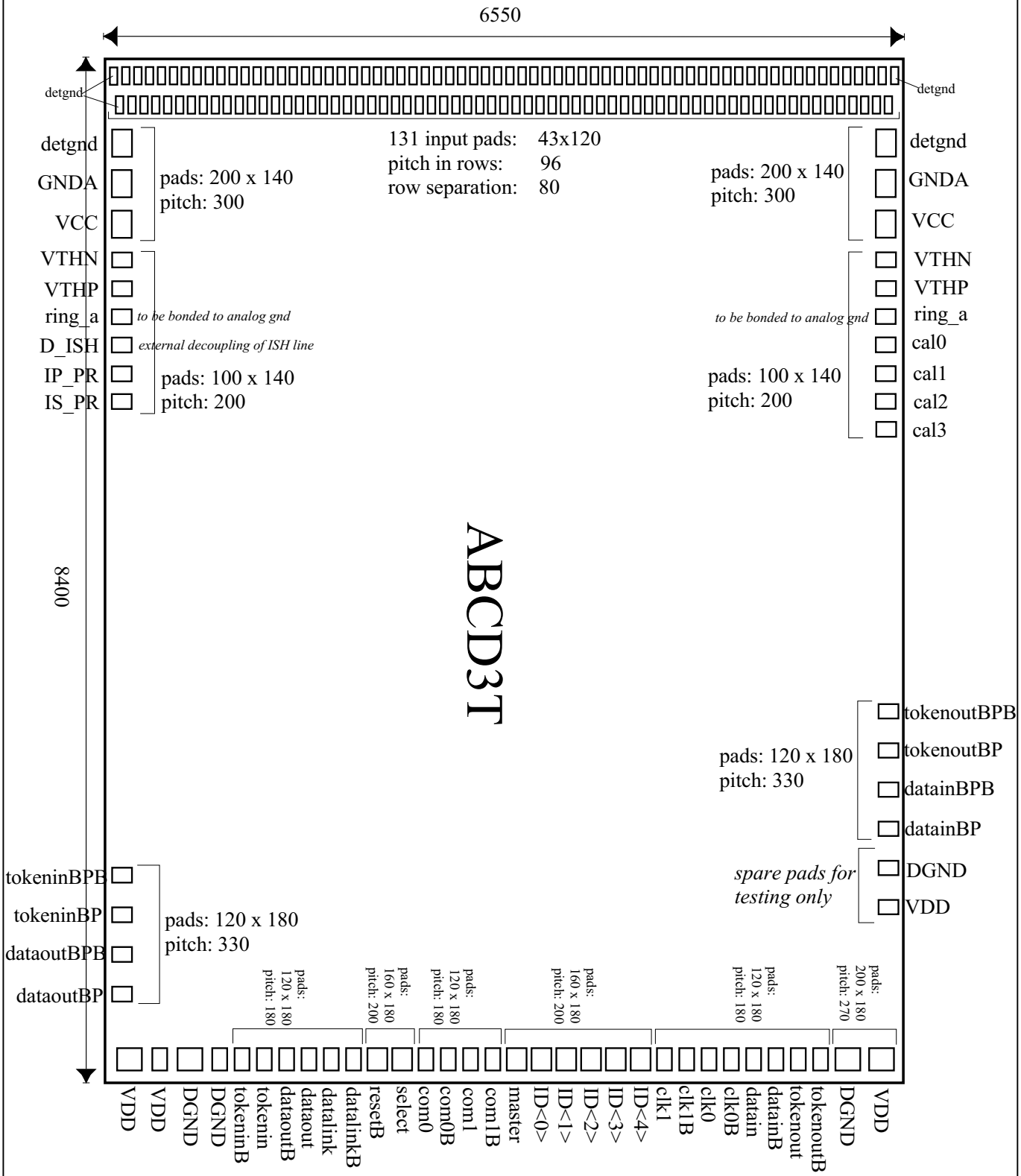

Figure 2.7: Pad Layout of the ABCD3T IC.

3 QUALIFICATION TESTING

The ABCD3T ICs are received from the foundry on untested wafers. Therefore all the chips needs to be fully tested and parameterised before dicing the wafers in order to select the chips which fulfil the SCT requirements with respect to:

- **correct functionality**
- **analogue performance**
- **speed performance of digital circuitry.**

The acceptance limits for various parameters are defined with sufficient margins allowing for degradation of parameters after full irradiation in the SCT environment

All chips are put through the full test procedure, even if they fail at some intermediate tests. The test data are then used for failure mode analyasis.

3.1 TEST FLOW

The test flow at wafer screening is shown in Figure 3.1. The test starts with the configuration register test. All the chips passing this basic digital test for the nominal condition of power supply and speed are examined and the results are saved for off-line analysis and tagging.

The following tables define the test conditions for each test.

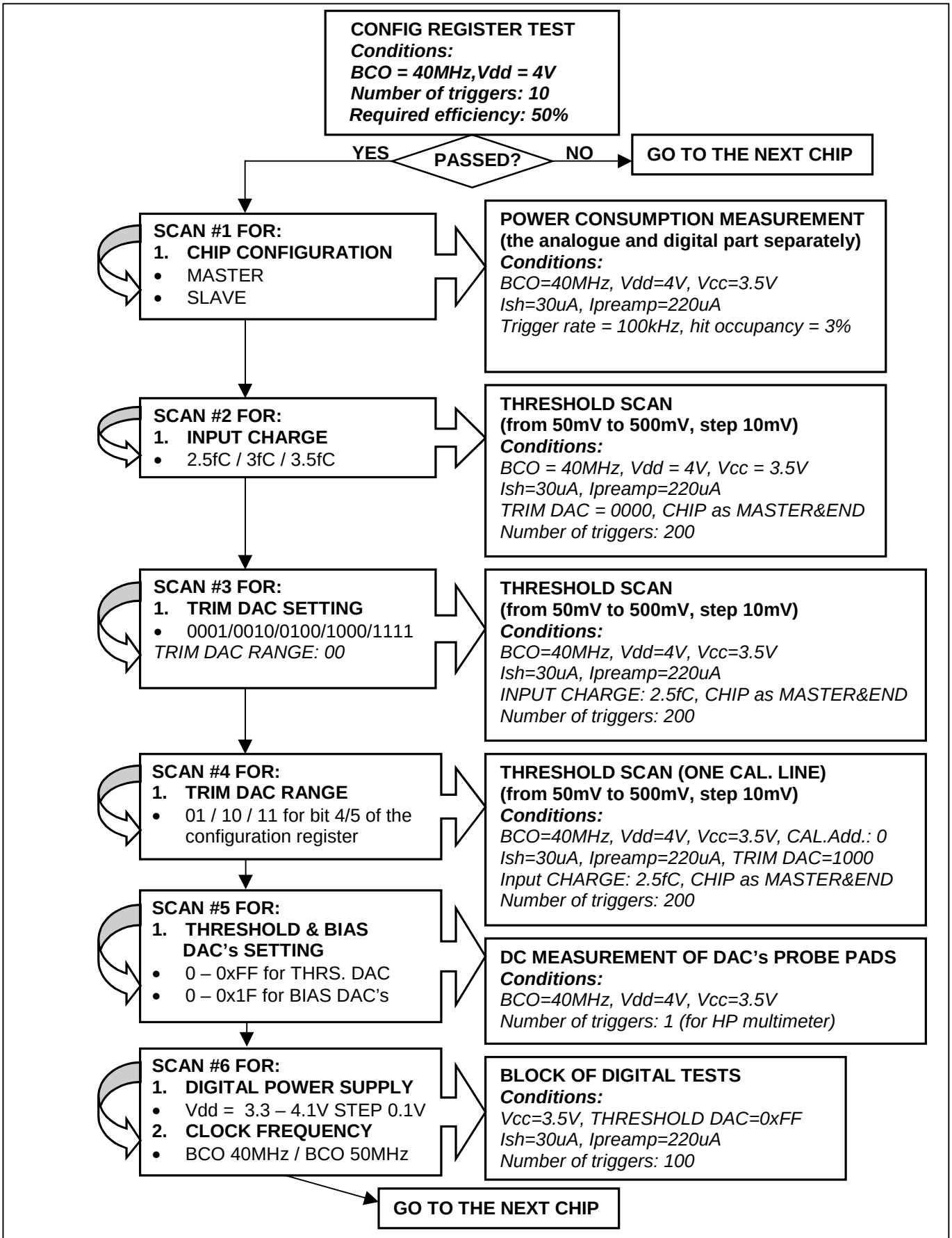

Figure 3.1: Test flow at screening of ABCD3T wafers.

3.1.1 POWER CONSUMPTION MEASUREMENT

The power consumption of both digital and analogue parts of the chip is measured. To simulate the nominal working conditions for the ATLAS SCT occupancy and L1 trigger rate, the measurement is done applying a 100kHz trigger with an occupancy of 3% (hits in 4 channels).

Table 3.1: Power consumption measurement.

SETTINGS	CHIP configuration	END | EDGE_ON | DATA_COMPRESSION_01X | DATA_TAKING_MODE | SELECT_0	
	CHIP bias	Ipreamp	220 μA
		Ishaper	30 μA
		Vcc	3.5 V
		Vdd	4 V
		BCO	40 MHz
		Threshold DAC	0xFF
	TRIM DAC	Value	0000
		Range	00
	CHIP address	Programmed = 1	
	COMMAND	Issue Calibration Pulse + 131 BCO delay + L1 trigger	
SCANS	LOOPS	1. Chip configuration = {MASTER, SLAVE}	
	Trigger rate	100 kHz	

3.1.2 ANALOGUE TESTS

3.1.2.1 MEASUREMENT OF GAIN, OFFSET AND NOISE

The goal of the test is to determine the basic analogue parameters of the front-end: gain, noise and discriminator offset for each electronic channel. For this purpose threshold scans for three values of input charge are performed for each channel.

Table 3.2: Gain, noise and offset measurement.

SETTINGS	CHIP configuration	MASTER | END | EDGE_ON | DATA_COMPRESSION_01X | DATA_TAKING_MODE | SELECT_0	
	CHIP bias	Ipreamp	220 μA
		Ishaper	30 μA
		Vcc	3.5 V
		Vdd	4 V
		BCO	40 MHz
	TRIM DAC	Value	0000
		Range	00
	CHIP address	Programmed = 1	
	COMMAND	Issue Calibration Pulse + 131 BCO delay + L1 trigger	
SCANS	LOOPS	INPUT CHARGE = {2.5fC, 3fC, 3.5fC} CALIBRATION ADDRESS = {0,1,2,3} THRESHOLD = [50mV – 500mV] step 10mV	
	No. of triggers	200	

3.1.2.2 CHARACTERIZATION OF THE TRIMDAC.

The TrimDAC response curve is measured for each channel for the basic range (00).

Table 3.3: : Characterisation of the TrimDAC.

SETTINGS	CHIP configuration	MASTER | END | EDGE_ON | DATA_COMPRESSION_01X | DATA_TAKING_MODE | SELECT_0	
	CHIP bias	Ipreamp	220 μA
		Ishaper	30 μA
		Vcc	3.5 V
		Vdd	4 V
		BCO	40 MHz
	Input Charge	2.5 fC	
	TRIM DAC	Range	00
	CHIP address	Programmed = 1	
	COMMAND	Issue Calibration Pulse + 131 BCO delay + L1 trigger	
SCANS	LOOPS	1. TRIM DAC VALUE = {0001, 0010, 0100, 1000, 1111} 2. CALIBRATION ADDRESS = {0,1,2,3} 3. THRESHOLD = [50mV – 500mV] step 10mV	
	No. of triggers	200	

3.1.2.3 CHARACTERIZATION OF THE TRIMDAC RANGE

The scan for the TRIM DAC RANGE setting is performed for one TRIM DAC value (1000). The TRIM DAC RANGE is calculated as an average of the values obtained from 32 scanned channels.

Table 3.4: Characterisation of TRIM DAC range.

SETTINGS	CHIP configuration	MASTER | END | EDGE_ON | DATA_COMPRESSION_01X | DATA_TAKING_MODE | SELECT_0	
	CHIP bias	Ipreamp	220 μA
		Ishaper	30 μA
		Vcc	3.5 V
		Vdd	4 V
		BCO	40 MHz
	CALIBRATION address	0	
	Input Charge	2.5 fC	
	TRIM DAC	Value	1000
	CHIP address	Programmed = 1	
	COMMAND	Issue Calibration Pulse + 131 BCO delay + L1 trigger	
SCANS	LOOPS	1. TRIM DAC RANGE = {01, 10, 11} 2. THRESHOLD = [50mV – 500mV] step 10mV	
	No. of triggers	200	

3.1.2.4 MEASUREMENT OF THE CHARACTERISTICS OF THE DIGITAL-TO-ANALOGUE CONVERTERS

Full response curves are measured for three DACs which provide common voltage/current for all channels in the chip:

- **Threshold DAC (8 bits)**
- **Input transistor current DAC (Ipreamp - 5 bit)**
- **Shaper current DAC (Ishaper – 5 bit).**

3.1.3 DIGITAL TESTS

Digital tests are designed to verify all digital circuitry in the ABCD3T chips and in particular to test the important functions: chip control, chip-to-chip communication and data compression. In order to determine the speed margins the digital tests are performed for different values of clock frequency and power supply.

3.1.4 TEST #1, CONFIGURATION REGISTER INPUT/OUTPUT TEST

The configuration register is written with random values, keeping the chip always as MASTER and END. The values are then compared with the data returned by the chip in the send identification mode.

Table 3.5: Configuration register input/output test.

SETTINGS	CHIP configuration	MASTER | END | SEND_ID_MODE | SELECT_0	
	CHIP bias	Ipreamp	220 μA
		Ishaper	30 μA
		Threshold DAC	0xFF
	TRIM DAC	Value	0000
		Range	00
	CHIP address	Universal address in command	
	COMMAND	L1 trigger	
SCANS	LOOPS		Random setting of the remaining configuration register bits
	No. of triggers		100

3.1.5 TEST #2, ADDRESSING TEST

The chip is given a random address and is configured using that address. The value is compared with the one returned in the chip data.

Table 3.6: Addressing test.

SETTINGS	CHIP configuration	MASTER | END | EDGE_ON | DATA_COMPRESSION_01X | SEND_ID_MODE | SELECT_0	
	CHIP bias	Ipreamp	220 μA
		Ishaper	30 μA
		Threshold DAC	0xFF
	TRIM DAC	Value	0000
		Range	00
	CHIP address	Random	
	COMMAND	L1 trigger	
SCANS	LOOPS		1. Random setting of address bits
	No. of triggers		100

3.1.6 TEST #3, INPUT REGISTER TEST

Four different patterns are loaded in the mask register and the input register is pulsed. Pulsing the input register issues one clock pulse to the channels allowed by the mask register. The data patterns read out from the chip are compared with the ones which are expected.

Table 3.7: Input register test.

SETTINGS	CHIP configuration	MASTER | END | EDGE_ON | DATA_COMPRESSION_01X | DATA_TAKING_MODE | SELECT_0	
	CHIP bias	Ipreamp	220μA
		Ishaper	30μA
		Threshold DAC	0xFF
	TRIM DAC	Value	0000
		Range	00
	CHIP address	Programmed = 1	
	COMMAND	Pulse Input Register + 129 BCO delay + L1 trigger	
SCANS	LOOPS	1. MASK = {mask#1, mask#2,mask#3,mask#4}	
	No. of triggers	100	

3.1.7 TEST #4, INPUT LINES TEST

The functionality of both input lines for the chip (basic 0 and redundant 1) is tested by injecting the four patterns through the mask register and sending the clocks and commands through both lines. The delay between SoftReset and L1 trigger is scanned in order to examine each row of the pipeline. The data output is compared with the injected patterns.

Table 3.8: Input lines test

SETTINGS	CHIP configuration	MASTER | END | EDGE_OFF | DATA_COMPRESSION_X1X | MASK | DATA_TAKING_MODE | SELECT_0	
	CHIP bias	Ipreamp	220μA
		Ishaper	30μA
		Threshold DAC	0xFF
	TRIM DAC	Value	0000
		Range	00
	CHIP address	Programmed = 1	
	COMMAND	SoftReset + Delay + L1 trigger	
SCANS	LOOPS	1. SELECT LINE = {0,1} MASK = {mask#1, mask#2,mask#3,mask#4} Delay = [150BCO - 161BCO] step 1BCO	
	No. of triggers	10	

3.1.8 TEST #5, FAKE SLAVE TEST

The chip is set as a master and middle chip. The token transmission for both lines (0 and 1) is checked.

Table 3.9: Fake slave test.

SETTINGS	CHIP configuration	MASTER | MIDDLE | EDGE_ON | DATA_COMPRESSION_01X | DATA_TAKING_MODE | SELECT_0	
	CHIP bias	Ipreamp	220μA
		Ishaper	30μA
		Threshold DAC	0xFF
	TRIM DAC	Value	0000
		Range	00
	CHIP address	Programmed = 1	
	COMMAND	Pulse Input Register + 129 BCO delay + L1 trigger + 5BCO delay + appended data pattern	
SCANS	LOOPS	1. {DATA_IN_0 & TOKEN_OUT_0, DATA_IN_1 & TOKEN_OUT_1}	
	No. of triggers	100	

3.1.9 TEST #6, SLAVE TEST

The chip is set as slave and end chip. The four patterns are injected through the mask register and the 8 tokens are sent after each 8 triggers through both input lines.

Table 3.10: Slave test.

SETTINGS	CHIP configuration	SLAVE | END | EDGE_OFF | DATA_COMPRESSION_X1X | MASK | DATA_TAKING_MODE | SELECT_0	
	CHIP bias	Ipreamp	220μA
		Ishaper	30μA
		Threshold DAC	0xFF
	TRIM DAC	Value	0000
		Range	00
	CHIP address	Programmed = 1	
	COMMAND	8xL1 trigger + 8xTOKEN	
SCANS	LOOPS	1. {TOKEN_IN_0 & DATA_OUT_0, TOKEN_IN_1 & DATA_OUT_1} 2. MASK = {mask#1, mask#2,mask#3,mask#4}	
	No. of triggers	10	

3.2 FAILURE ANALYSIS

In addition to the qualification of chips for the modules the wafers screening data are used for failure mode analysis. The results of failure analysis will be compared against the foundry data on Process Controll Monitor and will serve for monitoring of yield during production.

All tested chips are classified in such a way that each chip is assigned to a unique bin. The bin definitions are shown in Table 3.11. The algorithm used for assigning the chips to given bins is shown schematically in Figure 3.2.

Table 3.11: Definition of bins

BIN	DEFINITION
0	Good chip (after all tests)
2	failed DIGITAL TEST#1 @ 3.8V & 50MHz
3	failed DIGITAL TEST#2 (ADDRESSING) @ 3.8V & 50MHz
4	failed DIGITAL TEST#2 (L1 counter) @ 3.8V & 50MHz
5	failed DIGITAL TEST#4 (reading the mask) @ 3.8V & 50MHz
6	failed DIGITAL TEST#5 @ 3.8V & 50MHz
7	failed DIGITAL TEST#6 @ 3.8V & 50MHz
8	failed DIGITAL TEST#4 (reading the token) @ 3.8V & 50MHz
9	defect(s) in analog part #2 (channel offset out of the Trim DAC range 1 **or** gain different from the avarage by more than 25% **or** channel noise is 3 times higher than average noise of the chip **or** difference between average gain of the chip and average gain from the wafer is higher than 30%)
10	defect(s) in analog part #1 (no response to the calibration pulses)
11	[1 - 10] defects in the pipeline (low analog efficiency)
12	[10-100] defects in the pipeline (low analog efficiency)
13	> 100 defects in the pipeline (low analog efficiency)
14	high power consumption in digital part (Slave mode) (> 30% average)
15	high power consumption in analog part (Slave mode) (> 30% average)
16	low power consumption in digital part (Slave mode) (<30% average)
17	low power consumption in analog part (Slave mode) (<30% average)
18	Non-linear Threshold DAC (MAX ERR>10%)
19	Non-linear Bias1 (Preamp) DAC (MAX ERR>25%)
20	Non-linear Bias2 (Shaper) DAC (MAX ERR>25%)
21	Defect in the TRIM DAC (MAX ERR>25% **or** discrepancy between Trim DAC range 0 for a given channel and **TrDACRange0** is higher than 40%)
22	Defect in Trim DAC ranges (discrepancies between **TrDACRange0 + TrDACRange3** and averages from the wafer are higher than 40%)
23	Chip noise is outside of wafer noise distribution
24	Strict digital test failed at Vdd = 3.8 and 40MHz
25	Strict digital test failed at Vdd = 3.8 and 50MHz

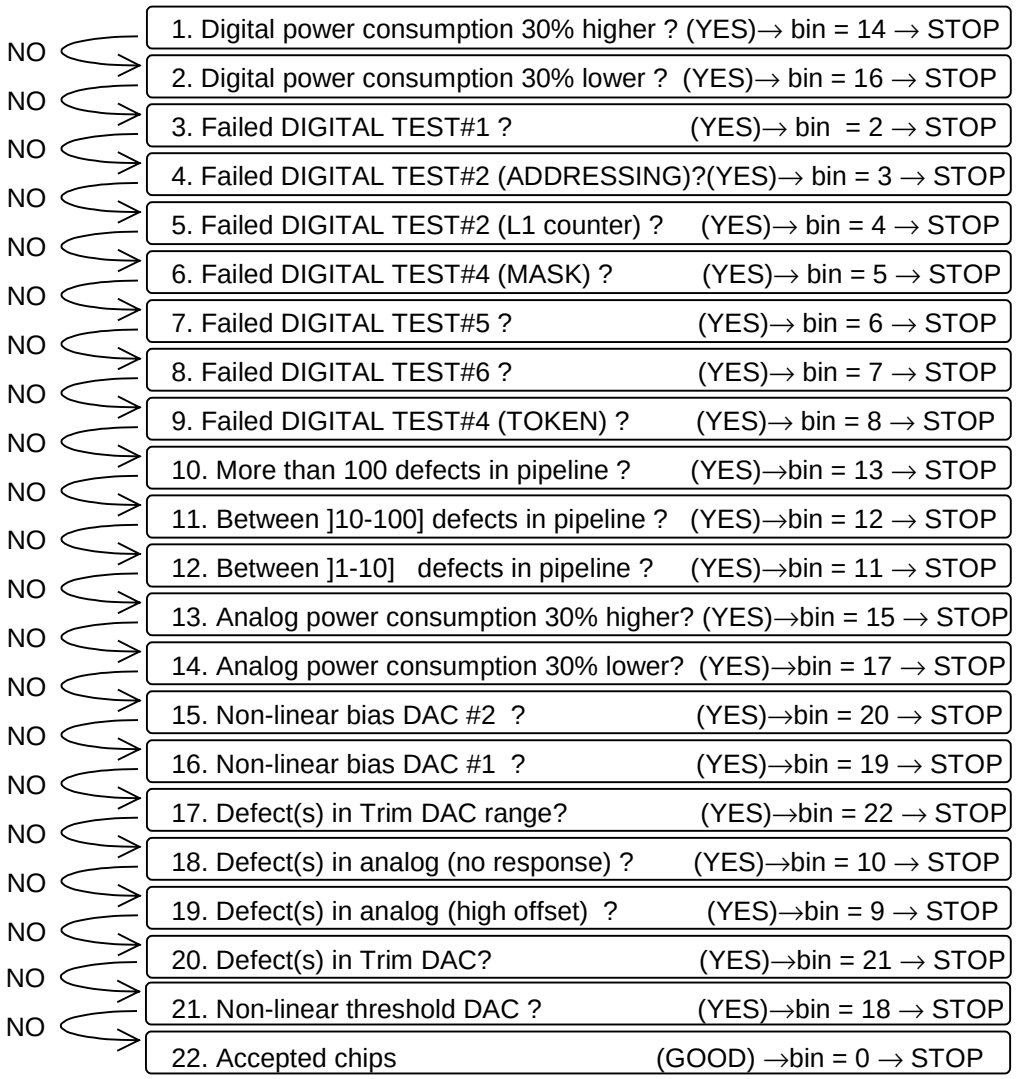

Figure 3.2: Algorithm for binning the test results.

4 INTERFACE TO THE SCT PRODUCTION DATABASE

4.1 PARAMETERS TRANSFERRED TO SCT DATABASE

Test parameters of all tested chips will be transferred to the ATLAS SCT production database. The parameters extracted from the wafer screening data and transferred to the database are listed in the following tables. All fields are mandatory.

Table 4.1: List of parameters transferred to the SCT database for the ITEM/ABCD article.

ITEM/CHIP unit	
MFR_SER_NO	BATCH-WAFER-XPOS-YPOS (example Z34685-W01-X05-Y05) – manufacturer serial number consist of number of batch, wafer number and x,y position of chip on the wafer
RECEIPT_DATE	Date of reception of material (wafers)
LOCATION	Location of the material (for example CERN)

Table 4.2: List of parameters transferred to the SCT database for the TEST_ABCD article.

TEST_ABCD unit	
MachineName	Name of the machine used for wafer screening
OnlineSoftRev	On-line software revision
OfflineSoftRev	Off-line software revision
PreampBias	Value of bias for the preamplifier stage used in the test [μA]
ShaperBias	Value of bias for the shaper stage used in the test [μA]
PrfFlg	Perfect flag – for absolutely perfect chips (depends on software revision)
DigFlg	Digital flag - for digitally perfect chips equal to 1
DppFlg	Digital Perfect Pattern flag (internal use)
Vdd0	Minimum Vdd [V] for which the chip is fully efficient for all digital tests @ 50MHz
Vdd0strict	Minimum Vdd [V] for which the chip is fully efficient for all **STRICT** digital tests @ 50MHz
VddTest1F0 (VddCnf0)	Minimum Vdd [V] for digital TEST vector #1 @ 50MHz
VddTest2F0 (VddAddr0)	Minimum Vdd [V] for digital TEST vector #2 @ 50MHz
VddTest3F0 (VddL1C0)	Minimum Vdd [V] for digital TEST vector #3 @ 50MHz
VddTest4F0 (VddInpReg0)	Minimum Vdd [V] for digital TEST vector #4 @ 50MHz
VddTest5F0 (VddInpLin0)	Minimum Vdd [V] for digital TEST vector #5 @ 50MHz
VddTest6F0 (VddFakeS0)	Minimum Vdd [V] for digital TEST vector #6 (
VddTest7F0 (VddSlave0)	Minimum Vdd [V] for digital TEST vector #7
VddTest8F0 (VddToken0)	Minimum Vdd [V] for digital TEST vector #8
Vdd1	Minimum Vdd[V] for which the chip is fully efficient for all digital tests @ 40MHz
Vdd1strict	Minimum Vdd[V] for which the chip is fully efficient for all **STRICT** digital tests @ 40MHz
VddTest1F1 (VddCnf1)	Same test as VddTest1F0 @ 40MHz
VddTest2F1 (VddAddr1)	Same test as VddTest2F0 @ 40MHz
VddTest3F1 (VddL1C1)	Same test as VddTest3F0 @ 40MHz
VddTest4F1 (VddInpReg1)	Same test as VddTest4F0 @ 40MHz
VddTest5F1 (VddInpLin1)	Same test as VddTest5F0 @ 40MHz
VddTest6F1 (VddFakeS1)	Same test as VddTest6F0 @ 40MHz
VddTest7F1 (VddSlave1)	Same test as VddTest7F0 @ 40MHz
VddTest8F1 (VddToken1)	Same test as VddTest8F0 @ 40MHz
ThrsDACSlope	Threshold DAC slope [mV/bit] obtained from linear fit to the measurement points.
ThrsDACErr	Maximum non-linearity error for Threshold DAC (maximum dispersion of the measurement point from the linear fit [mV])
PreampDACSlope	Preamplifier bias DAC slope [mV/bit] obtained from linear fit to the measurement points (direct values in mV readout from the probe pad)
PreamDACErr	Maximum non-linearity error for Preamplifier bias DAC (maximum dispersion of the measurement point from the linear fit [mV])
ShaperDACSlope	Shaper bias DAC slope [mV/bit] obtained from linear fit to the measurement points (direct values in mV readout from the probe pad)
ShaperDACErr	Maximum non-linearity error for Shaper bias DAC (maximum dispersion of the measurement point from the linear fit [mV])

MDigC	Power consumption (current) of the digital part in MASTER mode [A]
SDigC	Power consumption (current) of the digital part in SLAVE mode [A]
MAnaC	Power consumption (current) of the analogue part in MASTER mode [A]
SAnaC	Power consumption (current) of the analogue part in SLAVE mode [A]
NdNoResp	Number of channels not responding to calibration pulses (bin10)
NdPipeline	Number of channels with low analogue efficiency (pipeline defects)
NdNoise	Number of noisy channels (bin 9)
NdGain	Number of channels with degraded gain (bin9)
NdTrim	Number of channels with defects in TRIM DACs. Defects in the Trim DACs are verified for range 0 (data available for all channels of the chip). Conditions for verification are the same as for calculation of bin number 21.
NdHOffset0	Number of channels with offset out of the Trim DAC range 0
NdHOffset1	Number of channels with offset out of the Trim DAC range 1 (bin 9)
NdHOffset2	Number of channels with offset out of the Trim DAC range 2
NdHOffset3	Number of channels with offset out of the Trim DAC range 3
Ndead	Total number of unusable channels (channels with defects in analogue part).
Status	BIN status of the chip
StatusValid	Validation word for Status
AuxFlags	Auxiliary flags
AvGain	Average gain of the chip [mV/fC]
SGain	Sigma deviation of the channel gains on the chip [mV/fC]
MaxGain	Maximum channel gain in the chip [mV/fC]
MinGain	Minimum channel gain in the chip [mV/fC]
AvOffset	Average offset of the chip [mV]
SOffset	Sigma deviation of the channel offsets on the chip [mV]
MaxOffset	Maximum channel offset in the chip [mV]
MinOffset	Minimum channel offset in the chip [mV]
MaxTrDACErr	Maximum nonlinearity error for Trim DAC range 0 [mV]
MaxTrSlope	Maximum Trim DAC slope [mV/bit] of the Trim DAC characteristic (Range 0)
MinTrSlope	Minimum Trim DAC slope [mV/bit] of the Trim DAC characteristic (range 0)
TrDACRange0	Average of the ranges 0 of the trim DACs in the chip [mV]
TrDACRange1	Average of the ranges 1 of the trim DACs in the chip [mV]
TrDACRange2	Average of the ranges 2 of the trim DACs in the chip [mV]
TrDACRange3	Average of the ranges 3 of the trim DACs in the chip [mV]
AvNoise	Average output noise of the chip [mV] (extracted from point #1)
SNoise	Sigma deviation of the channel output noise on the chip [mV] (point #1)
MaxNoise	Maximum channel output noise in the chip [mV] (point #1)
MinNoise	Minimum channel output noise in the chip [mV] (point #1)
Qfactor	Quality factor defined as: gain/SQRT($soffset^2$+$sgain^2$)
Bin	Result of bin analysis (number from 0 to 28)

Table 4.3: List of the parameters transferred to the SCT database for the TSTABCDCHANNELS entity.

TSTABCDCHANNELS unit	
Chann_number	Channel number – primary key for this table
Gain	Gain for a given channel [mV/fC]
Offset	Offset for a given channel [mV]
Noise	Output noise for a given channel [mV]
TrDACSlope	Slope of the Trim DAC characteristic (Range 0) in [mV/bit]
TrDACErr	Maximum non-linearity error for Trim DAC (maximum dispersion of the measurement point from the linear fit [mV]) for Range 0
ChStatus	BIN status of channel

4.2 LOADING THE WAFER SCREENING RESULTS TO THE SCT DATABASE.

Uploading the chips to the database is done via a java application provided by the manager of the database. The encoding scheme for ITEMS.mfr_ser_no will be kept as a function of wafer_ser_no, XChipcoordinate, Ychipcoordinate.

Since the primary key of ITEMS is based only on the ITEMS.ser_no and no more constraints will be added to the ITEMS table, the application will be responsible for informing the user that the chips have not already been inserted into the database. The application will do that by checking the unique state of the ITEMS.MFR_SER_NO attribute before inserting the item chip.

An optional function to populate the SHIPS and SHIP_ITEMS automatically during the chips registration will also be implemented in this new java application. A special report will be generated to allow the users to make a shipment of a set of selected chips. The criteria for selecting the chips will be defined in future.

The report will give the possibility to automatically populate the SHIPS and SHIP_ITEMS tables with the record set by the criteria.

The web application already allow the users who are the owner of the shipped items and shipments to delete or update ITEMS, SHIPS and SHIP_ITEMS records.

When all the ship_items have been inserted (using the java application or the Web interface or else), the user is able "to send" (from a database point of view) the items to the destination person and institute, by updating the "Send Confirmation Date" field of the current shipment using his web browser.

ATLAS Project Document No.	Institute Document No.	Created:	Page: 1 of 4
SCT-BM-FDR-5.5		Modified: 10/05/01	Rev. No.: A

SCT Barrel Module FDR Document

Adhesives for the barrel modules

Prepared by:	Checked by:	Approved by:
Y. Unno, T. Kohriki, M. Gibson, R. Apsimon		

Distribution List

History of Changes

Rev. No.	*Date*	*Pages*	*Description of changes*
A	dd/mm/yy	All	First version

1 Introduction

The barrel modules are made of three major components: silicon microstrip sensors, baseboards, and hybrids. These components are fitted together with epoxy adhesives both thermally conductive and electrically conductive. In smaller parts, the readout ASICs are attached to the hybrids with an electrically conductive epoxy adhesive.

Both thermally and electrically conductive adhesives are used to adhere the baseboard and the sensors. A thermally conductive adhesive is required in order to transfer the heat generated in the sensors to the baseboard, especially after accumulating a large fluence of particles which damage the silicon bulk and induce many order of magnitude larger leakage current, together with increased full depletion voltage. Without an efficient transfer of heat from the sensors to the baseboard, the sensors may run away thermally through positive feedback of the leakage current and the temperature. An electrically conductive epoxy is required as the baseboard, made of carbon, is used for the electrical conductive path from the bias line on the hybrid to the backplane of the sensors.

Epoxy adhesives are chosen since they are known to be radiation-tolerant up to a very high fluence [1]. Although generally accepted radiation-tolerant, it is important that the electrical and thermal properties are demonstrated after receiving the full irradiation of $2*10^{14}$ 1 MeV-neutron equivalent/cm^2 fluence expected during the 10 years operation of detectors. To this end, the barrel community has adopted the epoxy adhesives, which have shown to work throughout the prototype modules and irradiation of the sub- and full modules.

In applying the epoxies, it is important to establish consistent quality among the module assembly sites. The barrel module community has arranged to acquire one each product for thermally and electrically conductive and provide the products to all sites, together with an appropriate documentation of specification, application procedure, curing schedule, and special precautions.

2 Thermally conductive epoxy

The thermally conductive epoxy of the choice is a 2 part, room temperature curing epoxy, supplied by Ciba-Geigy. The product is AW106/HV953U, known as its part number as Araldite 2011.

In order to enhance the thermal conductivity, a boron nitride filler is added, which is supplied by Advance ceramics, grade PT140S. The boron-nitride filler is chosen, over the alumina filler, after the test of the sensitivity in increasing the leakage current in the sensors [2]. The boron-nitride has a high thermal conductivity which helps to enhance the thermal conductivity of the epoxy mixture. The thermal conductivity of the mixture is estimated to be an order of 1 W/m/K.

The thermally conductive epoxy is used in the interfaces of

(1) the sensors and the baseboard, and
(2) the BeO facings of the baseboard and the steps of the hybrids.

The specification document is given in the appendix 4.1.

3 Electrically conductive epoxy

The electrically conductive epoxy of the choice is a 2 part, low temperature curing, supplied by

Eon Chemie Co. Ltd. The product is Eotite p-102. Although the curing schedule listed is above 50 °C, the epoxy is shown to cure at the room temperature. A caution is that it takes a long time in the room temperature, and it may not cure below 20 °C. A test data from the vendor in the appendix shows that the full curing takes 24 hrs. or more at 23 °C.

The thermal conductivity is good because of the silver filler and is measured to be 30 to 40 W/m/K, according to the vendor.

The electrically conductive epoxy is used in the interfaces of

(1) the sensors and the baseboard, and
(2) the ASICs and the hybrids.

The specification document is given in the appendix 4.2.

4 Appendix

4.1 ATLAS Barrel and Forward Module Structural Epoxy Specification, by M. Gibson and F.S. Morris

4.2 Conductive Epoxy Adhesive - Low Temperature Curing Type - Eotite P-102, by Eon Chemie Co. Ltd.

References

[1] E.g., H. Schönbacher, Radiation tests on epoxy resin NR 172, CERN LabII-RA-37.40-TM-74-6 (or any other better reference?)
[2] M. Gibson, Evaluation of Thermally Conductive Adhesive on the ‘p’ Side of Hamamatsu ATLAS Specified Silicon Detectors

8-12-98
issue 1

ATLAS Barrel and Forward Module Structural Epoxy Specification

M.Gibson
F.S.Morris

RAL, Didcot, Oxon 0X11 0QX, UK

Abstract
This document aims to specify the storage, handling, mixing and safety aspects of the approved ATLAS structural epoxy to be used in the construction of barrel and forward modules. The 2 part, room temperature curing epoxy (AW106/HV953U), has Boron Nitride (BN) additive to increase the thermal conductivity.

Materials.
Table 1 lists the basic constituents and the manufacturers of the loaded room temperature cure epoxy that has been agreed as the ATLAS standard for barrel and forward module construction. Table 2 lists the world suppliers for the boron nitride. Table 3 lists some of the Ciba-Geigy world offices who will supply the name of your local supplier.

TABLE 1

use	*item description*	*manufacturer*
structural epoxy	AW106/HV953U 2Kg pack part number 2011	Ciba-Geigy
filler	boron nitride grade PT140S	Advanced Ceramics

TABLE 2
boron nitride

European office	US Headquarters	UK office
Advanced Ceramics 54 Route de Clementy CH -1260 Nyon Switzerland	Advanced Ceramics PO box 94924 Clevland Ohio USA 44101-4924	Advanced Ceramics Unit 3 Vale Business Park Cow Bridge Glamorgan CF71 7PF
Phone (41) 22 361 50 08 Fax (41) 22 361 50 43	Phone (1) 703 426 0320	Phone (44) 1446 773826 Fax (44) 1446 773932

TABLE 3
Araldite

Australia	Germany	Japan	Spain
Ciba-Geigy Australia Ltd po box 332 Au-Thomastown Vic 3074	Ciba-Geigy Gmbh Postfach 1160/1180 D-79662 Wehr/Baden	Ciba-Geigy Japan Ltd 66-10 Miyuki-cho Takarazuka-city 665	Ciba-Geigy Sa Apartado 744 E-08080 Barcelona
phone (61) 3 282 0600 Fax (61) 3 282 0729	phone (49) 7762 820 fax (49) 7762 3727	phone(81) 797742439 Fax (81) 797742557	Phone (34) 3404 0300 Fax (34) 3404 0301
UK	USA		
Ciba-Polymers Duxford Cambridge CB2 4QA	Ciba-Geigy Corporation Formulated Systems Group 4917 Dawn Ave East Lancing Mi48823		
phone (44) 1223 83211	Phone (1) 517 3515900		

Preparation.

Fig 1 shows a typical mixing station, with P3 filters to limit dust, covered weighing station to protect the operative against splashes and extraction system to remove vapour. The resin, hardener and filler are mixed by weight in the following ratios.

Resin	Hardener	Filler
38.5 %	30.75 %	30.75 %
2.5 gm	2.0 gm	2.0 gm

Mixing.

Pour the required weight of resin and hardner into a small tall container and add the boron nitride. Mix by hand for about 2 minutes. At present there is no indication that it is necessary to evacuate the mixture to remove any dissolved air. The mix has a pot life of about 1 hour.

Storage.

The boron nitride is supplied by the manufacturer in sealed containers. The user should decant it into smaller, daily use containers and store in a dry atmosphere (e.g. in a sealed container with silica gel providing an atmsphere of approximately 23% RH @ 21deg C). The resin and hardner may be stored at room temperature (e.g. 45% RH @21deg C).

Safety.

Attached are copies of material safety data sheets as supplied by the manufactures. Users should obtain their own local versions.

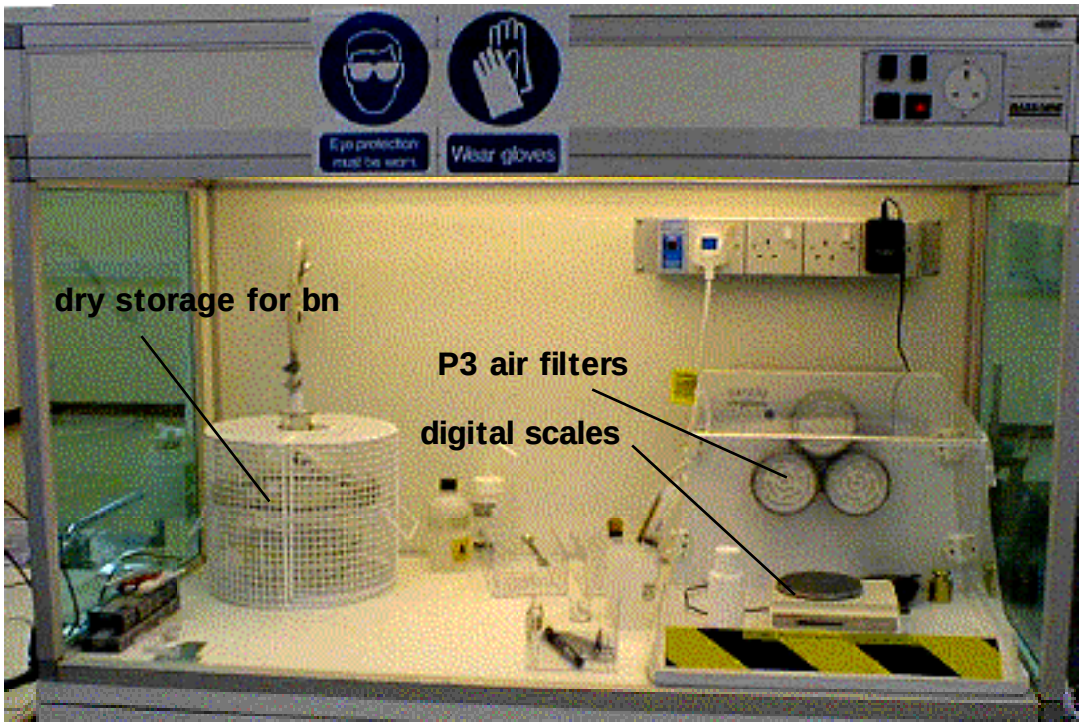

Fig 1

223

Ciba Polymers

SAFETY DATA SHEET

Araldite 2011 **August 1993**

1 SUBSTANCE/PREPARATION AND COMPANY IDENTIFICATION

CHEMICAL NATURE
Resin Component: Bisphenol A epoxy resin containing fillers
Hardener Component: Mixture of polyaminoamide and aliphatic polyamine
Preparations

COMPANY
Ciba Polymers
Duxford, Cambridge
England CB2 4QA

Tel: (0223) 832121
Fax: (0223) 838690

EMERGENCY TELEPHONE: +44 (0223) 832121

2 COMPOSITION/INFORMATION ON INGREDIENTS

RESIN COMPONENT CONTAINS
75-87% Bisphenol A epoxy resin (CAS No: 25068-38-6)
EEC-Symbol: Xi R phrases: 36/38-43

HARDENER COMPONENT CONTAINS
7-13% N(3-Dimethylaminopropyl)-1,3-propylenediamine (CAS No: 10563-29-8)
EEC-Symbol: Xi R phrases: 36/38-43

3 HAZARDS IDENTIFICATION

Irritating to eyes and skin. May cause sensitisation by skin contact.

4 FIRST-AID MEASURES

Skin Contact
Wipe with absorbent paper disposable towels. Wash with plenty of soap and water. Do not use organic solvents. In case of dermatitis get medical attention.

Eye Contact
Rinse immediately with water for at least 15 minutes and seek medical attention.

Inhalation
Move affected person to fresh air. In case of irritation of respiratory system or mucous membranes, or if you feel unwell or in case of prolonged exposure, get medical attention.

Ingestion
Immediately rinse the mouth repeatedly with water. If swallowing has occurred drink plenty of water. Seek medical attention promptly.

[redacted]ER COPY ISSUE DATE: 2/1/94
[redacted]T REMOVE QA APPROVED:

5 FIRE-FIGHTING MEASURES

Suitable Extinguishing Media
Water mist; Carbon dioxide; Foam; Dry powder

Unsuitable Extinguishing Media
High pressure water jet

Exposure Hazards
Do not release chemically contaminated water into drains, soil or surface water. Sufficient measures must be taken to retain water used for extinguishing. Dispose of contaminated water and soil according to local regulation.

6 ACCIDENTAL RELEASE MEASURES

Personal Precautions
Avoid contact with skin, eyes and clothing

Environmental Precautions
Prevent contamination of soil, drains and surface waters.

Methods for Cleaning
Take up with absorbent, inert material and place in suitable and closable container for disposal.

7 HANDLING AND STORAGE

Handling
Irritant, sensitising. Ensure good ventilation and local exhaust. Do not eat, drink or smoke at the workplace.

Storage
Keep away from food and drink. Store in the original container securely closed and at room temperature.

8 EXPOSURE CONTROLS/PERSONAL PROTECTION

Technical Protective Measures
No special measures required

Exposure Control Limits
None

Respiratory Protection
Not normally necessary. Work in well ventilated area.

Hand Protection
Wear suitable gloves

Eye Protection
Wear suitable goggles or face protection

Skin Protection
Wear overalls and closed footwear

9 PHYSICAL AND CHEMICAL PROPERTIES

RESIN COMPONENT

Appearance:	Cream liquid	Melting point/range:	Not applicable
Odour:	Slight	Boiling point/range:	Not available
Density:	1.15 - 1.25 g/cm³ at 25°C	Oxidizing properties:	Not available
Flashpoint:	> 200°C DIN 51758	Autoflammability:	Not available
Ignition:	Not available	Solubility in water:	Pract. insoluble at 20°C
pH value:	6 - 7 at 1:1 mixture with water	Vapour pressure:	0.1 Pa at 20°C
Viscosity:	24 - 45 Pa s at 25°C	Partition coeff.:	Not available
		Explosive properties:	Not available

HARDENER COMPONENT

Appearance:	Brownish yellow liquid	Melting point/range:	Not applicable
Odour:	Slight	Boiling point/range:	Not available
Density:	0.94 - 0.98 g/cm³ at 25°C	Oxidizing properties:	Not available
Flashpoint:	> 110°C DIN 51758	Autoflammability:	Not available
Ignition:	Not available	Solubility in water:	Pract. insoluble at 20°C
pH value:	12 at 1:1 mixture with water	Vapour pressure:	ca. 4 Pa at 20°C
Viscosity:	20 - 30 Pa s at 25°C	Partition coeff.:	Not available
		Explosive properties:	Not available

10 STABILITY AND REACTIVITY

Thermal Decomposition: > 200°C

Conditions to Avoid: Static discharges

Materials to Avoid: Strong acids, strong bases and strong oxidizing agents

Hazardous Decomposition Products
Thermal decomposition or burning may release oxides of carbon and other toxic gases or vapours.

11 TOXICOLOGICAL INFORMATION

	RESIN COMPONENT	HARDENER COMPONENT
LD_{50} Acute oral toxicity in rats:	> 5000 mg/kg	> 5000 mg/kg
Eye irritation tested in rabbits:	Not irritant	Not irritant
Skin irritation tested in rabbits:	Not irritant	Not irritant
Skin sensitisation in guinea pigs:	May cause sensitisation by skin contact	May cause sensitisation by skin contact

12 ECOLOGICAL INFORMATION

Prevent contamination of soil, drains or surface water.

	RESIN COMPONENT	HARDENER COMPONENT
LC_{50} Zebra fish (96h):	Not available	Not available
LC_{50} Rainbow trout (96 h):	Not available	Not available
EC_{50} Daphnia magna (24 h):	Not available	Not available
Biodegradability (Sturm test):	Not available	Not available
Algae Inhibition Test:	Not available	Not available
Sludge toxicity:	Not available	Not available

13 DISPOSAL CONSIDERATION

Incineration or landfill in accordance with local regulations. Contaminated packaging materials should be disposed of identically to the product itself. Packaging materials that are not contaminated should be treated as household waste or as recycling material. For easy disposal any unmixed resin and hardener can be mixed and allowed to cure. Once fully cured Araldite 2011 can be disposed of as normal household waste.

14 TRANSPORT INFORMATION

RID/ADR:	Free
IMDG-Code:	Free
IATA:	Free
Flashpoint:	> 110°C DIN 51758

15 REGULATORY INFORMATION

RESIN COMPONENT

Symbol:	Xi
Contains:	Bisphenol-A epoxy resin
R 36/38:	Irritating to eyes and skin.
R 43:	May cause sensitisation by skin contact.
S 24/25:	Avoid contact with skin and eyes.

HARDENER COMPONENT

Symbol:	Xi
Contains:	N (3-Dimethylamino propyl)-1, 3-propylenediamine
R 36/38:	Irritating to eyes and skin
R 43:	May cause sensitisation by skin contact
S24/25:	Avoid contact with skin and eyes

16 OTHER INFORMATION

Product Use:	Araldite 2011 is a two-component, room temperature curing epoxy industrial adhesive.
Note:	Araldite 2011 is available in larger pack sizes under designation Araldite AW 106 and Hardener HV 953U.

Edition: 01 according to Directive 91/155/EEC
Editor: Product Safety & Registration Fax +44 (0223) 838690

Advanced Ceramics
CORPORATION

MATERIAL SAFETY DATA SHEET

POLAR THERM™

1. CHEMICAL PRODUCT & COMPANY IDENTIFICATION

Advanced Ceramics Corporation
P.O. Box 94924, Cleveland, OH 44101-4924
11907 Madison Ave., Lakewood, OH 44107-5026
(216) 529-2900

EMERGENCY TELEPHONE NO.:
24 hr. CHEMTREC: 1-800-424-9300

TRADE NAME: Polar Therm™ Grade 203

MSDS NUMBER: 203

CHEMICAL NAME: Boron Nitride

SYNONYMS: Not Applicable

PREPARED BY:
Clayton Environmental Consultants, Inc.

DATE OF ISSUE/REVISION:
October 2, 1995/April 22, 1997

2. INGREDIENTS

Component	CAS #	Percent	ACGIH (TLV)	OSHA (PEL)	Units
Boron Nitride	10043-11-5	> 95	10 (T) 3 (R)	15 (T) 5 (R)	mg/M³ mg/M³
Boric Oxide	1303-86-2	< 5	10 (T)	15 (T) 5 (R)	mg/M mg/M
Proprietary Filler	NA	< 5	Not Est.	Not Est.	Not Est.

The total concentration of the Boric Oxide and Proprietary Filler components of the product is less than 5%.

T = Total Dust
R = Respirable Dust

3. HAZARDS IDENTIFICATION

EMERGENCY OVERVIEW

Product is a white powder with no odor. Dusts may cause eye, skin, and respiratory tract irritation. Wear appropriate personal protective equipment. Keep individuals not involved in the cleanup out of the area. Pick up with appropriate implements and place in suitable containers for reuse or disposal. Although the product itself is considered non-hazardous, all wastes generated during cleanup operations should be treated as hazardous unless specific testing, including TCLP, shows them to be non-hazardous. The product is not expected to present an environmental hazard.

3. HAZARDS IDENTIFICATION (Continued)

POTENTIAL HEALTH EFFECTS:

Eye: May cause irritation.

Skin Contact: May cause irritation.

Skin Absorption: Not absorbed through the intact skin.

Ingestion: No known effects.

Inhalation: May cause irritation.

Chronic & Carcinogenicity: **Prolonged exposures to high concentrations of the product may cause a benign pneumoconiosis.** The product is not known to be a carcinogen or suspected carcinogen. May possibly aggravate pre-existing lung or skin disorders.

4. FIRST AID MEASURES

Inhalation: Remove exposed person to fresh air. If breathing is difficult, oxygen may be administered. If breathing has stopped, artificial respiration should be started immediately. Seek medical attention.

Eyes: Flush with tepid water for at least 20 minutes holding the eyelids wide open. Seek medical attention if irritation develops.

Skin: Wash thoroughly with mild soap and water. Seek medical attention if irritation develops. Remove any contaminated clothing and launder thoroughly before reuse.

Ingestion: Not expected to be an important route of entry into the body. If large amounts of the product are ingested, give 2 glasses of water. Never give anything by mouth to an unconscious person. Seek medical attention.

5. FIRE FIGHTING MEASURES

FLASH POINT: NA **LEL:** NA **UEL:** NA **AUTO IGN. TEMP.:**

Product is non-flammable. Product in or near fires should be cooled with water spray or fog, if compatible with the other materials involved in the fire. Self-contained breathing apparatus, operating in the positive pressure mode and full fire fighting protective equipment should be worn for combating all fires.

6. ACCIDENTAL RELEASE MEASURES

Pick up with suitable implements and return to original or other appropriate container if product is reusable. If not reusable, place in DOT approved containers for disposal. See Section 13. Keep unnecessary personnel out of area. Wear appropriate personal protective equipment.

7. HANDLING AND STORAGE

Do not store with or near incompatible materials cited in Section 10. Store in tightly closed containers out of contact with the elements. Good housekeeping engineering practices should be employed to prevent the generation and accumulation of dusts. Wet mopping or vacuuming with a unit that contains a HEPA filter is recommended to clean up any dusts that may be generated during handling and processing.

8. EXPOSURE CONTROL - PERSONAL PROTECTION

ENGINEERING CONTROLS: Local exhaust ventilation should be provided to maintain exposures below the limits cited in Section 2. Design details for local exhaust ventilation systems may be found in the latest edition of "Industrial Ventilation: A Manual of Recommended Practices" published by the ACGIH Committee on Industrial Ventilation, P.O. Box 16153, Lansing, MI 48910. The need for local exhaust ventilation should be evaluated by a professional industrial hygienist. Exhaust ventilation systems should be designed by a professional engineer.

RESPIRATORY: If exposures exceed the limits cited in Section 2 by less than a factor of ten, use as a minimum a NIOSH approved 1/2 facepiece respirator equipped with cartridges approved for particulate matter with an exposure limit of not less than 0.05 mg/M^3. If exposures exceed 10 times the recommended limits, consult a professional industrial hygienist or your respiratory protective equipment supplier for selection of the proper equipment. The evaluation of the need for respiratory protection should be determined by a professional industrial hygienist.

EYE PROTECTION: Safety glasses with side shields are recommended for most operations.

PROTECTIVE GLOVES: Polymeric gloves are recommended to prevent possible irritation.

GENERAL: Polymeric coated apron or other body covering is recommended where there is a possibility of regular work clothing becoming contaminated with the product. All soiled or dirty clothing and personal protective equipment should be thoroughly cleaned before reuse.

9. PHYSICAL AND CHEMICAL PROPERTIES

APPEARANCE & PHYSICAL STATE: White powder

VAPOR DENSITY (AIR=1): Not Applicable

VAPOR PRESSURE: Not Applicable

ODOR: None

% VOLATILE BY VOLUME: Not Volatile

% SOLUBILITY (H_2O): <5% Filler, Boron Nitride/Boric Oxide = Insoluble

pH: Not Applicable

MELT POINT: Filler = [illegible] Boron Nitride/Boric Oxide Sublimes at 3000 F [illegible]

OCTANOL/WATER PARTITION COEFFICIENT: Not Applicable

EVAPORATION RATE BuOAC = 1: Applicable

SPECIFIC GRAVITY/BULK DENSITY: SG = 2.1 - 2.2 g/cc

BOILING POINT: Not Determined

OTHER: Not Applicable

10. STABILITY AND REACTIVITY

STABILITY & POLYMERIZATION: Product is stable. Hazardous polymerization will not occur.

INCOMPATIBILITY (CONDITIONS TO AVOID): Strong oxidizing and reducing agents.

HAZARDOUS DECOMPOSITION PRODUCTS: Combustion or thermal decomposition of the proprietary filler may liberate oxides of carbon and low molecular weight organic materials whose composition and toxicity has not been determined. The boron nitride/boric oxide components of the product are stable to 3000 F (1650 C), at which point sublimation occurs.

SPECIAL SENSITIVITY: None that are known.

11. TOXICOLOGICAL INFORMATION

Soluble boron compounds are known to have a toxic effect on the central nervous system at high exposure levels. The boron compounds present in the product are present in an insoluble, inert matrix and are not expected to be bio-available.

The proprietary filler has been shown to cause developmental abnormalities in the offspring of rats who were fed a minimum of 600 grams per kilogram of body weight per day for the three months prior to and during pregnancy. These results are not meaningful to the human model since the minimum daily dose rate required to produce the observed adverse effects is equivalent to 60% of the body weight of the average female.

12. ECOLOGICAL INFORMATION

Product is inert. It is not expected to present an environmental hazard.

13. DISPOSAL CONSIDERATIONS

As prepared, product is considered non-hazardous. It should be disposed of in an EPA approved landfill in accordance with all local, state, and federal regulations. If used or waste product is disposed of, testing including TCLP, should be conducted to determine hazard characteristics. Empty containers will have product residues. Observe proper safety and handling precautions. Do not allow empty containers or packaging to be used for any purpose except to store or ship original product.

14. TRANSPORTATION INFORMATION

Not currently regulated under DOT.

15. REGULATORY INFORMATION

OSHA Hazard Communication Categories: Irritant.

The product is not reportable under Section 313 of Title III of the Superfund Amendments and Reauthorization Act of 1986.

16. OTHER INFORMATION

NA = Not Applicable

HMIS Classification: Health = 1, Fire = 0, Reactivity = 0

All components of the product are included in the Toxic Substances Control Act (TSCA) inventory.

NOTICE TO USERS: Advanced Ceramics requests the users of this product to study this material safety data sheet (MSDS) and become aware of product hazards and safety information. To promote safe use of this product, a user should (1) notify its employees, agents, and contractors of the information on this MSDS and any product hazard and safety information, (2) furnish this same information to each of its customers for the product and, (3) request such customers to notify their employees and customers of the product hazards and safety information.

The opinions expressed herein are those of qualified experts within Advanced Ceramics. We believe that the information contained herein is current as of the date of this MSDS. Since the use of this product is not within the control of Advanced Ceramics, it is the user's obligation to determine the conditions of safe use of this product.

Conductive Epoxy Adhesive

- Low Temperature Curing Type -

EOTITE P-102

EOTITE P-102 is a two-component type Epoxy resin adhesive with fine-grained silver cured under a low temperature. Two parts of the hardner shall be added to 100 parts of the resin by weight for curing.

The adhesive is applicable for bonding metals, ceramics, plastics, carbon, glass, phenolic resin, epoxy resin, ferite, etc. requiring a perfect electroconductivity of the adhesive to be used for bonding .

Characteristics

1. Cured at low temperature of 50°C - 80°C.
2. Easy to mix the resin and the hardner with a creamy paste resin.
3. No shrinkage with cure. Suitable for filling and potting.
4. High bond strength. No sagging.
5. Excellent storage stability of one year at an ordinally temperature.

Specifications

	Resin	Hardner
Main Component	Silver / Epoxy	Polyamine
Mix Ratio (% by weight)	100	2
Specific Gravity (@20°C)	3.0 - 3.2	1.0
Viscosity (@20°C)	creamy paste	30 - 40 cps.
Purity (% of Ag)	99.5 or more	-
Particle Size (μ m,diameter)	0.5 - 1.2	-
Condition for Curing	50°C x 2 hrs - 80°C x 15 min.	
Volume Resistivity	5×10^{-4} Ω・cm	
Surface Resistivity	0.05 Ω/□	
Pot Life after Mixed	3 - 5 hrs. at 25°C 100 - 120 hrs. at -20°C	
Storage Stability (@20°C)	approx. 1 year	

Curing Condition (100 pts of resin / 2 pts of hardner by weight)

Condition		Volume Resistivity (Ω・cm)
Temperature (°C)	Time Heating	
50	2 hrs.	1.5×10^{-2}
60	2 "	1.0×10^{-2}
70	20 min.	8.0×10^{-3}
80	15 "	5.0×10^{-4}
100	10 "	5.0×10^{-4}

Cautions on Handling

1. Allowed to be stored at room temperature avoiding a direct sunlight.
2. Keep the cap of the container tightly protect against moisture after use.
3. Avoid to contact with skin. Preferable to wear a mask and gloves.
4. Wash hands thoroughly after use.

Correlation between Amount of Hardner and Bond Strength

(Result by change of amount of hardner to 100 pts. resin by weight)

Tensile Shear Strength (kg / cm)

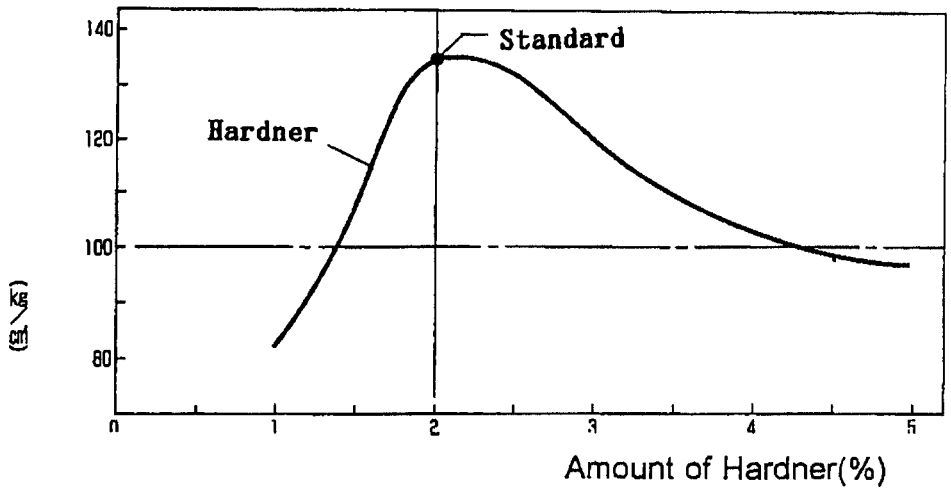

(Bonded Steel to Steel)

Bond Strength

Substrates	Tensile Shear Strength	Remark
Steel / Steel	140.0 kg · cm^2	Cohesive Failure
Epoxy / Epoxy	83.5 "	Broken Substrate
Phenolic / Phenolic	66.5 "	" "

Mix Ratio: 100 pts of Resin / 2 pts of Hardner
Curing Condition: 80°C x 15min.
Measured after aged for 24 hours at room temperature.

Heat Resistance

- Heated for 1 hour at 190°C -

Aging Time after Cured	Tensile Shear strength	Volume Resistivity
0 min.	145 kg / cm^2	---
15 "	135 "	5×10^{-4} Ω · cm
24 hrs.	145 "	5×10^{-4} "

Bonded Substrates: steel / steel
Curing Condition: 80°C x 15 min.
Tested after aged for 24 hours at room temperature.

How to Use EOTITE P-102

1. Weigh correctly the resin and the hardner.
2. Mix well.
3. Use the mixed adhesive within 2 - 3 hours after mixed.
   Preferable to weigh an adequate quantity to finish to use within a time of pot life.

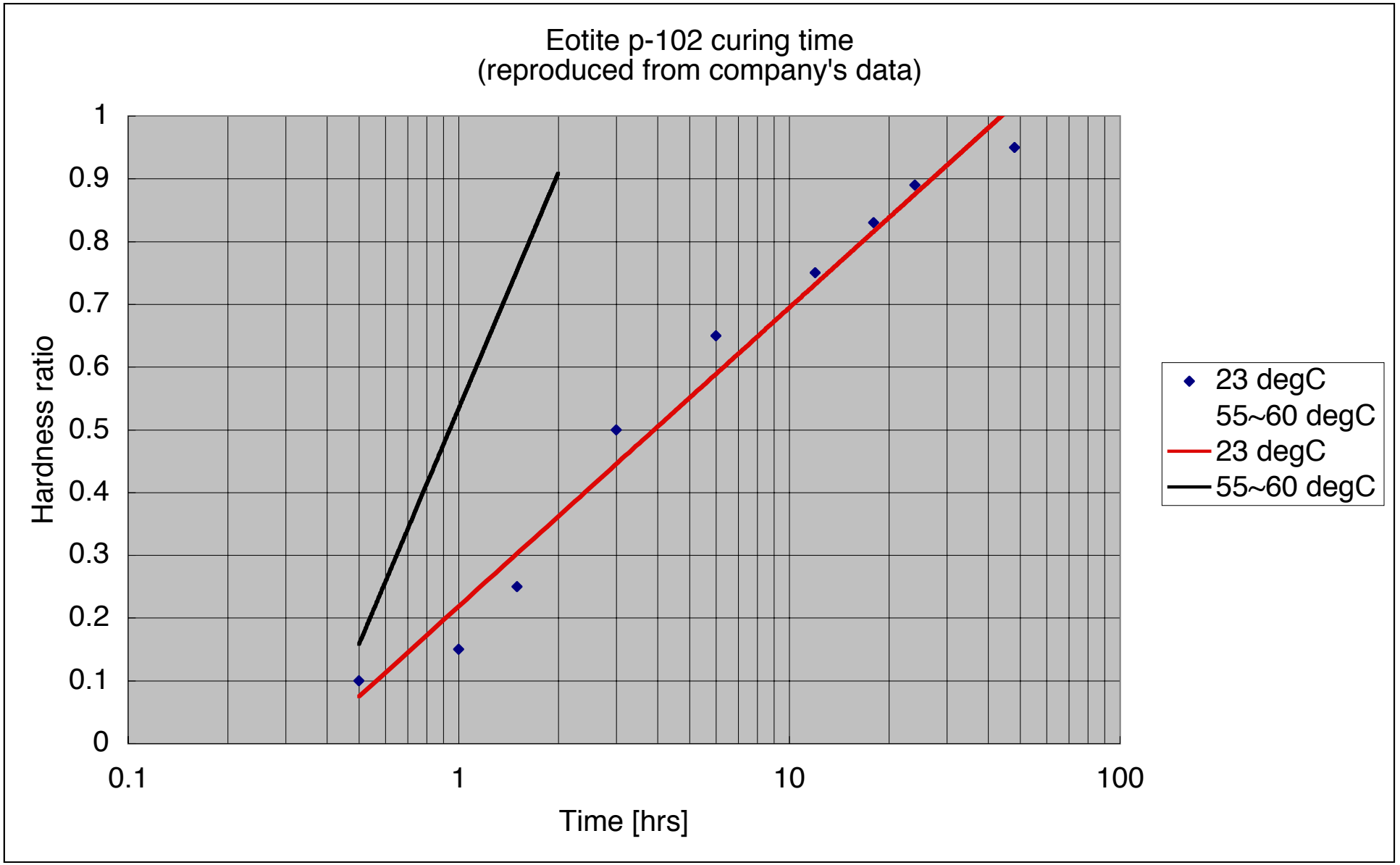
Eotite p-102 curing time
(reproduced from company's data)
Hardness ratio
1
0.9
0.8
0.7
0.6
0.5
0.4
0.3
0.2
0.1
0
0.1
1
10
100
Time [hrs]
23 degC
55~60 degC
23 degC
55~60 degC

M　S　D　S
（製品安全性データーシート）

名称	導電性エポキシ系接着剤・イオタイトＰ－１０２
物質の特定	化学名：エポキシ樹脂、銀粉、安定剤・硬化剤ﾎﾟﾘｱﾐﾝ を含む混合物 既存化学物質汎用グレード NO.７－１２８３（Epoxy resin) ＣＡＳ NO.７４４０－２２－４（Silver Compound) 輸出（入）統計品目 NO.７１０６　(Silver Compound)
性状	導電性（銀系）エポキシ接着剤はエポキシ基２個以上を含む可溶性の　ﾌﾟﾚﾎﾟﾘﾏｰ　で硬化剤:ﾎﾟﾘｱﾐﾝを加えて加熱により、接着力を発揮し強力に接着する、接着後の収縮はない
危険性 有害性	引火性なし、ただし硬化剤なしでも 70°c 以上で重合反応をおこす アレルギー体質の人はヒフが刺激されカユミや炎症を生じることがある。飲み込むと咽喉や胃に刺激を感じるから注意 硬化剤ﾎﾟﾘｱﾐﾝ は触れると発疹を起こす
応急処置	目に入った時：ただちに流水で洗眼し、医師の手当てを受ける ヒフ付着の時：付着の部位を石けんで良く洗い、炎症が生じたときは医師の手当てを受ける 飲み込んだ時：多量の水または食塩水を飲ませて吐かせ、直ちに医師の手当てを受ける 吸入した時　：新鮮な空気を入れ替え、通風の良い場所に寝かせ、医師の手当てを受ける 硬化剤ﾎﾟﾘｱﾐﾝがﾋﾌに 触れたときは、その部位を、ただちに石鹸水でよく 洗う
火災時の措置	消火方法：火元の燃焼源を断ち、消火剤を使用して消火する消火に当たっては呼吸用保護具を着用する 消火剤　：粉末（ＡＢＣ）、アルコホーム
漏洩時の措置	ⓐ少量の場合は布等で拭き取り、その後アルコール等でよく拭く ⓑ大量の場合はフロアー用のワイパーやヘラ等でかき集めて、空の容器へ回収する、その後洗剤と水でよく洗い流しておく
取扱および貯蔵上の注意 取扱上の注意	ⓐ容器からの出し入れは遺漏のないように注意する ⓑ作業時は目、ヒフおよび着衣にふれないようにし、必要に応じて保護具を着用する ⓒ作業場所は換気をおこなう、なるべく局所排気装置を設置する ⓓ使用済の容器は廃棄業者に依託する ⓔ使用時は熱源を避ける
貯蔵上の注意	ⓐ冷暗所（20°c以下）に密閉して保存する ⓑ直射日光ならびに熱源近くの場所には貯蔵してはいけない ⓒ湿気を避けて貯蔵する

暴露防止装置

管理濃度 ・ 特になし　　許容濃度 ・ 特になし

設備対策 ・ 作業場所にはなるべく局所排気装置を設け、熱源は避ける

防護具 ・ 状況に応じ、保護マスク、保護メガネ、保護手袋を着用する

物理／化学的性質（主剤）

外観 ・	銀色ペースト状	沸点 ・	-----
粘度 ・	25±30 ps/20°c	蒸気圧 ・	0.1mmHg 以下
比重 ・	3.0 ～3.2 /20°c	融点 ・	-----
臭気 ・	微臭	溶解度 ・	水に不溶、有機溶剤に可溶

不純物イオン濃度

Ｎａ ・ １０ppm 以下　at 100°c×20hrs 抽出

Ｃｌ ・ １０ppm 以下　at 100°c×20hrs 抽出

有害情報

急性毒性 ・ LD_{50}(ラット経口) 50～100g ····· Ag：推定値

刺激性 ・ 人によっては刺激臭を感じる

感作性 ・ 人によっては刺激臭を感じる

環境負荷化学物質含有量

ＰＲＴＲ（化学物質排出管理法）： 該当なし

輸送上の注意

ⓐ運搬に際しては容器に漏れのないことを確認し、容器の損傷がないように梱包に注意して輸送する

ⓑ輸送中に水分が当たらないように注意する

廃棄上の注意

ⓐ廃棄は所定の容器に入れ、産業廃棄物認可業者に依託する

ⓑ主剤、硬化剤が付着している容器も同様に依託する

適用法令

労働安全衛生法・・・・該当なし

毒物及び劇物取締法・・該当せず

危険物船舶運送及び貯蔵規制・・該当なし

引用文献

１）環境庁・環境安全課：ＰＲＴＲ指定化学物質リスト

２）１３７００の化学商品（化学工業日報社）

３）化審法化学物質リスト

平成 12年 9 月 26 日

〒331-0063

埼玉県大宮市プラザ８２番８号

イオンケミー株式会社

TEL 048-624-9582 FAX 048-624-9592

P-102

営業所・〒101 東京都千代田区鍛冶町2-8-6

TEL 03-3255-9655 FAX 03-3256-8776

SCT BARREL MODULE Document

SCT Barrel Module: ASSEMBLY PROCEDURES & JIGS

Abstract

This document describes the barrel module assembly procedures and the jigs that are used..

Prepared by :	*Checked by :*	*Approved by :*
A. Carter, O.Dorholt, M.Gibson, Y. Unno		

Table of Contents

1. SCOPE OF THE DOCUMENT

This document describes the barrel module assembly jigs and procedures used by the four barrel clusters. It also describes a module transport and test box in Appendix 1.

2. MODULE ASSEMBLY STEPS

2.1 Overview

The barrel module assembly contains five specific operations. The manner in which these are carried out in the four assembly clusters in Japan, UK, Scandinavia and US has developed differently in some details, but each cluster is required to produce high quality modules that meet the same defined specifications. The encouraging achievements are presented and discussed in Sections 8 and 9, and documents are appended that discuss individual cluster procedures. In the initial step all the module component parts are inspected and their serial numbers checked against those in the construction database. Next the four silicon sensors have to be positioned precisely onto a baseboard to produce a detector-baseboard sandwich. A third step is attaching ASICs on the hybrids, and then in the module assembly the hybrids are mounted onto the detector-baseboard sandwich. Finally the ASIC inputs are connected to the individual sensor readout channels with wire bonds, and the sensor biasing connections are made.

2.2 Sensor-Baseboard Assembly

A great amount of effort has been put into developing procedures and jigs in this phase since the most demanding mechanical precision is required at this step. The elements involved are a pair of sensors on top and bottom of the baseboard. Requirements are to align each pair of sensors in the x-y plane, and also align the top and the bottom pair relative to each other and to the module reference point, the dowel holes. It is also important to minimise module distortion out of the x-y plane, i.e. in the z direction, and to prevent any mechanical damage to the sensors. All these are very demanding requirements.

2.2.1 Assembly station

The basic assembly procedure consists in having a station for aligning a pair of sensors, by using two sets of (x,y,Θ) stages, and large x and y stages to move the (x,y,Θ) stages under a microscope. One such arrangement of stages is shown in Figure 1. Some variations exist at the different clusters depending on the specific stages that are used.

A pair of aligned sensors are transferred to a pick-up jig with vacuum-chucking. Experimentally it was shown that optimised precision during the transfer process requires that the vacuum of the stages of the assembly station and the transfer jig are applied sequentially to avoid asymmetric forces on the aligned sensors. In order to confirm that the sensors have not moved beyond allowed tolerances, the transfer jigs have inspection holes at the fiducial marks through which co-ordinates are visually inspected before and after the transfer.

The surfaces of silicon sensors are protected at all stages, when in contact with jigs, by the use of clean-room paper that is renewed before each separate operation.

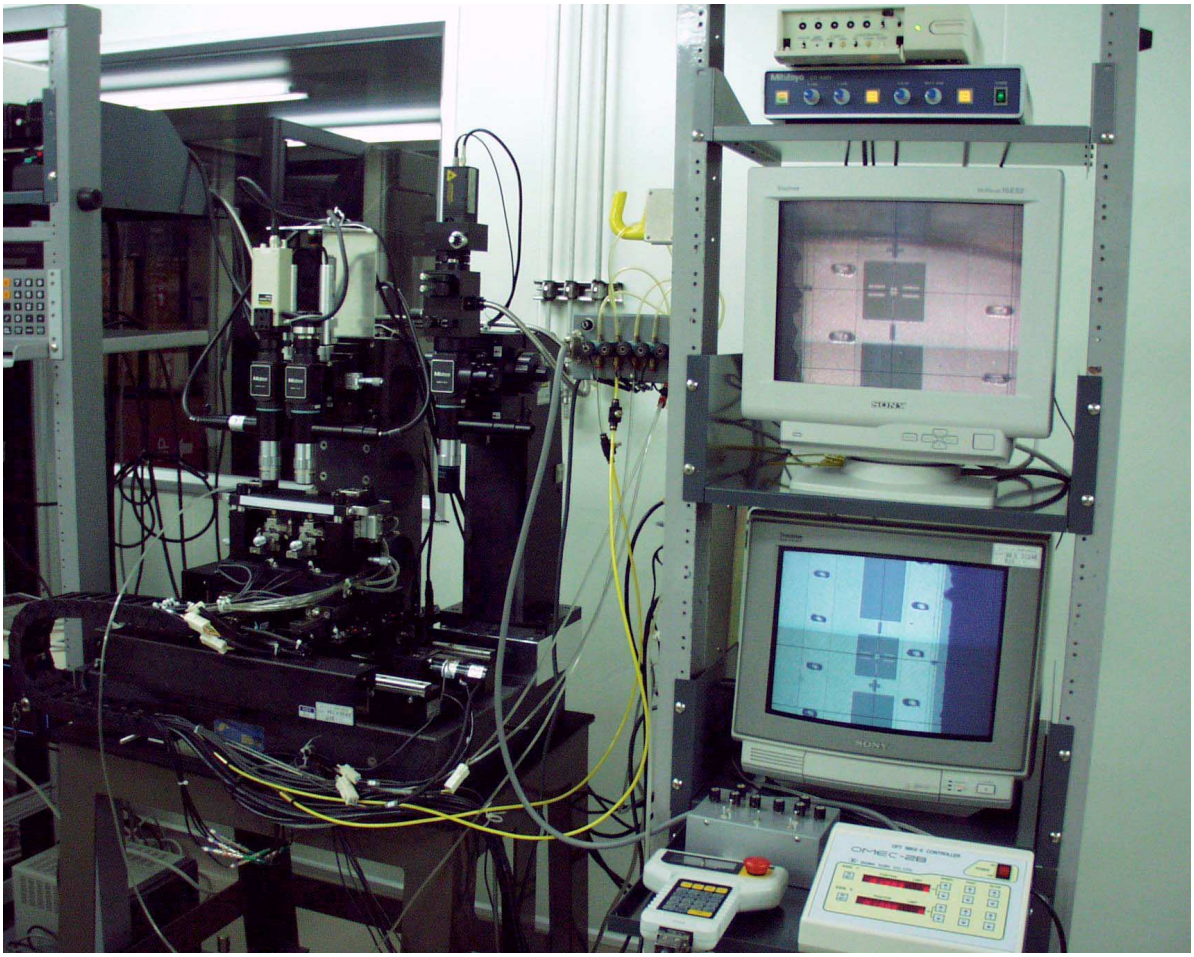

Figure 1 An example of assembly station

2.2.2 Gluing step and glue dispensing

In gluing the sensors to baseboards experience has shown that the preferred procedure is to hold the central baseboard area with a vacuum chuck and apply glue to the accessible surface and hence produce the completed sandwich assembly in a two-step process.

The detectors and the baseboard are glued with a room temperature curing epoxy glue, Araldite 2011, with a boron-nitride filler to improve the thermal conductivity[1]. A pre-defined amount of the epoxy glue is applied to the baseboard to ensure a specified glue thickness, and this is conveniently done using a dispensing machine which combines xyz stages with a glue dispensing unit. An example is shown in Figure 2.

There are two glue spots per sensor where electrical connection is made to the back-side with Eotite p-102, the same silver-loaded electrically conductive epoxy that is used for attaching the ASICs to the hybrid.

[1] M. Gibson, F.S. Morris, ATLAS Barrel and Forward Module Structural Epoxy Specification, http://hepunx.rl.ac.uk/atlasuk/sct/moduleAssembly/adhesivespec.pdf

Figure 2 Glue dispensing system which is made of (1) a xyz stage where the baseboard is on the xy stage and a glue-syringe is attached on the z-axis, and (2) a dispensing controller.

2.2.3 Documentation for the assembly sites

Details of the assembly station and assembly steps are described in the appended documents:

Appendix 2: Assembly jigs and procedures for the Japanese Cluster

Appendix 3: Assembly jigs and procedures for the UK-B and US Clusters

Appendix 4: Assembly jigs and procedures for the Scandinavian Cluster

3. ASIC ATTACHMENT AND BACK-END WIRE BONDING ON THE HYBRIDS

The hybrids for the barrel modules are to be delivered to the module assembly clusters with passive components surface-mounted, but without ASICs. Firstly, defined wire-bond pull-tests are carried out to ensure bondability before ASICs are attached and then fully bonded.

ASICs are glued on the chip pads with an electrically conductive epoxy, Eotite p-102[1] which has been chosen after showing successful electrical performance and suffering no adverse affects after irradiation in prototype modules. During the application of the adhesives and attaching the ASICs, care is taken to protect bonding pads from surface contamination. The adhesive is cured at a temperature at 50 ^{o}C for a period of greater than 2hrs.

After curing the ASIC adhesives, the back-end wire-bonding is carried out so that the ASICs electrical performance can be tested.

4. MOUNTING THE HYBRID

In the barrel module, the hybrid is wrapped around the sensor-baseboard assembly and this is most conveniently done with a customised tool. Details of this are given in the appended assembly documents, and positioning tolerances of ±50 μm in both the x and y directions are achieved

5. FULL WIRE-BONDING

Following the hybrid mounting and curing of adhesives, a set of electrical connections are made:

Firstly, individual connections are made to the supply bias and for the return current from the detectors. The electrical bias connection to the backside of the sensors is made through the conducting baseboard and the hybrid connections are wire-bonded to electrical connections on the upper-side beryllia facings which have been directly connected with conducting epoxy to the baseboard substrate. The ground return is wire-bonded from the bias ring on the strip side of the detector to a trace on the fan-in and then into the pre-amplifier ground contact.

Secondly, the high density wire-bonds are made from the ASIC to the fan-ins, and from the fan-ins to the sensor, and from the sensor to the sensor. There are in total 4608 of these bonds per module. This step uses a dedicated automatic wire-bonder. With 80μm pitch there is no problem bonding under fully automatic control. Particular care is, however, required to bond from the step down between fan-ins and sensors, which is about 1 mm. It is estimated that one complete module can be bonded and inspected within 4 hours during series production, dependent upon interleaving the necessary operations.

Full details of the wire-bonding scheme are provided in the document *ATLAS SCT Barrel module wire-bonding scheme*[2].

[1] Eotite p-102, http://atlas.kek.jp/~unno/SCTSGmod/glue/eotitep102.pdf

[2] T. Kohriki et al., http://atlas.kek.jp/~unno/SCTSGmod/mod00/Wirebondscheme.pdf

Appendix 1 Module Transport and Test Box

1 OVERVIEW AND REQUIREMENTS

A barrel module is a delicate device with well-defined mechanical, thermal and electrical properties. Its fabrication is described elsewhere in these FDR documents, and the present document addresses the box into which it is placed immediately after its construction. The module remains in this box until it is mounted on the barrel cylinder assembly, and during this potentially significant period of time the following operations are expected to be carried out:

(i) electrical testing [and thermal cycling where necessary] and storage

(ii) transport to the barrel module mounting site

(iii) storage and subsequent mounting on to a barrel cylinder

To be appropriate for these functions the box must include a basic module carrier, possess a cooling interface which is serviced internally by fluid flow, and have appropriate connections for the fluid and for attachment of an external inert gas supply. It has to be fitted with an integrated PCB and the appropriate electrical connectors. Whilst in the carrier the module must be protected at all stages by top and bottom cover plates. Various prototype boxes have been produced to meet these needs and shown to provide the necessary functions. However, further global requirements are needed for the final box, as in the module series production phase more than one thousand of these units will be needed. This requires the unit to be produced at an acceptable cost and in a process capable of medium scale production. Such a working example is given below to show that at least one solution already exists. The final box will be agreed shortly when all prototypes have been evaluated. Figure 1 shows an initial prototype box, and Figure 2 shows its latest design, where the engineering drawings are converted into a virtual solid model.

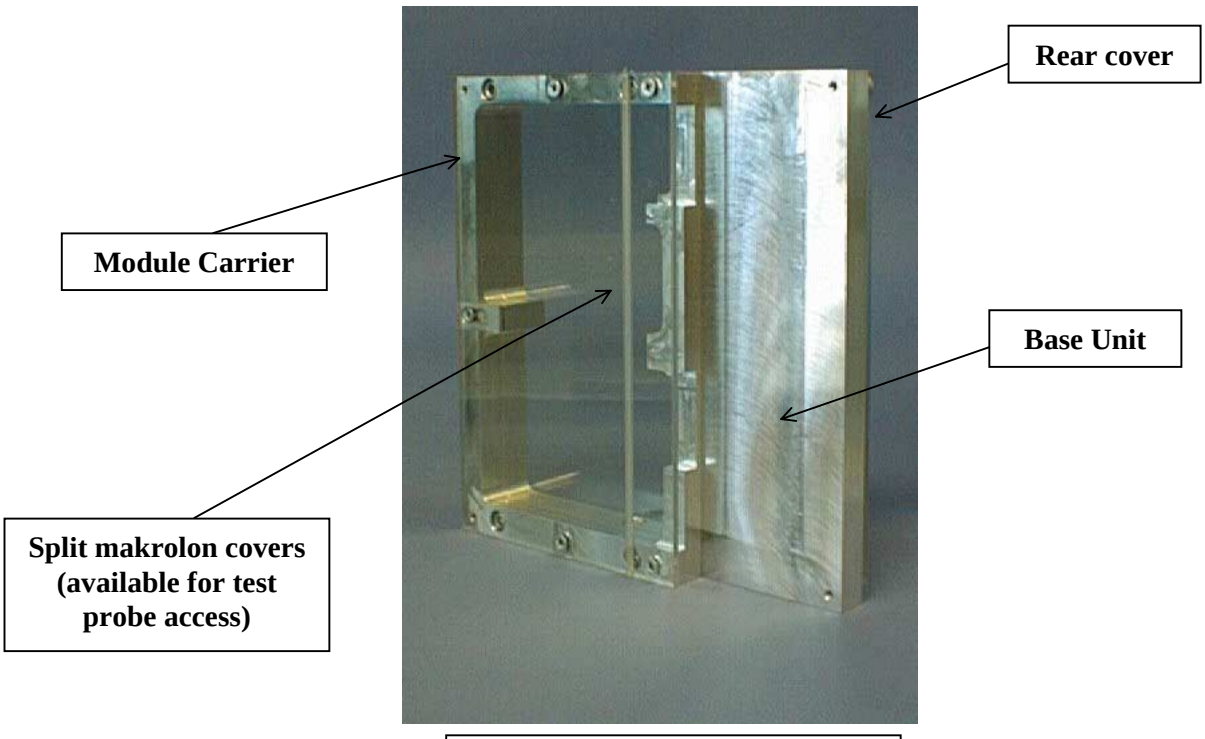

Figure 1. Initial prototype box

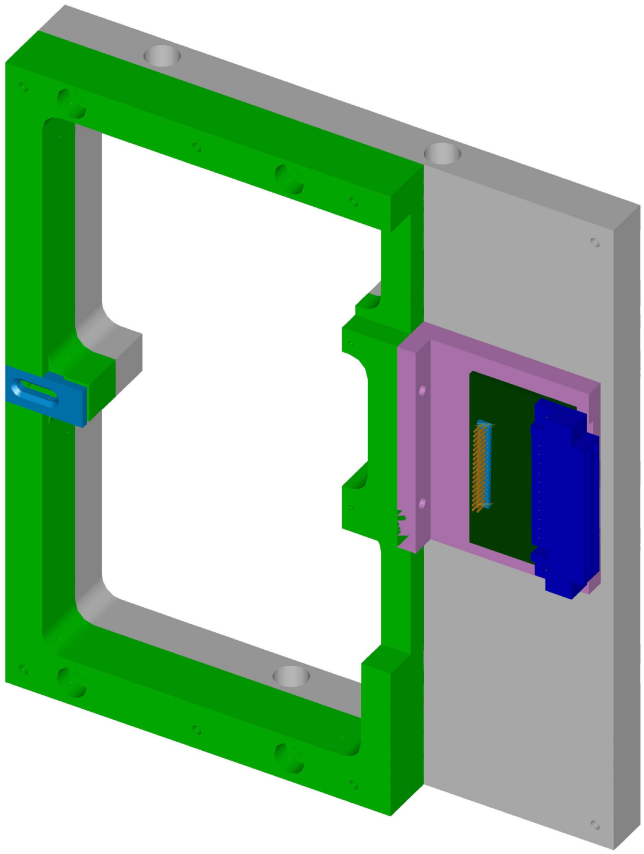

Figure 2. Virtual solid model of latest carrier and test box

2 COMPONENT ITEMS

(1) Module Carrier:

This is machined from cast aluminium tooling plate to a general tolerance of ±0.1mm, with the areas where the module is supported being machine to a higher precision of ±0.05mm. These regions also correspond to where the module-mounting robot requires direct access to attach to the module itself. The module is fixed to the carrier by two screws through the large cooling facings, and the far side of the module is restrained from moving out of the plane by a sliding clamp incorporated into the carrier frame. Oversize makrolon covers are attached to the front and back of the carrier to protecting the kapton electrical pigtail and its connector that emerge from the body of the module. The makrolon can be further strengthened at its two outer corners by the addition of two 15mm PCB-style spacers that hold the front and rear covers apart. An angled bracket fixed to the side of the framework allows the pigtail interface card and its components to be retained for each individual carrier. In total more than 1000 of these units could be needed.

(2) Base Unit:

This is machined from the same material as the carrier and to the same tolerances and aperture profile. There are four connections to the unit (two entries and two exits) two to allow coolant fluid to flow through the base unit and two to provide the inert gas environment for the active module. The fluid passes directly beneath the cooling-side facing, while the gas is distributed throughout the full volume of the box, with the pipe fittings being appropriate for connection to push-fit 6mm tubing. Each module-testing site will require a few of these, and the total number should be about 20 units.

3 BASIC OPERATIONS

- In storage and transport mode: the module is fitted within the carrier, and the large covers are in place, and inert gas supplied as required.

- In module test mode: the rear cover is removed and the module within its carrier is attached on to the base unit and electrical, fluid and gas connections are made. If test access is required the top cover can be removed and the carrier unit fitted with split test covers.

4 SUMMARY

By separating the carrier and module test functions it has been possible to reduce the number of components for this unit and hence reduce the overall system costs. In this way modules can undergo initial tests in a safe manner after their construction, be stored and transported safely, and have minimum handling through to mounting on the barrel cylinders, by allowing access for the mounting robot directly in to the box. Agreement on the final version of the box and its accessories will be made shortly, and production will start during summer 2001 and be completed by the end of 2001.

Module assembly jigs and assembly steps of the barrel modules

T. Kohriki[a], T. Kondo[a], S. Terada[a], Y. Unno[a], K. Hara[b], R. Takashima[c], I. Nakano[d], Y. Iwata[e], T. Ohsugi[e]

[a]KEK
[b]Tsukuba University
[c]Kyoto University of Education
[d]Okayama University
[e]Hiroshima University

Abstract

The second version module assembly jigs are developed at KEK by feeding back the experience and issues identified in the first jigs. An overview of the second version jigs, in comparison with the first ones, is presented, followed by descriptions of the assembly station, individual jigs, and step-by-step assembly process.

I. Introduction

During the fabrication of first version of module assembly jigs and building more than five precision mechanical module, we have gained experience and insights into the jigs and assembly steps. These first version assembly jigs and the precision of assembled mechanical modules were reported in the SCT weeks in Nov. 1998 [1] and Feb. 1999 [2]. Having feedback from these results and experience, we have developed a new set of assembly jigs, the second version. This note describes the new set of module assembly jigs and assembly steps.

Although the full module assembly includes the assembly of hybrid on the baseboard and wire-bondings, this note describes the fabrication jigs which requires precision, i.e, aligning the detectors, in plane and back-to-back, and to the dowel holes in the baseboard. The hybrid alignment and wire-bondings are much less stringent in precision than these detector and dowel alignment.

II. Assembly jigs

A. Feedback from the first version assembly jigs

The first version module assembly jigs were developed in the process of evaluating, improving, and simplifying the Rutherford jigs. The first version jigs fabricated the detector-baseboard units with a precision less than about 4μm. Although the precision was within the tolerance of the module [3], the observations were

1. linear bearings-pins introduced 2 to 5 μm errors due to elastic deformation,
2. location of the linear bearings-pins introduced displacement not only in angle but also alignment between the top and the bottom detectors, i.e., back-to-back alignment, due to the lever-arm if there was moment to the top or bottom transfer plates when they were mated,
3. removing the baseboard from the fixed dowel pin was difficult because the dowel pins and holes were made without play,
4. aligning detectors in plane could be made easier if the axis of transfer plates is pre-rotated by 20 mrad, leaving the detectors aligned in one direction, x-axis, which, then requiring small correction in rotation and in the translation in transverse to the strip direction, y-axis.

These issues requested usage of the jigs with great attention. The concept of 1st assembly station is shown in the figure in the appendix.

B. Overview of the second version jigs

Consideration to the issues in the first version jigs has lead to a design of the second version jigs. A conceptual view of the second jigs is shown in Figure 1. The collection of the second version jigs can be seen in Figure 2. The modifications to the first version jigs are

1. location of the linear bearings-pins is moved to the ends of the detectors in the strip direction and in the centre axis of the detectors, in order to have a larger separation of two bearings-pins and a shorter distance to the detector's side-edges, which reduces the influence of the elastic move of the pins,
2. the axis of the linear bearings-pins is rotated 20 mrad to the x-axis of the rotation-translation and the main translation stages,
3. the dowel pins are made movable by using linear bearings-pins, so that the pins can be moved down when the baseboard is taken out of the jig,
4. introducing a master gauge which defines the location of the master pins and the dowel-pins, from which the locations of linear bearings in associated jigs are copied, even to the multiple sets of jigs required for parallel operation of module assembly,
5. introducing a detector pre-alignment fixture, which eases the detector handling in an open space, simplifies the top table of the rotation stage which allows to make the assembly station concise,
6. use of disposable clean-room paper, which is porous enough to transmit vacuum, on the surface of the jigs where a detector touches, which is a common practice in a detector vendor.

The rotation-translation stage of the assembly station is shown in Figure 3, where detectors are vacuum-chucked on the rotation tables. Descriptions of the jigs are given in the next section. Most part of the jigs are made of an aluminium alloy, except the master gauge which is made of a steel alloy.

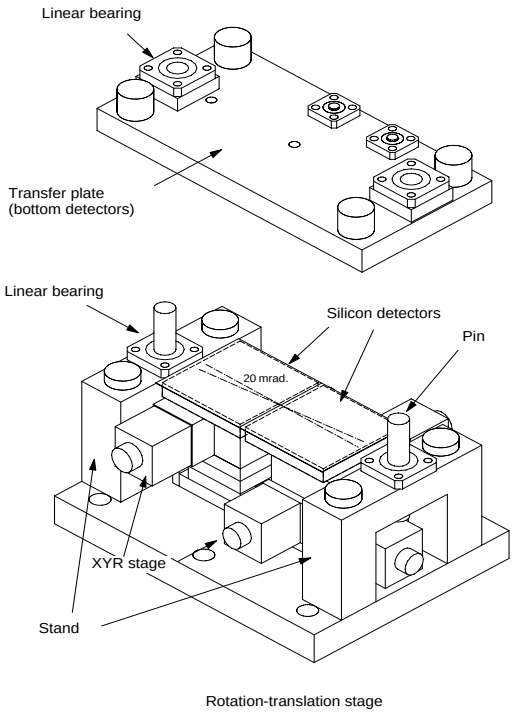

Figure 1: Conceptual view of the second version module assembly jigs

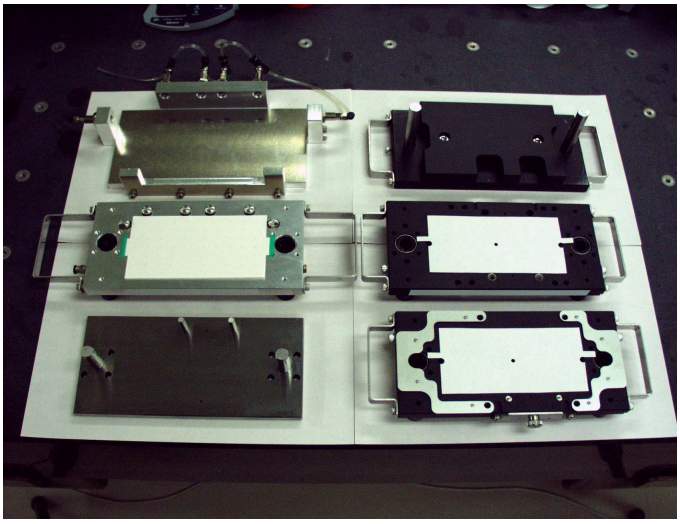

Figure 2: Overview of the second version barrel module assembly jigs: Master gauge (bottom-left), Detector pre-alignment fixture (top-left), Bottom fixture (top-right), Bottom detector transfer plate (bottom-right), and Top detector transfer plate (middle-right)

C. Jig description

1) Assembly station

An overview of the assembly station is shown in Figure 4, where the main components are a microscope-based rotation-translation stage and a video screen to display the view of the microscope. The assembly station is made of two blocks of stages: the main xy stage, X0 and Y0, and a pair of rotation-translation stages, (x1,y1, θ1) and (x2, y2, θ2). The sequence of the motion stages are, from the top,

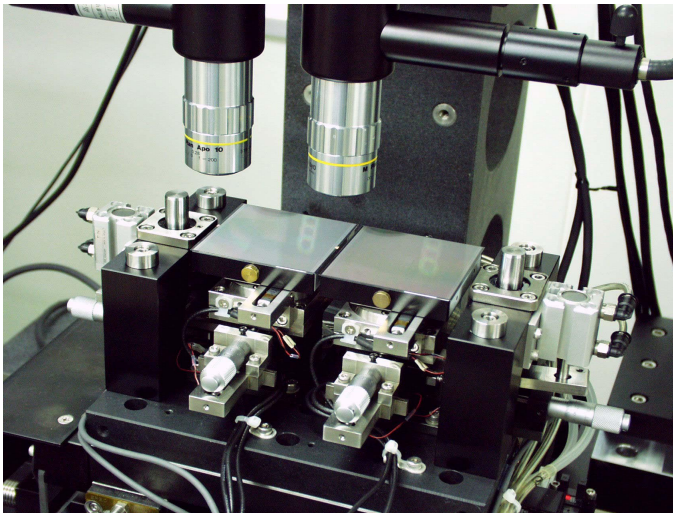

Figure 3: Rotation-translation stage in the assembly station

1. θ1 and θ2 -- rotation stages of two detectors, programme driven,
2. x1 and x2 -- small x-axis translation stage, programme driven,
3. y1 and y2 -- small y-axis translation stage, programme driven,
4. Y0-- main y-axis translation stage, programme driven,
5. X0-- main x-axis translation stage, programme driven.

The main xy stage and the microscope unit can be any of existing equipment as long as the precision fulfils requirement. The small rotation-translation stage is a specific for the detector-baseboard alignment purpose.

The rotation-translation stage of the assembly station has linear bearings for holding master pins for the detector transfer plates. The axis of the linear bearings is rotated 20 mrad to the x-axis of the rotation-translation stage and of the main xy stage. The setting of the 20 mrad axis is described in the section of rotation-translation stage setting.

2) Master gauge

One of the major issue in the assembly jig is to make identical copies. Since the required tolerance is less than an order of 5 μm, it is very costly if all the jigs are machined individually to the accuracy. A simple and economical method is to make a precision master gauge and adjust parts of associated jigs to mate the gauge. This copying of the master gauge is made possible with the use of flange-type linear bearings. The flange of the linear bearing is fixed in the associated jigs after mating the pins of the master gauge.

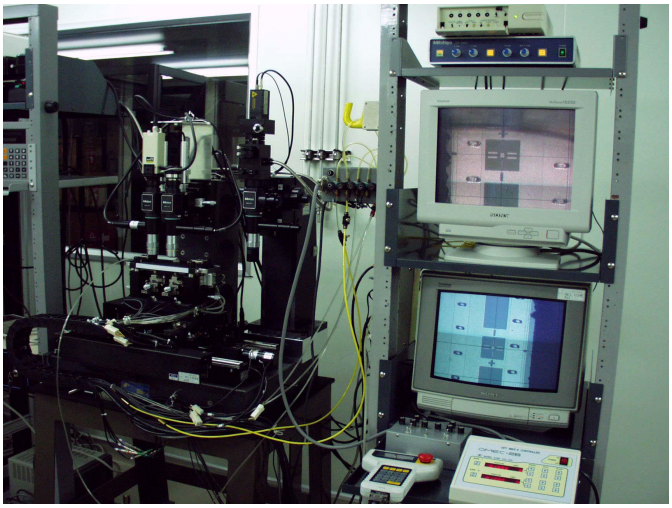

Figure 4: Overview of the barrel module assembly station. The left screen displays the centre fiducial mark of the barrel detector which is being set on the rotation-translation stage of the assembly station.

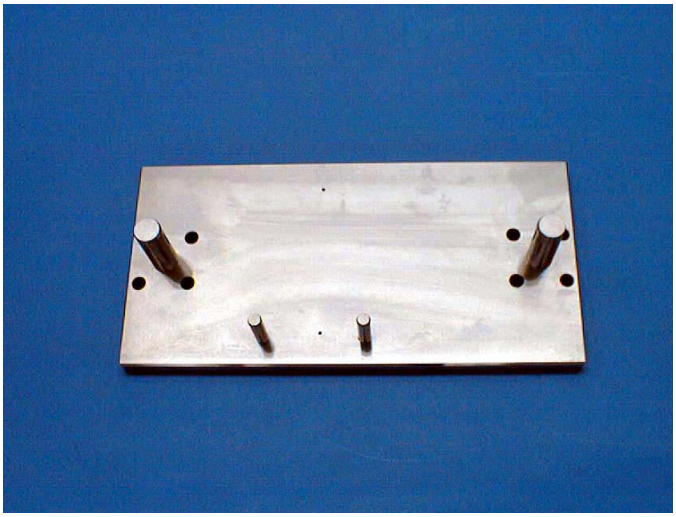

Figure 5: Master gauge. The large two pins are for the detector alignment and the small two pins are for the dowel hole and slot alignment.

The master gauge of the second version jigs is shown in Figure 5. There are two master pins for detector alignment and two small pins for the dowel holes in the baseboard. These master and small pins are made by planting a thicker pins and machining to a diameter a few microns thicker than the diameter of the mating linear bearings. The machining ensures the diameters and the normality of pins. Around the master pins there are four holes so that the screws of the flanges can be fixed through the master gauge when fitted. The gauge is made of a steel-alloy.

Ideally, the axis of the master pins will be the centre line of the module and the module centre will be defined from the location of the dowel pins. Critical dimensions are, as shown in Figure 6,

1. parallelism of the master and the small pins,
2. distance between the axes of the master and dowel pins.

Any offsets from the above can be corrected, but, introduces complexity in the aligning the detectors in the assembly station.

3) Detector pre-alignment fixture

The detector pre-aligning is required so that the centre of the rotation stage is at the centre of the detector in order to separate the movement in translation and in rotation. In the first version jigs, the alignment pins were planted on the rotation table. There were two issues in the step of the pre-alignment:

1. it was possible to work on placing the detectors on the rotation tables in the assembly station, but was awkward because of other objects such as the microscope,
2. the alignment pins chip the detector edge when the detectors are transferred out of the table.

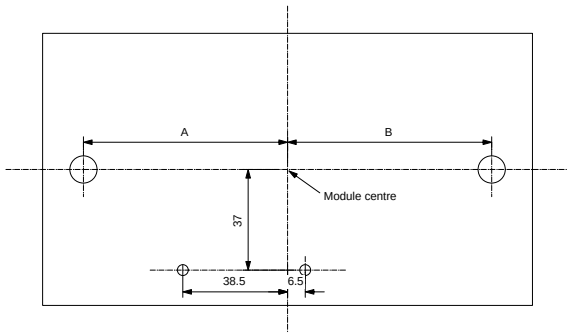

Figure 6: Critical dimensions of the Master gauge. The exact values of “A” and “B” are not critical but the module centre must be known within a required precision.

In order to solve these issues, a detector pre-alignment fixture, shown in Figure 7, is designed, which allows

1. placing the detectors in a separate open space and being able to work simultaneously with precision alignment in the assembly station,
2. alignment pins to be retracted off from the detectors once the detectors are vacuum-chucked to the fixture.

The two master pins in the fixture are pins inserted to linear bearings in the fixture The locations of the linear bearings are copied from the master gauge, although a full precision is not required in these pins.

The surface protection of the detectors and the fixture is made by using a clean-room paper which will be disposed every time when new detectors are placed. The clean-room paper is porous enough to transmit vacuum in order to vacuum-chuck detectors. The use of this clean-room paper for the surface pro-

tection is a common practice in testing detectors in a detector vendor.

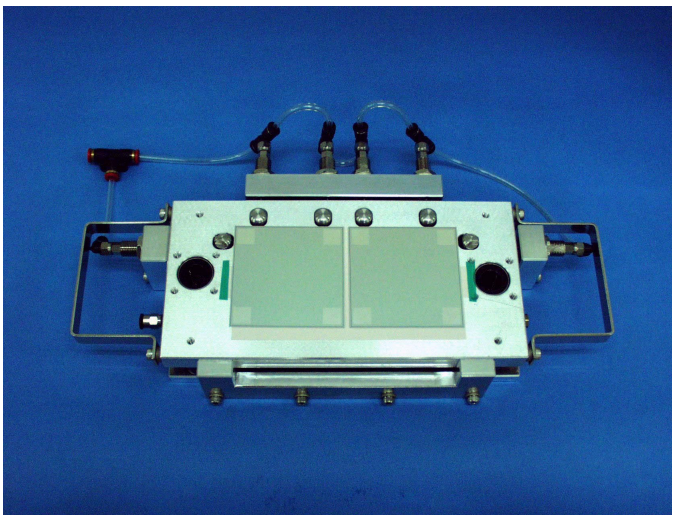

Figure 7: Detectors pre-alignment fixture. The white section is a disposable clean paper. The detector alignment pins will be retracted after the detectors are vacuum-chucked to the fixture.

4) Bottom fixture

Stacking is the concept of the module assembly jigs: from the bottom, the bottom detectors, the baseboard, and the top detectors. The detectors are aligned and vacuum-chucked in transfer plates. In order to stack the transfer plates, a base plate called the Bottom fixture, is designed to hold the master pins and to make clearance for the flanges of the linear bearings of the Bottom-detector transfer plate. The Bottom detector transfer plate itself is described in the next section. The fixture is shown in Figure 8. No critical accuracy is required to the location of the master pins which are being held loosely in the fixture.

5) Bottom detector transfer plate

There are two detector transfer plates. One is for the bottom detectors and the other for the top detectors. The bottom detector transfer plate is shown in Figure 9. The transfer plate carries the master linear bearings which are hidden with the frame-spacer, the dowel pins, with which the baseboard is aligned to the detectors, and a frame-spacer, which defines the thickness of the detector-baseboard unit, surrounding the detector chucking area.

The shiny metal frame is the frame-spacer, which has cut-outs for the detectors, the master pins, and the dowel pins. The linear bearings for the master pins are hidden under the frame-spacer. The dowel pins are pins inserted in the linear bearings. The heads of a thicker pins are machined to be the diameter of the dowel screws of the module mounting. The dowel pins are movable, being able to be pushed down, with a metal plate seen in the edge of the jig, connected to the pins. This helps removing the baseboard from the dowel pins since the dowel pins and the dowel holes in the baseboard are designed without play.

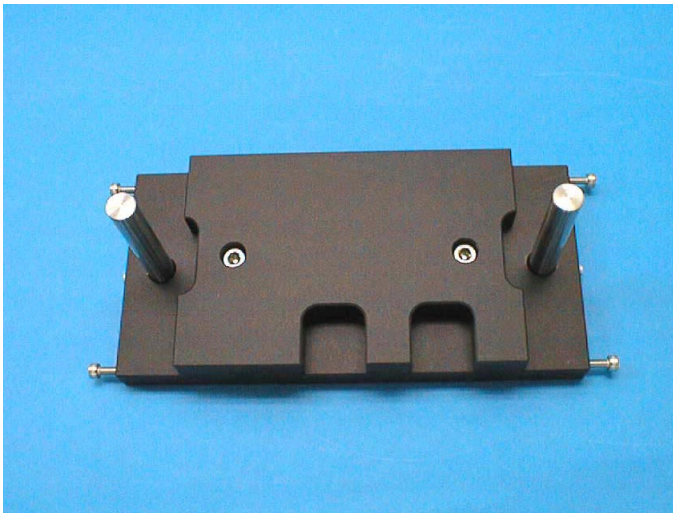

Figure 8: Bottom fixture. A simple pedestal fixture making clearance for the heads of the linear bearings and holding the master pins.

The detector area is covered with the disposable clean-room paper for detector protection. The jig and the clean-room paper have holes along the centre line of the module in order to inspect the location of the fiducial marks from the back after vacuum-chucking the detectors. The thickness uniformity of the clean-room paper is important because the thickness must be counted into the thickness of the frame-spacer. A measurement has shown the uniformity is good. In addition, the thickness can be monitored by sampling the lots.

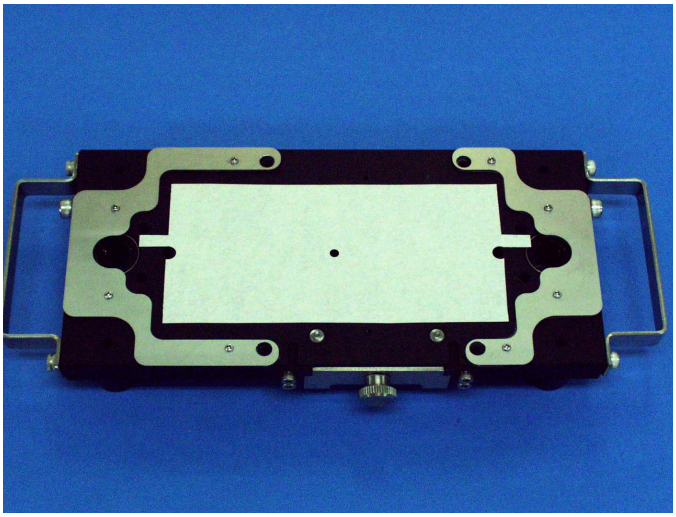

Figure 9: Bottom detector transfer plate. The shiny metal frame is a spacer defining the module thickness, i.e., the distance between the surfaces of the top and the bottom detectors sandwiching the baseboard. The white centre piece is a disposable clean-room paper. The two pins at the bottom-centre is the dowel pins for the dowel holes of the baseboard.

6) Top detectors transfer plate

A pair to the bottom detector transfer plate is the top detector transfer plate, shown in Figure 10. The jig is basically the same as the bottom detector transfer plate, except the dowel pins, for which female holes are machined in the mirror positions. The linear bearings of the master pins are visible in the jig. The frame-spacer can be attached to the top detector transfer plate as well.

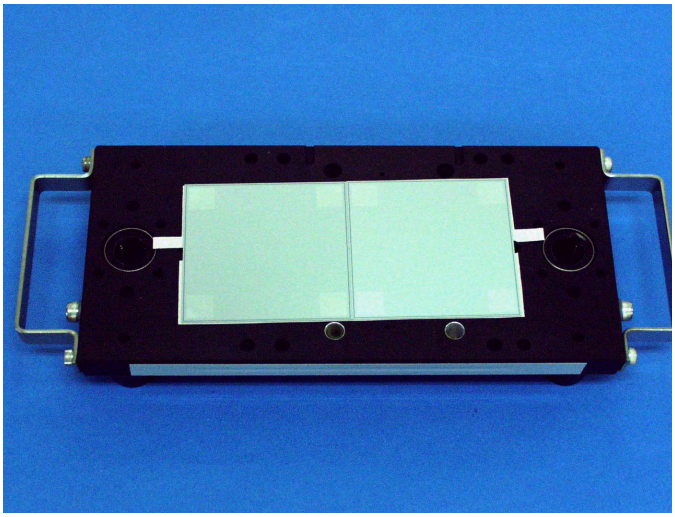

Figure 10: Top detectors transfer plate. The white piece is a disposable clean paper.

7) Glue dispensing machine

The detectors and the baseboard are glued with a room-temperature curing epoxy glue, e.g., Araldite 2011, with a Boron-Nitride filler to help thermal conductivity. The epoxy glue is applied to the both sides of the baseboard with pre-defined amount to ensure the glue thickness. The application is made with a glue dispensing machine which is a combination of a xyz stage and a glue dispensing unit. Use of a glue dispensing machine is a clean way of applying glues, by touching the baseboard only when it is placed and removed from the machine.

Since the glue hardenes in several hours in the room temperature, the viscosity of the glue changes in time, and, in addition, after several hours the glue has to be disposed. An economical glue dispensing is to use a disposable syringe, which is driven by pressure. The change of the viscosity can be compensated by changing the pressure, which is effective for applying dot patterns, and/or changing the speed of head movement, effective for applying line patterns

A machine being used at KEK is shown in Figure 11, which has capability of programming pressure in time [4]. Empirical pressure adjustment curve is shown in Figure 12 for the Araldite 2011 with BN filler in compensating the change of viscosity. The variation of dispensed amount is less than 5% even after one hour from the mixing.

Figure 11: Glue dispensing system which is made of (1) a xyz stage where the baseboard is on the xy stage and a glue-syringe is attached on the z-axis, and (2) a dispensing controller.

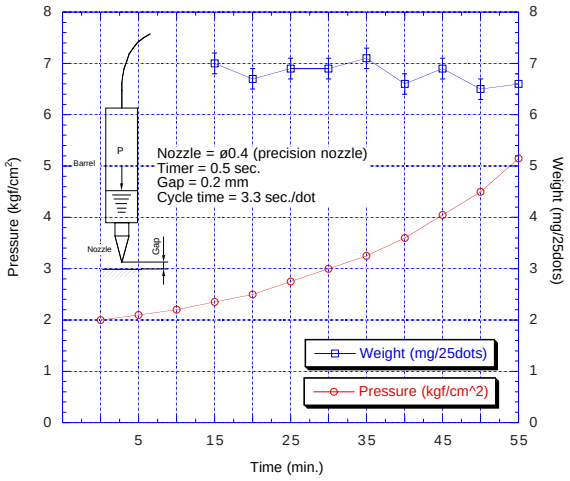

Figure 12: Pressure compensating the change of viscosity of the Araldite 2011 with BN filler (circle) and the weight of dispensed glue in 25 dots (square)

D. Copying the Master gauge

1) Rotation-translation stage

The rotation-translation stage aligning the detectors will have the master pins to which the transfer plates are slided down. The location of the master pins is copied from the master gauge by adjusting the location of the linear bearings of the rotation-translation stage, as shown in Figure 13. Separate master pins, which diameters are measured to match the master pin of the master gauge, are, then, inserted into the linear bearings of the rotation-translation stage.

The location of the linear bearings is at 20 mrad rotation to

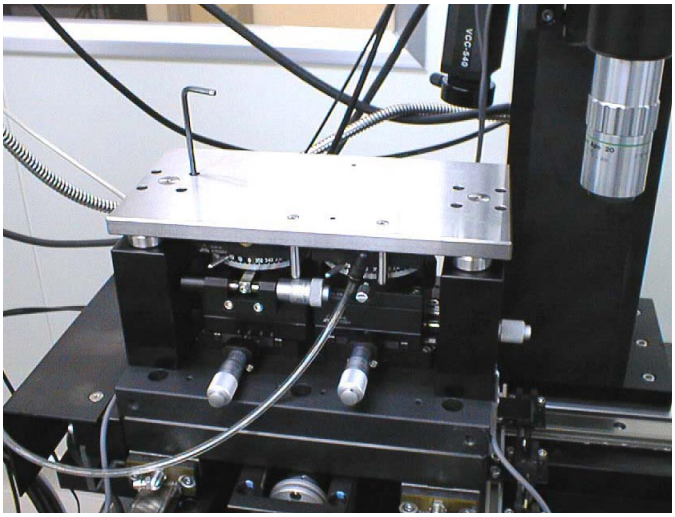

Figure 13: Copying the master pin locations to the linear bearings of the rotation-translation stage from the master gauge

the x-axis, but imperfect because of the required play for the process of copying the master gauge.

2) Transfer plates

The locations of the master (and small) pins of the master gauge are copied to the bottom detector transfer plate by sliding in the transfer plate on to the master gauge and fixing the flanges of the linear bearings. The mating of the master gauge and the bottom detector transfer plate is shown in Figure 14. The similar process is repeated to the top detector transfer plate to copy the master gauge.

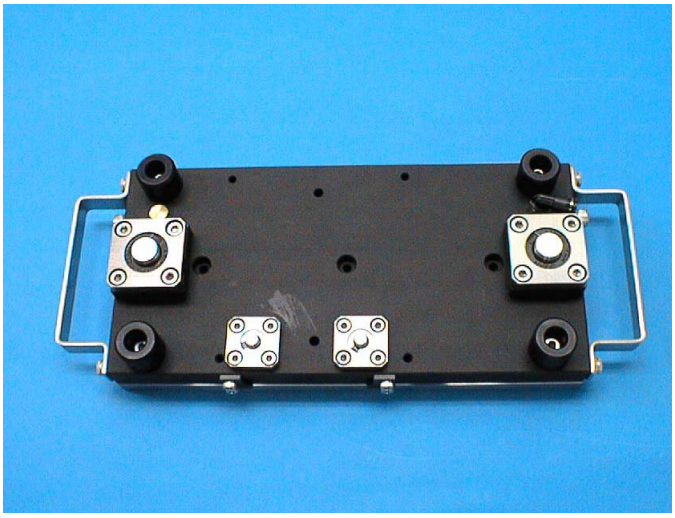

Figure 14: Copying the pin locations from the master gauge to the bottom detectors transfer plate for both the detector and the dowel linear bearings

E. Rotation-translation stage setting

In order to ease the aligning of the detectors, the axis of the master pins of the rotation-translation stage is rotated 20 mrad to the x-axis of the x-translation stages, x1 and x2. With the rotation, if perfect, the detectors, which must be rotated 20 mrad to the module centre line, i.e., the axis of the master pins, is aligned along the x-axis of the stages, as shown in Figure 15. The detectors, then, require only a small correction in the rotation in $\theta 1$ and $\theta 2$ and a small correction in the translation in y2, since the detectors are pre-aligned in the pre-alignment fixture. One remaining relatively large motion is along the x-axis, x2, since a large gap is left between two detectors on the pre-alignment fixture in order to allow a safe operation in the rotation and the y-translation.

The accurate 20 mrad rotation of the axis of the master pins to the x-axis of the main x-translation stage is made by making correction to the unit of rotation-translation stage:

1. the centres of the master pins are obtained by measuring the outer circles of the pins optically,
2. the centres of the pins are referenced to the fiducial marks on the unit of rotation-translation stage,
3. the unit is moved until the fiducial marks are in the preset positions such that the axis of the centres of the master pins is rotated 20 mrad to the x-axis of the main x-translation stage.

The fiducial mark, after setting the rotation-translation stage, is displayed on the video screen in Figure 16. Because of this correction to the rotation-translation stage, there arises a small correlation in the small xy stages, x2 and y2, in the rotation-translation stage, in reality.

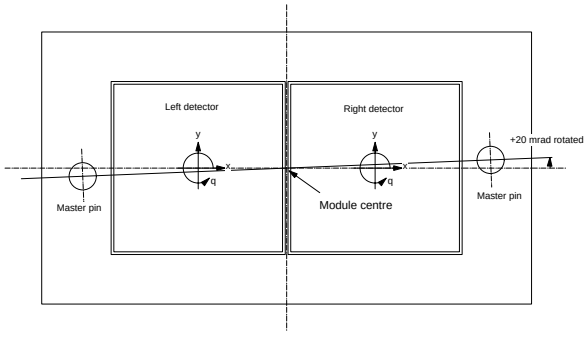

Figure 15: Rotated axis of the master pins in the rotation-translation stage to make the move of the detectors minimum

III. Assembly steps

The detector-baseboard assembly sequence proceeds in the steps of, pre-aligning detectors, transferring detectors to the rotation-translation stage, aligning detectors in precision, transferring detectors to the transfer plates, placing the baseboard on the bottom detector transfer plate with the bottom detectors vacu-

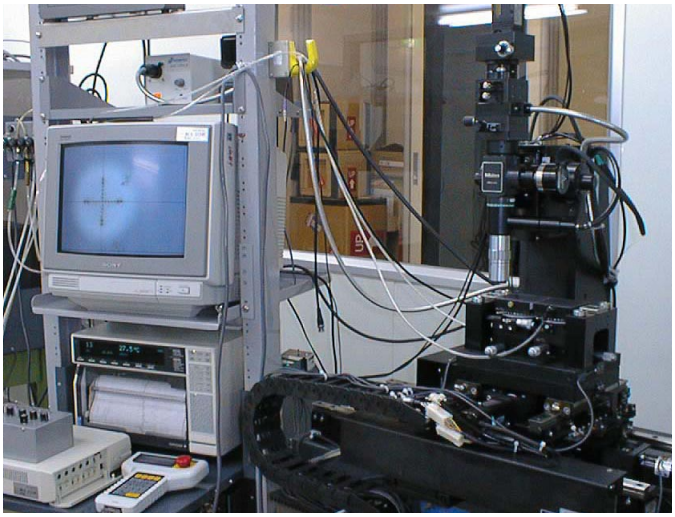

Figure 16: Setting the axis of the master pins of the rotation-translation stage rotated 20 mrad to the x-axis of the main x-stage

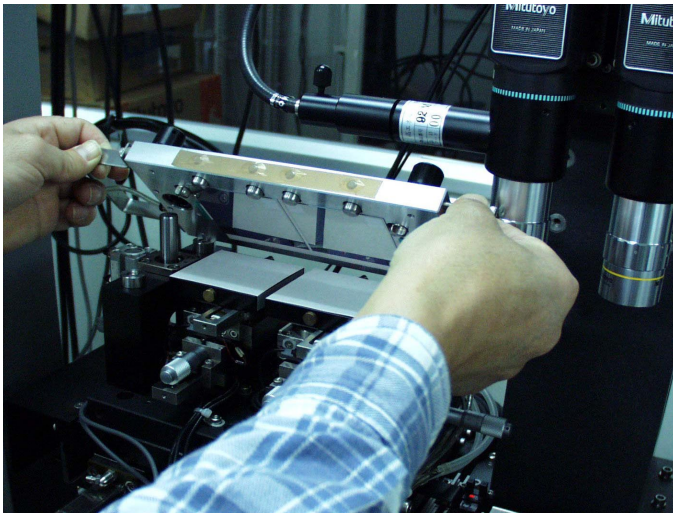

Figure 18: Placing the chucked detectors on the detector pre-alignment fixture to the rotation-translation stage

um-chucked, and mating the top detector transfer plate with top detectors vacuum-chucked.

1) Pre-aligning detectors

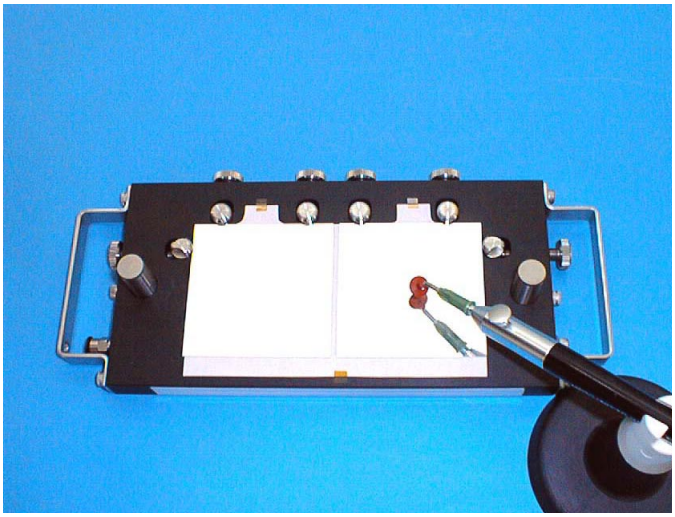

Figure 17: Placing the detectors on the detector pre-alignment fixture. A vacuum picker can be used in holding detectors.

A detector is picked up from the detector envelope with a vacuum picker by chucking the backside of the detector. With the alignment pins pressed to the nominal positions, two detectors are placed to touch the alignment pins at each edge, as shown in Figure 17. Once the detectors are vacuum-chucked to the pre-alignment fixture, the alignment pins are retracted off the detectors to a safe position.

2) Transferring to the rotation-translation stage

The pre-alignment fixture is transferred to the rotation-translation stage while vacuum-chucking the detectors, as shown in Figure 18. A spacer is ensuring such that there is a gap of 10 to 20 µm between the surface of the detectors and the surface of the rotation tables. The detectors are transferred to the rotation table by turning off the vacuum of the pre-alignment fixture and, sequentially, turning on the vacuum of the rotation table. It is not critical in this step, but critical in the precision process, to turn the vacuum off and on sequentially. It is found that when the both vacuum are on, the stages move and there arises random move in the detector position of 5 to 10 µm, due to imperfect flatness or parallelism in the two jigs.

3) Aligning detectors in precision

Two detectors on the rotation-translation stage are aligned in precision by observing the fiducial marks on the detectors, as shown in Figure 19. Since the rotation of the 20 mrad is already taken care of by the axis of the master pins, after small correction in rotation, a move of two detectors in the x-direction with a small correction in y-direction can set the fiducial marks to pre-defined positions, defined from the module centre in the master gauge, relatively in straight-forward way.

4) Transferring to the detector transfer plates

Once the detectors are aligned in precision, the detectors are transferred to the transfer plate. The bottom detector transfer plate being placed on the stage is shown in Figure 20. A gap of 10 to 20 µm is ensured, with a spacer, between the surface of the detectors and the transfer plate. The detectors are transferred by turning the vacuum of the rotation tables off, first, and, then, turning the transfer plate on, sequentially. It is important to confirm the coordinates of the fiducial marks of the detectors, after transferring, viewed through the observation holes, so that there is little move in the transferring.

The bottom detector transfer plate with detectors being vacuum-chucked and placed on the bottom fixture is shown in

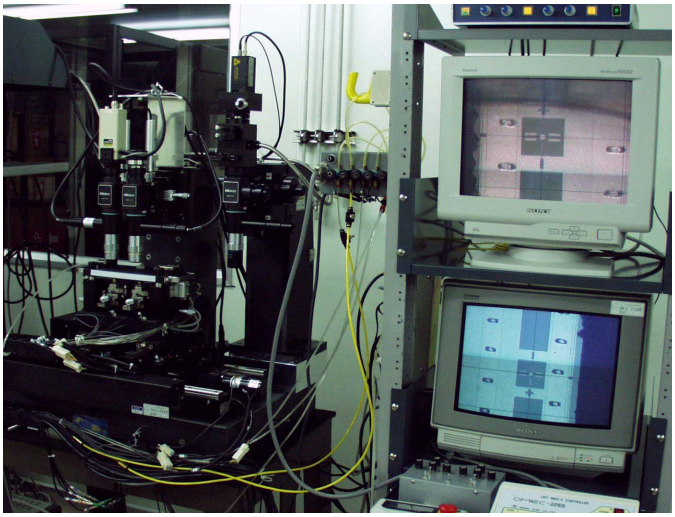

Figure 19: Aligning detectors

Figure 21. The top detectors are also aligned in precision and transferred to the top detector transfer plate

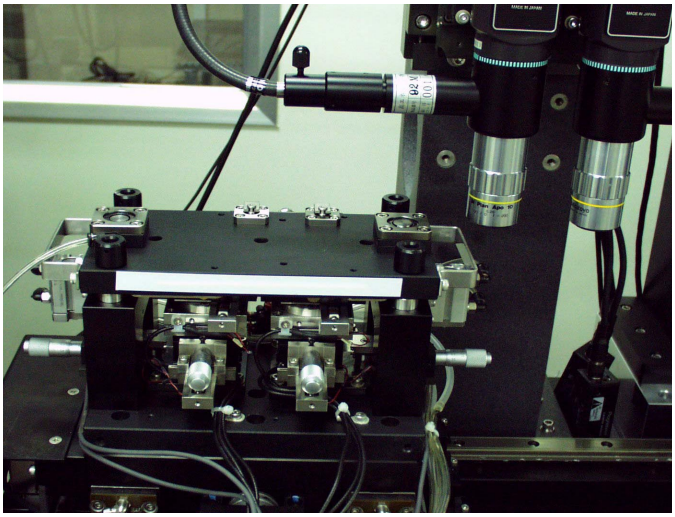

Figure 20: Transferring detectors from the rotation-translation stage to the bottom detector transfer plate. The fiducial marks of the detectors can be seen through the observation holes.

5) Placing baseboard on the bottom detectors transfer plate

In “one-step” gluing, the baseboard is with glues applied in both sides is placed over the bottom detectors on the bottom detector transfer plate, as shown in Figure 22. The alignment of the baseboard is made by using the dowel pins in the transfer plate and the dowel holes in the baseboard.

6) Mating the top and the bottom detectors transfer plates

Immediately after the baseboard is placed on the bottom detector transfer plate, the top detector transfer plate with top detectors being vacuum chucked is slided in, in order to sandwich

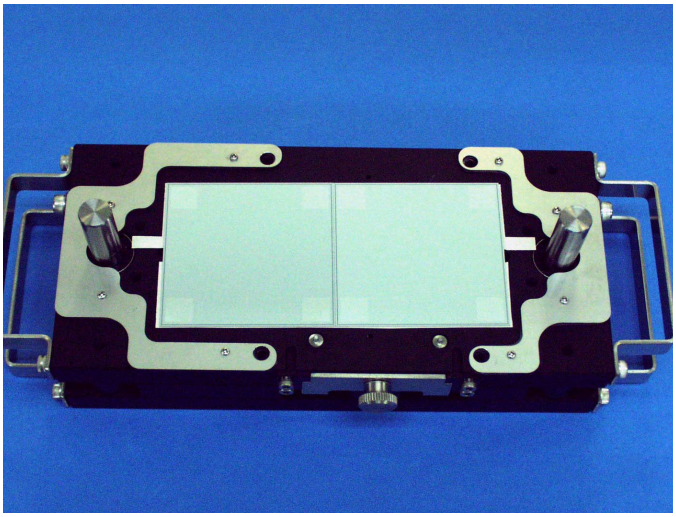

Figure 21: Aligned detectors chucked on the bottom detector transfer plate

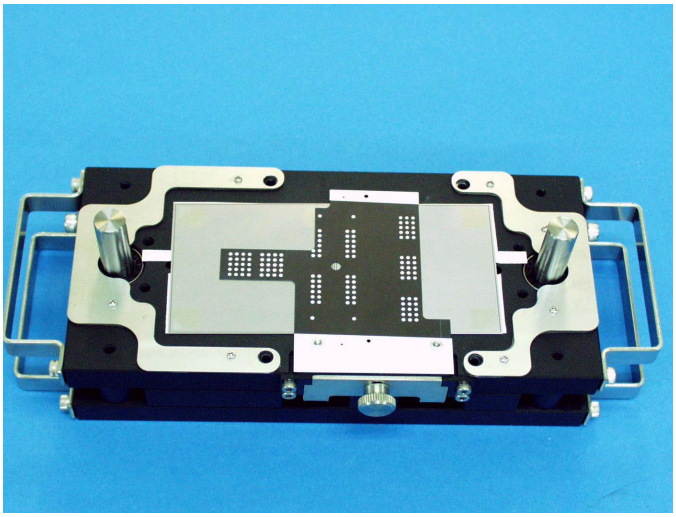

Figure 22: Baseboard is being placed over the bottom detectors. The alignment of the baseboard to the detectors are being made with the use of dowel pins in the bottom detector transfer plate and the dowel holes in the baseboard.. The baseboard and the glue pattern is of the “narrow nose” type. The latest baseboard is of the “wide nose” and the glue pattern has been updated.

the baseboard with the top and the bottom detectors, as shown in Figure 23. The top and the bottom detector transfer plates are, then, pressurized with screws and left in the room temperature for several hours until the glue is cured. The completed detector-baseboard assembly, on the jig, is shown in Fig.xx.

7) Two-step gluing of the assembly

After analysing the assembled modules, the flatness of the module was found to be affected by the deformation in the neck between the facings and the main part. In the “one-step” gluing, the baseboard was constrained, at the facings, so that the loca-

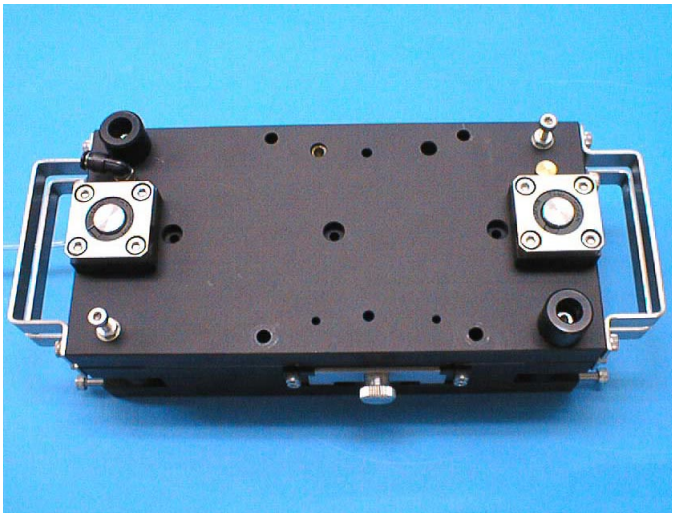

Figure 23: Mating the top detectors and the bottom detectors transfer plates

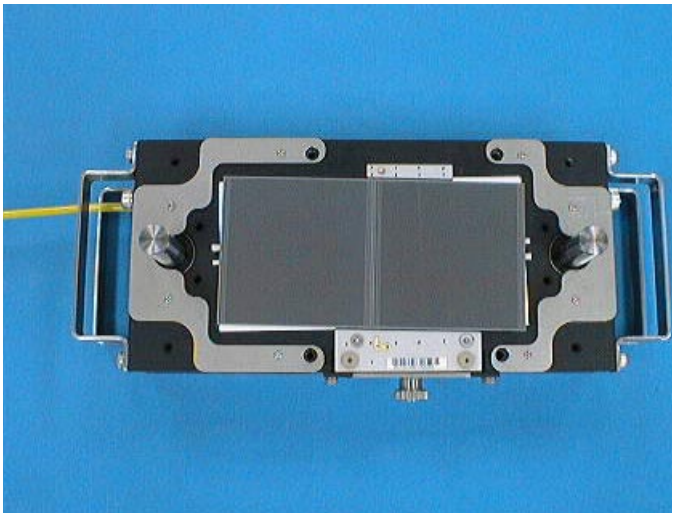

Figure 24: Completed detector-baseboard assembly

tion in height of the baseboard is constrained. This constraint did not work since the viscosity of the glue was much higher than adjusting the glue thickness by the constraint. Instead, the constraint introduced distortion in the neck between the sensor and the facings, which introduced distortions in the flatness of the modules, together.

In order to make the facings free and constrain the baseboard, the baseboard must be held in the main area. This holding the main area of the baseboard with vacuum-chuck transfer plate helps to flatten the baseboard, in addition. Since the glue can not be applied to the vacuum-chucking side, the gluing step is now step-by-step: one side first and then the other side, i.e., "two-step gluing".

In the "two-step gluing", the usage sequence of the transfer plates is reversed. Topside sensors are aligned first, picked up with the top transfer plate, and placed on the bottom fixture. The baseboard is placed on the bottom transfer plate using the dowel pins, vacuum-chucked. Applying the glue on the baseboard, the baseboard is placed over the sensors on top of the top transfer plate and glue is cured. The bottom sensors are aligned and picked up with the bottom transfer plate which is freed from the baseboard, with the dowel pins being recessed. Applying the glue on the baseboard of the baseboard-top sensors assembly still held on the top transfer plate, the bottom transfer plate is mated over the baseboard assembly and the glue is cured.

IV. Summary

A second version of module assembly jigs has been designed and fabricated at KEK by feeding back the experience and the issues found in the first version of the jigs. The major modifications in the second version are the move of the location of the master pins, introduction of the master gauge, the pre-alignment fixture, and the 20 mrad rotation of the axis of the master pins in the rotation-translation stage. Experience of the assembling and the precision of the assembled modules will be reported in a separate document.

V. Appendix

A conceptual view of the first assembly jigs is shown Figure 25

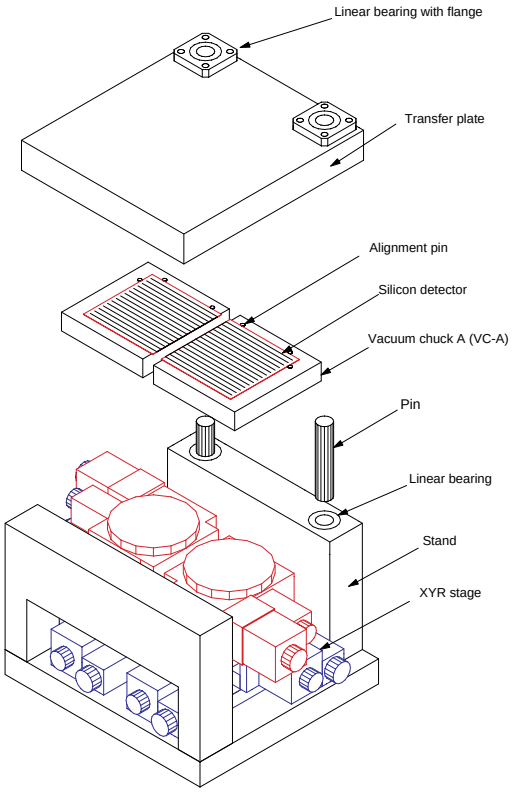

Figure 25: Concept of the first version assembly station and a detector transfer plate

VI. REFERENCES

[1] T. Kohriki et al., “Assembly of precision mechanical modules at KEK”, SCT week, Nov., 1998

[2] T. Kohriki et al., “Construction of Barrel Precision Modules”, SCT week, Feb., 1999

[3] ATLAS Inner detector technical design report, CERN/LHCC/97-17, ATLAS TDR 5, 30 April 1997, pp 467-470

[4] A pressure-programmable dispenser, ML-808EX, and a xyz stage, SHOTMASTER3, made by MUSASHI engineering, inc. Tokyo, Japan. A similar equipment, ACCURA9 for the dispenser and Ez-ROBO for the xyz stage (an OEM of SONY’s ROBOKIDS), is available from IWASHITA engineering, IEI, Tokyo, Japan.

ATLAS SCT Barrel Module FDR/2001

ATLAS Project Document No.	*Institute Document No.*	*Created:*	*Page:*
SCT-BM-FDR-6 appendix 2		*Modified:*	*Rev. No.:* **A**

SCT Barrel Module Document

Appendix 2 to SCT-BM-FDR-6

Assembly Jigs & Procedures for the Japanese Cluster

abstract

This document describes the procedures of the barrel module assembly and the jigs as developed for the Japanese Cluster

Prepared by:	*Checked by:*	*Approved by:*
Y. Unno, T. Kohriki, et al., KEK		

Distribution List

Module assembly jigs and assembly steps of the barrel modules

T. Kohriki[a], T. Kondo[a], S. Terada[a], Y. Unno[a], K. Hara[b], R. Takashima[c], I. Nakano[d], Y. Iwata[e], T. Ohsugi[e]

[a]KEK
[b]Tsukuba University
[c]Kyoto University of Education
[d]Okayama University
[e]Hiroshima University

Abstract

The second version module assembly jigs are developed at KEK by feeding back the experience and issues identified in the first jigs. An overview of the second version jigs, in comparison with the first ones, is presented, followed by descriptions of the assembly station, individual jigs, and step-by-step assembly process.

I. Introduction

During the fabrication of first version of module assembly jigs and building more than five precision mechanical module, we have gained experience and insights into the jigs and assembly steps. These first version assembly jigs and the precision of assembled mechanical modules were reported in the SCT weeks in Nov. 1998 [1] and Feb. 1999 [2]. Having feedback from these results and experience, we have developed a new set of assembly jigs, the second version. This note describes the new set of module assembly jigs and assembly steps.

Although the full module assembly includes the assembly of hybrid on the baseboard and wire-bondings, this note describes the fabrication jigs which requires precision, i.e, aligning the detectors, in plane and back-to-back, and to the dowel holes in the baseboard. The hybrid alignment and wire-bondings are much less stringent in precision than these detector and dowel alignment.

II. Assembly jigs

A. Feedback from the first version assembly jigs

The first version module assembly jigs were developed in the process of evaluating, improving, and simplifying the Rutherford jigs. The first version jigs fabricated the detector-baseboard units with a precision less than about 4μm. Although the precision was within the tolerance of the module [3], the observations were

1. linear bearings-pins introduced 2 to 5 μm errors due to elastic deformation,
2. location of the linear bearings-pins introduced displacement not only in angle but also alignment between the top and the bottom detectors, i.e., back-to-back alignment, due to the lever-arm if there was moment to the top or bottom transfer plates when they were mated,
3. removing the baseboard from the fixed dowel pin was difficult because the dowel pins and holes were made without play,
4. aligning detectors in plane could be made easier if the axis of transfer plates is pre-rotated by 20 mrad, leaving the detectors aligned in one direction, x-axis, which, then requiring small correction in rotation and in the translation in transverse to the strip direction, y-axis.

These issues requested usage of the jigs with great attention. The concept of 1st assembly station is shown in the figure in the appendix.

B. Overview of the second version jigs

Consideration to the issues in the first version jigs has lead to a design of the second version jigs. A conceptual view of the second jigs is shown in Figure 1. The collection of the second version jigs can be seen in Figure 2. The modifications to the first version jigs are

1. location of the linear bearings-pins is moved to the ends of the detectors in the strip direction and in the centre axis of the detectors, in order to have a larger separation of two bearings-pins and a shorter distance to the detector's side-edges, which reduces the influence of the elastic move of the pins,
2. the axis of the linear bearings-pins is rotated 20 mrad to the x-axis of the rotation-translation and the main translation stages,
3. the dowel pins are made movable by using linear bearings-pins, so that the pins can be moved down when the baseboard is taken out of the jig,
4. introducing a master gauge which defines the location of the master pins and the dowel-pins, from which the locations of linear bearings in associated jigs are copied, even to the multiple sets of jigs required for parallel operation of module assembly,
5. introducing a detector pre-alignment fixture, which eases the detector handling in an open space, simplifies the top table of the rotation stage which allows to make the assembly station concise,
6. use of disposable clean-room paper, which is porous enough to transmit vacuum, on the surface of the jigs where a detector touches, which is a common practice in a detector vendor.

The rotation-translation stage of the assembly station is shown in Figure 3, where detectors are vacuum-chucked on the rotation tables. Descriptions of the jigs are given in the next section. Most part of the jigs are made of an aluminium alloy, except the master gauge which is made of a steel alloy.

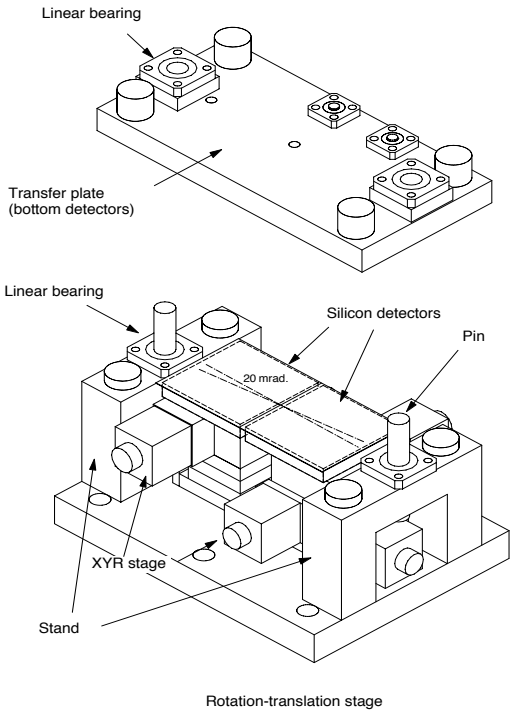

Figure 1: Conceptual view of the second version module assembly jigs

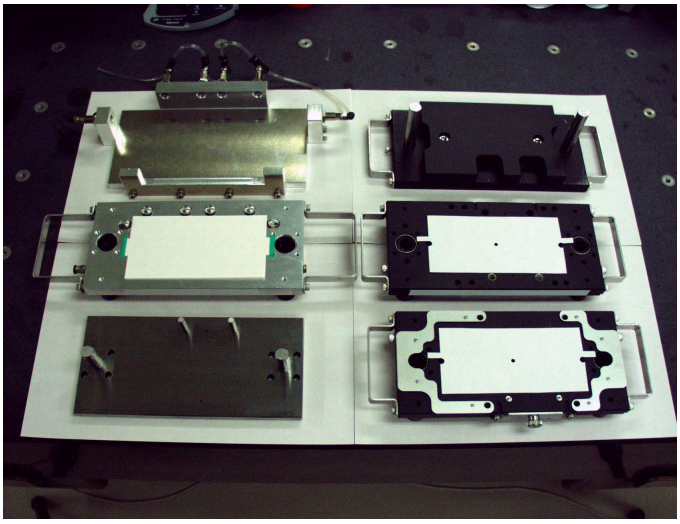

Figure 2: Overview of the second version barrel module assembly jigs: Master gauge (bottom-left), Detector pre-alignment fixture (top-left), Bottom fixture (top-right), Bottom detector transfer plate (bottom-right), and Top detector transfer plate (middle-right)

C. Jig description

1) Assembly station

An overview of the assembly station is shown in Figure 4, where the main components are a microscope-based rotation-translation stage and a video screen to display the view of the microscope. The assembly station is made of two blocks of stages: the main xy stage, X0 and Y0, and a pair of rotation-translation stages, (x1,y1, θ1) and (x2, y2, θ2). The sequence of the motion stages are, from the top,

1. θ1 and θ2 -- rotation stages of two detectors, programme driven,
2. x1 and x2 -- small x-axis translation stage, programme driven,
3. y1 and y2 -- small y-axis translation stage, programme driven,
4. Y0-- main y-axis translation stage, programme driven,
5. X0-- main x-axis translation stage, programme driven.

The main xy stage and the microscope unit can be any of existing equipment as long as the precision fulfils requirement. The small rotation-translation stage is a specific for the detector-baseboard alignment purpose.

The rotation-translation stage of the assembly station has linear bearings for holding master pins for the detector transfer plates. The axis of the linear bearings is rotated 20 mrad to the x-axis of the rotation-translation stage and of the main xy stage. The setting of the 20 mrad axis is described in the section of rotation-translation stage setting.

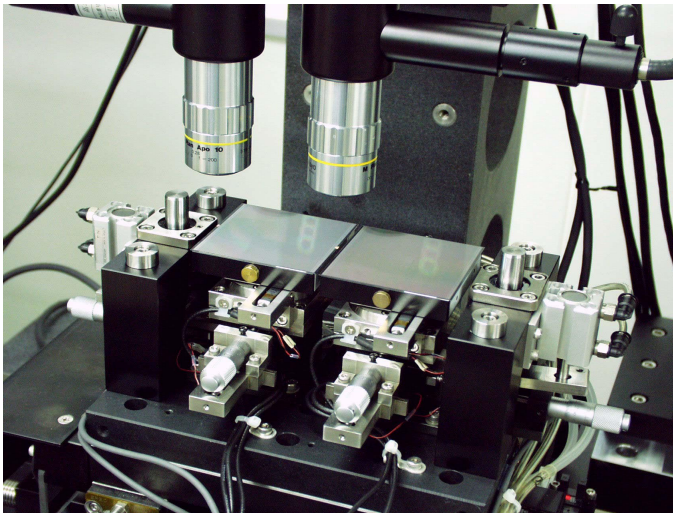

Figure 3: Rotation-translation stage in the assembly station

2) Master gauge

One of the major issue in the assembly jig is to make identical copies. Since the required tolerance is less than an order of 5 μm, it is very costly if all the jigs are machined individually to the accuracy. A simple and economical method is to make a precision master gauge and adjust parts of associated jigs to mate the gauge. This copying of the master gauge is made possible with the use of flange-type linear bearings. The flange of the linear bearing is fixed in the associated jigs after mating the pins of the master gauge.

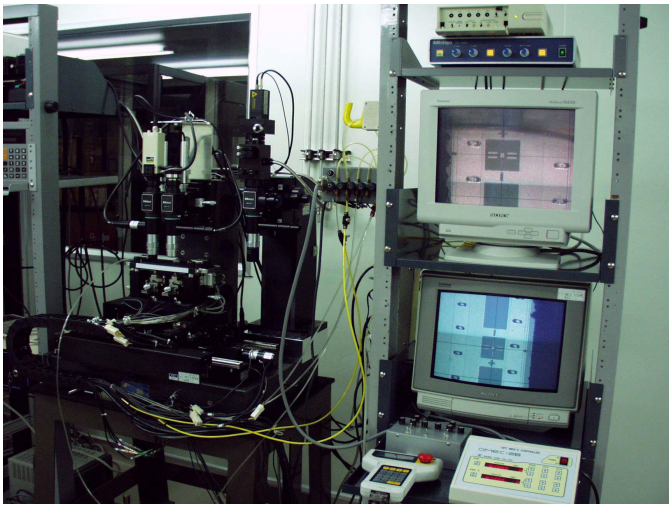

Figure 4: Overview of the barrel module assembly station. The left screen displays the centre fiducial mark of the barrel detector which is being set on the rotation-translation stage of the assembly station.

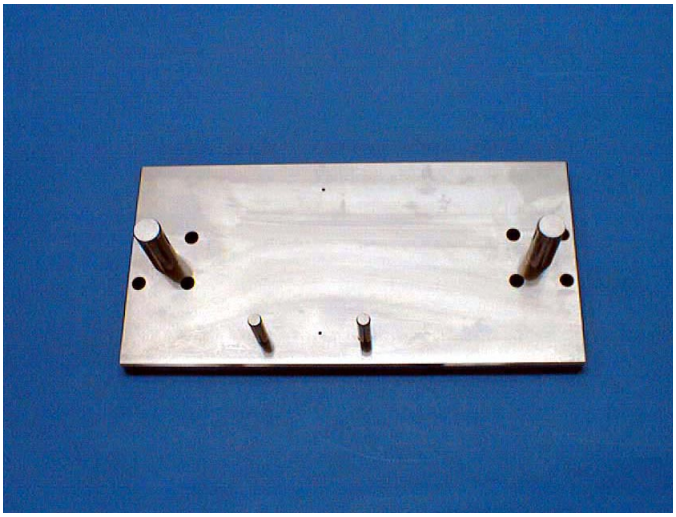

Figure 5: Master gauge. The large two pins are for the detector alignment and the small two pins are for the dowel hole and slot alignment.

The master gauge of the second version jigs is shown in Figure 5. There are two master pins for detector alignment and two small pins for the dowel holes in the baseboard. These master and small pins are made by planting a thicker pins and machining to a diameter a few microns thicker than the diameter of the mating linear bearings. The machining ensures the diameters and the normality of pins. Around the master pins there are four holes so that the screws of the flanges can be fixed through the master gauge when fitted. The gauge is made of a steel-alloy.

Ideally, the axis of the master pins will be the centre line of the module and the module centre will be defined from the location of the dowel pins. Critical dimensions are, as shown in Figure 6,

1. parallelism of the master and the small pins,
2. distance between the axes of the master and dowel pins.

Any offsets from the above can be corrected, but, introduces complexity in the aligning the detectors in the assembly station.

3) Detector pre-alignment fixture

The detector pre-aligning is required so that the centre of the rotation stage is at the centre of the detector in order to separate the movement in translation and in rotation. In the first version jigs, the alignment pins were planted on the rotation table. There were two issues in the step of the pre-alignment:

1. it was possible to work on placing the detectors on the rotation tables in the assembly station, but was awkward because of other objects such as the microscope,
2. the alignment pins chip the detector edge when the detectors are transferred out of the table.

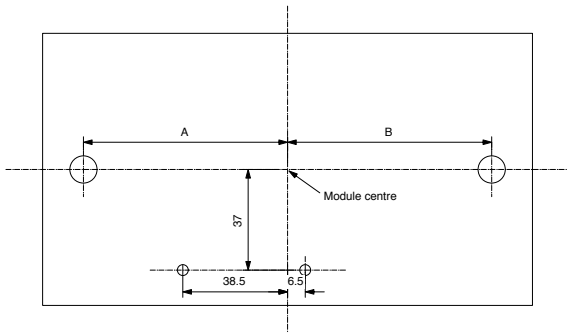

Figure 6: Critical dimensions of the Master gauge. The exact values of "A" and "B" are not critical but the module centre must be known within a required precision.

In order to solve these issues, a detector pre-alignment fixture, shown in Figure 7, is designed, which allows

1. placing the detectors in a separate open space and being able to work simultaneously with precision alignment in the assembly station,
2. alignment pins to be retracted off from the detectors once the detectors are vacuum-chucked to the fixture.

The two master pins in the fixture are pins inserted to linear bearings in the fixture The locations of the linear bearings are copied from the master gauge, although a full precision is not required in these pins.

The surface protection of the detectors and the fixture is made by using a clean-room paper which will be disposed every time when new detectors are placed. The clean-room paper is porous enough to transmit vacuum in order to vacuum-chuck detectors. The use of this clean-room paper for the surface pro-

tection is a common practice in testing detectors in a detector vendor.

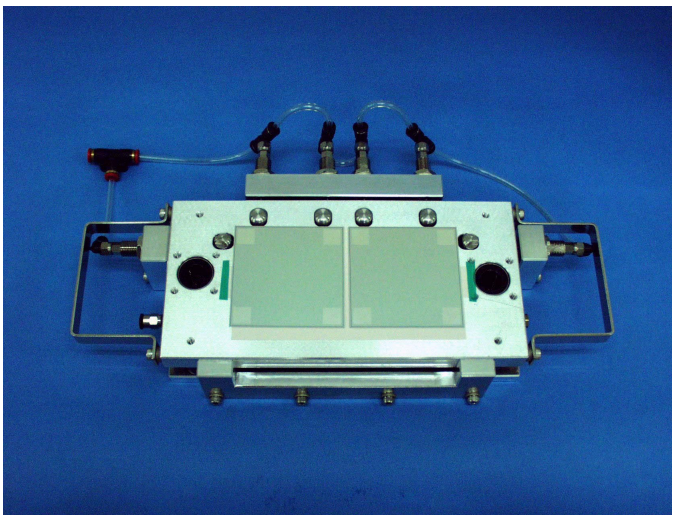

Figure 7: Detectors pre-alignment fixture. The white section is a disposable clean paper. The detector alignment pins will be retracted after the detectors are vacuum-chucked to the fixture.

4) Bottom fixture

Stacking is the concept of the module assembly jigs: from the bottom, the bottom detectors, the baseboard, and the top detectors. The detectors are aligned and vacuum-chucked in transfer plates. In order to stack the transfer plates, a base plate called the Bottom fixture, is designed to hold the master pins and to make clearance for the flanges of the linear bearings of the Bottom-detector transfer plate. The Bottom detector transfer plate itself is described in the next section. The fixture is shown in Figure 8. No critical accuracy is required to the location of the master pins which are being held loosely in the fixture.

5) Bottom detector transfer plate

There are two detector transfer plates. One is for the bottom detectors and the other for the top detectors. The bottom detector transfer plate is shown in Figure 9. The transfer plate carries the master linear bearings which are hidden with the frame-spacer, the dowel pins, with which the baseboard is aligned to the detectors, and a frame-spacer, which defines the thickness of the detector-baseboard unit, surrounding the detector chucking area.

The shiny metal frame is the frame-spacer, which has cut-outs for the detectors, the master pins, and the dowel pins. The linear bearings for the master pins are hidden under the frame-spacer. The dowel pins are pins inserted in the linear bearings. The heads of a thicker pins are machined to be the diameter of the dowel screws of the module mounting. The dowel pins are movable, being able to be pushed down, with a metal plate seen in the edge of the jig, connected to the pins. This helps removing the baseboard from the dowel pins since the dowel pins and the dowel holes in the baseboard are designed without play.

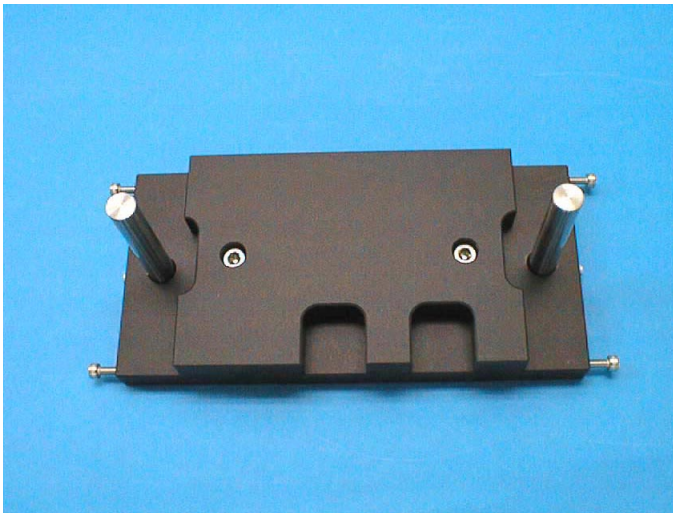

Figure 8: Bottom fixture. A simple pedestal fixture making clearance for the heads of the linear bearings and holding the master pins.

The detector area is covered with the disposable clean-room paper for detector protection. The jig and the clean-room paper have holes along the centre line of the module in order to inspect the location of the fiducial marks from the back after vacuum-chucking the detectors. The thickness uniformity of the clean-room paper is important because the thickness must be counted into the thickness of the frame-spacer. A measurement has shown the uniformity is good. In addition, the thickness can be monitored by sampling the lots.

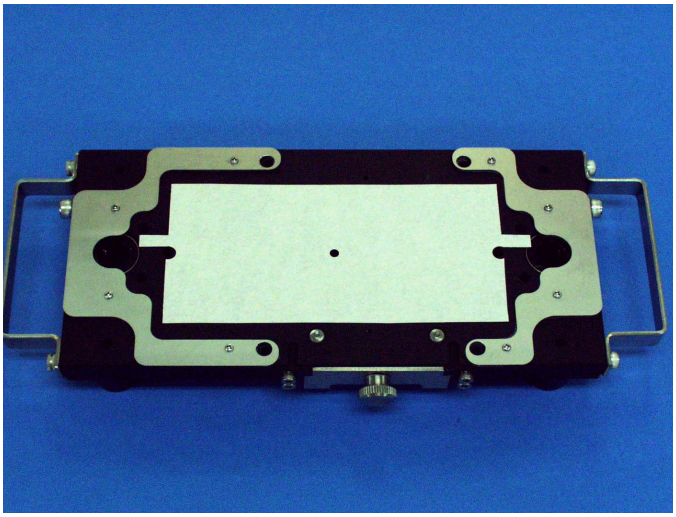

Figure 9: Bottom detector transfer plate. The shiny metal frame is a spacer defining the module thickness, i.e., the distance between the surfaces of the top and the bottom detectors sandwiching the baseboard. The white centre piece is a disposable clean-room paper. The two pins at the bottom-centre is the dowel pins for the dowel holes of the baseboard.

6) Top detectors transfer plate

A pair to the bottom detector transfer plate is the top detector transfer plate, shown in Figure 10. The jig is basically the same as the bottom detector transfer plate, except the dowel pins, for which female holes are machined in the mirror positions. The linear bearings of the master pins are visible in the jig. The frame-spacer can be attached to the top detector transfer plate as well.

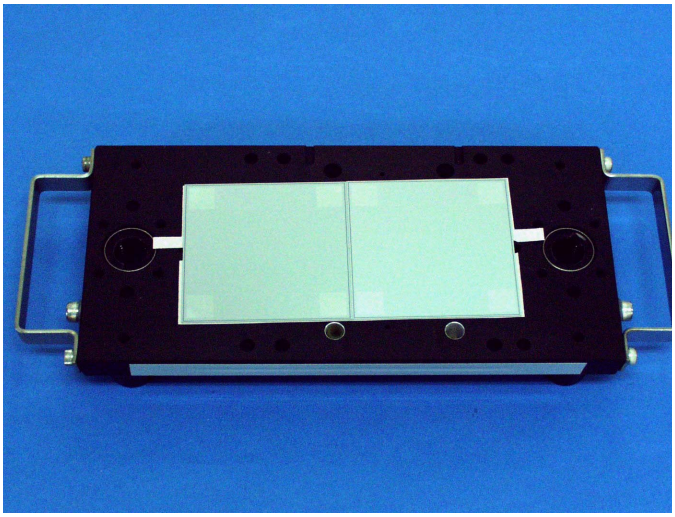

Figure 10: Top detectors transfer plate. The white piece is a disposable clean paper.

7) Glue dispensing machine

The detectors and the baseboard are glued with a room-temperature curing epoxy glue, e.g., Araldite 2011, with a Boron-Nitride filler to help thermal conductivity. The epoxy glue is applied to the both sides of the baseboard with pre-defined amount to ensure the glue thickness. The application is made with a glue dispensing machine which is a combination of a xyz stage and a glue dispensing unit. Use of a glue dispensing machine is a clean way of applying glues, by touching the baseboard only when it is placed and removed from the machine.

Since the glue hardenes in several hours in the room temperature, the viscosity of the glue changes in time, and, in addition, after several hours the glue has to be disposed. An economical glue dispensing is to use a disposable syringe, which is driven by pressure. The change of the viscosity can be compensated by changing the pressure, which is effective for applying dot patterns, and/or changing the speed of head movement, effective for applying line patterns

A machine being used at KEK is shown in Figure 11, which has capability of programming pressure in time [4]. Empirical pressure adjustment curve is shown in Figure 12 for the Araldite 2011 with BN filler in compensating the change of viscosity. The variation of dispensed amount is less than 5% even after one hour from the mixing.

Figure 11: Glue dispensing system which is made of (1) a xyz stage where the baseboard is on the xy stage and a glue-syringe is attached on the z-axis, and (2) a dispensing controller.

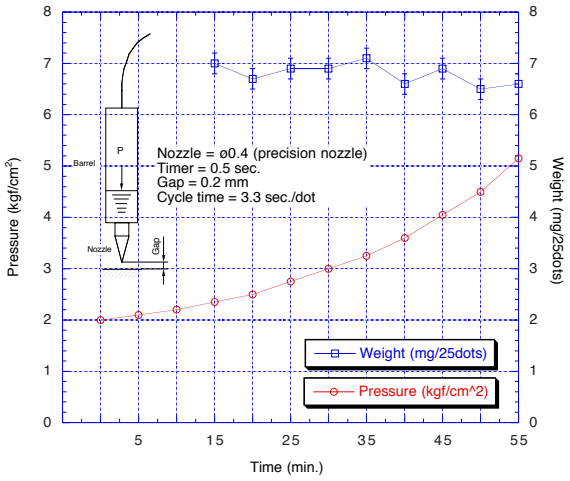

Figure 12: Pressure compensating the change of viscosity of the Araldite 2011 with BN filler (circle) and the weight of dispensed glue in 25 dots (square)

D. Copying the Master gauge

1) Rotation-translation stage

The rotation-translation stage aligning the detectors will have the master pins to which the transfer plates are slided down. The location of the master pins is copied from the master gauge by adjusting the location of the linear bearings of the rotation-translation stage, as shown in Figure 13. Separate master pins, which diameters are measured to match the master pin of the master gauge, are, then, inserted into the linear bearings of the rotation-translation stage.

The location of the linear bearings is at 20 mrad rotation to

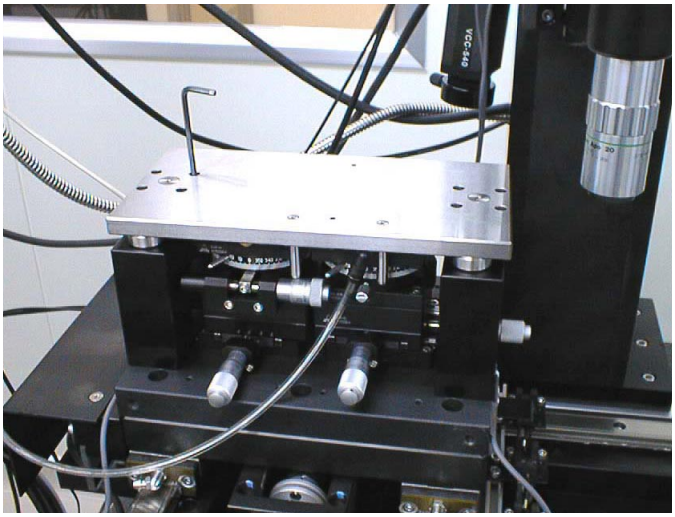

Figure 13: Copying the master pin locations to the linear bearings of the rotation-translation stage from the master gauge

the x-axis, but imperfect because of the required play for the process of copying the master gauge.

2) Transfer plates

The locations of the master (and small) pins of the master gauge are copied to the bottom detector transfer plate by sliding in the transfer plate on to the master gauge and fixing the flanges of the linear bearings. The mating of the master gauge and the bottom detector transfer plate is shown in Figure 14. The similar process is repeated to the top detector transfer plate to copy the master gauge.

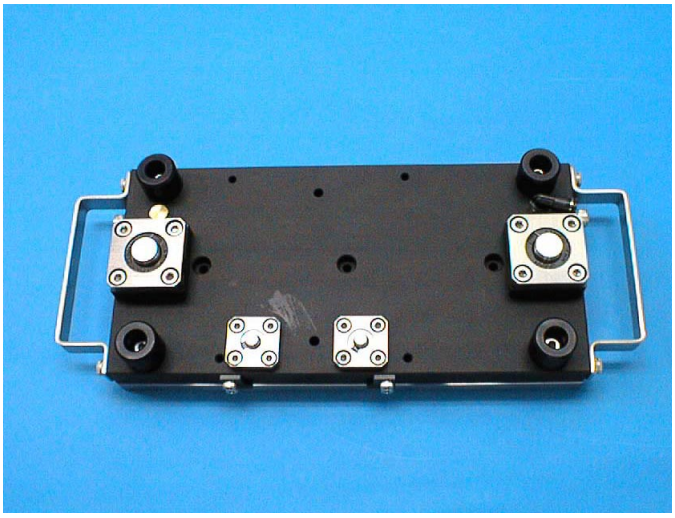

Figure 14: Copying the pin locations from the master gauge to the bottom detectors transfer plate for both the detector and the dowel linear bearings

E. Rotation-translation stage setting

In order to ease the aligning of the detectors, the axis of the master pins of the rotation-translation stage is rotated 20 mrad to the x-axis of the x-translation stages, x1 and x2. With the rotation, if perfect, the detectors, which must be rotated 20 mrad to the module centre line, i.e., the axis of the master pins, is aligned along the x-axis of the stages, as shown in Figure 15. The detectors, then, require only a small correction in the rotation in θ1 and θ2 and a small correction in the translation in y2, since the detectors are pre-aligned in the pre-alignment fixture. One remaining relatively large motion is along the x-axis, x2, since a large gap is left between two detectors on the pre-alignment fixture in order to allow a safe operation in the rotation and the y-translation.

The accurate 20 mrad rotation of the axis of the master pins to the x-axis of the main x-translation stage is made by making correction to the unit of rotation-translation stage:

1. the centres of the master pins are obtained by measuring the outer circles of the pins optically,
2. the centres of the pins are referenced to the fiducial marks on the unit of rotation-translation stage,
3. the unit is moved until the fiducial marks are in the preset positions such that the axis of the centres of the master pins is rotated 20 mrad to the x-axis of the main x-translation stage.

The fiducial mark, after setting the rotation-translation stage, is displayed on the video screen in Figure 16. Because of this correction to the rotation-translation stage, there arises a small correlation in the small xy stages, x2 and y2, in the rotation-translation stage, in reality.

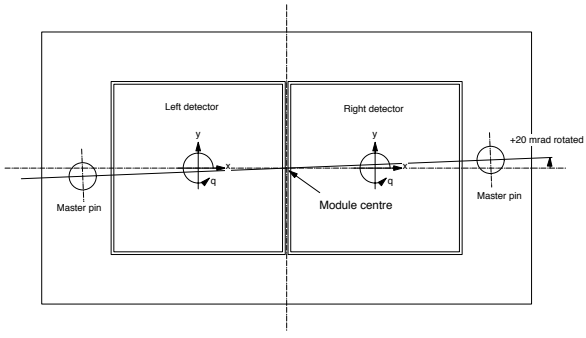

Figure 15: Rotated axis of the master pins in the rotation-translation stage to make the move of the detectors minimum

III. Assembly steps

The detector-baseboard assembly sequence proceeds in the steps of, pre-aligning detectors, transferring detectors to the rotation-translation stage, aligning detectors in precision, transferring detectors to the transfer plates, placing the baseboard on the bottom detector transfer plate with the bottom detectors vacu-

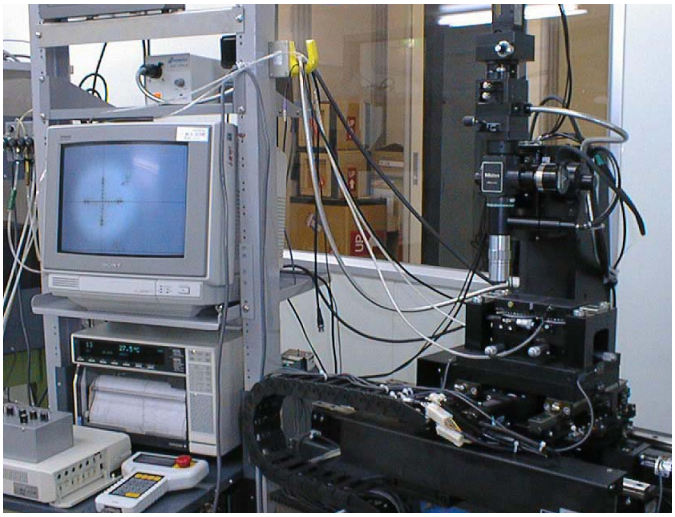

Figure 16: Setting the axis of the master pins of the rotation-translation stage rotated 20 mrad to the x-axis of the main x-stage

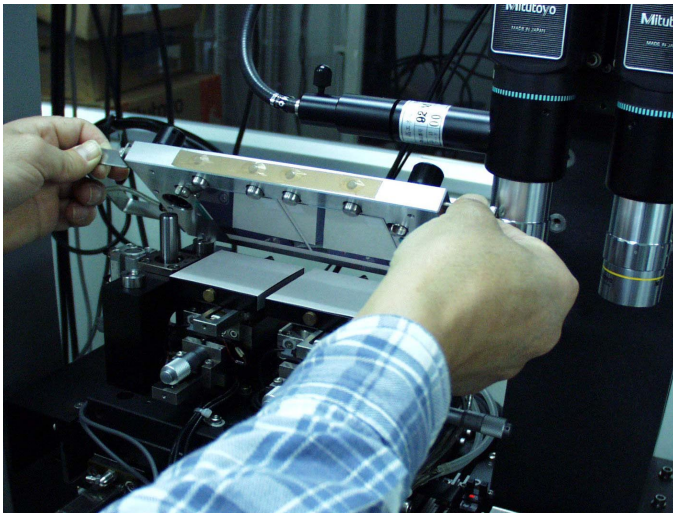

Figure 18: Placing the chucked detectors on the detector pre-alignment fixture to the rotation-translation stage

um-chucked, and mating the top detector transfer plate with top detectors vacuum-chucked.

1) Pre-aligning detectors

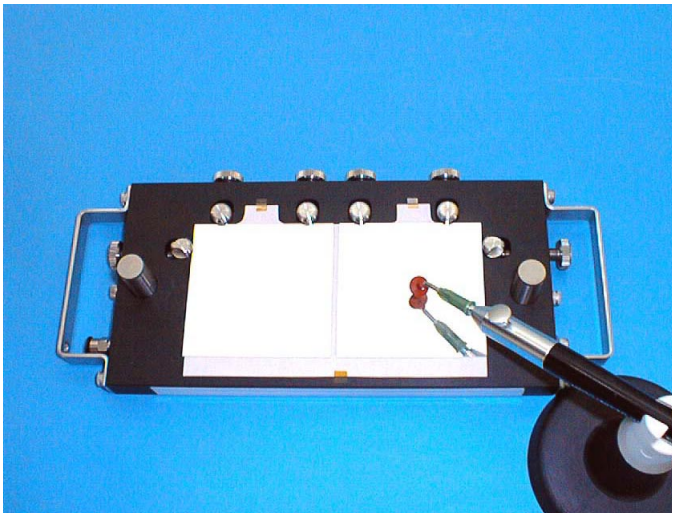

Figure 17: Placing the detectors on the detector pre-alignment fixture. A vacuum picker can be used in holding detectors.

A detector is picked up from the detector envelope with a vacuum picker by chucking the backside of the detector. With the alignment pins pressed to the nominal positions, two detectors are placed to touch the alignment pins at each edge, as shown in Figure 17. Once the detectors are vacuum-chucked to the pre-alignment fixture, the alignment pins are retracted off the detectors to a safe position.

2) Transferring to the rotation-translation stage

The pre-alignment fixture is transferred to the rotation-translation stage while vacuum-chucking the detectors, as shown in Figure 18. A spacer is ensuring such that there is a gap of 10 to 20 μm between the surface of the detectors and the surface of the rotation tables. The detectors are transferred to the rotation table by turning off the vacuum of the pre-alignment fixture and, sequentially, turning on the vacuum of the rotation table. It is not critical in this step, but critical in the precision process, to turn the vacuum off and on sequentially. It is found that when the both vacuum are on, the stages move and there arises random move in the detector position of 5 to 10 μm, due to imperfect flatness or parallelism in the two jigs.

3) Aligning detectors in precision

Two detectors on the rotation-translation stage are aligned in precision by observing the fiducial marks on the detectors, as shown in Figure 19. Since the rotation of the 20 mrad is already taken care of by the axis of the master pins, after small correction in rotation, a move of two detectors in the x-direction with a small correction in y-direction can set the fiducial marks to pre-defined positions, defined from the module centre in the master gauge, relatively in straight-forward way.

4) Transferring to the detector transfer plates

Once the detectors are aligned in precision, the detectors are transferred to the transfer plate. The bottom detector transfer plate being placed on the stage is shown in Figure 20. A gap of 10 to 20 μm is ensured, with a spacer, between the surface of the detectors and the transfer plate. The detectors are transferred by turning the vacuum of the rotation tables off, first, and, then, turning the transfer plate on, sequentially. It is important to confirm the coordinates of the fiducial marks of the detectors, after transferring, viewed through the observation holes, so that there is little move in the transferring.

The bottom detector transfer plate with detectors being vacuum-chucked and placed on the bottom fixture is shown in

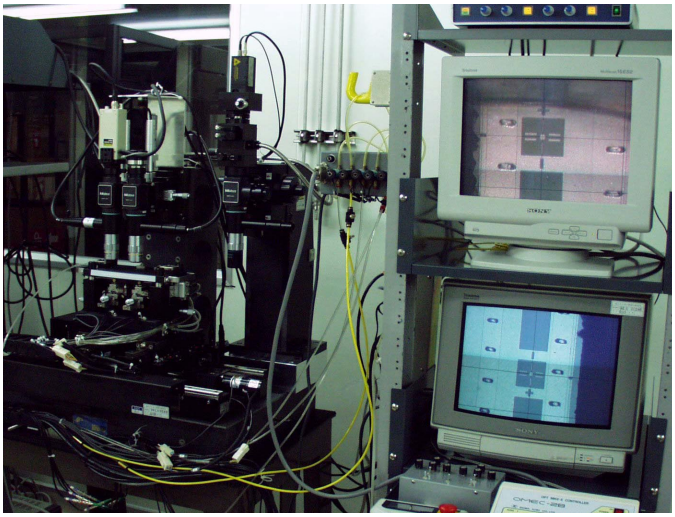

Figure 19: Aligning detectors

Figure 21. The top detectors are also aligned in precision and transferred to the top detector transfer plate

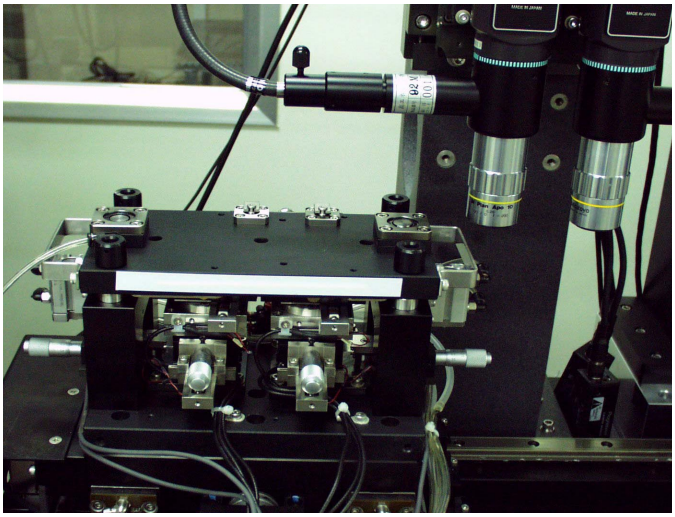

Figure 20: Transferring detectors from the rotation-translation stage to the bottom detector transfer plate. The fiducial marks of the detectors can be seen through the observation holes.

5) Placing baseboard on the bottom detectors transfer plate

In "one-step" gluing, the baseboard is with glues applied in both sides is placed over the bottom detectors on the bottom detector transfer plate, as shown in Figure 22. The alignment of the baseboard is made by using the dowel pins in the transfer plate and the dowel holes in the baseboard.

6) Mating the top and the bottom detectors transfer plates

Immediately after the baseboard is placed on the bottom detector transfer plate, the top detector transfer plate with top detectors being vacuum chucked is slided in, in order to sandwich

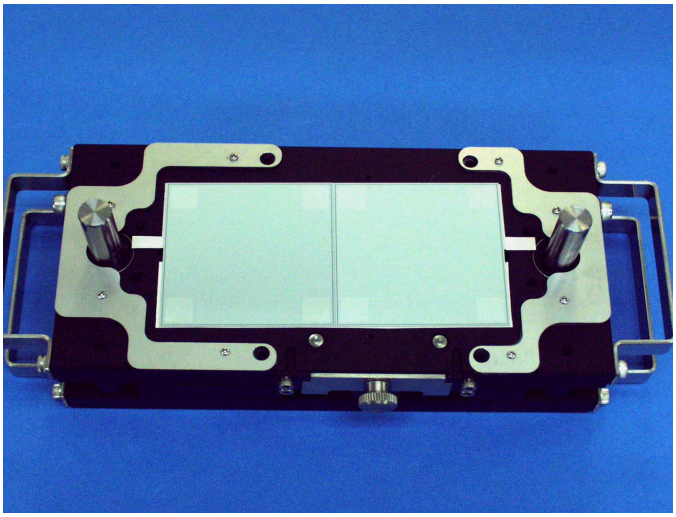

Figure 21: Aligned detectors chucked on the bottom detector transfer plate

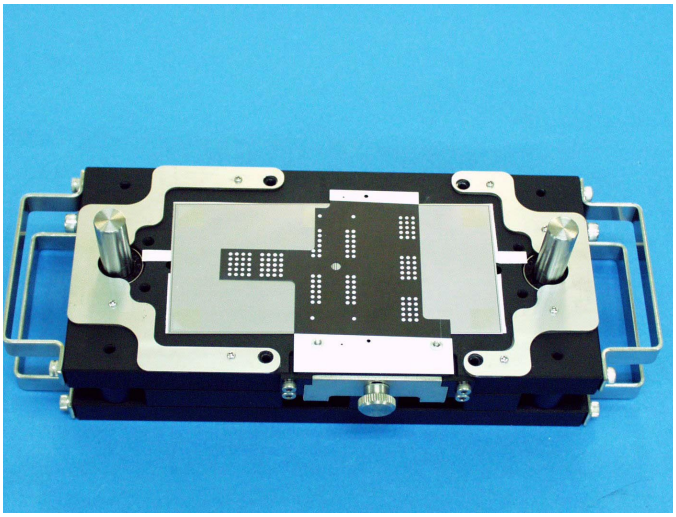

Figure 22: Baseboard is being placed over the bottom detectors. The alignment of the baseboard to the detectors are being made with the use of dowel pins in the bottom detector transfer plate and the dowel holes in the baseboard.. The baseboard and the glue pattern is of the "narrow nose" type. The latest baseboard is of the "wide nose" and the glue pattern has been updated.

the baseboard with the top and the bottom detectors, as shown in Figure 23. The top and the bottom detector transfer plates are, then, pressurized with screws and left in the room temperature for several hours until the glue is cured. The completed detector-baseboard assembly, on the jig, is shown in Fig.xx.

7) Two-step gluing of the assembly

After analysing the assembled modules, the flatness of the module was found to be affected by the deformation in the neck between the facings and the main part. In the "one-step" gluing, the baseboard was constrained, at the facings, so that the loca-

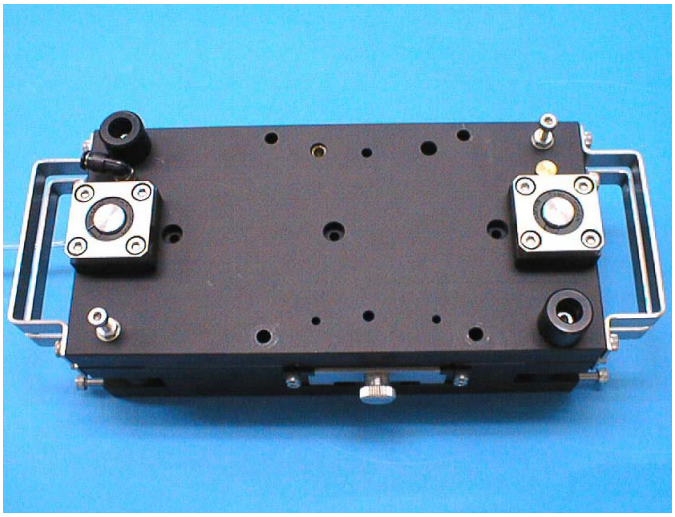

Figure 23: Mating the top detectors and the bottom detectors transfer plates

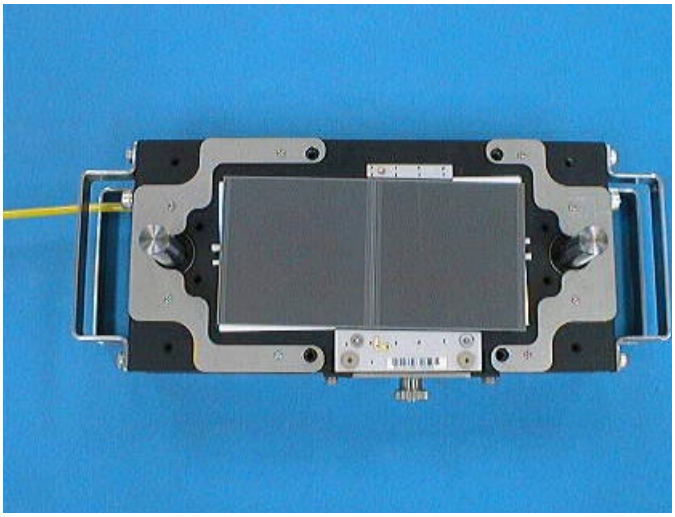

Figure 24: Completed detector-baseboard assembly

tion in height of the baseboard is constrained. This constraint did not work since the viscosity of the glue was much higher than adjusting the glue thickness by the constraint. Instead, the constraint introduced distortion in the neck between the sensor and the facings, which introduced distortions in the flatness of the modules, together.

In order to make the facings free and constrain the baseboard, the baseboard must be held in the main area. This holding the main area of the baseboard with vacuum-chuck transfer plate helps to flatten the baseboard, in addition. Since the glue can not be applied to the vacuum-chucking side, the gluing step is now step-by-step: one side first and then the other side, i.e., "two-step gluing".

In the "two-step gluing", the usage sequence of the transfer plates is reversed. Topside sensors are aligned first, picked up with the top transfer plate, and placed on the bottom fixture. The baseboard is placed on the bottom transfer plate using the dowel pins, vacuum-chucked. Applying the glue on the baseboard, the baseboard is placed over the sensors on top of the top transfer plate and glue is cured. The bottom sensors are aligned and picked up with the bottom transfer plate which is freed from the baseboard, with the dowel pins being recessed. Applying the glue on the baseboard of the baseboard-top sensors assembly still held on the top transfer plate, the bottom transfer plate is mated over the baseboard assembly and the glue is cured.

IV. Summary

A second version of module assembly jigs has been designed and fabricated at KEK by feeding back the experience and the issues found in the first version of the jigs. The major modifications in the second version are the move of the location of the master pins, introduction of the master gauge, the pre-alignment fixture, and the 20 mrad rotation of the axis of the master pins in the rotation-translation stage. Experience of the assembling and the precision of the assembled modules will be reported in a separate document.

V. Appendix

A conceptual view of the first assembly jigs is shown Figure 25

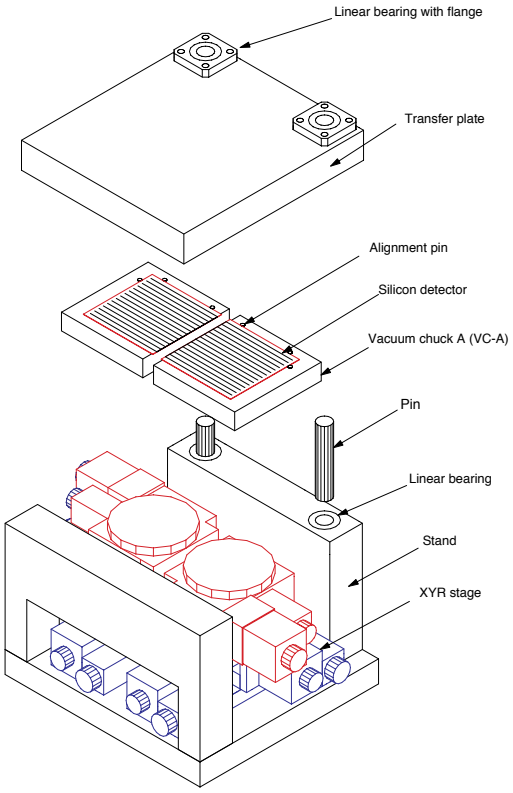

Figure 25: Concept of the first version assembly station and a detector transfer plate

VI. REFERENCES

[1] T. Kohriki et al., "Assembly of precision mechanical modules at KEK", SCT week, Nov., 1998

[2] T. Kohriki et al., "Construction of Barrel Precision Modules", SCT week, Feb., 1999

[3] ATLAS Inner detector technical design report, CERN/LHCC/97-17, ATLAS TDR 5, 30 April 1997, pp 467-470

[4] A pressure-programmable dispenser, ML-808EX, and a xyz stage, SHOTMASTER3, made by MUSASHI engineering, inc. Tokyo, Japan. A similar equipment, ACCURA9 for the dispenser and Ez-ROBO for the xyz stage (an OEM of SONY's ROBOKIDS), is available from IWASHITA engineering, IEI, Tokyo, Japan.

SCT Barrel Module Document

Appendix 3 to SCT-BM-FDR-6 Assembly Jigs & Procedures for the UK-B and US Clusters

Abstract

This document defines the procedures of the barrel module assembly and the jigs as developed for the UK-B and US Clusters

Prepared by :	*Checked by :*	*Approved by :*
M.Gibson		

Distribution List

Table of Contents

MODULE ASSEMBLY

JIGS AND THEIR USE

MODULE ASSEMBLY

1 Assembly Steps.

This document describes the steps and actions necessary for the alignment and fabrication of an ATLAS barrel module at RAL. The various steps are summarised below.

1) Detector alignment and transfer to the jig plates.
2) Fitting of the baseboard into the module assembly frame, and fitting the baseboard support plate.
3) Applying both the adhesives to side A of the baseboard.
4) Fitting one of the jig plates.
5) Transferring back into the adhesive dispenser for the second side application.
6) Fitting the second jig plate.
7) Removal of sub-assembly from the assembly frame.
8) Parameterisation of the IV characteristics of the detectors after construction of the sub-assembly.
9) Metrology of the sub-assembly.
10) Fitting of the hybrid.

1.1 Detector Alignment.

Figure 1 shows the general arrangement of the hardware. The necessary actions are listed below. The alignment of the detectors to each other and to a reference fiducial is automated and runs with custom LabView software.

1.1.1 The detector alignment chucks are positioned in their home positions and the four location blocks, two for each chuck, advanced to their minimum position.
1.1.2 A new piece of disposable pre-cut clean room paper is placed on each of the alignment chucks.
1.1.3 The detectors are placed, strip side up, in the correct orientation onto the chucks, the vacuum to each being turned on in turn. Vacuum warning lights indicate the quality of the vacuum.
1.1.4 The route card is completed.
1.1.5 The auto-alignment software now aligns the two detectors to each other and a to a reference fiducial on the wall.
1.1.6 When stage 2.1.5 is completed a new piece of double sized pre-cut clean room paper is laid on the strip side of the detectors.
1.1.7 The trolley (Figure 2) on which the jig plates are stored is connected to both the vacuum and power.
1.1.8 Because of manufacturing tolerances, each jig plate has its own software corrections, so it is important to place the appropriate jig plate into the linear bearings and lower into contact with the detectors.
1.1.9 Remove the vacuum from the alignment chucks and apply to the jig plate, checking that the warning lights are green.
1.1.10 Remove the jig plate and store on the trolley, detector side uppermost.
1.1.11 Repeat for the second pair of detectors.

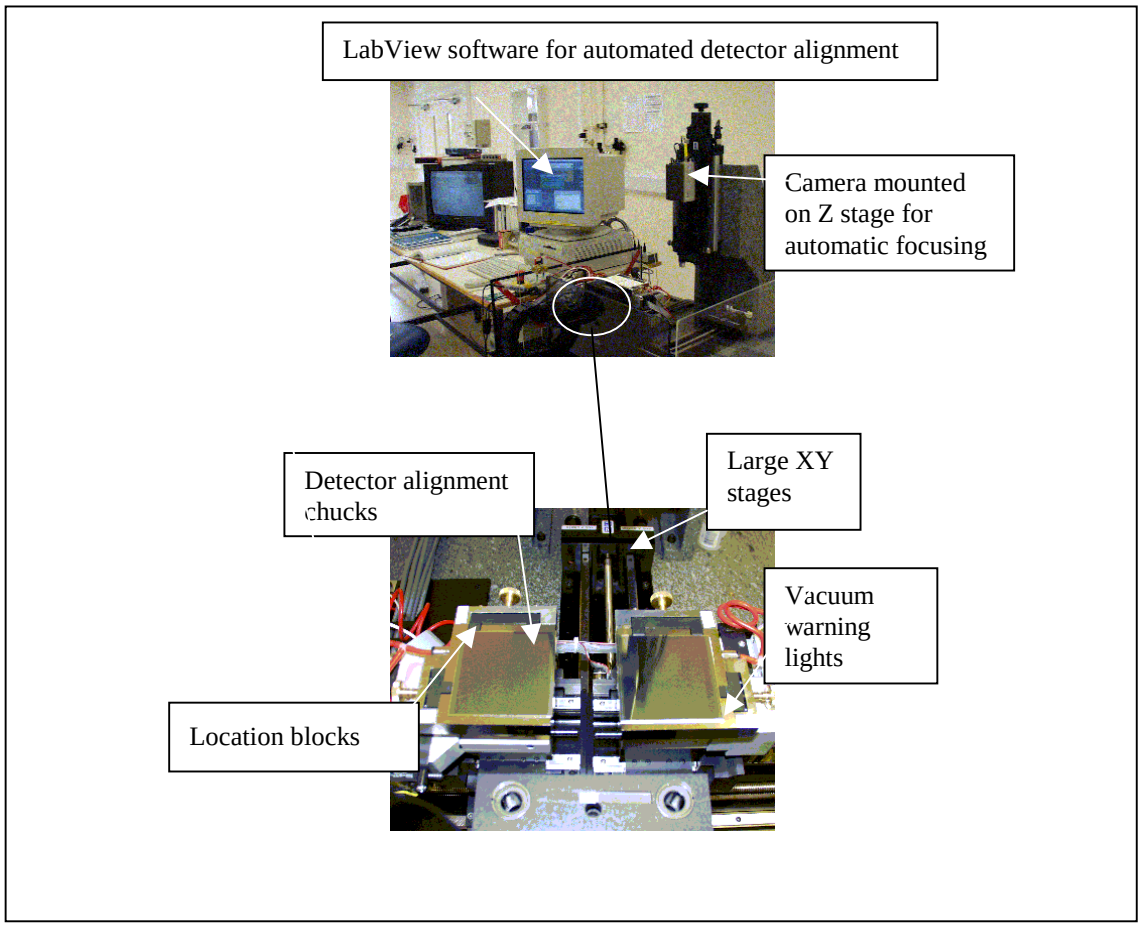

Figure 1

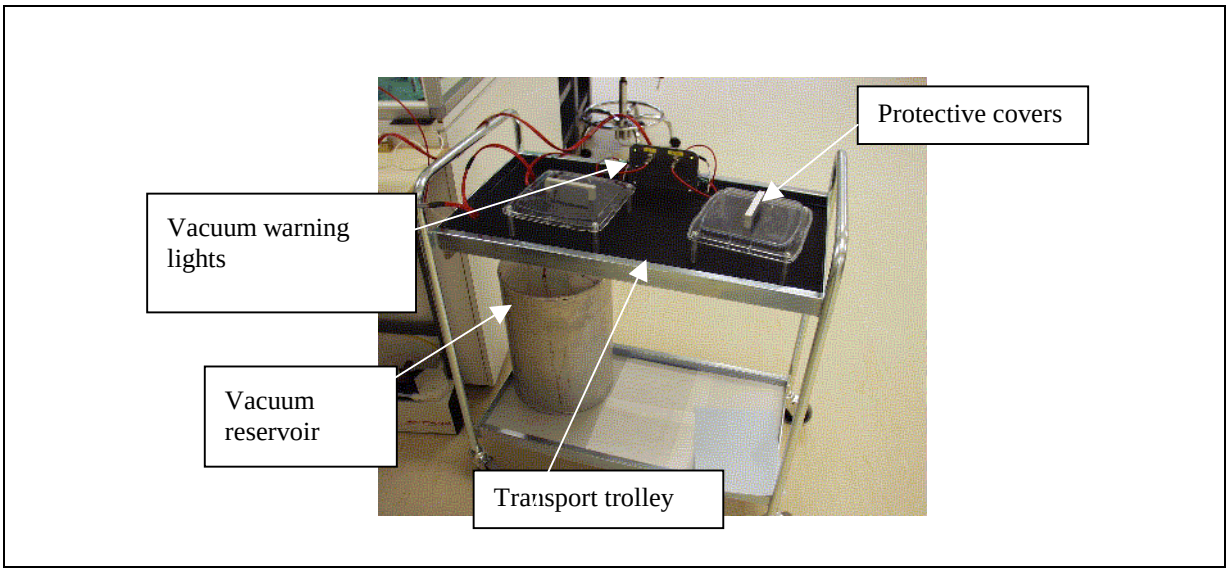

Figure 2

1.2 Baseboard to Assembly Frame.

Figures 3a and 3b shows an empty assembly frame with detailed close up of the baseboard kinematic supports.
A mounted but unsupported baseboard is shown in Figure 4a and a supported one ready for the adhesive to be applied in Figure 4b.

1.2.1 The thickness of the detectors and the baseboard are evaluated to ensure that the assembly jig spacers are of the correct value.
1.2.2 The two spring loaded custom screws are removed along with their springs.
1.2.3 The far end clamp is also removed.
1.2.4 The baseboard is laid onto the kinematic supports.
1.2.5 Each of the two spring loaded screws is refitted to restrain the baseboard.
1.2.6 The far side clamp is refitted.
1.2.7 The ATLAS serial number of the baseboard is recorded in the route card.
1.2.8 A new sheet of pre-cut clean room paper is fitted onto the baseboard support plate.
1.2.9 This is fitted into the jig and bolted in using the same holes as for the jig plate.
1.2.10 A visual check is now made to ensure that all components fit closely.
1.2.11 If necessary this jig may be adjusted in z independently of the assembly jig spacers.

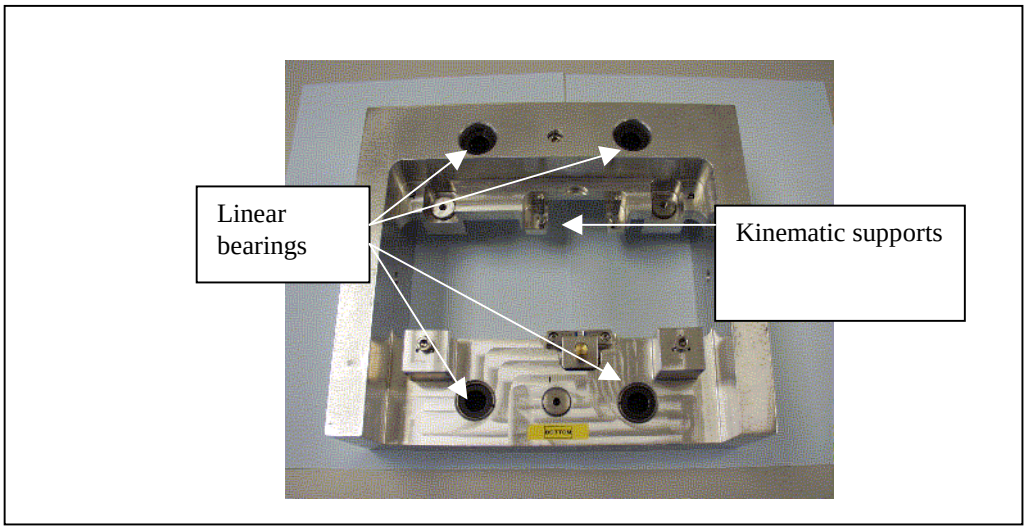

Figure 3a

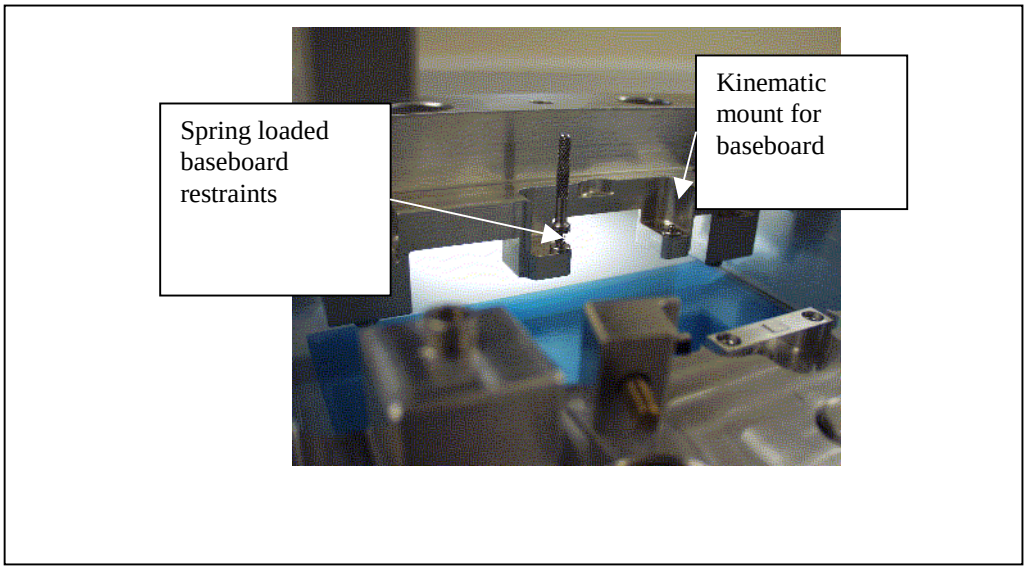

Figure 3b

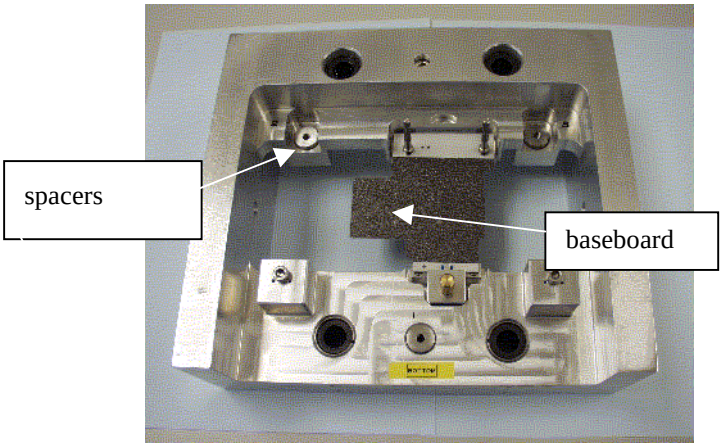

Figure 4a

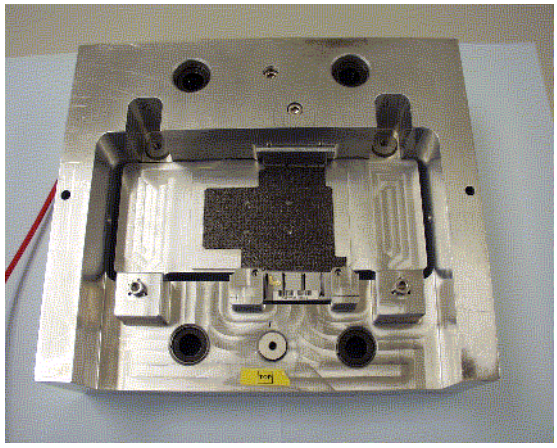

Figure 4b

1.3 Adhesive Application.

Figure 5 shows the 3 axis high precision dispensing workstation used for adhesive application in barrel module assembly. The stand-alone unit uses a standard Sony tabletop robot with 0.02mm X, Y, Z position resolution. The Y axis stage is modified to accommodate the barrel module assembly jig directly. The dispense system is mounted onto the 'X, Z' axis and consists of a Dispensit Model 802-30 Positive Displacement Pinch Tube Valve using an EFD controller. The dispensing workstation is also fitted with a camera and monitor to assist in programming the position of adhesive spots. This system is used to dispense the high viscosity adhesive mix of Ciba-Geigy AW106/HV953V(2011) and Boron Nitride Grade PT140S filler. The mix by weight being 2.5g resin, 2g hardener, 2g filler. The adhesive pattern dispensed Consists of 154 dots arranged as shown if figure 6. The time to complete the dispensing operation including loading the Adhesive into the dispenser and purging adhesive through the dispense system is less than 10 minutes.
The silver loaded conducting epoxy is applied manually after the assembly jigs are removed from the dispensing workstation.

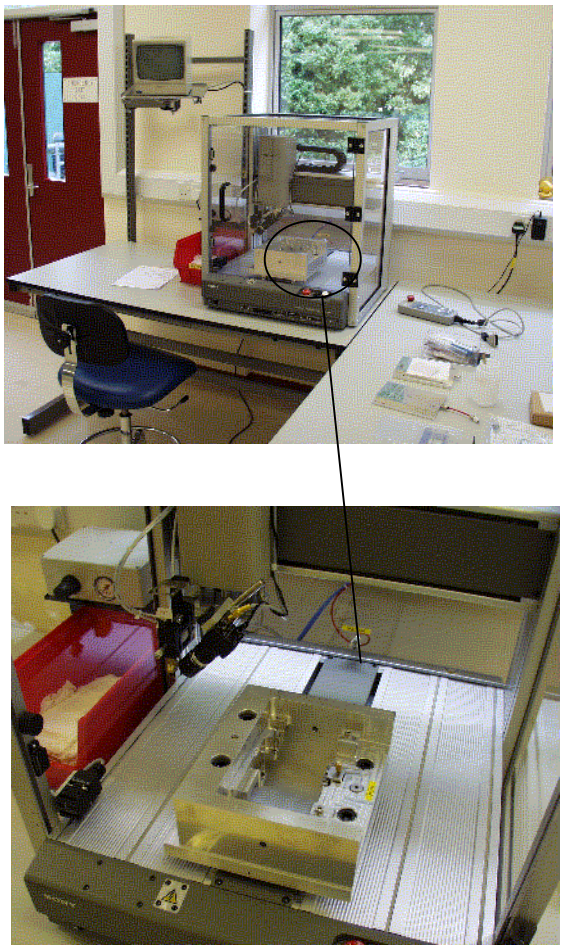

Figure 5

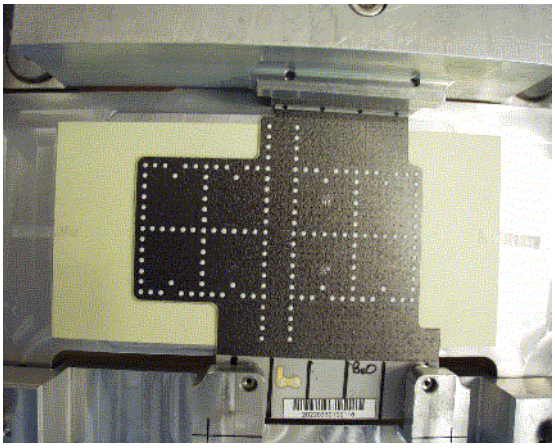

Figure 6

1.4 Fitting The Top Jig Plate.

The previously aligned detectors are held under vacuum on the two jig plates. The dowel pins in the top plate simply Slide into the linear bearings of the main jig as seen in figure 4b. It is retained by 3 screws. This assembly is then placed to one side to cure.

1.5 Transferring Back into The Adhesive Dispenser.

The vacuum is turned off and the baseboard support plate is removed. The whole assembly consisting of the main frame and the top jig plate is returned to the adhesive dispenser and the glue for the second (bottom) side dispensed.

1.6 Fitting The Bottom Jig Plate.

This operation is simply a repeat of step 1.4.

1.7 Removal of the Completed Sub-Assembly

The completed sub-assembly is removed from the assembly jig by removing all the baseboard retaining fixings and lifting it out on the top jig plate, leaving free access to the top of the module so that the universal handling tool (fig 7) may be fitted.

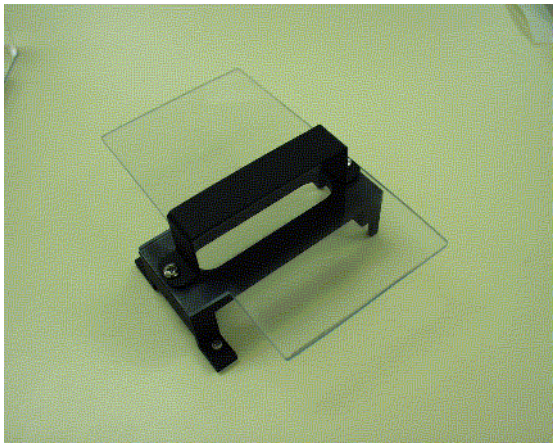

Figure 7

1.8 Parameterisation of The IV Characteristics of The Detectors After Construction of The Sub-Assembly.

The prototype system is described below and in figure 8. The main differences between this and the production version are that the module frame that at present is unique to this process will be replaced by a frame that is also used for sub-assembly testing, hybrid mounting and wire bonding.

1.8.1 The 4-detector sub-assembly is placed in the frame.

1.8.2 A check is made for electrical continuity between the far top bias and the spring loaded bias connection on the cooled upper facing.

1.8.3 This assembly is then fitted onto the custom support.

1.8.4 This is now positioned underneath the optics and locked in position.

1.8.5 The manual prober is now used to position a probe needle onto the relevant bias pad.

1.8.6 All internal lights are turned off and the door shut to isolate the detectors.

1.8.7 Custom software is then used which checks the ATLAS database for detector compatibility, biases the detectors and produces the IV characterisation curves which have pass/fail parameters.

1.8.8 After successfully testing the top two detectors the frame is removed, inverted and reinstalled for testing the second side.

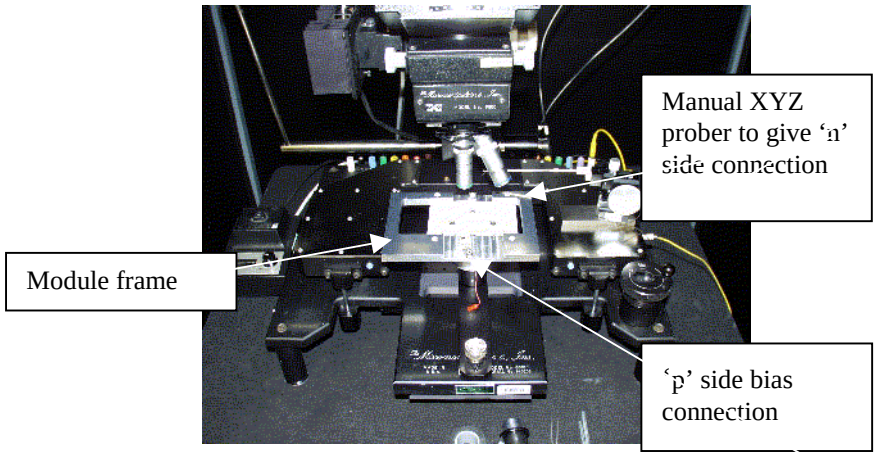

Figure 8

1.9 Metrology of The 4 Detector Sub-Assembly.

Metrology of the module in XY and Z planes with data from both the top and bottom detectors requires a technique of registration between the two sets of data. This is achieved by equipping the module frame with 4 thin pinholes to obtain the XY reference and 3 surfaces to obtain the Z plane datum. Figure 9 shows the completed item.

1.9.1 The module is fitted into the module frame by using the universal-handling tool.

1.9.2 The handling tool is removed.

1.9.3 The sub-assembly is restrained within the frame by the module restraining clips.

1.9.4 Metrology of the top is completed.

1.9.5 The module frame is inverted and replaced on the support plate that is fitted with kinematic supports.

1.9.6 Metrology of the bottom is then completed.

1.9.7 The module is removed and transferred to a storage box or the hybrid-mounting frame.

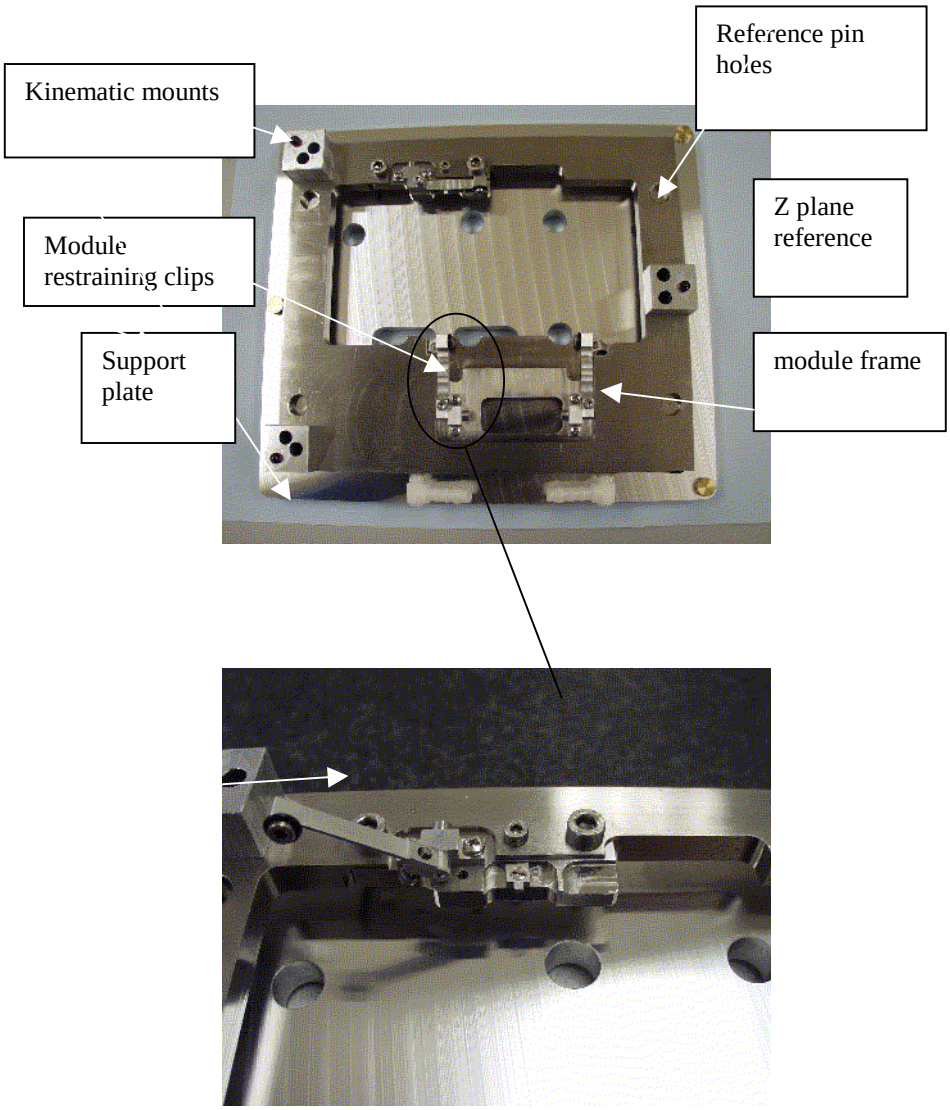

Figure 9

1.10 Hybrid Mounting Procedure.

The procedure describes the necessary steps for aligning and mounting hybrids. Dedicated optics with an integrated custom graticiule allows viewing of both features on the hybrid and the detectors at the same time to ensure correct positioning. Figure 10 illustrates the hardware involved.

1.10.1 Mounting the upper hybrid.

The hybrid is placed onto the positioning lift, under the hybrid vacuum platen at position A. Once positioned, the platen is lowered and vacuum is applied to retain the hybrid. The z-adjustment is used to lift the hybrid away from its carrier, to the end of its travel. The positioning lift is carefully removed. The 4-detector sub assembly is secured to the underside of the platen, under the upper hybrid and the whole assembly slid to position B, for a preliminary alignment check. Once alignment is assured, the platen is moved to position B. The adhesive is mixed, and applied to the two feet of the upper hybrid. The module carrier is returned to position B and the hybrid lowered into position and alignment rechecked. The long 'pot' life of the adhesive allows ample time for repositioning.

1.10.2 Mounting the lower hybrid.

The hybrid has a flexible joint situated between the upper and lower sections, which wraps around the detector assembly. This operation is 'once only', so adhesive is applied beforehand. The platen is moved to position A, the adhesive is applied and the 4 detector sub- assembly is flipped about its non-cooled edge, taking with it the previous mounted upper hybrid. The Platen is slid to position B for the alignment to be checked

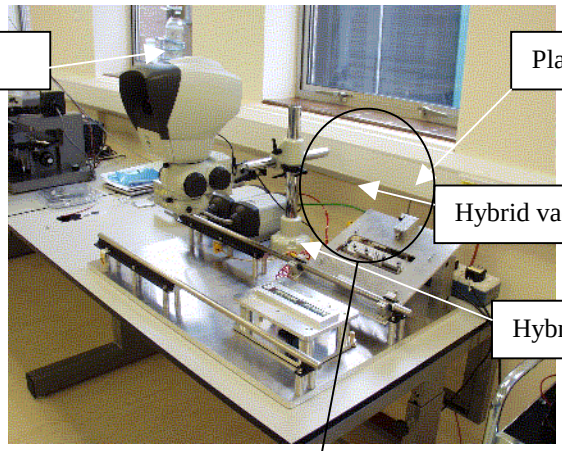
Optics
Platen
Hybrid vacuum platen
Hybrid

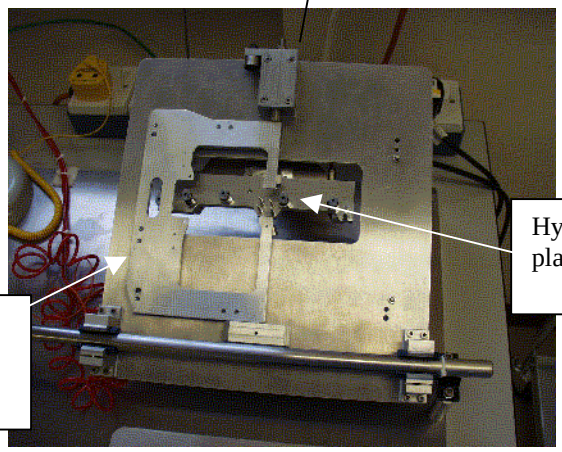
Hybrid vacuum platen
4 detector sub-assembly carrier

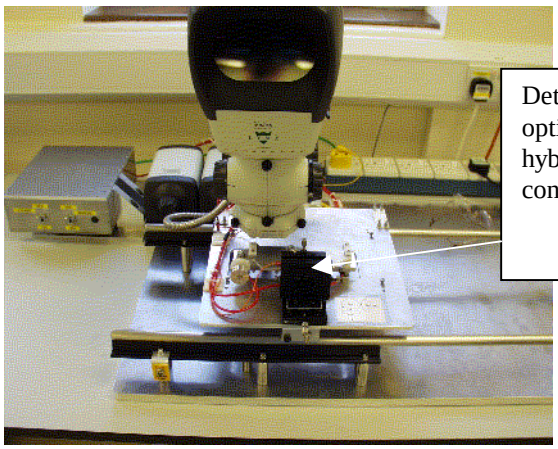
Detail of platen under optics in position B with hybrid XYZ and rotate control

Figure 10

Jigs and their Use

This section of the document describes all the jigs, fixtures and fittings used at the Rutherford Appleton Laboratory for the fabrication of ATLAS Barrel modules in their order of use.

1) Washer mounting jig.

Currently baseboards are supplied to RAL from CERN without either mounting washers or bushes. These are fitted by hand using the jig and fixtures shown in figure 1 and described by the drawings listed in table 1.

Table 1

Drawing number	Description	Drawing number	Description
A0-TB-0059-440-01	GA	A3-TB-0059-448-00	Spacer block
A3-TB-0059-440-02	Location jig datum washers & handling points	A3-TB-0059-449-00	Datum pin
A1-TB-0059-441-00	Base plate	A3-TB-0059-450-00	Obround pin
A3-TB-0059-442-00	Sealing plate	A3-TB-0059-451-00	Tooling ball holder
A3-TB-0059-443-00	Guide block large	A3-TB-0059-452-00	Spacer washer
A3-TB-0059-444-00	Adjustable stop large	A3-TB-0059-453-00	Tooling ball
A3-TB-0059-446-00	Adjustable stop small	A2-TB-0059-454-00	Clamp plate
A2-TB-0059-447-00	Top plate	A3-TB-0059-455-00	Location screw

Description of use

The washer mounting jig allow one baseboard per day to be equipped with both the handling bushes and the alignment washers. The position of the handling bushes on any baseboard is not a critical parameter while that of the alignment of the washers is. In order to accelerate the fabrication of these assemblies the handling bushes are temporarily fixed with superglue to the baseboard using the clamp plate. The two custom alignment washers are fitted over the two accurately machined pins that pass through the baseboard and are constrained in the Z plane by spring loaded plungers mounted on the top plate. Epoxy (Araldite 2011) is applied around the circumference of the washers and handling bushes.

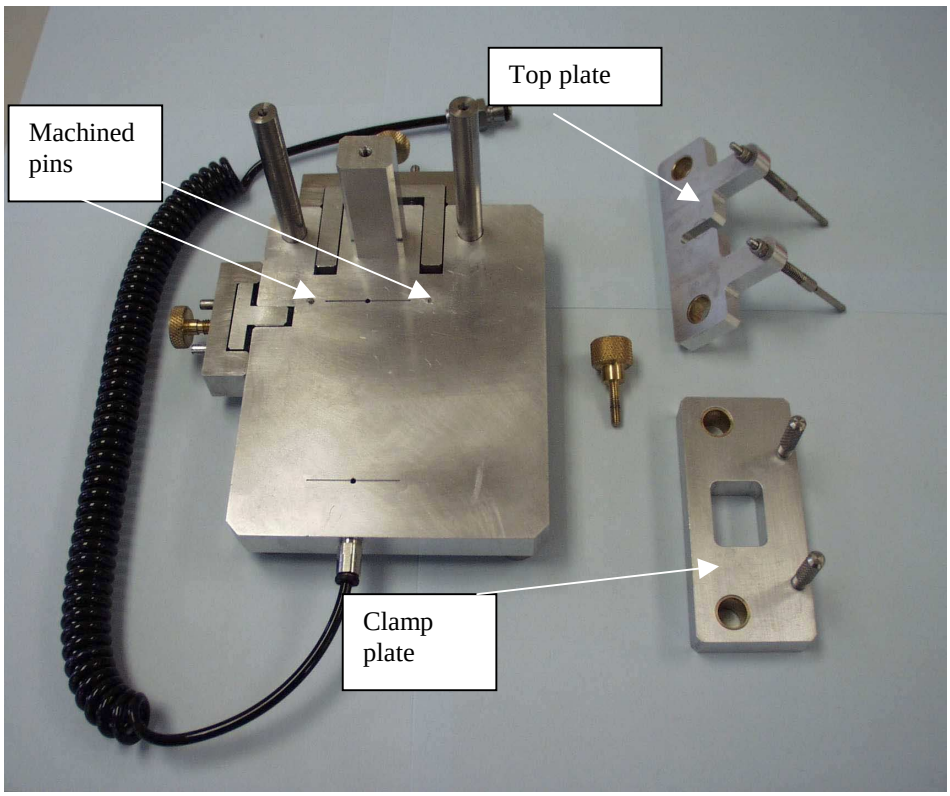

figure 1

2) Module assembly jigs

The following text describes the various jigs and fixtures required to construct an ATLAS barrel 4 detector sub-assembly as described in drawing TB-0059-601-02.

The jigs and fixtures are shown in figure 2, and described by the drawings listed in table 2.

Table 2

Drawing number	Description	Drawing number	Description
A0-TB-0059-400-00	Detector support chuck.	A0-TB-0059-422-00	Body drilling
A0-TB-0059-401-00	Base Right Hand Side	A0-TB-0059-423-00	Jig plate assembly
A0-TB-0059-402-00	Bridge piece large	A0-TB-0059-424-00	Jig plate machining
A0-TB-0059-403-00	Bridge piece small	A0-TB-0059-425-00	Location screw
A0-TB-0059-404-00	Double location block	A0-TB-0059-426-00	Clamp
A0-TB-0059-405-00	Single location block	A0-TB-0059-427-00	Location ball
A0-TB-0059-406-00	Protective film	A0-TB-0059-428-00	Captivated screw
A0-TB-0059-407-00	Adjusting screw modified	A0-TB-0059-429-00	Location spacer
A0-TB-0059-410-00	Detector support chuck left hand side	A0-TB-0059-430-00	Location spacer block
A0-TB-0059-411-00	Base left hand side	A0-TB-0059-431-00	Location bush
A0-TB-0059-420-00	Module assembly jig	A0-TB-0059-432-00	Location spacer
A0-TB-0059-421-00	Body final machining	A0-TB-0059-433-00	Protective film

Description of use

The module assembly jig is equipped with 4 linear bearings, which are positioned to provide the +-20 milliradians of rotation for the two sets of detectors relative to the baseboard. Small positional errors in manufacturing being corrected with the automatic alignment system. Accurate positioning of the baseboard is provided by kinematic supports. A pair of aligned detectors are held under vacuum on each of the two jig plates (each of which is equipped with 2 dowel pins). These jig plates slide onto the module assembly jig using the linear bearings. Additional temporary support for the baseboard while the first side is fitted it is provided by the baseboard support plate.

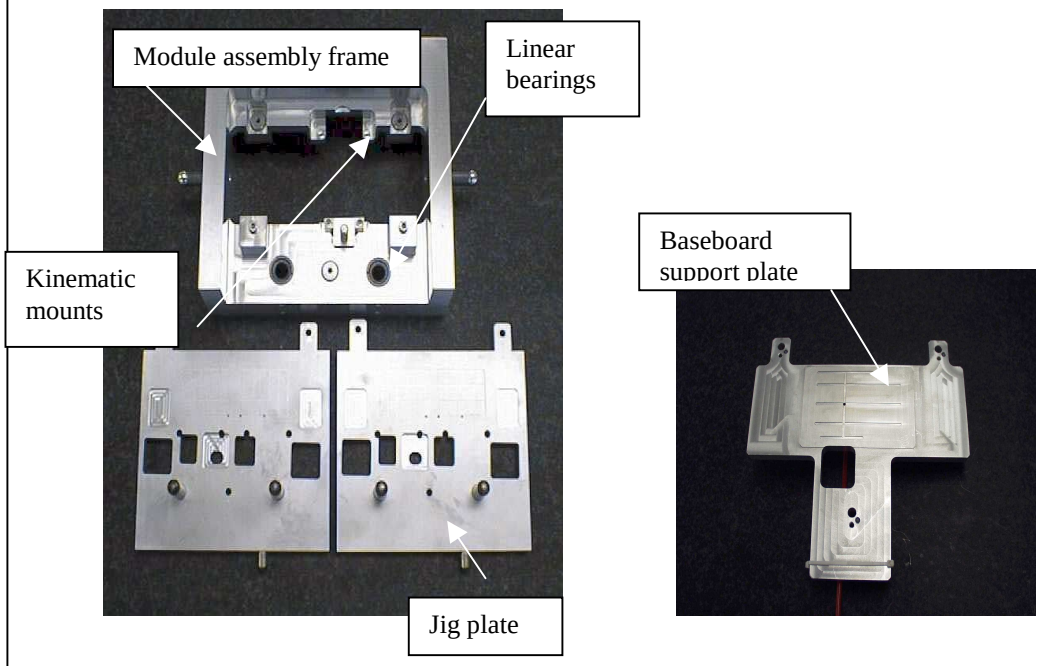

figure 2

3) Sub assembly tester.

The following text describes the jig and fixtures required to bias and parameterise the IV characteristics of the 4 individual detectors after mounting onto the baseboard but before fitting the hybrid. This allows a comparison between the values previously recorded for the separate items. A prototype item exists and is shown in figure 3.

Description of use.

This jig provides support for 4 detector sub-assembly with temporary electrical connection to the metal bias pad on the top facing. The second electrical connection is via a probe needle manually positioned by the XYZ prober. The jig also provides the ability to invert the sub-assembly and repeat for the second side. This removes any requirement for temporary wire bonding.

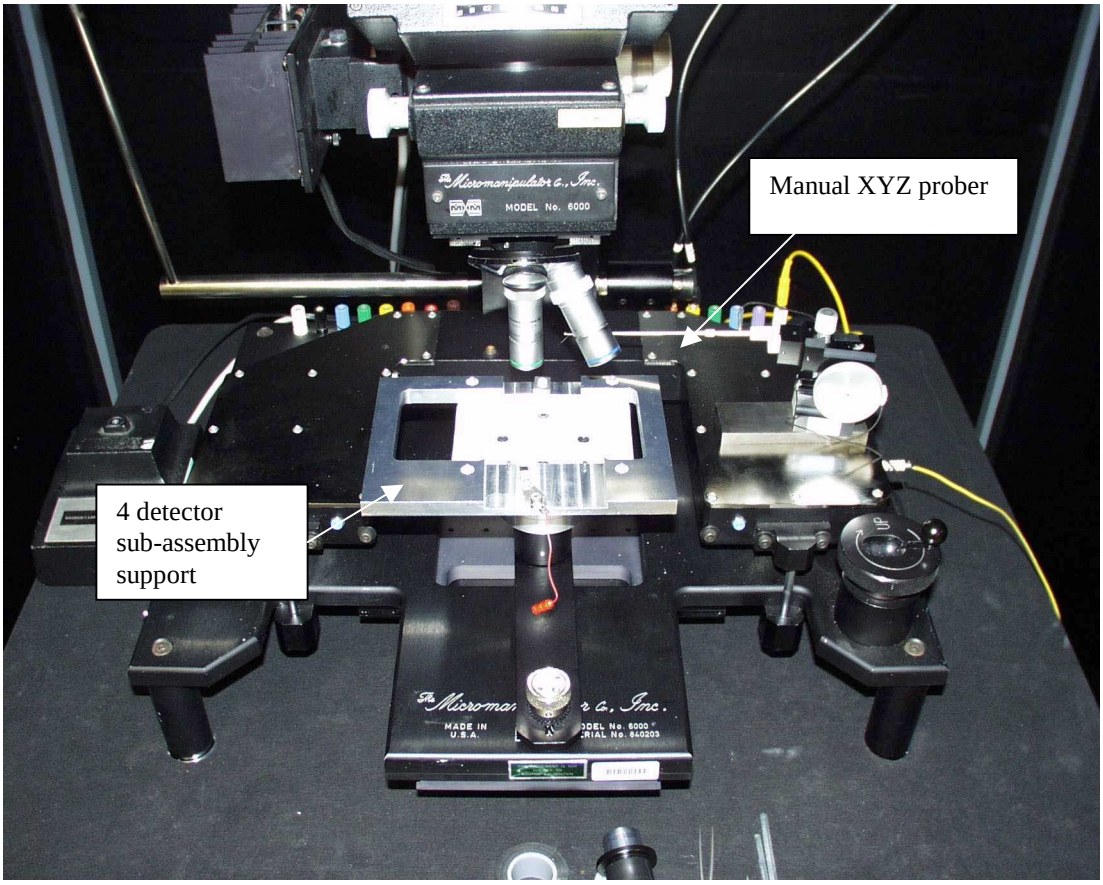

figure 3

4) Metrology.

The following text describes the jig required to support an ATLAS barrel 4 detector sub-assembly for metrology. The prototype is shown in figure 4, and described by the drawings listed in table 3.

Table 3

Drawing number	Description	Drawing number	Description
A1-TD-1009-100-03	Mounting Plate	A3-TD-1009-105-01	Spring Clip Support
A2-TD-1009-101-02	Edge Piece	A3-TD-1009-106-01	M2 Shoulder Screw
A3-TD-1009-103-01	M3 Shoulder Screw	A3-TD-1009-107-01	O Ring Screw
A3-TD-1009-104-01	Spring Clip	A3-TD-1009-109-01	M2.5 Shoulder Screw

Description of use.

This item provides the reference frame for metrology of the 4 detector sub-assembly before fitting of a tested hybrid. The module is clamped into the frame with 3 flexible clips allowing unobstructed viewing of the two mounting washers. 4 reference pinholes provide the back and front positional correlation.

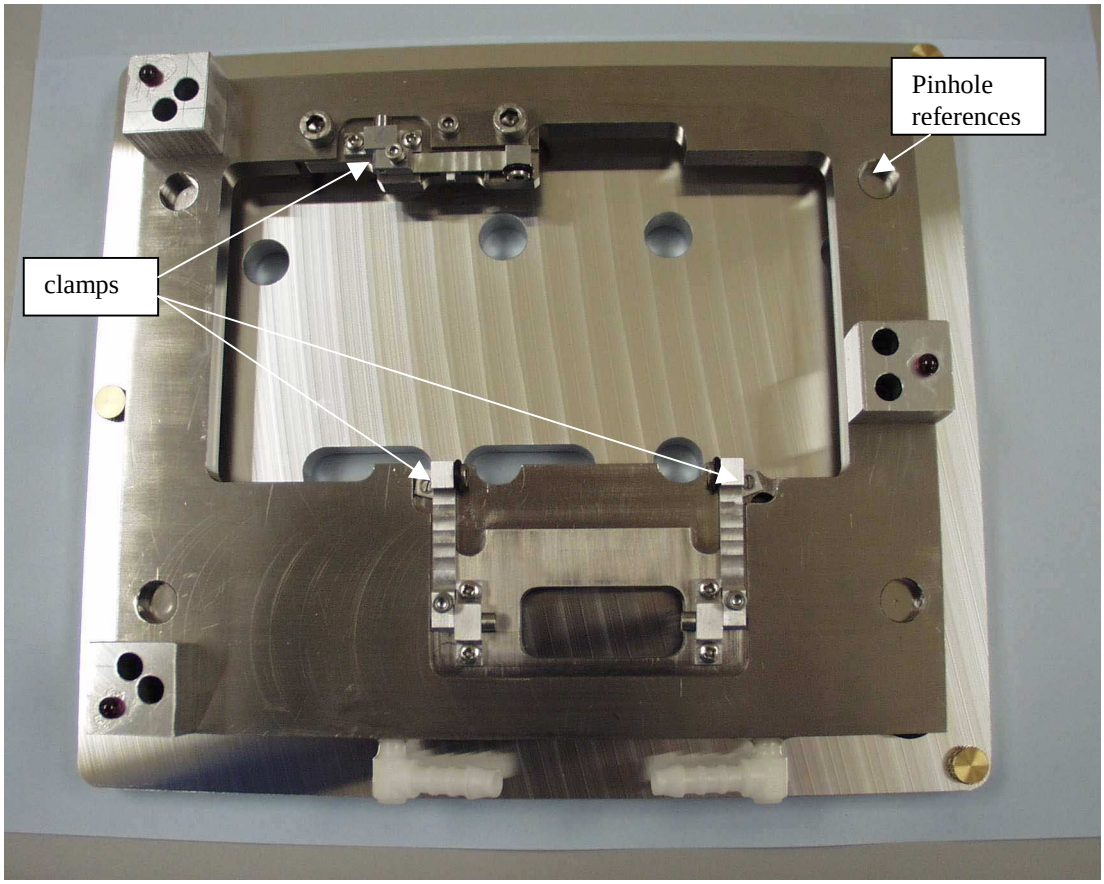

figure 4

5)Hybrid mounting jigs

The following text describes the various jigs and fixtures required to optically align and fit a hybrid onto a previously constructed 4 detector sub-assembly. A prototype item exists and is shown in figures 5 to 7 and described in the drawings listed in table 4.

Drawing number	Description	Drawing number	Description
TD-1009-303	G.A.	TD-1009-320	Module plate
TD-1009-318	GA for carrier assembly	TD-1009-326	Left hand clamp
TD-1009-390	Vacuum plate	TD-1009-329	Lower clamp
TD-1009-393	standoffs	TD-1009-331	Upper clamp
TD-1009-392	Cup fitting	TD-1009-327	Location pin
TD-1009-385	Angle bracket	TD-1009-316	Cover A
TD-1009-335	Module carrier	TD-1009-317	Cover B

Description of use.

This assembly kit provides all the actions necessary align and fit the hybrid relative to the detector Readout strips on each side of the sub-assembly using the detector strips and the pitch adapter on The hybrid. This is retrained within the hybrid vacuum pick up tool with a mixture of vacuum suction cups and pins, while the module is fitted into the support frame.

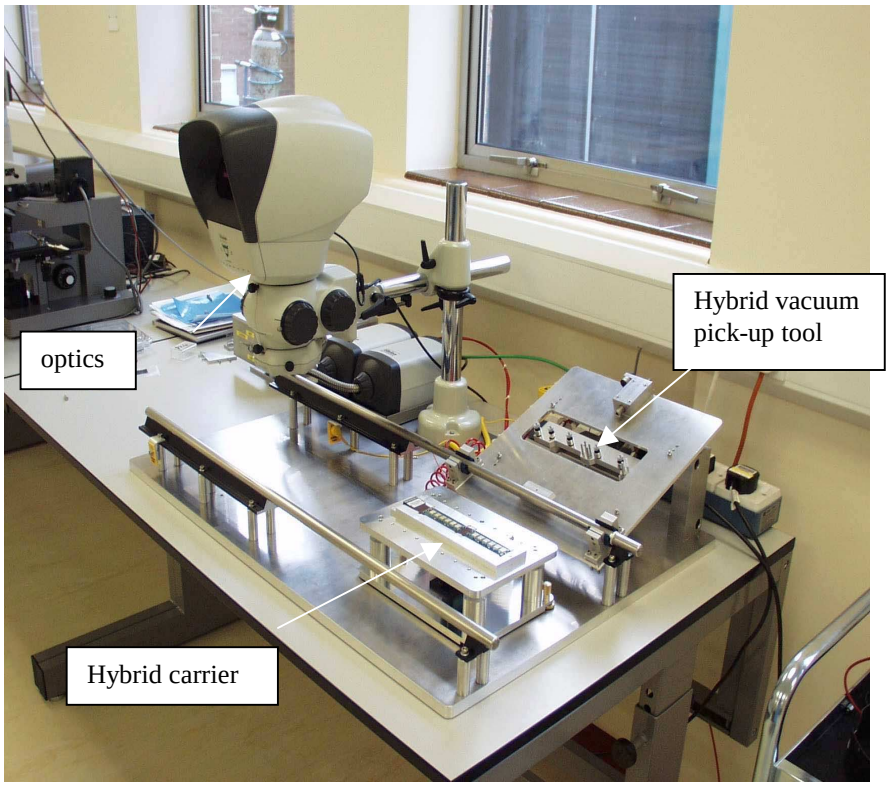

figure 5

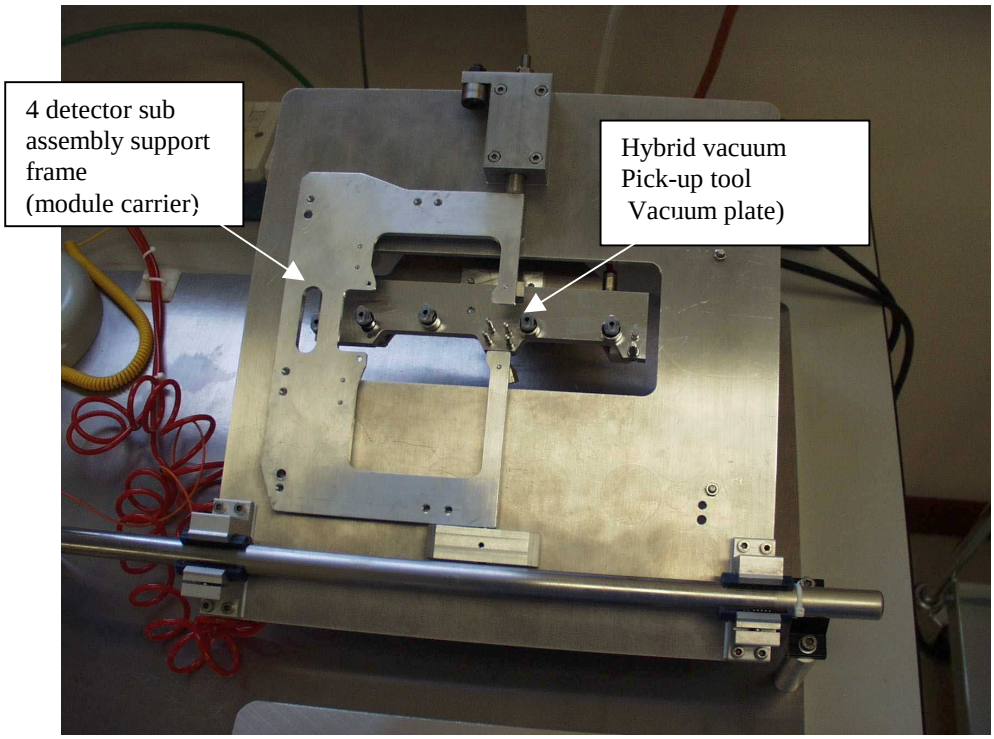

figure 6

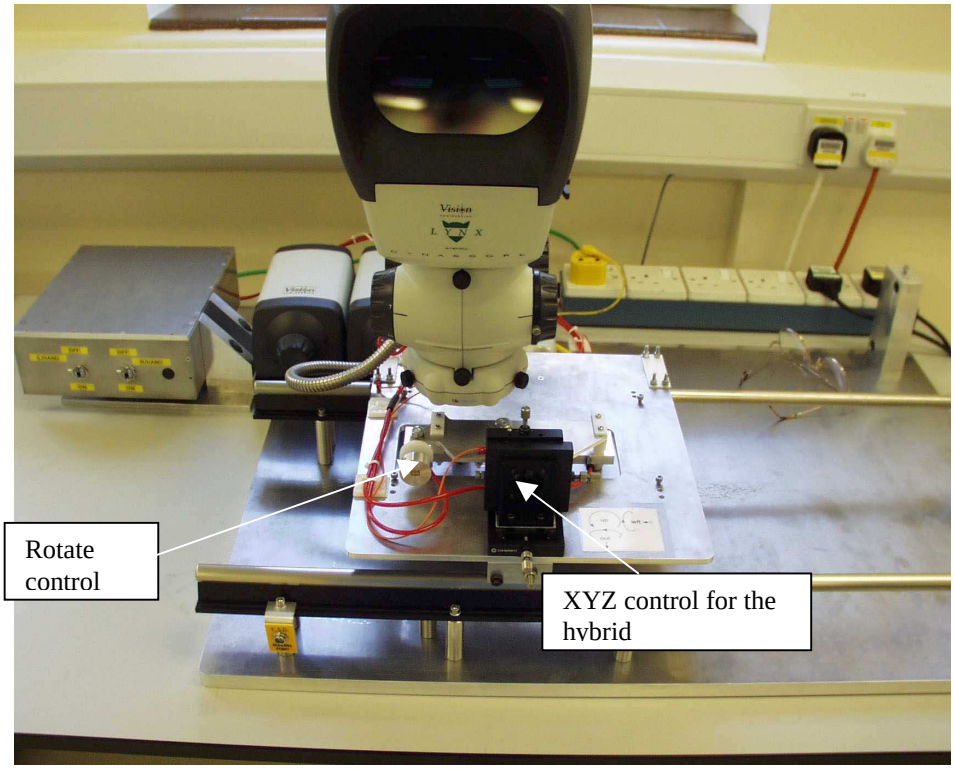

figure 7

5) Universal module handling tool.

At various points in the construction sequence the sub-assembly may have to be moved between the various jigs or stored awaiting testing or delivery of components. The handling tool below (figure 8) allows movement between all of the above jigs and current storage boxes (figure 9).

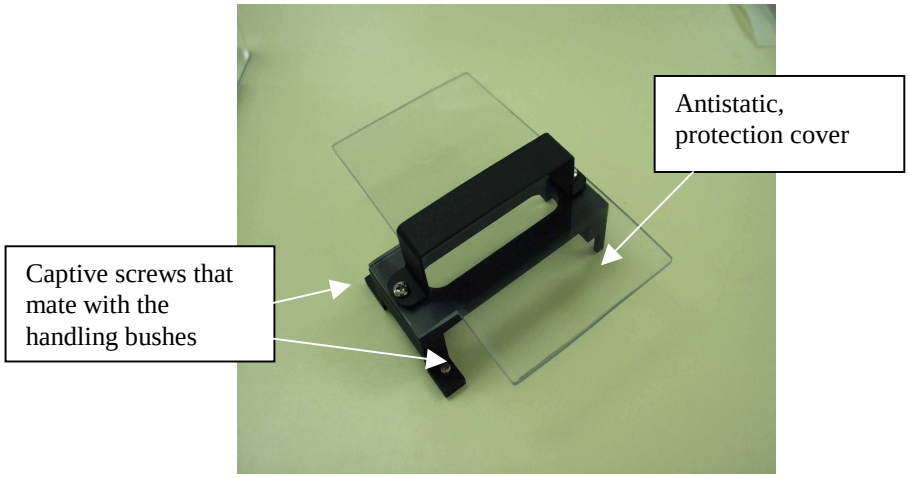

figure 8

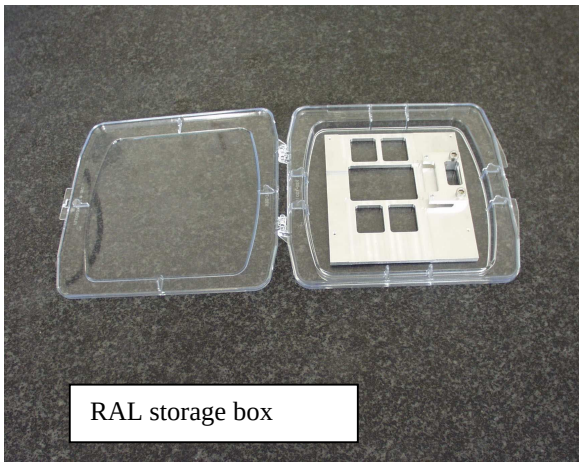

figure 9

APPENDIX 4 TO SCT-BM-FDR-6

ASSEMBLY JIGS AND PROCEDURES FOR THE SCANDINAVIAN CLUSTER

O. Dorholt

Jigs and their use in Oslo.

This document describes all the jigs, used at The University of Oslo for the fabrication of ATLAS Barrel modules.

1 Alignment.

1.1 Detector Alignment.

The Alignment -jig is used for placing the detectors at the correct position to the module.
All angles of the module, are implemented in the line-up process.

The jig is placed on a XY stepper motor system that allows to move the jig under the camera.
There are also 6 stepper motors that place each of the detectors individually.
(XY and rotation) (fig. 1).

On top of the rotation stepper motors, there are vacuum chucks holding the detectors.

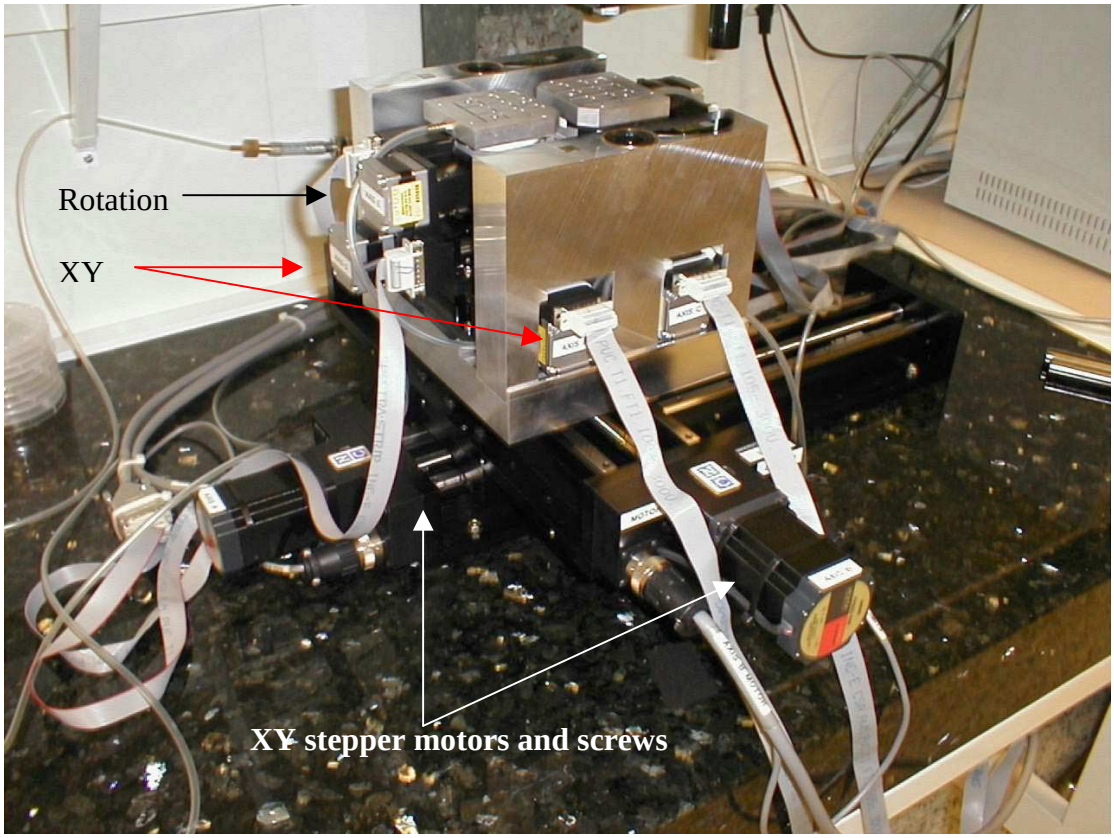

fig.1

1.2 Bearings and Shafts.

To be able to pick up the detectors after alignment, there are two linear ball bearings, one on each “sidewall” of the jig.
Those bearings are tuned to the accuracy needed by a tube of Brass (Fig. 2).
By using precision shafts in the bearings, we are able to slide the Pickup-jigs correctly down onto the Alignment-jig, and pick up the detectors (Fig. 3 and 4).

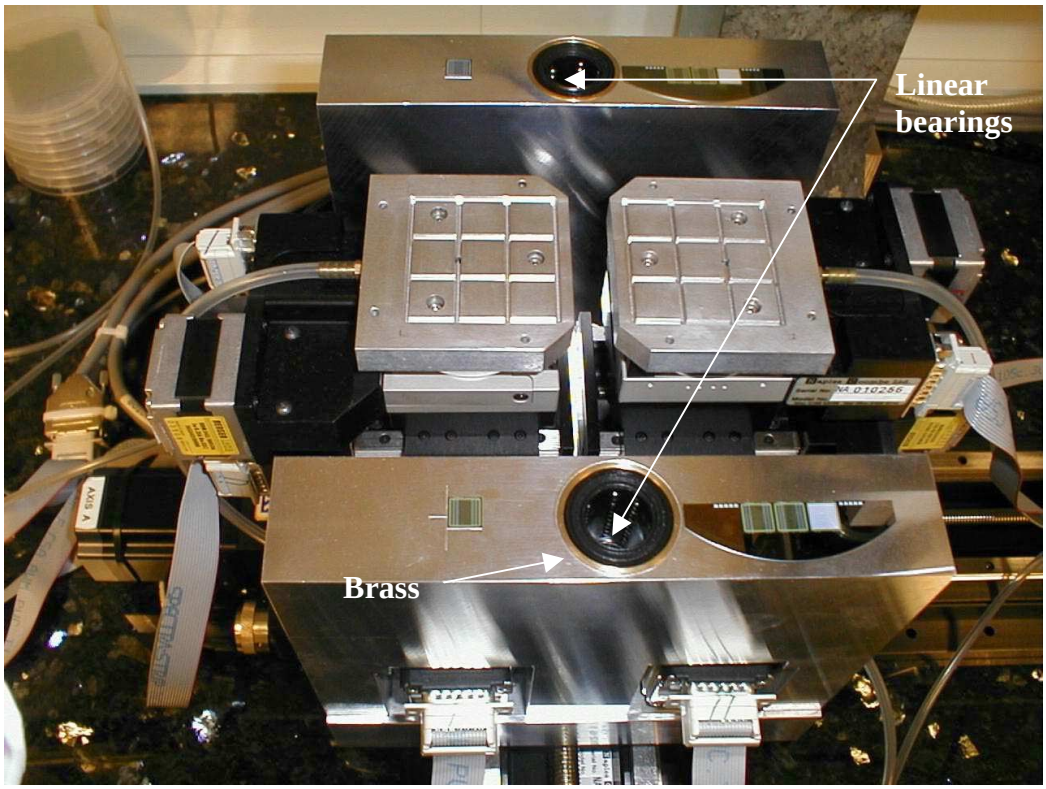

Fig.2

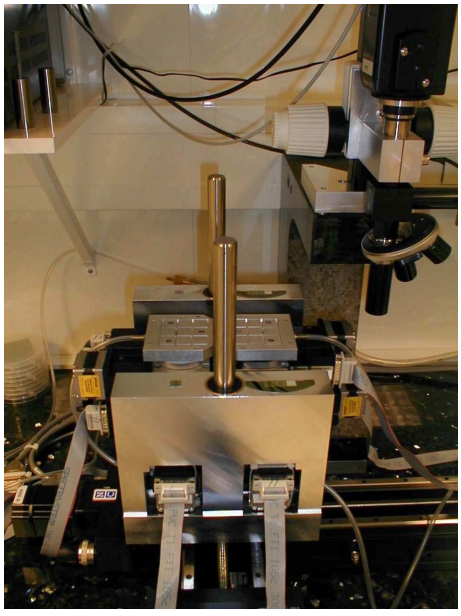

Fig. 3

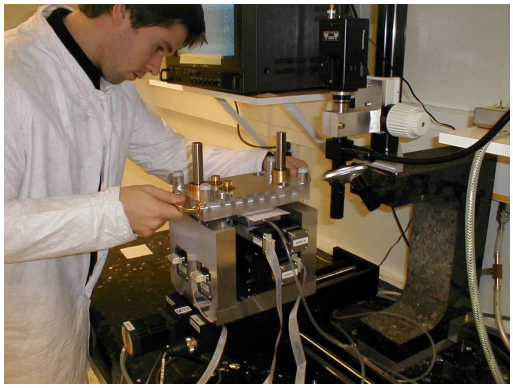

Fig.4

The bearings on the jig are placed with an angle of ~20 mrad compared with the jig itself.

This is done so that the camera follows the edge of the aligned detectors while the jig moves.

1.3 Components and materials.

Components	Type	Supplier
Aluminium	ALPLAN 5083 (AlMg4.5Mn)	Astrup
Linear ball bearings	CBCR 20-2LS	SKF Multitec
Precision Shafts	High-grade steel 20 mm ∅ Tolerance h6	SKF Multitec

2 Vacuum jigs.

2.1 Pickup jigs.

There are two different jigs used to alignment detectors from the Alignment-jig.
The first used in the process, has positioning screws for the baseboard.
This jig always holds the lower side of the module.

The other Pickup-jig is similar to the first one, but without the baseboard positioning screws. (Fig 4.)

2.2 Baseboard-jig.

To be able to glue the module in two steps, we need a similar jig to the Pickup-jigs to hold the baseboard during gluing the first step of the module. (fig. 4)

Fig. 4

2.3 Materials.

Components	Type	Supplier
Aluminium	ALPLAN 5083 (AlMg4.5Mn)	Astrup

3 Glue-jig.

3.1 Baseboard-support.

To be able to handle the baseboard during the dispensing of glue, we have a Support-jig. This jig clamps the baseboard carefully, using brass-clamps with rubber underneath. The clamps are supported by spring-loads.
To position the baseboard, there are pins that fit into the baseboard mounting holes. A mechanical support for the baseboard is mounted on the jig used when dispensing onto a bare baseboard. (Fig. 5)

3.2 Positioning the frame.

The Baseboard-jig has a Position-jig mounted onto the glue dispenser. These part fits together with linear bearings and precision shafts. The Baseboard-jig fits onto the Position-jig with either of its flat sides facing up, but with the Baseboard-jigs fiducial pointing in one direction only.

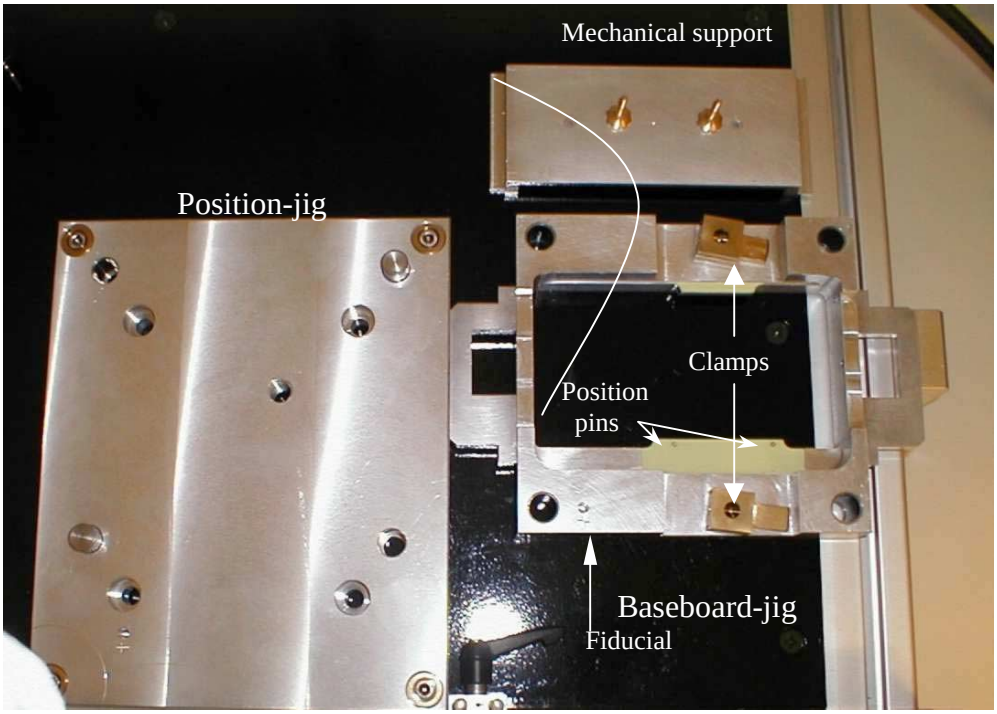

Fig. 5

3.3 Materials

Components	Type	Supplier
Aluminium	Alcoa Alca Plus	The Empire
Linear bearings	PG 12 1420 F	SKF Multitec
Precision Shafts	High-grade steel 12 mm ∅ Tolerance h6	SKF Multitec

Module building in Oslo

1.1 Detectors:

Detectors, either from Hamamatsu or Sintef, will arrive to Oslo after testing in Bergen.

1.2 Baseboards:

The baseboards, will be sent us from CERN.

1.3 Glue:

The thermal conductive glue, is Araldite 2011- AW 106/HV 953U supported by a Norwegian vendor: “Lindberg og Lund”.

The filler, Boron nitride, was delivered from RAL.
The electrically conductive glue is delivered from KEK.

1.4 Storing the parts:

All the parts will be stored in our clean-room under controlled temperature and humidity. They will remain in the original packets until they are to be used.

The glues are stored at room temperature approx. 22° C, and the Boron nitride is stored in the original bag, containing silicon gel as well.

1.5 Other parts in the process:

We are using clean-room paper in between the different vacuum chucks, and the detectors.

This has been a problem to get from vendors, but for the moment we use
“Rice paper H44-001B” from Metron TechnologyNordic AB.

2. Dispensing the glue

2.1 Mixing the Glue:

Both the glue-types used for the detectors, are mixed by hand.
To fill the syringe with the thermal conductive glue, we use a special designed plastic pouch, like a cornet. (Picture 1)

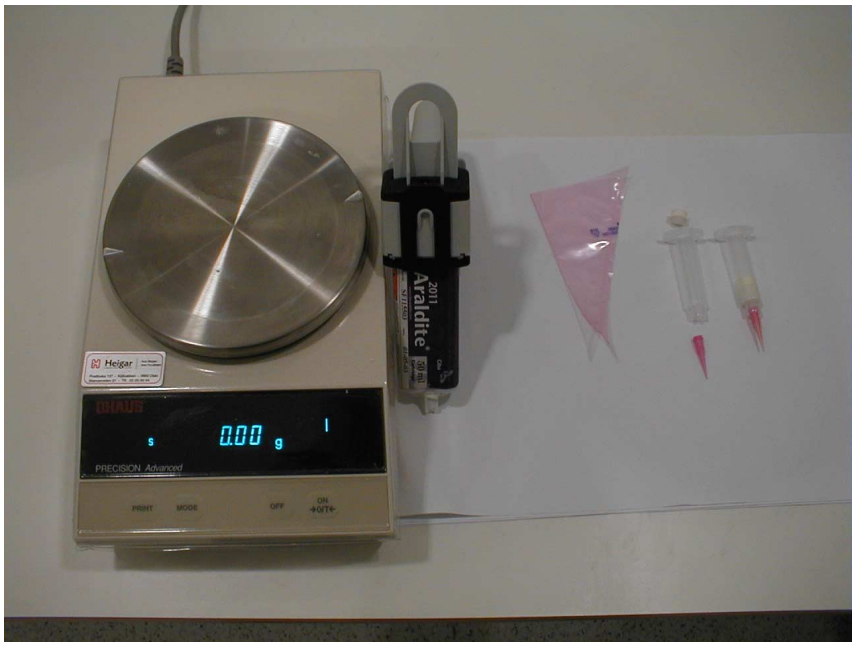

Picture 1

2.2 Glue dispenser:

This unit is capable to read for instance Gerber –files, and convert it to a steering-program for the unit. (Picture 2)

Picture 2

2.3 Baseboard jig:

To be able to treat the baseboard during the dispensing, we are using a jig that holds the baseboard in a careful way, with to pins into the baseboard holes, and two clamps with rubber legs touching the Beryllia facing.
This jig is designed to hold a single baseboard, or a baseboard with to detectors glued on one side (half-module). That allows us to glue the modules in to steps. (4.1)

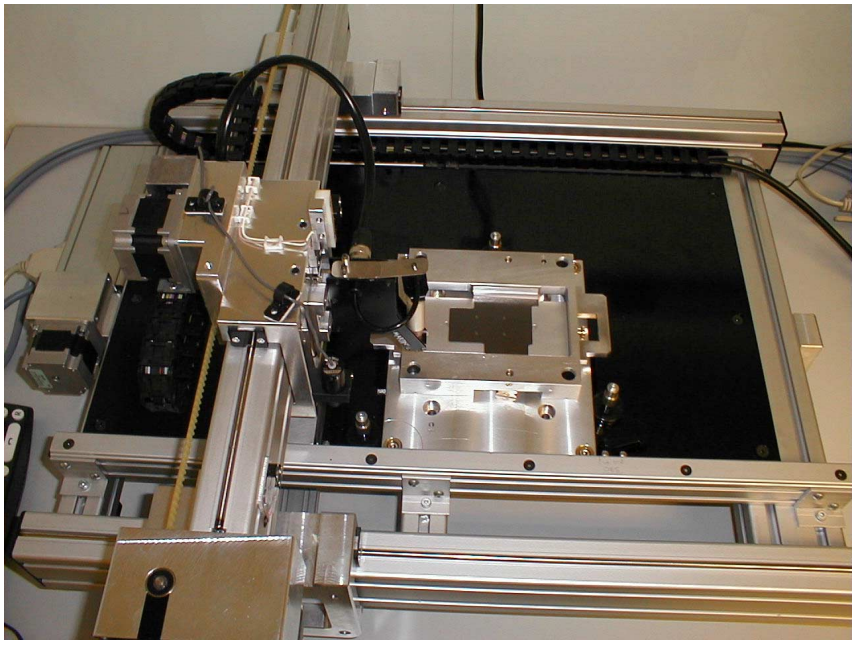

Picture 3

2.4 Moving the Baseboard:

To move the Baseboard from its original box to the glue-jig, and between the dispenser and the module-assembly jigs, we are using either the handling-tool provided by Martin Gibson, or a similar tool built in Oslo.
This tool uses the handling points on the Baseboard.

2.5 Testing the glue dispenser:

To test the glue-dispenser, we have used dummy components in Plexiglas and brass, to learn and understand more of what's going on in-between the detectors and the Baseboard.
(Picture 4)

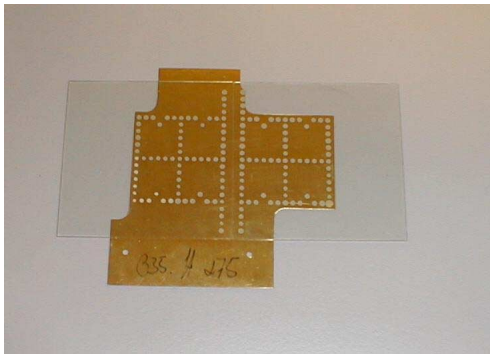

Picture 4

3. Lining up detectors

3.1 Pick up the detectors:

To pick up the detectors from the transportation packets, we are using a handheld vacuum-pen with plastic foot. This tool is placed directly to the top surface.
To prevent damaging the detector, we also have clean-room paper in-between the detector and the pen. (Picture 5)

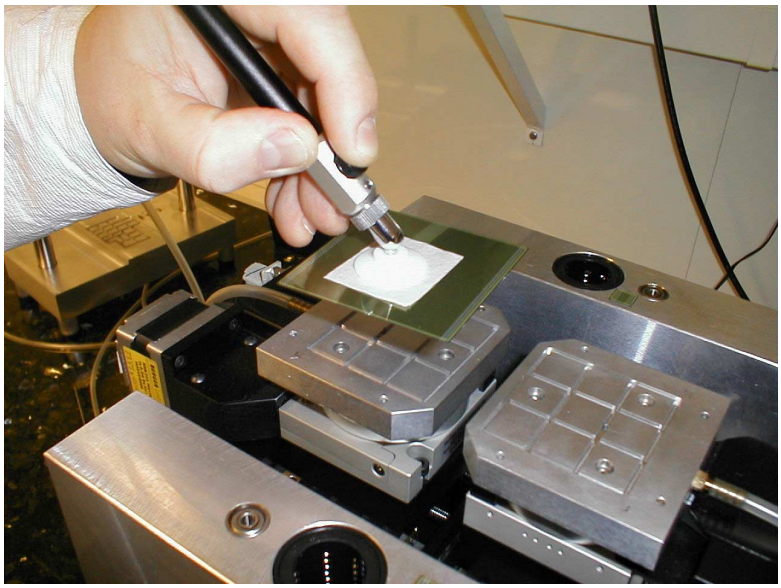

Picture 5

3.2 Alignment:

The alignment of the detectors is done with our step-engines jig, using software from Manchester, and a Labview program developed in Oslo.

3.3 Pickup jigs:

To be able to transfer the aligned detectors from the alignment jig, and to the gluing process, we pick them up with the gluing jigs directly, using vacuum.

The jigs used for this purpose, are lowered onto the detectors, with a sheet of clean-room paper in-between. They slide down on to dowel pins as shown in picture 6.

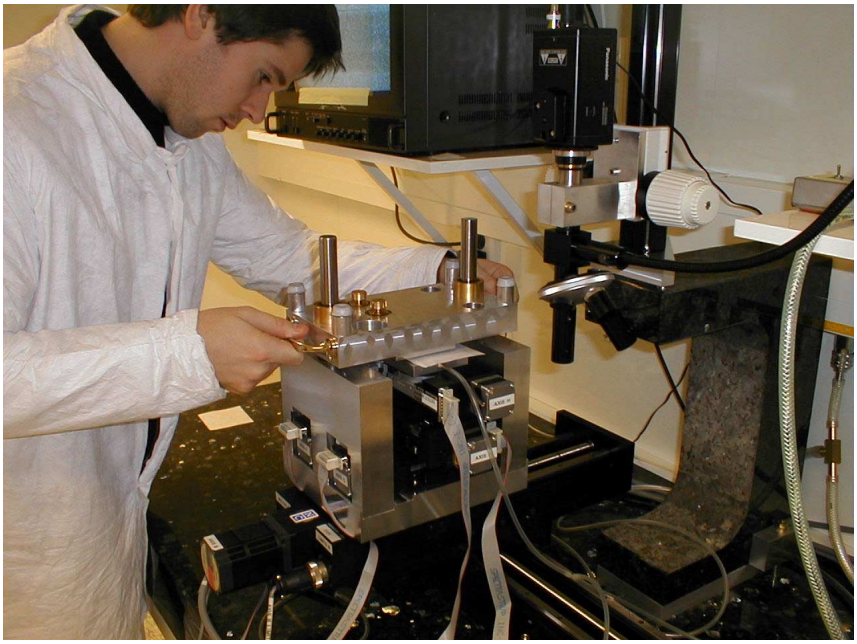

Picture 6

We have two different jigs for picking up detectors. One of them has also two small pins for positioning the Baseboard trough its holes. (Picture 7)

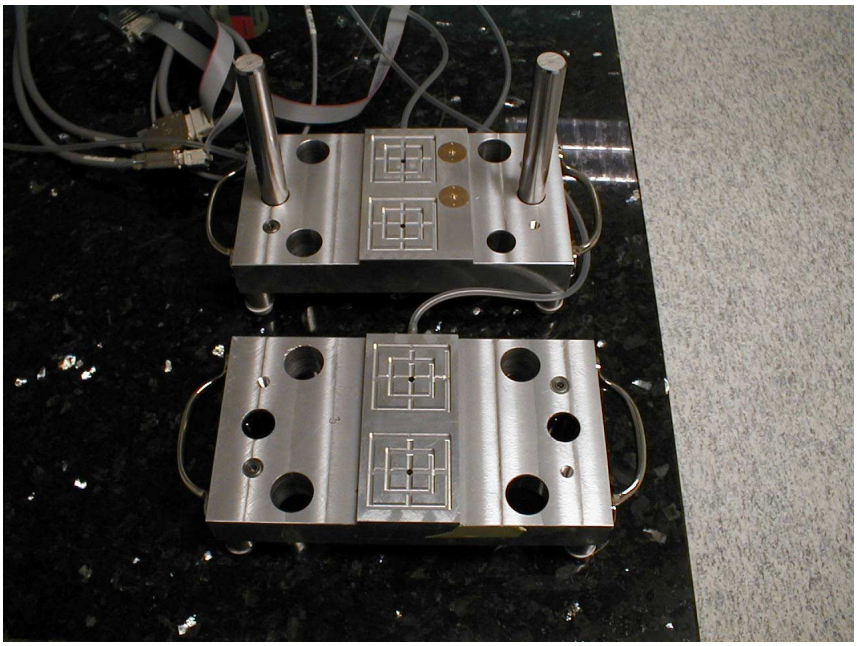

Picture 7

4. Gluing the module:

4.1 Two step gluing:

To be able to do the “Two step” gluing, we have developed a jig to hold the baseboard in the right position while doing the first step. (Picture 8)
This support the Baseboard with vacuum, so that the pins used for positioning no longer are needed, and they will be unscrewed from the jig.

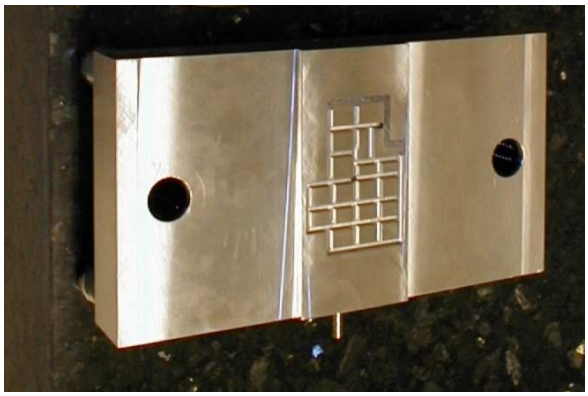

Picture 8

After hardening the first step, the “half”- module is placed back in the gluing-jig (Picture 3), and glue is dispensed on the other side of the Baseboard.
Then the “half”- module goes back to its originally gluing jig, and the second half of the module is glued, using the other pickup-jig.

4.2 Spacers:

To control the glue-thickness of the modules, we will use spacers in-between the jigs.
Those give us the possibility of controlling the thickness of the glue on each side.

5 Transportation:

After the modules are glued in Oslo, they will be transported to Uppsala, for metrology measuring, hybrid mounting and testing.

ATLAS project	**ATLAS SCT Barrel Module FDR/2001**				
SCT-BM-FDR-7	*Institute Document No.*				
		Modified:	15/05/01	*Rev. No.*	

SCT Barrel Module FDR Document

SCT Barrel Module : MODULE QA

Abstract

This document describes the quality assurance procedure to be applied for the SCT barrel module production.

Prepared by :	***Checked by :***	***Approved by :***
R. Apsimon, J. Carter, D. Charlton, L. Eklund, P. Phillips, Y. Unno		

Distribution List

Table of Contents

1 SCOPE OF THE DOCUMENT

This document describes the QA procedure to be applied to barrel modules during the construction process. The QA procedures for the individual components are dealt with in other documents (see SCT-BM-FDR-5). Tests are made during assembly to check that the components have not been damaged, for example in transport or in the first stages of module construction. Post-assembly testing validates the quality of the completed module: most tests will be performed on all produced modules, but some destructive or very time-consuming tests are performed on a sample subset of modules.

The procedures and tests described here aim to investigate a wide range of potential failures and problems. This extensive testing will be applied during the first part of the module series production, but is time consuming. In the later parts of the production, where the production rate is higher and experience of previously produced modules has been gained, the procedures will be reduced in areas that do not show failures.

The results of all tests will be logged to the SCT database. In some cases a simple yes/no result is obtained, for most tests characteristic performance data will be logged in addition to the flag of whether the module passes the relevant QA criteria.

The aim of the QA procedures is to ensure that each SCT Barrel Module fulfils all aspects of the specification. The same QA procedures and criteria will be applied at all the four barrel module production sites.

2 QA DURING MODULE ASSEMBLY

The following QA steps are performed during the assembly of a module. The criteria for accepting a module as ‘good’ are for initial use, and will evolve with experience.

2.1 Assembly of ASICs onto hybrids

Before delivery to the assembly site, the individual components have already been subject to QA procedures as described in SCT-BM-FDR-5.3 for the Hybrids and in SCT-MB-FDR-5.4 for the ASICs.

2.1.1 Tests of Distributed Passive-Component Mounted Hybrids

Hybrids with passive components mounted but without ASICs are distributed to the hybrid assembly sites. After transport a subset of the acceptance tests for hybrids are repeated to check that no damage has occurred in transport. For similar reasons, a visual check is made of each hybrid. The glass fan-in on the hybrid is also checked visually for any damage.

Before ASIC attachment, pull-tests are also made on each hybrid, requiring pull strength values of 6 gm for 30% height to distance ratio setting.

2.1.2 Electrical Tests of Hybrids after ASIC Attachment

After attachment of ASICs to the hybrids all wire bonds between hybrid and ASICs are made. At this stage an electrical test is made of the hybrid to ensure that all ASICs perform properly and that all wire bonds are functional. This is done by performing a Characterisation Sequence (see section 3.3).

2.1.3 Long Term Test of Hybrids with ASICs

In addition to the full ASIC characterisation on the hybrids, a longer duration test is performed on assembled hybrids. The aim of this test is to catch infant mortality problems in the front-end ASICs. The test is therefore performed at the first feasible stage, i.e. immediately after the ASICs are mounted on to the hybrids. (It should be noted that experience to-date has shown no long-term failures of ASICs).

The test consists of a long duration run at elevated temperature. The temperature and length of the run will be adjusted during production in the light of experience gained, but initially a 100 hour test will be made with a temperature measured by the hybrid thermistors of 45^{o}C. During the test the hybrids are powered, clocked and configured and triggered at the nominal L1A trigger frequency of 100kHz. The currents drawn by, and the temperatures of, the hybrids are monitored every few minutes. Every few hours a test to establish correct functionality of the hybrid is performed, so that if problems do develop the time structure of the failures can be observed.

2.1.4 Final Electrical Test of Hybrids

After the long term test, the ASICs are bonded to the hybrid pitch adapter. A final electrical Confirmation Sequence (see section 3.3) is performed to ensure that no inadvertent damage has been caused.

2.2 Construction of the Baseboard – Detector Sandwich

Before delivery to the assembly site, the individual components have already been subject to QA procedures as described in SCT-BM-FDR-5.1 for the Detectors and in SCT-BM-FDR-5.2 for the Baseboards.

2.2.1 Visual Inspection

Before use, the four silicon detectors and the baseboard are all visually inspected to ensure that no damage has occurred in transit. The criteria for detector acceptance is the same as on their first delivery from the contractor. The baseboard is checked to ensure that it is free from any cracks or defects.

Following the gluing of the detectors to the baseboard, the assembly is checked visually.

2.2.2 Detector Leakage Currents

After the detectors are glued to the baseboard, the I-V curve is recorded for each detector individually up to a bias of 500V. If any current (normalised to 20^{o}C) at 500V bias differs by more than 1μA from that last recorded in the database for the detector, the assembly is put to one side for further visual checks and current stability measurements.

2.2.3 Metrology

The full set of metrology survey measurements (see section 3.2) is performed on the baseboard-detector assembly. If the results are outside specification the assembly is rejected.

2.3 Mounting the Hybrid

2.3.1 Electrical Check of Hybrid

On receipt at the module assembly site, the hybrid is checked for its continued correct electrical functionality before mounting on the module. This is done with the Confirmation Sequence as described in Section 3.3.

The glass fan-in on the hybrid is also checked visually for any damage.

2.3.2 Detector Leakage Current Check

After the hybrid is mounted on the module, the detector bias is bonded, and the leakage current checked up to 500V bias. This is a diagnostic step, to establish whether any subsequent leakage current problems that may be observed have occurred before or after the detector strip bonding.

3 QA OF THE COMPLETED MODULE

The following QA steps are performed on fully assembled modules. The criteria for accepting a module as 'good' are for initial use, and will evolve with experience.

3.1 Leakage Current Tests of Each Completed Module

3.1.1 I-V Scan to 500V

With the ASICs unpowered, the detector I-V curve of the completed module is recorded up to 500V bias at room temperature. For a good module, the total leakage current of the module will differ from the sum of those for the four individual detectors by no more than 4μA at 500V. Outside this limit, the module will be visually inspected for any signs of damage to the detectors, and subjected to long-term current tests at a range of bias voltages.

3.1.2 Long Term Leakage Current Stability

All modules will be tested for long-term leakage current stability over a 24 hour period in an environmental chamber containing cold dry air (nitrogen). The ASICs are powered, clocked and triggered, and the detector bias is maintained at 150V, with the

current monitored every 15 minutes over the period. The temperature is adjusted so that it is -10^{o}C measured by the hybrid thermistors. The maximum increase in leakage current over the period should be less than 4μA for a good module, after an initial settling time of 5 minutes.

This test can be performed in parallel with the long-term electrical test on modules, section 3.5 below.

3.2 Metrology

After completing the detector-baseboard assembly or the assembly of module, the object will be surveyed for mechanical precision. The precision is characterised by in-plane and out-of-plane parameters. For the in-plane survey, a well-defined set of fiducial marks on the sensors is used. For the out-of-plane survey, a matrix of points with equal spacing is measured. A 3D measuring machine is required for the out-of-plane survey

3.2.1 In-Plane Survey

The in-plane survey characterises the relative positions of the four sensors and the dowel hole/slot of the baseboard. Figure 1 shows a typical setup for the measurement. A module is placed on a frame and is held at three points. The frame has a number of transparent fiducials so that the measurements of the front and the back sides can be correlated.

The x and y coordinates of a sensor are obtained from the measurements of the nine fiducial marks *A* (see SCT-BM-FDR-5.2 for their description). The reduced parameter set, however, does not rely in the end on which fiducial marks are used. For the front side, the centres of the dowel hole and slot are obtained from the measurements of the perimeter of the hole and the slot.

From the 34 (x,y) coordinates measured, the module coordinate and a reduced parameter set are obtained as shown in Figure 2. The coordinate origin is the geometrical centre of four sensors. The stereo angle is that between the axis of the front pair, C1C2, and the back pair, C3C4, where C1 to C4 are the geometrical centres of sensors1 to 4, respectively. The half-stereo angle defines the x coordinate, X_m, and then the y coordinate, Y_m. In this coordinate system, the reduced parameter set is listed in Table 1, with the design values and the tolerances specified.

3.2.2 Out-of-Plane Survey

The surface of the module is measured at a matrix of 5x5 points for each sensor with a 3D measuring machine having a z measurement precision of better than 10 μm. In addition to the surface points on the sensors, three points Z1, Z2, and Z3 are measured on the surfaces of the cooling contact and the far-end BeO facings on the back side of the module, as shown in Figure 1. The three points define the *module plane* as mounted on the bracket on the barrel cylinder. The locations of Z1 and Z2 are close to the dowel hole and slot, while Z3 is near the third module mounting point. The front-back correlation is made through the measurement of the transparent fiducials on the frame. There are in total 100 (x, y, z) data points for which the (x,y) module coordinates are defined in the in-plane survey, and the z coordinate with the origin at the centre of the module calculated from the *module plane*.

The out-of-plane tolerances are constrained by two factors; the requirement to keep at least a 1mm `stay clear' distance between modules mounted on the barrel (see SCT-BM-FDR-4, section 4), and the physics tracking requirement for the residuals in z-flatness. These are discussed in Appendix 1. For the `stay clear' distance, the requirements for a good module is

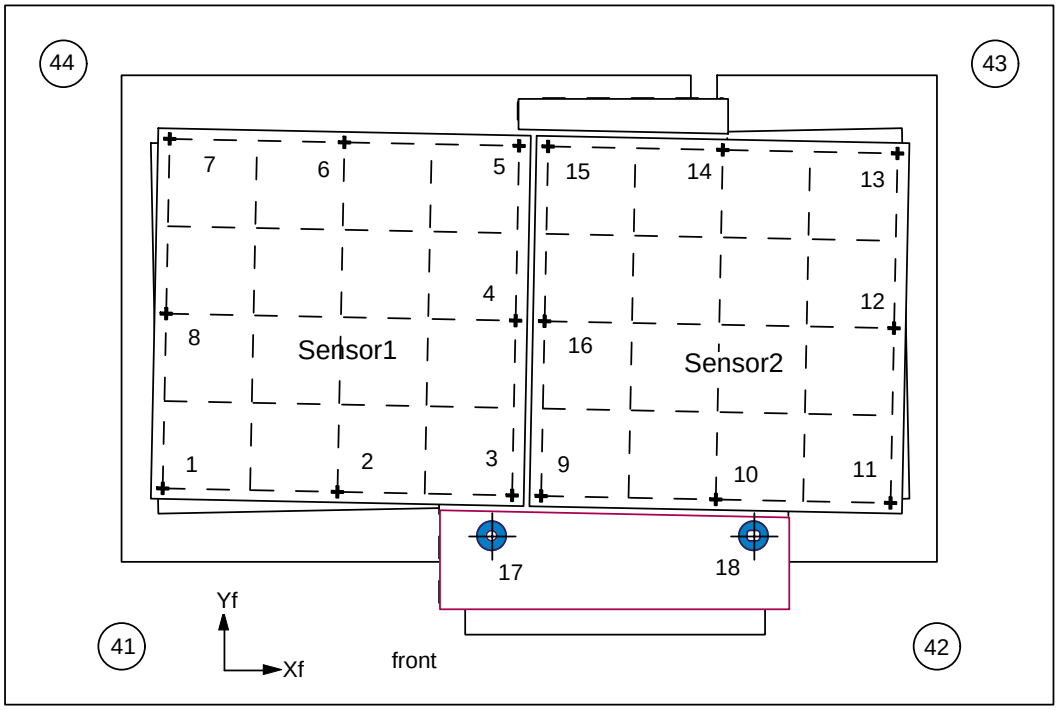

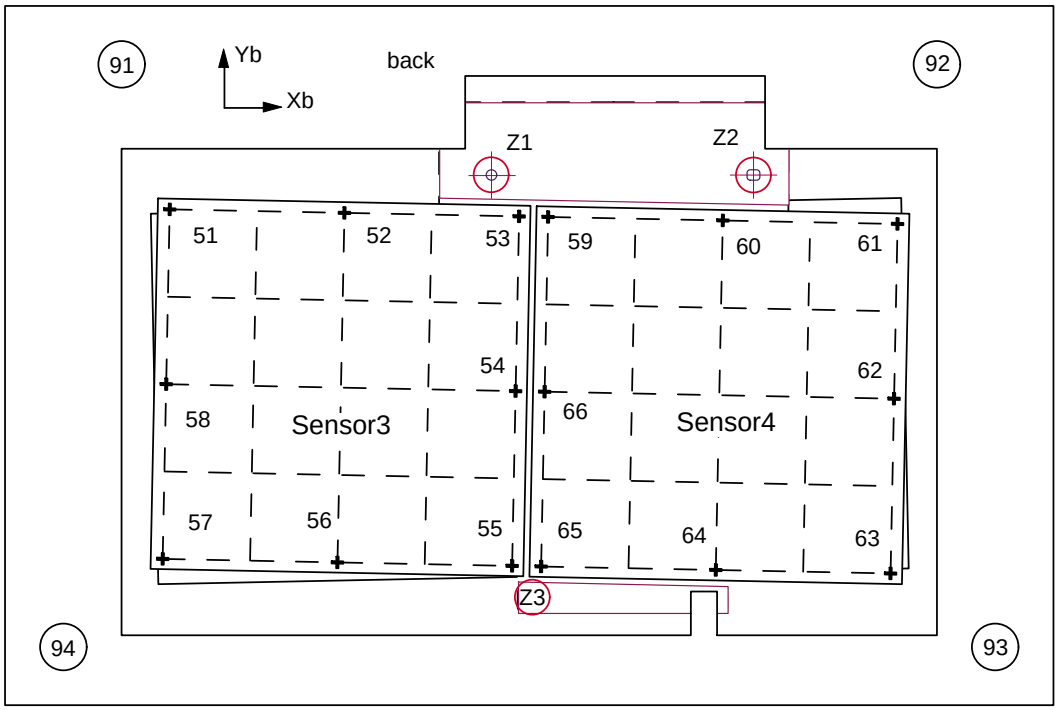

Figure 1 Survey points on a barrel module. Sensors 1 and 3 are on the left when the module is drawn in the conventional orientation. "+" represents the fiducial mark A on the sensors. Points 1-18, 41-44, and 51-66 are for the in-plane survey. Point 17 is the centre of the mounting hole and Point 18 of the mounting slot. For the out-of-plane survey, points on a 5x5 matrix are measured for a sensor, in addition to the points Z1, Z2, and Z3 in the back in order to define the module reference plane. Points 41-44 and 91-94 are transparent fiducials to correlate the measurements of the front and the back sides.

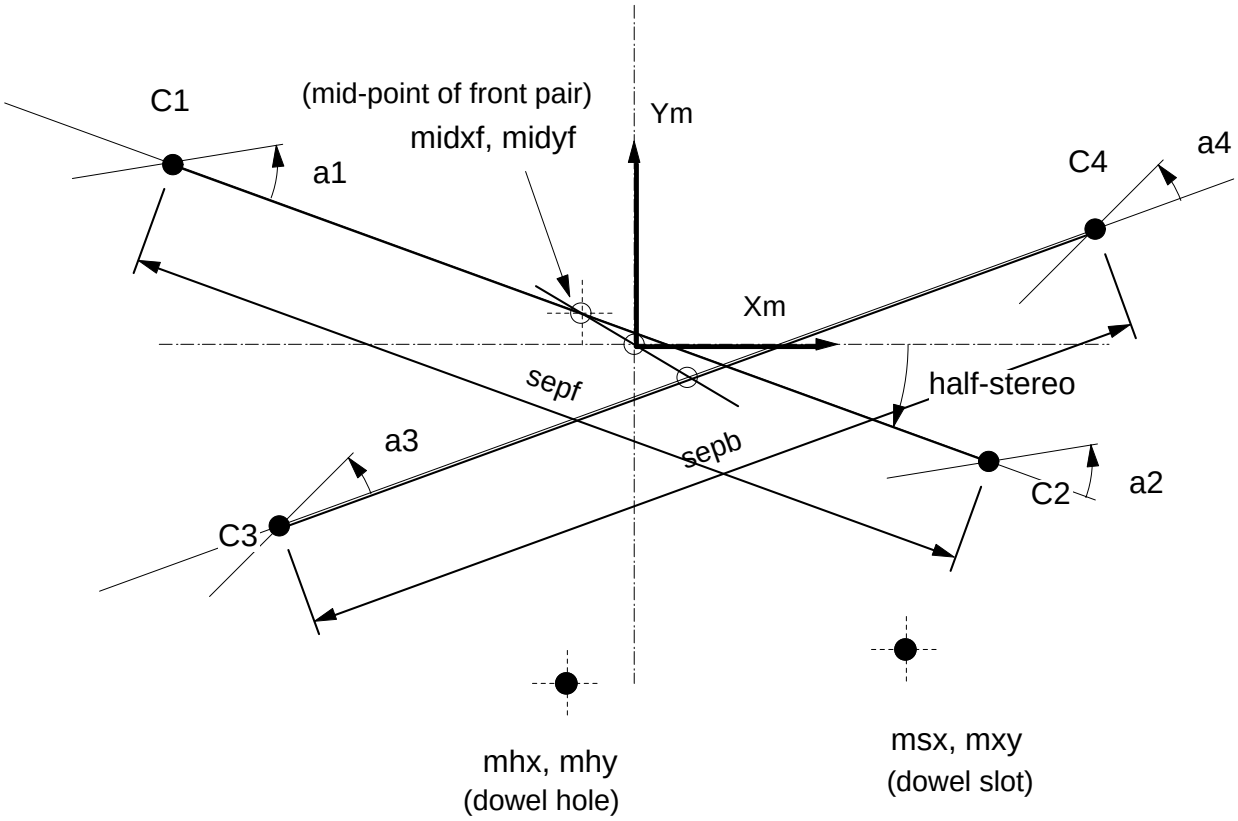

Figure 2 Definition of the parameters which describe the geometry of a module. The black circles C1 to C4 are the measured centres of the four sensors. The dashed line through each centre gives the measured orientation of each sensor. Open circles are the centre points of lines. The module is described in the database by 13 numbers: the coordinate pairs of the dowel hole, slot, and centre of front/back pair: (mhx, mhy), (msx, msy) and (midxf, midyf), the sensor separations: sepf, sepb, sensor angles: a1, a2, a3, a4, and the half-stereo angle. The stereo angle is measured from the X_m axis and sensor angles from the stereo axis, with anti-clockwise rotation being positive.

that the maximum height of a sensor surface from the nominal should be < 200 μm. The requirement on the residuals in z-flatness, after `minimal use' (see Appendix 1) of z data, is that the value should be < 50 μm.

Parameter	Design Value	Tolerance
Dowel hole, mhx [µm]	-6500	30
Dowel hole, mhy [µm]	-37500	30
Dowel slot, msx [µm]	38500	100
Dowel slot, msy [µm]	-37500	30
Mid-point of front pair, midxf [µm]	0	10
Mid-point of front pair, midyf [µm]	0	5
Separation of front pair, sepf [µm]	64090	10
Separation of back pair, sepb [µm]	64090	10
Sensor1 angle, a1 [mrad]	0	0.13
Sensor2 angle, a2 [mrad]	0	0.13
Sensor3 angle, a3 [mrad]	0	0.13
Sensor4 angle, a4 [mrad]	0	0.13
Half stereo angle, half-stereo [mrad]	-20	0.13

Table 1: Module in-plane geometry parameters

3.3 Electrical Tests

An extensive suite of both hardware and software[1] has been developed to facilitate module testing. The readout system is based around the VME modules CLOAC, MuSTARD and SLOG. The prototype low voltage and high voltage modules, SCTLV and SCTHV, are also part of the system.

Two largely automated series of tests[2] have been devised to simplify the testing procedure, as outlined in table 1. The *Characterisation Sequence* aims to perform the full characterisation of a hybrid or module whereas the shorter *Confirmation Sequence* provides a reduced set of information. The *Confirmation Sequence* ensures that the digital part of the ASICs is functioning, none of the critical wire-bonds have been damaged and that the basic analogue performance of a module has not deteriorated. It is anticipated that the *Confirmation Sequence* would be repeated at regular intervals during the long-term tests and each time that a hybrid or module is shipped between institutes.

[1] http://sct.home.cern.ch/sct/sctdaq.html

[2] The tests are described fully in http://hepwww.rl.ac.uk/atlas-sct/documents/Electrical_Tests.htm

	Characterisation	Confirmation
Power On Tests / Verification of Response to Hard Reset	√	
Clock and Command Reception Test	√	√
Bypass Functionality Test	√	√
Pipeline Efficiency Test	√	
Strobe Delay Scan	√	√
Three Point Estimation of Gain, Noise and Offset	√	√
TrimRange Scan	√	
Determination of the Response Curve	√	
Noise Occupancy Scan	√	
Timewalk Scan	√	

Table 1: The Characterisation and Confirmation Sequences

In general, the analogue performance of a module/hybrid is measured with respect to the internal calibration circuitry of the ABCD3T chip. Hence it is necessary to make a correction for the variation of the calibration capacitance between batches of ASIC wafers.

There follows a brief description of the individual tests to be performed as part of the electrical QA procedure. The description contains the method in general terms, the purpose of the tests and in quantitative terms the criteria for PASS/FAIL cuts. A summary of the results of each test will be recorded in the SCT database.

A module is classed as `good' if at least 99% of its readout strips will operate efficiently with low noise occupancy at 1fC threshold.

3.3.1 Power on Tests / Verification of Response to Hard Reset

The module/hybrid is clocked and the power is switched on. The operator must verify that each data-link responds with CLK/2 and that, after the chips have been configured, the clock feed-through signal stops. The analogue and digital currents are then recorded. Finally Hard Reset is issued to bring back the CLK/2 signal.

This test verifies that the Clock, Command and Hard Reset signals are received correctly, that the chips can be configured and that the current consumption is reasonable. The test will identify modules/hybrids with severe failures. Every module must pass this test without error.

This is the only test that would normally require operator intervention.

3.3.2 Clock and Command Reception / Addressing Error Test

The chips are configured to return the contents of the Mask Register and a burst of triggers is issued for each of the Primary and Redundant Clock and Command options. Prior to each event, a different bit pattern is loaded in the Mask Register such that consecutive events are not the same.

By comparing the received data with expectation it is verified that both the Primary and Redundant Clock and Command signals are received correctly and that the top address bit of each chip changes as the Clock/Command source is varied, as specified in the

module design. This test will identify modules/hybrids with faulty command reception or addressing errors. Modules/hybrids with such defects would be considered to have failed pending further investigation and possible rework.

3.3.3 Bypass Functionality Test

A trigger burst is recorded with the module/hybrid programmed to each of a number of different configurations, sufficient to exercise all data/token passing links between the chips. In each case the chips are configured to return the contents of the Mask Register such that the expected data is accurately known. The test is repeated across a range of digital supply voltages.

This test determines the minimum value of the digital supply voltage needed for each of the data/token passing links to work. Any link that did not work at the designated supply voltage, and which could not be identified as being due to a missing wirebond and subsequently repaired, would cause a module/hybrid to be rejected.

3.3.4 Pipeline Efficiency Test

For this test, a Soft Reset command is sent to reset the pipeline followed a certain number of clock periods later by a Pulse Input Register command and L1A trigger. In this way, a known pattern is injected into a given location in the pipeline. By varying the distance between the Soft Reset and Pulse Input Register commands it can be verified that each of the eleven blocks within the pipeline is free of defects.

Zero occupancy for a particular number of clock periods between the Soft Reset and Pulse Input Register commands would indicate a dead cell in the corresponding block of the pipeline. Zero occupancy for all values would indicate a dead channel. Modules/hybrids with a large number of dead Pipeline cells or dead channels will be rejected.

3.3.5 Strobe Delay Scan

This scan is performed to determine the correct Strobe Delay setting, corresponding to the timing of the charge injection pulse, to be used during the Analogue Tests.

3.3.6 Three Point Estimation of Gain, Noise and Offset

Threshold scans are taken for three injected charges to facilitate a quick measurement of gain, noise and the discriminator offset. Pathological channels are categorised as FAULTY if the defect would result in the channel having a reduced but non-zero detection efficiency in ATLAS, or as LOST if the defect would result in the channel having zero efficiency:

- **Lost: Dead, Stuck, Unbonded or Noisy channels**
- **Faulty: Inefficient, Low Gain or Partially Bonded channels**

Modules/hybrids having any chips with abnormal gain or high noise will be rejected, for potential re-work, as will those with large numbers of pathological channels.

3.3.7 Trim Range Scan

For each of the four possible TrimRange settings, a series of Threshold scans are performed for a subset of the sixteen possible TrimDAC settings, all with 1fC injected charge. For each TrimRange setting a straight line is fitted to the data for each channel to characterise the TrimDAC response and to determine the TrimDAC slope. The number of trimmable channels and the spread of the resultant trimmed thresholds are also recorded. The optimised TrimDAC settings and a list of channels to be masked are produced for use in the subsequent analogue tests.

The chips used to build modules will have been selected such that all channels may be trimmed using the smallest TrimRange. Modules which do not meet this specification on at least 99% of channels will be rejected, for potential rework, as will those where a particular TrimRange has a slope other than that expected.

3.3.8 Response Curve

Threshold scans are performed for a series of input charges and, for each channel, an appropriate function is fitted to the resulting response curve. From this the Gain, Noise and discriminator Offset are extracted.

The parameters from the fit are stored since they describe the correspondence between the Threshold, in mV, and input charge, in fC. The categorisation of pathological channels is repeated as described for the Three Point Gain. Modules/hybrids with a large number of pathological channels will be rejected.

3.3.9 Noise Occupancy Scan

A high statistics Threshold scan is performed at the nominal ATLAS trigger rate of 100kHz, without any injected charge, to determine the Noise Occupancy of each channel as a function of Threshold. The analogue and digital current consumption as a function of Threshold is recorded.

Channels with high Noise Occupancy will be added to the list of masked channels.

3.3.10 Timewalk Scan

This test performs a series of Strobe Delay scans with the Threshold set to 1 fC, varying the input charge from 1.25 to 10 fC. In each case a fit is made to the rising edge of the pulse to determine the Strobe Delay value needed to obtain 50% occupancy.

The Timewalk is defined as the time variation in the crossing of a threshold of 1fC over a signal range of 1.25 to 10.0fC. This parameter is calculated and recorded.

3.4 Thermal cycling

For every module a thermal cycle from -30^{o} to +50^{o}C will be carried out ten times, in an inert atmosphere. The module(s) will be placed inside an environmental test chamber and purged with nitrogen for sufficient time to achieve at least 3 volume changes within the chamber. During the test, each module will be clocked and triggered and the ASIC currents will be checked. The test cycle will start and end at room temperature and the first temperature excursion will be to +50^{o}C. The ramp up/down times will be approximately 30 minutes (2-3^{o}C/minute) and the soak time about 30 minutes at each temperature. The total test time will therefore be about 20 hours. This test could also be extended to carry out long-term electrical tests at the operating temperature.

3.5 Long-term electrical test

In addition to detailed electrical testing and characterisation, a longer duration test will be performed on assembled modules at the ATLAS operating temperature. This test verifies that modules will function electrically at reduced temperatures.

The test consists of an extended (24 hour) run at reduced temperature, defined to be –10^{o}C as measured by the hybrid thermistors. During the test the hybrids are clocked and triggered. The currents drawn by, and the temperatures of, the hybrids are monitored continuously. Every few hours a *Confirmation Sequence* is performed. At the end of the test, a *Characterisation Sequence* is performed while the modules are kept cold.

This test may be performed in parallel with the long-term leakage test (section 3.1.2).

4 SAMPLING QA ON COMPLETED MODULES

The fraction of modules to be used initially for the sub-sample tests is indicated in each of the following sections.

4.2 Irradiation Tests

A very small sample of the completed barrel modules (approximately 10 per annum during the construction period) will be fully and uniformly irradiated in the SCT facility at the CERN PS to a fluence of $3x10^{14}$ pcm^{-2} 24 GeV/c protons. They will be annealed for 7 days at 25^{o}C following the irradiation and then checked for mechanical integrity and for noise performance, for full ASIC functionality and for detector leakage current when run cold at the SCT operating temperature. Several of these modules will also be tested in the beam for signal:noise and efficiency performance.

4.3 Readout Performance with Particles

4.3.1 Beam Tests

A small number (approximately 20 per annum during the construction period) of the barrel modules will be fully tested in the H8 beam at CERN, with a magnetic field and with varying angles of incidence of the particles to check their continued performance characteristics. Modules will also be tested in the beam at KEK.

4.3.2 Source Tests

It is anticipated that a fraction of the modules will, at least initially, be read out in the laboratory when exposed to a Ru^{106} beta source. This will allow signal:noise values to be confirmed for the different batches of delivered ASICs.

4.3.3 Laser Tests

A subset of the produced modules may also be submitted to scanning Laser tests. A focused LASER of wavelength e.g. 1050 nm is mounted on a x-y stage and scanned over the module. This test provides very precise position information, hence the correct functionality of all channels can be verified.

5 SUMMARY

The QA procedures for the Barrel SCT module are designed to ensure the quality and performance for each individual module produced. They should cover all aspects of the module, such as mechanical tolerances, electrical performance and long-term stability. These goals should be achieved uniformly during the production cycle, regardless of production site, for all batches of constituent components and for the assembled modules..

Appendix 1: Tolerances on Out-of-Plane Metrology Data

One limitation on the out-of-plane data comes from the `stay clear' distance required between the surfaces of adjacent modules, see SCT-BM-FDR-4, section 4. To ensure a 1.0 mm stay clear distance, the maximum allowed out-of-plane deviation of a module from the nominal is 200 μm.

With the `optimal use' of the 100 metrology data points per module in a reconstruction program, i.e., 100 points times 2112 barrel modules, no further requirement is necessary for the out-of-plane tolerance. However, this cannot be regarded as practical solution.

`No use' of the z metrology data would require the module z-deviations from perfect flatness to be limited to the value allowed from the physics requirements, which is less than about 50 μm. From the experience of the modules so far constructed, `no use' is not a practical solution as there is intrinsic bowing in the sensors and in the baseboards.

The `minimal use' of z data is the procedure adopted, and this is carried out in two steps:

(1) The `mid-plane' calculated from the top and the bottom surface of the sensors is fitted (separately in the left and the right side sensors) to a plane, $z = ax + by + c$. These 6 parameters per module express any asymmetry in the construction or non-planar properties of the baseboard for the module.

(2) The `common profile' of the surface is calculated at the 100 measured points. Thus, 100 points express the bowing of the sensors, common to all modules which use sensors from a particular vendor.

After the above two corrections, the residual is regarded as the error in z-flatness, which has to be smaller than the tolerance from the physics requirements.

SCT Barrel Module FDR Document

SCT Barrel Module : Mechanical and Thermal Performance

Abstract

This document describes module metrology results and the measurements of a thermal module.

Prepared by :	*Checked by :*	*Approved by :*
R. Apsimon, A Carter, J. Carter, Y. Unno		

Distribution List

Table of Contents

1 SCOPE OF THE DOCUMENT

Metrology results are presented for barrel modules in section 2 and thermal results in section 3. The measured thermal properties of modules are compared with FEA calculation. Over a period of several years during the evolution of the module design, special *thermal modules* have been built for detailed thermal study, and in particular to check the FEA calculations regarding thermal runaway of irradiated detectors. Agreement has been good. A new thermal module has recently been constructed and first results are presented in section 3.

2 BARREL MODULE METROLOGY RESULTS

2.1 Metrology of completed modules

Assembled modules have been surveyed for their mechanical precision, both in-plane and out-of-plane, as defined in SCT-BM-FDR-7. The measurements were made with a 3D metrology machine. One such machine used is shown in Figure 1. This machine has an absolute precision of better than 1 μm in the (x y) - plane over a span of 100 mm x 100 mm, and better than 10 μm in the z direction with auto-focusing.

Figure 1 A 3D metrology machine, Mitutoyo QuickVision Pro250

2.2 In-Plane Survey

The reduced parameter set is defined for the in-plane survey in SCT-BM-FDR-7, section 3.2.1. The parameter and tolerance list is reproduced in Table 1. The survey results, giving deviations from the design values, are shown in Figures 2 to 4 for a sample of seven modules constructed by the Japanese cluster. Figure 2 shows the positions of the dowel hole and slot, Figure 3 the centre and separation of the pairs of sensors, and Figure 4 the rotation of the sensors and the half-stereo angle. In each figure, the tolerance on the quantity is half the span of the horizontal axis. Similar results are obtained for modules made by the UK-B cluster[1]

Parameter	Design Value	Tolerance
Dowel hole, mhx [µm]	-6500	30
Dowel hole, mhy [µm]	-37500	30
Dowel slot, msx [µm]	38500	100
Dowel slot, msy [µm]	-37500	30
Mid-point of front pair, midxf [µm]	0	10
Mid-point of front pair, midyf [µm]	0	5
Separation of front pair, sepf [µm]	64090	10
Separation of back pair, sepb [µm]	64090	10
Sensor1 angle, a1 [mrad]	0	0.13
Sensor2 angle, a2 [mrad]	0	0.13
Sensor3 angle, a3 [mrad]	0	0.13
Sensor4 angle, a4 [mrad]	0	0.13
Half stereo angle, half-stereo [mrad]	-20	0.13

Table 1: Module in-plane geometry parameters

For all the parameters, the main parts of the distributions are well within the tolerances. However, occasionally, there is a measurement at the limit of the tolerance. Also, there are slight offsets in the centres of the distributions of the sensor angles. From these measurements we conclude:

(1) The present assembly jigs and assembly processes conform to the requirements

(2) Although the jigs are engineered to the limit, some fine tuning may still be possible

(3) Good control can be maintained during series production through the measurement and monitoring of these distributions, feeding the results back into the module assembly process.

[1] http://www.slac.stanford.edu/~stevemc/metrology.pdf

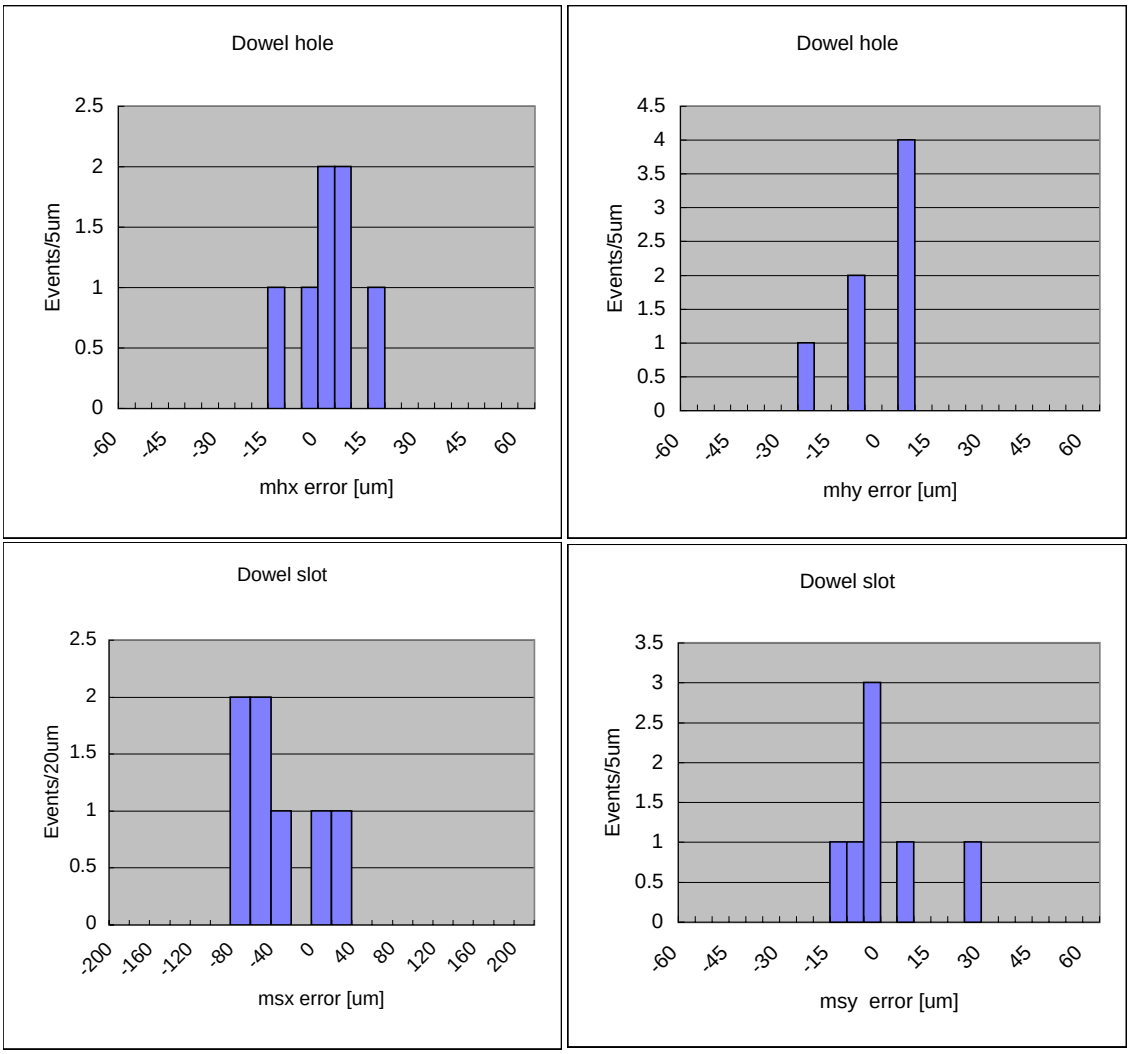

Figure 2 In-plane survey: deviations from the nominal of mhx and mhy of the dowel hole and msx and msy of the slot in the BeO facing

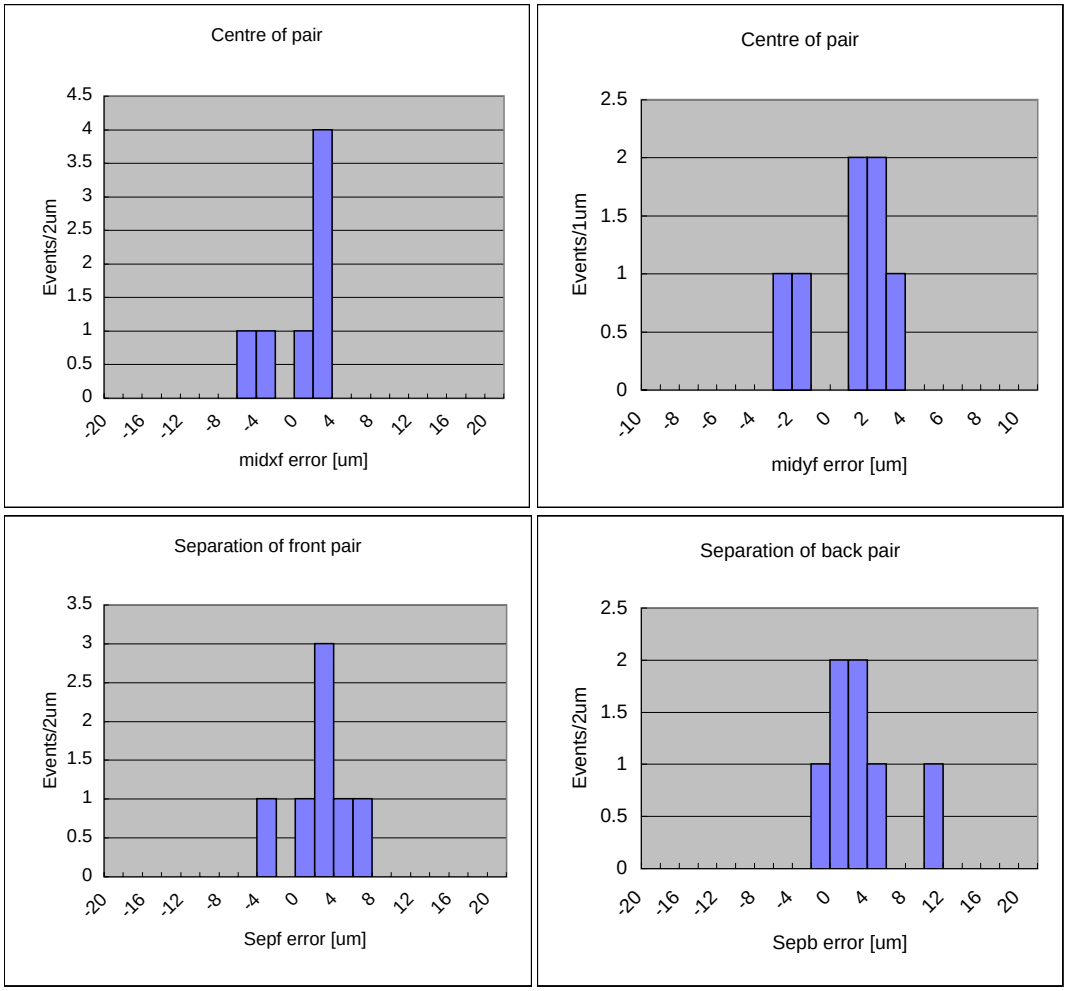

Figure 3 In-plane survey: deviations from the nominal of the centre of the front pair of sensors, midxf and midyf, and the separation of the front pair, sepf, and the back pair, sepb

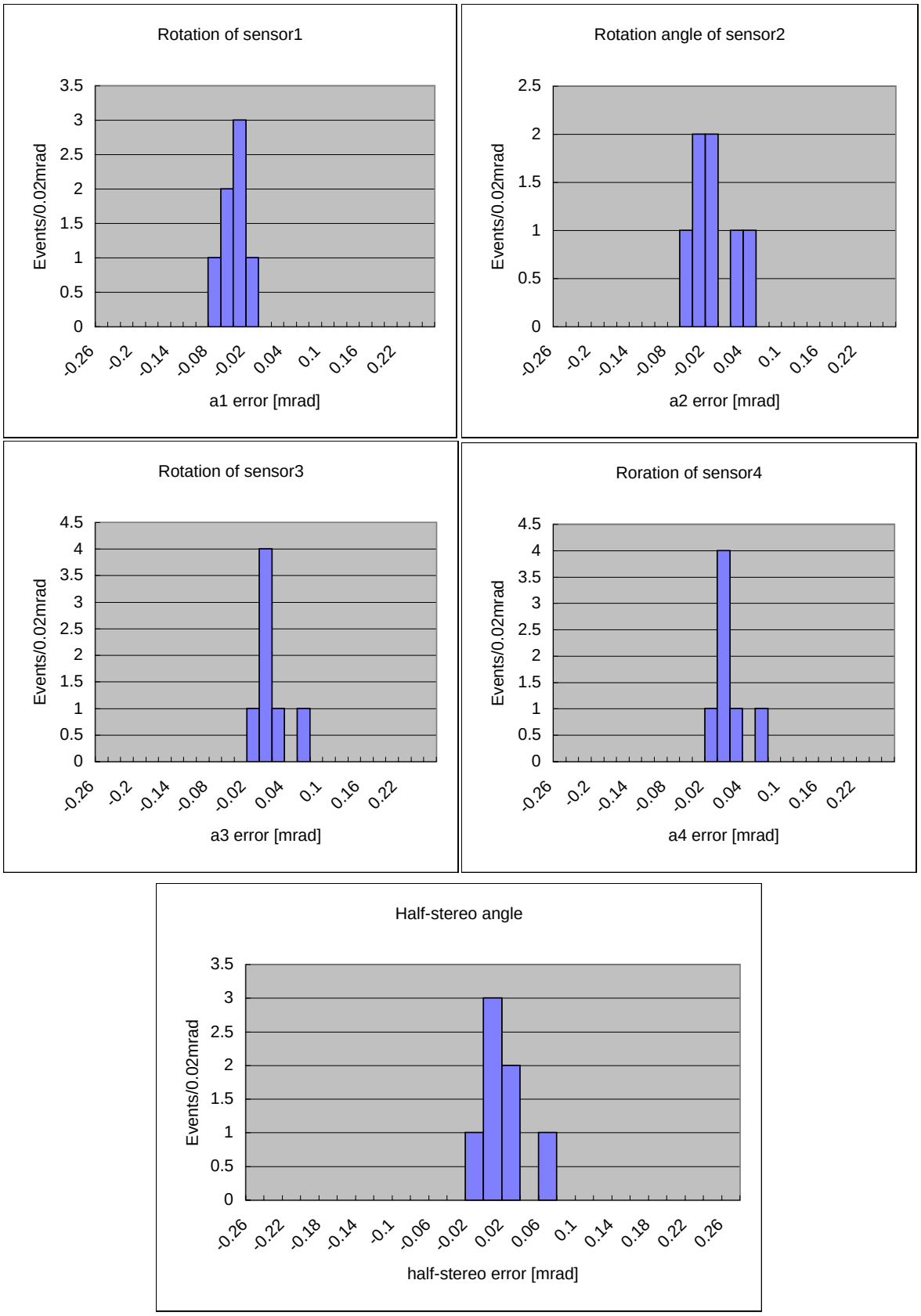

Figure 4 In-plane survey: deviations from the nominal of the rotations of the sensors, a1, a2, a3, and a4, and the half-stereo angle

2.3 Out-of-Plane Survey

Two tolerance limits are placed on the out-of-plane deviations, as described in SCT-BM-FDR-7. One is the maximum deviation of the z-height of the sensor surface from the nominal, which should be <200 μm. The other is that the maximum z-flatness residual, after the 'minimal use' of the z data, should be < 50 μm.

2.3.1 Maximum z Deviations

Results are presented on the z-profiles of 8 modules constructed by the Japanese cluster and measured at KEK using a 3D metrology machine. The z coordinates at three locations Z1, Z2 and Z3 on the BeO facings, as defined in Figure 1 of SCT-BM-FDR-7, are used to define a plane. The nominal half-thickness of the BeO facing – VHCPG baseboard assembly, 0.46 mm, is added to this measured plane, to define the *module plane*. The nominal top and bottom sensor surfaces are at +0.575mm and -0.575 mm from the module plane, respectively, since the nominal module thickness is 1.15mm in the sensor area. The deviations of the z-heights of the top and bottom sensor surfaces from the nominal are measured. The distribution of the maximum z deviation from the nominal for both sides of each module is shown in the left-hand plot of Figure 5.

It is seen that all the modules satisfy the tolerance of 200 μm for the maximum deviation of the z-height of the sensor surface from the nominal. The majority of data are within ±80 μm. Two module surfaces are outside this range; one module giving +83 μm for its top surface and a different module giving -176 μm for its bottom surface.

2.3.2 Minimal z Errors

In order to systematise the deviations in z seen above, the 'minimal use' of z data has been applied, as described in Appendix 1 of SCT-BM-FDR-7. After fitting the mid-planes of the modules, separately for the left and right sides, the 'minimal z' profiles from the fitted mid-plane are measured. These are averaged over the sample of 8 modules to obtain the *mean profile*. The 'minimal z'-profiles are shown for a typical module in Figure 6, together with its 'minimal z errors', that is, the deviations from the mean profile.

The top-left plot of Figure 6 shows the z-coordinates of the surface of the four sensors along the strip direction for different lateral positions. The bottom-left plot shows the z-coordinates, perpendicular to the strips, for different longitudinal positions. It is seen that the top and bottom sensors are symmetric and curling inwards towards the ends of the module where the sensors are free from the baseboard. This is caused by the intrinsic bow of the sensors.

The minimal z errors are shown in the right-hand plots of Figure 6. The top-right plot shows the z deviation from the mean profile along the strip direction for different lateral positions, for all four sensors. The bottom right plot shows the z deviation from the mean profile perpendicular to the strip direction for different longitudinal positions, for all four sensors.

The distribution for all modules of the maximum of the 'minimal z errors' of four sensors is shown in Figure 5, in the top-right plot, and the rms of the 'minimal z error' is shown in the bottom-right plot. It is seen that the maximum deviation of any sensor from the mean profile is below 30 μm, and the rms of this deviation is less than 10 μm. Thus all these modules satisfy the specification of a deviation of <50 μm from the mean profile.

The out-of-plane specifications can therefore be met with the present assembly jigs, assembly processes and module components.

Figure 5: Out-of-plane survey: the left-hand plot shows the maximum measured z deviations of sensors from the nominal top and bottom module surfaces. The right-hand plots show the results after the 'minimum use' of z data; top right the resulting maximum z errors of the 4 sensors, and bottom right the rms of the z errors of the 4 sensors.

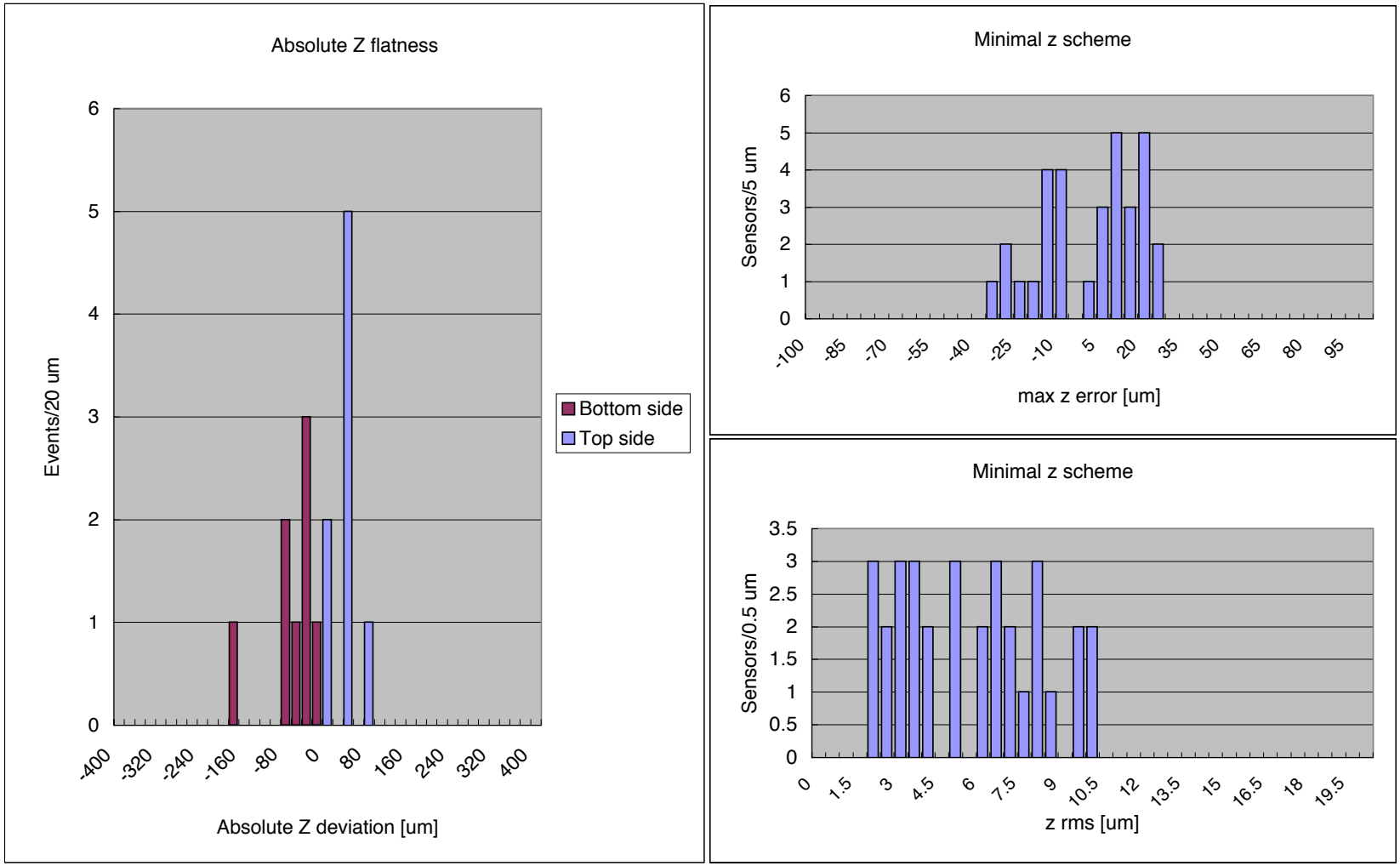

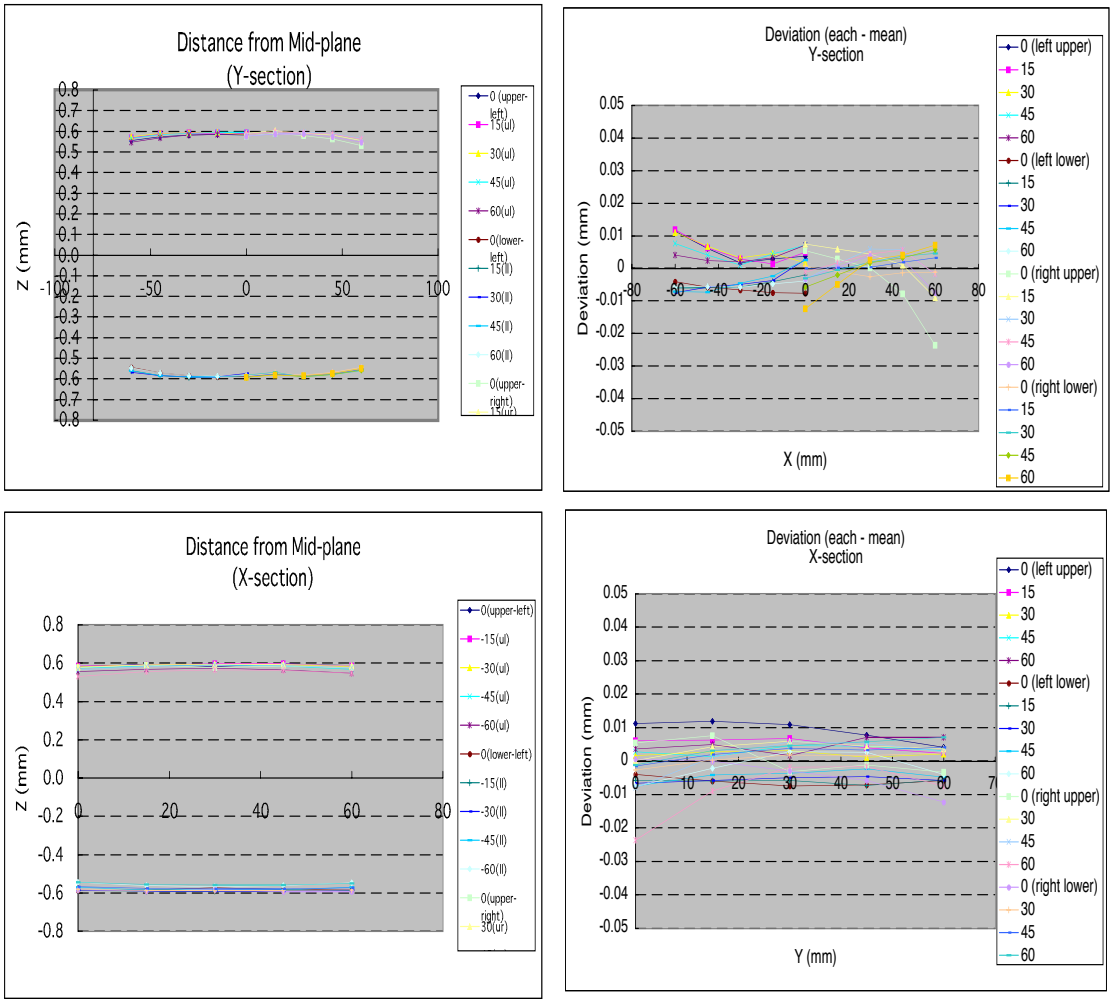

Figure 6: Out-of-plane measurements for module 20220170100035. The top-left plot shows the z-coordinates of the surface of the four sensors along the strip direction for different lateral positions. The bottom-left plot shows the z-coordinates, perpendicular to the strips, for different longitudinal positions. The top-right plot shows the z deviation from the mean profile along the strip direction for different lateral positions, for all four sensors. The bottom right plot shows the z deviation from the mean profile perpendicular to the strip direction for different longitudinal positions, for all four sensors.

2.3.3 Thermal Cycling and Long-term Tests

A number of modules have been subjected to thermal cycling and long-term readout tests. The thermal cycle sequence was from room temperature to –30 ^{o}C and +60 ^{o}C, repeated 5 times. In the long-term tests, the module was operated, with hybrid power on, for 24 hrs with the hybrid temperature at around 30 ^{o}C. The same in-plane and out-of-plane metrology was repeated after the thermal cycles and the long-term test.

The in-plane surveys show that there is essentially no change in the in-plane parameters. The changes in the out-of-plane measurements before and after thermal cycling and long-term testing are shown in Figure 7. The left plot shows the change in the maximum z deviations before and after the thermal cycles, and the right plot before and after the long-term tests.

Figure 7: Out-of-plane survey: change in the maximum z deviation before and after thermal cycling (-30 ^{o}C to +60 ^{o}C, 5 times) (left). And change following the thermal cycling after the long-term test (24 hours operation, hybrid power on) (right).

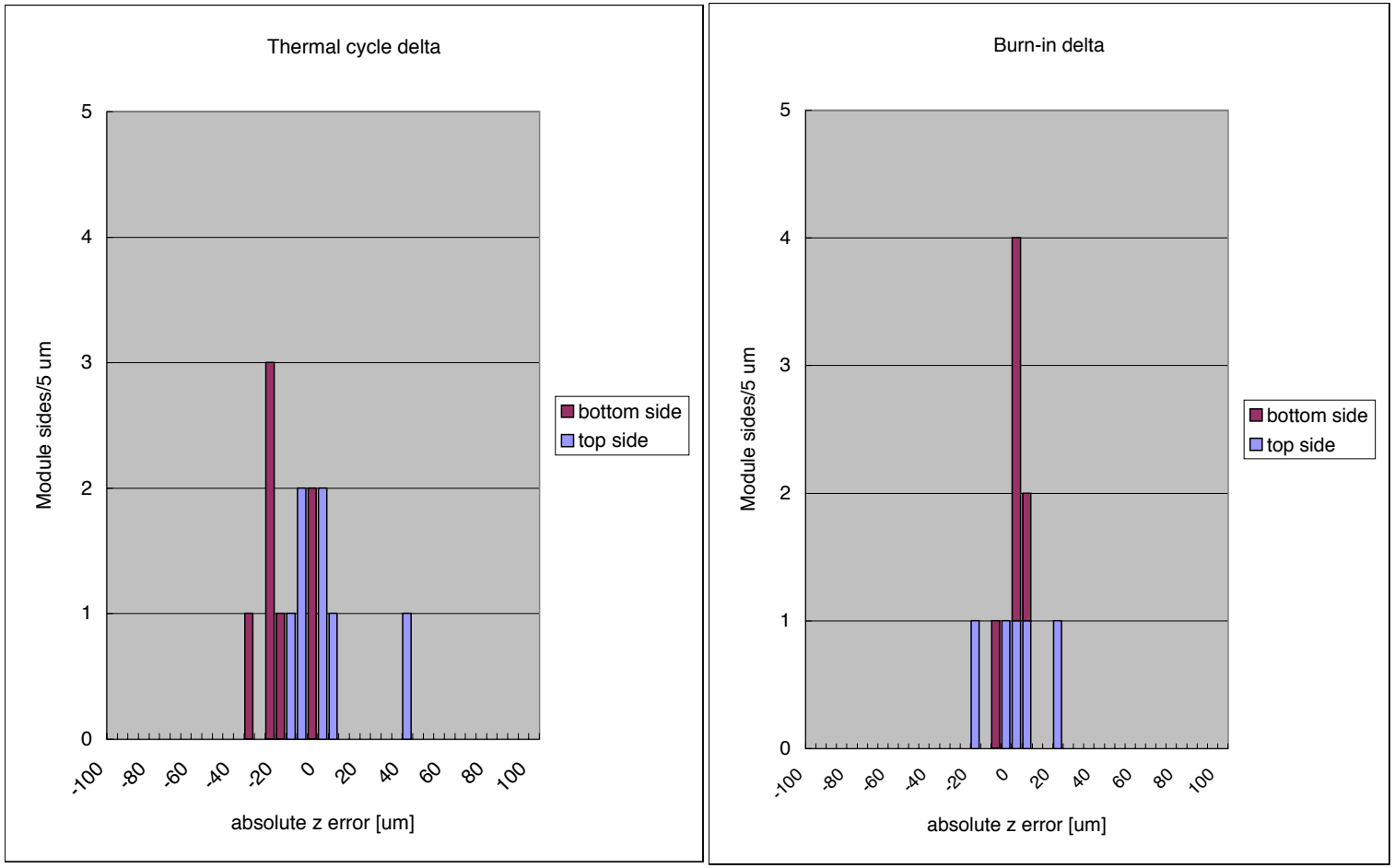

Since the long-term test is a steady-state operation, no change is anticipated. The distribution shows that the majority of the data are within 10 μm, with a few points extending out to 20 μm. These data are comparable with the measurement errors of the metrology machine, although the larger values could be caused by a real deformation.

Thermal cycling is more dynamic and some deformation is anticipated. As seen from the plot, the majority of results are within 20 μm, and comparing these data with the long-term test distribution, there could be a deformation of order 10 μm or less. One module, however, showed a larger deviation of 41 μm. This was the module that showed the second largest deviation before thermal cycling. The maximum z deviation of this module was changed from 83 μm before to 123 μm after the thermal cycles.

Although there is some deformation associated with thermal cycling, all modules still have a maximum z deviation of <200 μm. Also, all modules satisfy the tolerance of <50 μm for the minimal z errors.

3 BARREL MODULE THERMAL RESULTS

3.1 Thermo Profile Measurements made with a Thermo Viewer

The temperature profile has been measured for a sample of unirradiated modules by using a thermo viewer. Although a thermo viewer measurement is desirable because of its remote sensing nature, it involves the following practical difficulties:

(1) estimating or determining the reflectivity of the surface, which depends on the surface and the material

(2) shielding infra-red light from the external environment

(3) the infra-red transparency of silicon

The transparency of silicon to infra-red wave-lengths precludes the measurement of the temperature of the silicon sensors. Thus the measurement is only useful for estimating the temperature of the hybrids and the BeO facings. Thermo viewing is not a technique that will be used for every module during production, but can be a useful diagnostic tool.

A typical example of the measured temperature profile of the hybrid and of the facing is shown in Figure 8, with an ASIC power of 5.3 W. In the figure, the temperatures are given with respect to the top of the BeO cooling facing. With respect to this, the highest temperature on the hybrid was 11 – 12 ^{o}C at the location of the ASICs. The temperature at the hybrid thermistor was about 6^{o}C. The thermal FEA simulation is consistent with these measurements. This is illustrated in Figure 9, which shows a thermal simulation of the hybrid plus ASICs with the same ASIC power of 5.3W. The highest temperature of the hybrid with respect to the BeO cooling facing is about 12^{o}C, as in the data.

Figure 8 The thermo profile of the hybrid of a module measured with a thermo viewer. The temperatures are normalised to the temperature of the top of the BeO cooling facing.

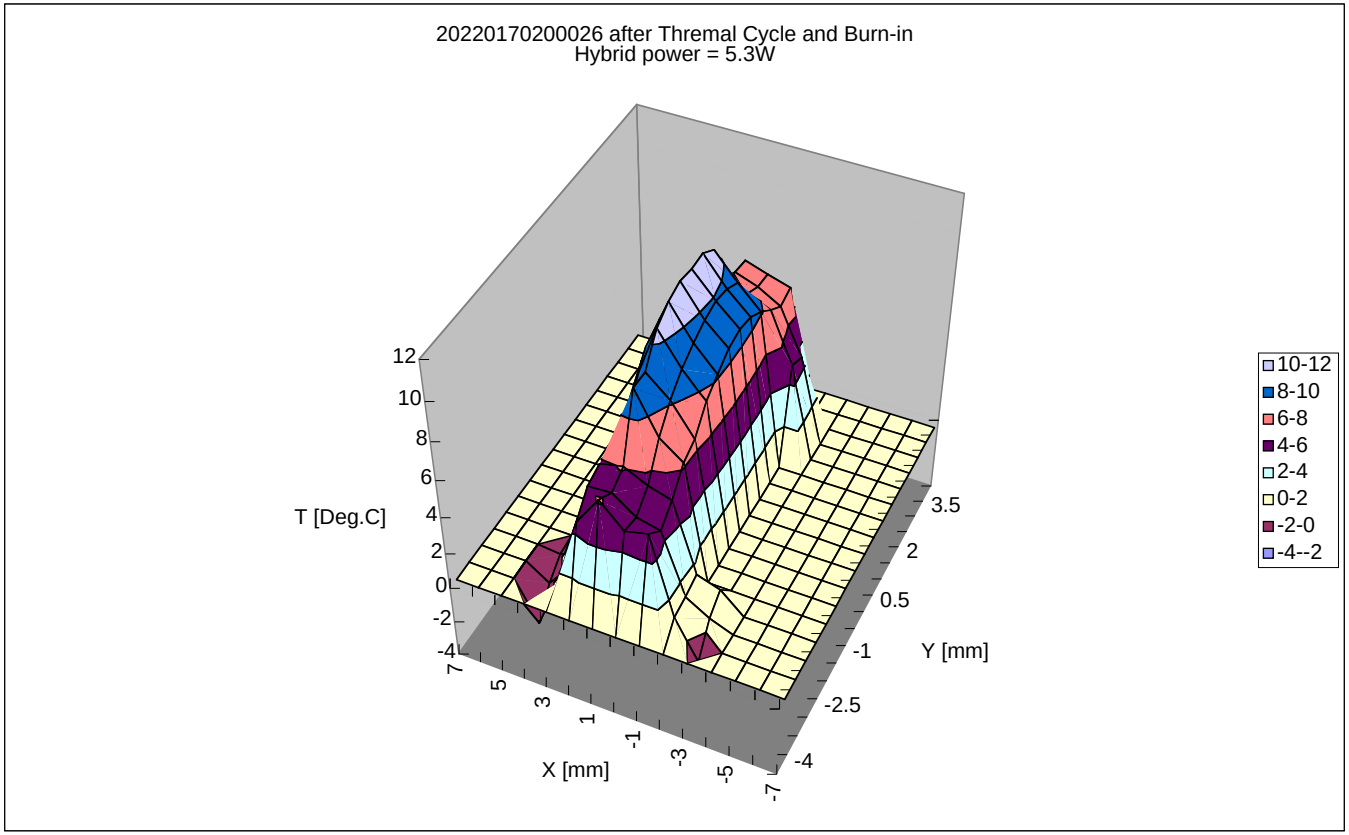

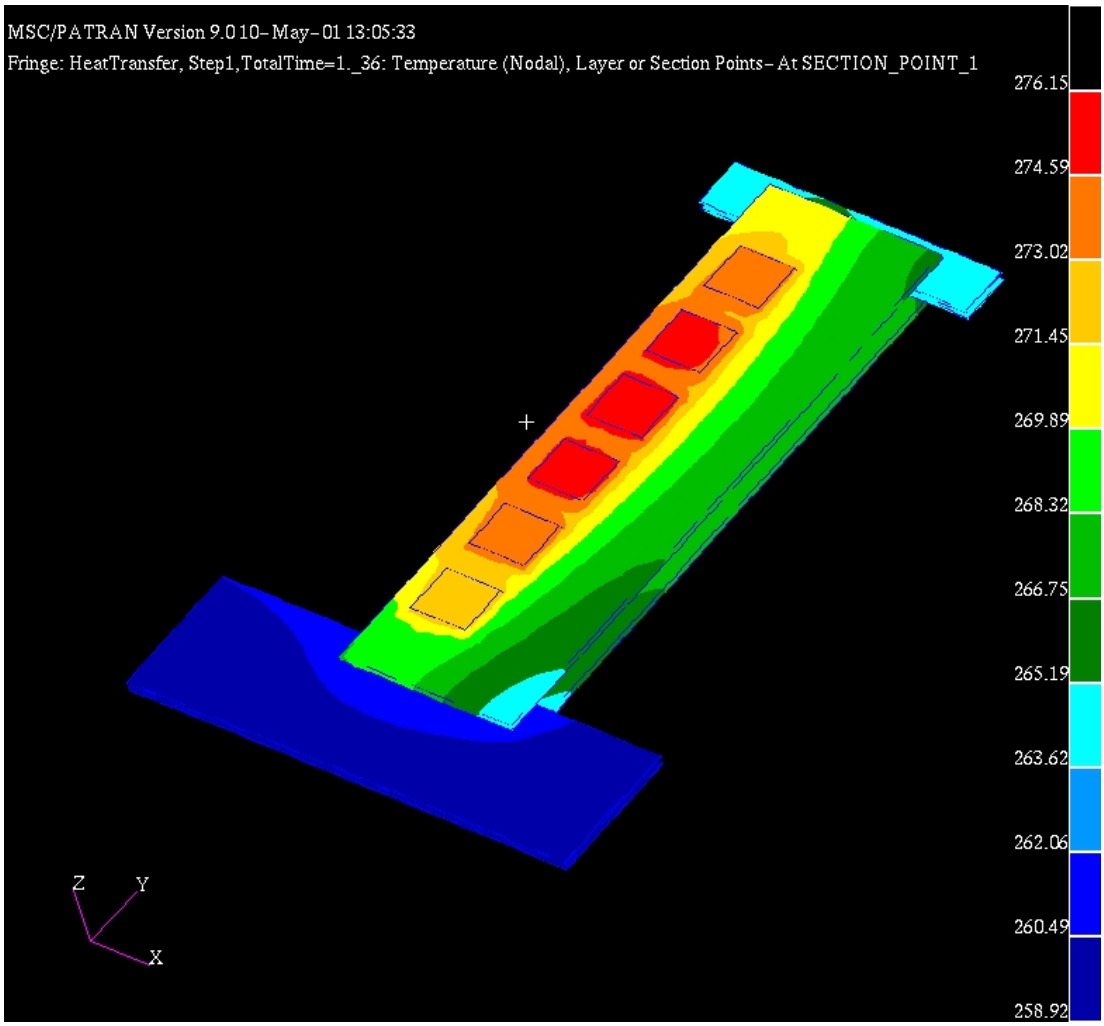

Figure 9: FEA simulation of a hybrid and ASICs, with an ASIC power of 5.3W.

3.2 Thermal Module Results

3.2.1 Thermally Induced Distortions.

Studies have been carried out on the elastic and non-elastic thermally induced distortions on barrel SCT mechanical modules. A total of four modules were built, using non-electrically working but thermally realistic components. Each module was measured under a non-contact 3D metrology system with a measurement accuracy of better than 1μm in the 'xy' plane and around 4μm in the 'z' plane. The 'z' measurements are made by an automated depth of focus algorithm running at high (x800) magnification. Each module was then heated and cooled over a temperature range of +39˚C to –17˚C. At five specific temperatures (-17˚C, -6˚C, +7˚C, +21˚C and +39˚C) the module was allowed to reach equilibrium and the profile measurements were repeated.

Each module was then thermally cycled ten times between -30˚C and +100˚C in a nitrogen atmosphere and the profile re-measured. No variations in the 'xy' measurements were observed. The 'z' variations were only measurable at the unsupported corners of the detectors. The average

movement seen over all temperature variations for the 4 modules, prior to thermal cycling, was 1.29µm/˚C. After thermal cycling, the average value was found to be 1.33µm/˚C, that is, essentially unchanged.

An allowance for elastic deformation will be applied to room temperature survey data to predict the final module shape at the operating temperature.

3.2.2 Thermal performance.

A module has been built using irradiated p-in-n silicon detectors. The detectors were assembled to a pre-series BeO/VHCPG baseboard and the thermal module was completed by the addition of a pre-series copper/kapton hybrid, complete with carbon-carbon bridge supports. The detectors were biased in the normal way and the front-end chips were simulated using 2.2Ω silicon chip heaters. The module was equipped with a number of Pt100 thermal sensors, as illustrated in Figure 10, that provided temperature readout of the two hybrid bridges, three of the detector corners, the upper cooled facing, the cooling block and the ambient gas temperature. The cooling was provided by a mixture of water and antifreeze flowing in a copper pipe, and the cooling interface was a copper block of approximately correct dimensions brazed to the pipe. The block was connected via thermal grease (DC 340) to a 3 mm thick piece of aluminium frame and this in turn was connected to the beryllia facing of the module through another layer of DC 340. The pipe and cooling block were sprung so that the connection of the aluminium to copper was by spring pressure. The connection of the facing to the aluminium was by screws. The layout is thus representative of the principles to be used in the final SCT.

A summary of the results to-date are given in Tables 2 and 3.

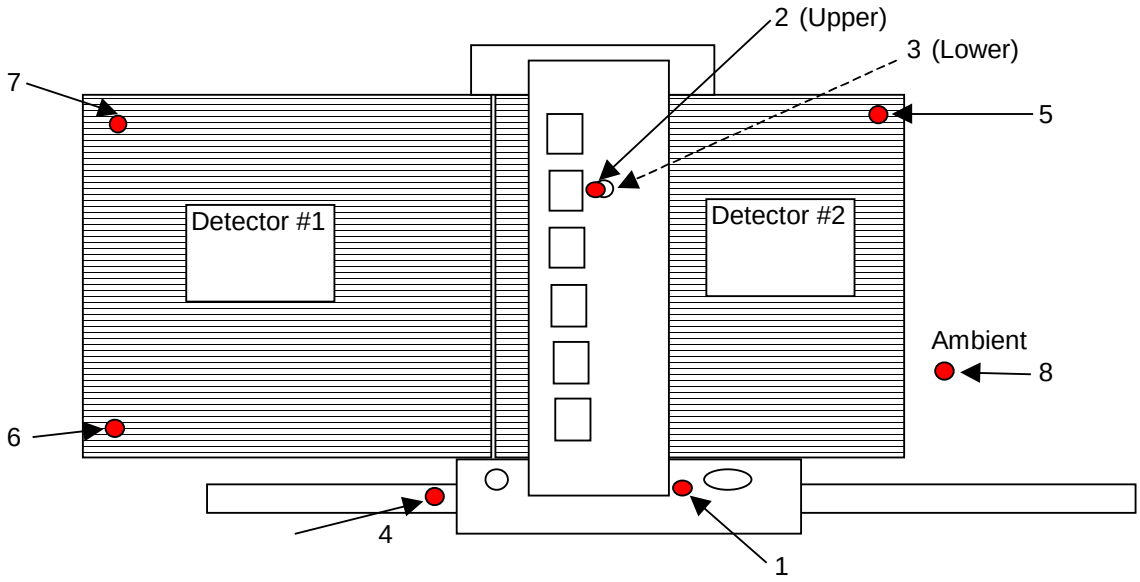

Figure 10: Layout of the thermal module, showing the positions of the temperature sensors, labelled 1 to 8.

Hybrid power (W)	Detector power (W)	Coolant ^{o}C	Ambient ^{o}C .	Cooled facing ^{o}C	Hottest hybrid ^{o}C	Hottest detector ^{o}C
0	0	-6.82	-6.03	-4.03	-3.90	-4.31
6.36	0	-7.52	-5.16	0.96	12.53	1.95
6.35	0.52	-7.51	-4.64	1.70	13.56	3.09
6.35	1.01	-8.02	-4.47	2.04	14.04	3.36
6.35	0.28	-6.84	-4.19	1.85	13.63	3.14
8.11	0.00	-8.52	-4.19	2.73	17.52	4.11
8.11	0.35	-7.33	-4.01	3.13	18.11	4.76
8.11	0.65	-7.54	-3.70	3.49	18.67	5.43
8.11	1.30	-6.95	-3.52	4.08	19.58	6.37
8.11	1.24	-10.13	-7.48	-0.42	15.14	2.32
8.12	1.64	-10.93	-8.73	-1.45	14.08	1.40
8.12	3.03	-11.25	-6.43	-0.24	15.61	3.18
8.30	3.32	-10.34	-4.99	1.65	18.09	5.51

Table 2: Thermal module temperatures as a function of hybrid and detector power

Hybrid power	Detector power	δT coolant – facing	δT facing - hybrid	δT facing - detector	δT ambient - coolant
0.00	0.00	2.79	0.13	-0.28	0.79
6.36	0.00	8.48	11.58	0.99	2.36
6.35	0.52	9.20	11.86	1.40	2.87
6.35	1.01	10.06	12.00	1.33	3.55
6.35	0.28	8.69	11.77	1.29	2.65
8.11	0.00	11.25	14.79	1.39	4.33
8.11	0.35	10.46	14.98	1.63	3.32
8.11	0.65	11.03	15.18	1.94	3.83
8.11	1.30	11.03	15.50	2.29	3.44
8.11	1.24	9.71	15.56	2.74	2.65
8.12	1.64	9.48	15.53	2.86	2.20
8.12	3.03	11.00	15.86	3.42	4.81
8.30	3.32	11.98	16.44	3.86	5.35

Table 3: Differential temperatures as measured on a thermal module

The module has been designed using FEA that has been verified up to thermal runaway through previous thermal module prototypes. The present experimental results show stable running at a coolant temperature of around –10.5 ^{0}C with a detector power dissipation of about 130 μW/mm^2 normalised to 0 ^{o}C. The FEA predicts thermal runaway at around 135 μW/mm^2 at such a coolant temperature. Thus the results confirm the designed thermal operation of the module, that is, its

stable operation and large safety factor against thermal runaway with the envisaged coolant temperatures of ATLAS.

4. SUMMARY

The metrology data show that the module design, components and assembly methods are appropriate to the SCT specifications. Thermal data support the FEA calculations used to optimise the module design, and hence the thermally robust nature of the barrel module.

SCT Barrel Module FDR Document

SCT Barrel Module : Electrical Performance

Abstract

This document summarises the measured electrical readout performance of barrel modules in the laboratory, in beam tests at CERN and KEK and in the SCT system test at CERN.

Prepared by :	*Checked by :*	*Approved by :*
J.Carter, L.Eklund, G.Moorhead, M.Morrissey, J.Pater, P.Phillips, Y.Unno, M.Vos		

Distribution List

Table of Contents

1 SCOPE OF THE DOCUMENT

This document summarises results on the electrical performance of barrel modules read out with the ABCD2T, ABCD3T and the current ABCD3T-A versions of the SCT binary ASICs. It includes

- Noise occupancy versus binary threshold and extracted noise for modules read out individually in the laboratory, both before and after irradiation to a fluence of $3x10^{14}$ pcm^{-2} 24 GeV/c protons.
- Tracking efficiency, charge collection and resolution measurements for both non-irradiated and irradiated modules as measured in test beams at CERN and at KEK.
- First results from an assembly of 10 modules mounted together on a barrel sector in the SCT system test at CERN.

2 PERFORMANCE GOALS

The anticipated performance of SCT barrel modules as recorded in the Inner Detector TDR in 1997 was:

- Signal:noise of about 14:1 pre-irradiation, reducing to about 11.5:1 after 10 years of operation in ATLAS (Figure 11-36, page 435)
- Noise occupancy < $5x10^{-4}$
- Tracking efficiency > 99%

Much has changed in the intervening 4 years, including the detector type (p-in-n rather than n-in-n) and specification, and the evolution of the ABCD ASIC. Nevertheless, the noise occupancy and tracking efficiency specifications remain as the electrical performance goals of the barrel modules.

3 AVAILABLE ELECTRICAL MODULES

The number of electrical barrel modules so far constructed by the SCT has been limited by the supply of ASICs. For this reason data are included from modules constructed with previous versions of the ASIC (SCT-BM-FDR-5.4) - the ABCD2T and ABCD3T, as well as the current ABCD3T-A. The modules from which results have been obtained are listed in Table 1.

Module ID	ASIC type	Detector type	Irradiated	Data		
				Lab	Test beam	System Test
K3103	ABCD2T	HP <111>	No	√	√ (KEK)	√
K3104	ABCD2T	HP <111>	No	√		√
K3111	ABCD2T	HP <111>	No	√		
K3112	ABCD2T	HP <100>	No	√	√ (CERN)	√
K3113	ABCD2T	HP <100>	Detectors	√	√ (CERN)	
RLT5	ABCD2T	HP <111> 325μm thick	No	√	√ (CERN)	
RLT4	ABCD2T	HP <111> 325μm thick	Yes	√	√ (CERN)	
RLT9	ABCD2T	HP <111>	Detectors	√	√ (CERN)	
RLT10	ABCD2T	HP <100>	Detectors	√	√ (CERN)	
RLK6	ABCD2T	HP <111>	No	√	√ (CERN)	
Scand1	ABCD2T	Sintef <100>	No	√	√ (CERN)	√
20220170100004	ABCD3T	HP <111>	No	√		√
20220170100011	ABCD3T	HP <100>	No	√	√ (KEK)	√
20220170100022	ABCD3T (thinned and metallised)	HP <100>	No	√	√ (KEK)	√
20220170100003	ABCD3T	HP <100>	Yes	√	√ (KEK)	
20220170100026	ABCD3T	HP <100>	No	√		√
20220170100001	ABCD3T	HP <111>	Yes	√		
20220170100008	ABCD3T (attached with non-conducting glue)	HP <111>	No	√		√
20220170100009	ABCD3T	HP <111>	No	√		√
20220170100020	ABCD3T-A	HP <100>	Yes	√		
20220170100037	ABCD3T-A	HP <100>	Yes	√		
20220170100016	ABCD3T-A	HP <111>	No	√		
20220170100018	ABCD3T-A	HP <111>	No	√		
20220170100019	ABCD3T-A	HP <111>	No	√		
20220170100035	ABCD3T-A	HP <100>	No	√		
20220170100036	ABCD3T-A	HP <100>	No	√		

Table 1: SCT Barrel Electrical Modules Constructed and Tested as at 2nd May 2001

4 RESULTS FROM INDIVIDUAL MODULES

The ASICs are powered with the prototype SCT low voltage power supply, SCTLV2, and readout electrically via an SCT CLOAC-MuSTARD-SLOG system[1].

4.1 Noise and Noise Occupancy at 1fC Threshold for Unirradiated Modules

The noise and noise occupancy are quoted for the modules with ABCD3T and ABCD3T-A ASICs. Non-linearity of the ABCD2T calibrates gives rise to some uncertainty in determining absolute noise values for these modules.

The noise of the ASIC decreases as the temperature is reduced The standard laboratory measurements are made with the hybrid temperature at about 27°C. At this temperature, the measured noise for the ABCD3T modules is in the region of 1400-1700 ENC. This is illustrated in Figure 1, which shows the average noise values for each of the 12 readout ASICs on nine of the ABCD3T(-A) modules.

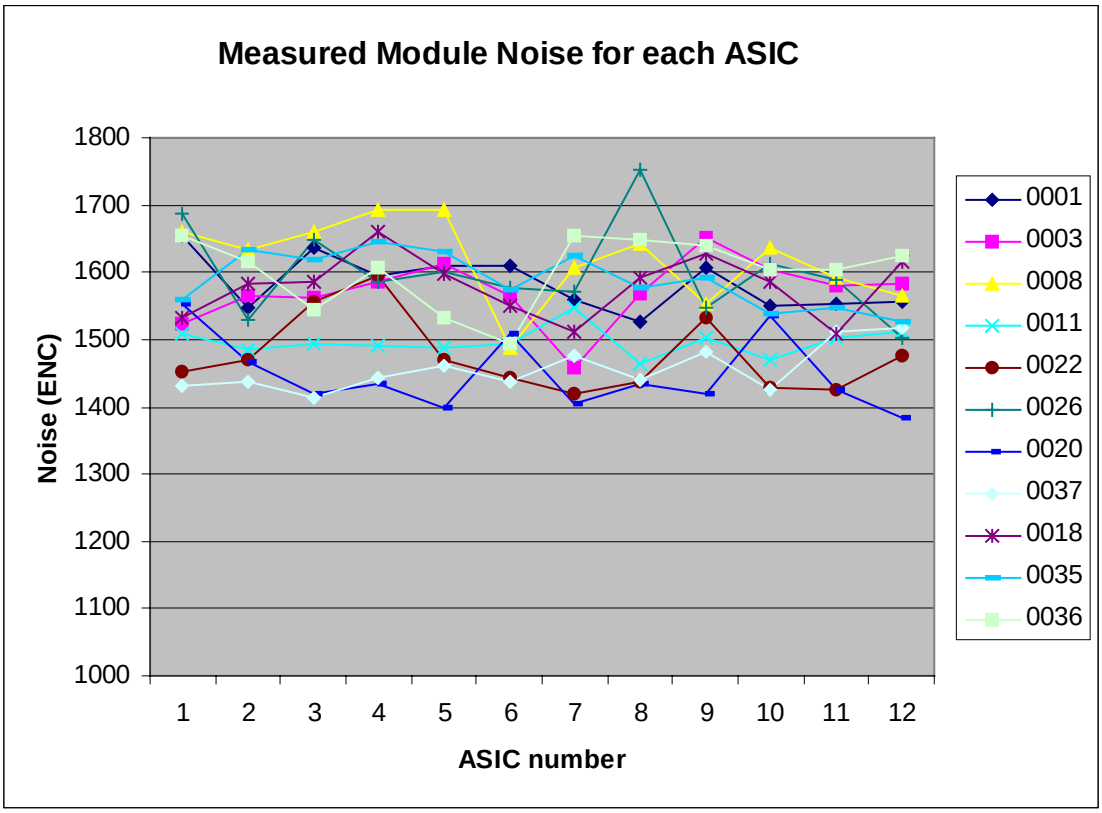

Figure 1: Measured noise (ENC) on each of the 12 ASICs of nine of the modules made with ABCD3T or ABCD3T-A ASICs. The temperature of the hybrid was about 27°C. Each curve is labelled with the four least significant digits of the corresponding module number.

[1] http://sct.home.cern.ch/sct/sctdaq.html

At the SCT operating temperature of ~0°C on the hybrid, the noise is reduced to typically about 1350 ENC for the ABCD3T modules for cold operation. This corresponds to an expected signal:noise value of better than 14:1, thus satisfying the pre-irradiation performance goal of section 2. Signal:noise values for modules as measured in a test beam are consistent with this expectation, and presented in section 5.

The noise of each individual readout channels of an ABCD3T-A module, operated warm, is shown in Figure 2. A uniform noise distribution is seen, apart from a single channel on the module that is bonded to only a 6 cm length of detector.

The SCT design goal is to set the ASIC single-strip binary readout threshold at 1fC, to ensure high tracking efficiency for particles traversing the silicon at inclined angles, depositing charge on more than one readout strip. The noise occupancy of the individual unirradiated modules at this threshold, even when operated warm, is ~10^{-5} (that is, << 10^{-4}), which is satisfactory for the SCT (section 2). This is illustrated in Figure 3.

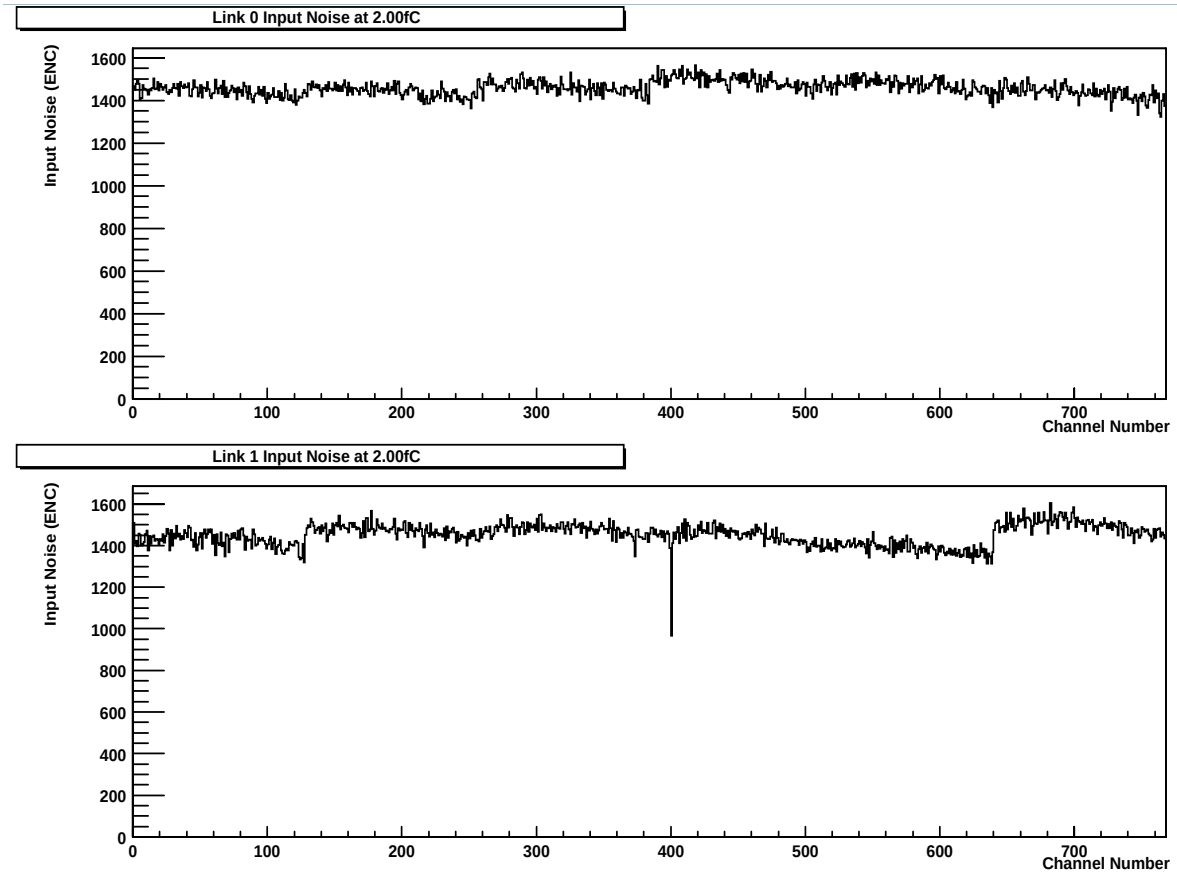

Figure 2: Measured noise values (ENC) on all channels of ABCD3T-A module 20220170100018

4.2 Uniformity of Threshold

Good channel to channel uniformity of the nominal 1fC threshold is essential for operation of a binary readout system. This is ensured through the ASIC threshold correction circuit, where each channel is provided with a trim DAC of 4 bit resolution with four selectable ranges (see SCT-BM-

FDR-5.4). The first range (0 mV – 60 mV) is used pre-irradiation, which gives a maximum channel to channel variation of 4mV (or ~ 0.08 fC). This is to be compared with the noise value of ~ 0.25 fC. The effect of this channel to channel threshold spread is to give a contribution to the noise occupancy at 1fC equivalent to less than a 1% increase in the intrinsic channel noise.

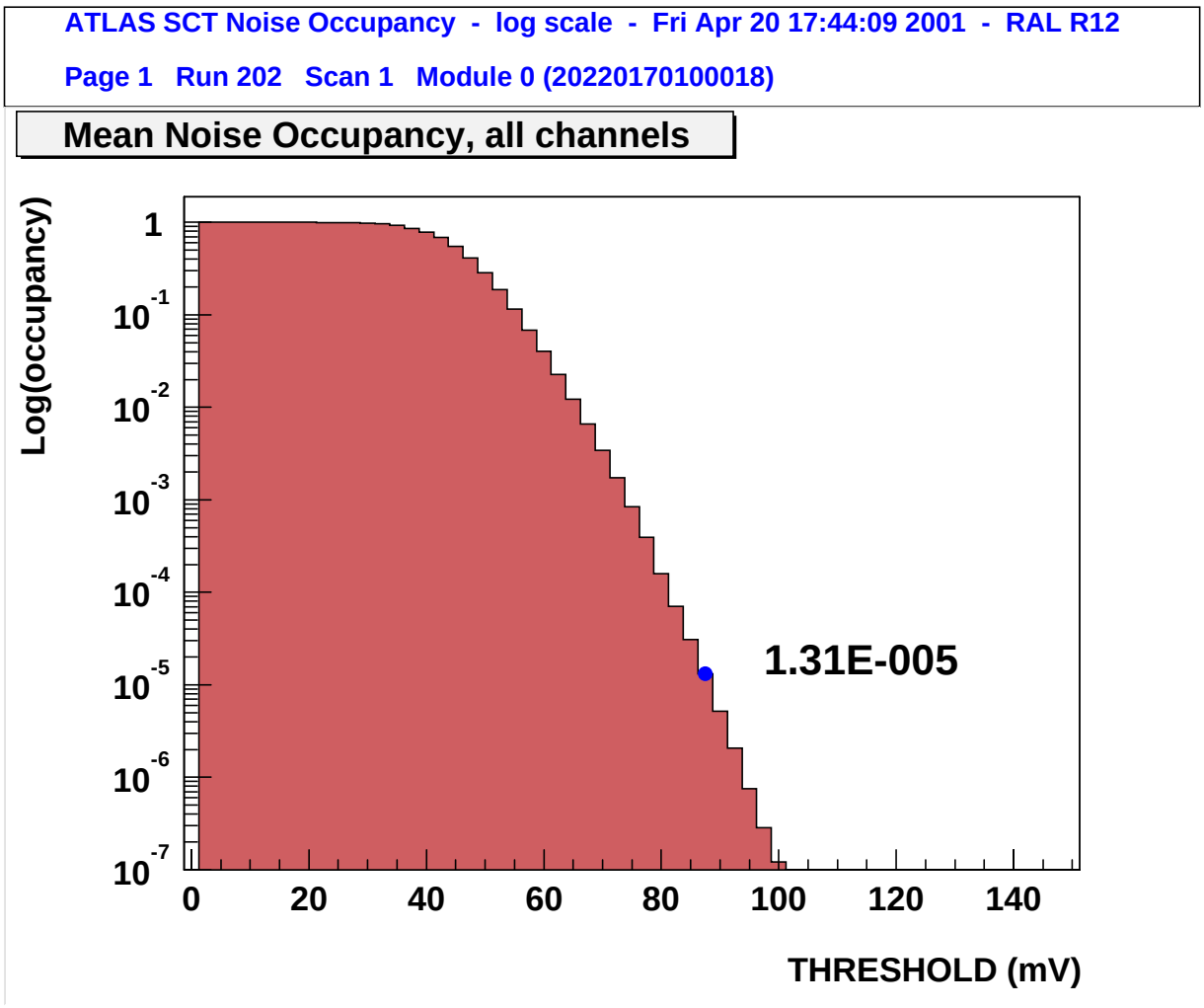

Figure 3: Mean noise occupancy of all channels of ABCD3T-A module 20220170100018, measured warm. The noise occupancy at 1fC threshold is 1.31x10^{-5}.

4.3 Module Stability

Figure 4 shows example plots of occupancy versus threshold for all individual channels from the first readout side of the ABCD3T-A module 20220170100018. We take the smoothness and regularity of these curves as a very sensitive test of the intrinsic stability of a module. The data of Figure 4 show good regularity. In general, with the ABCD3T(-A) ASICs and 220nF V_{cc} and V_{dd} decoupling capacitors on the hybrid (see SCT-BM-FDR-5.3), some small irregularities are seen in these 'S-curves' for typically up to four chips on a module, predominantly on the second readout side. This is illustrated in Figure 5, showing this second readout side for the module 20220170100018, where some irregularities appear for the last two ASICs. It should be noted that these effects occur below 0.5fC threshold, and create no apparent instability in the modules under normal operating conditions.

4.4 Timewalk

The ASIC requirement (see SCT-BM-FDR-5.3) is that the timewalk should be <16 ns. Here timewalk is defined as the maximum time variation in the crossing of the time stamp threshold over a signal range of 1.25 to 10 fC, with the comparator threshold set to 1fC. Figure 6 shows measured data for the ABCD3T-A module 20220170100018. The top row of curves shows time in strobe delay units versus injected charge (fC) for each ASIC and the bottom row the timewalk distribution in nsec of the channels of each of the readout chips of the first side. The specification is satisfied for all channels.

4.5 Noise and Noise Occupancy at 1fC Threshold for Irradiated Modules

Results are so far available for two ABCD3T modules that have been fully irradiated at the CERN PS to a fluence of $3x10^{14}$ pcm^{-2} 24 GeV/c protons (modules 20220170100001 and 3). For these, the measured ASIC noise value when operated cold, with the hybrid around $0^{o}C$, averages about 2050 ENC.

As will be illustrated through the test beam data of section 5, the charge collection efficiency of the irradiated silicon is close to 100% at bias voltages above about 400V. Thus the signal:noise value found for fully irradiated barrel modules is in the region of 10:1 at the SCT operating temperature. This is lower than the target (because of the higher noise). However, noise occupancy at 1fC threshold as measured in the test beam is about $3x10^{-4}$. It is thus anticipated that the 1fC threshold can be maintained post-irradiation, to provide maximum tracking efficiency after 10 years of ATLAS operation.

After the maximum fluence, the ASICs may be operated with a very safe margin using the coarsest trim DAC range, trim range 3. After irradiation this range is decreased (typically 0 mV – 190 mV) giving maximum channel to channel variation at the 12mV bin level. This gives a contrbution to the noise occupancy equivalent to a ~ 4% increase in noise.

In the ABCD3T, all trim DAC ranges could not be selected reliably after irradiation. This was corrected in the ABCD3T-A version of the chip (see SCT-BM-FDR-5.4). The ABCD3T-A modules 20220170100020 and 20220170100037 have been irradiated in the PS in April 2001, and both have fully functional trim circuitry after exposure to the full dose of $3x10^{14}$ pcm^{-2} 24 GeV/c protons. Figure 7 illustrates the functionality of all the trim DAC ranges for the second readout side of module 20220170100020. All channels can infact be aligned using trim range 2. The corresponding trim DAC settings and the resultant trimmed thresholds are shown in Figure 8.

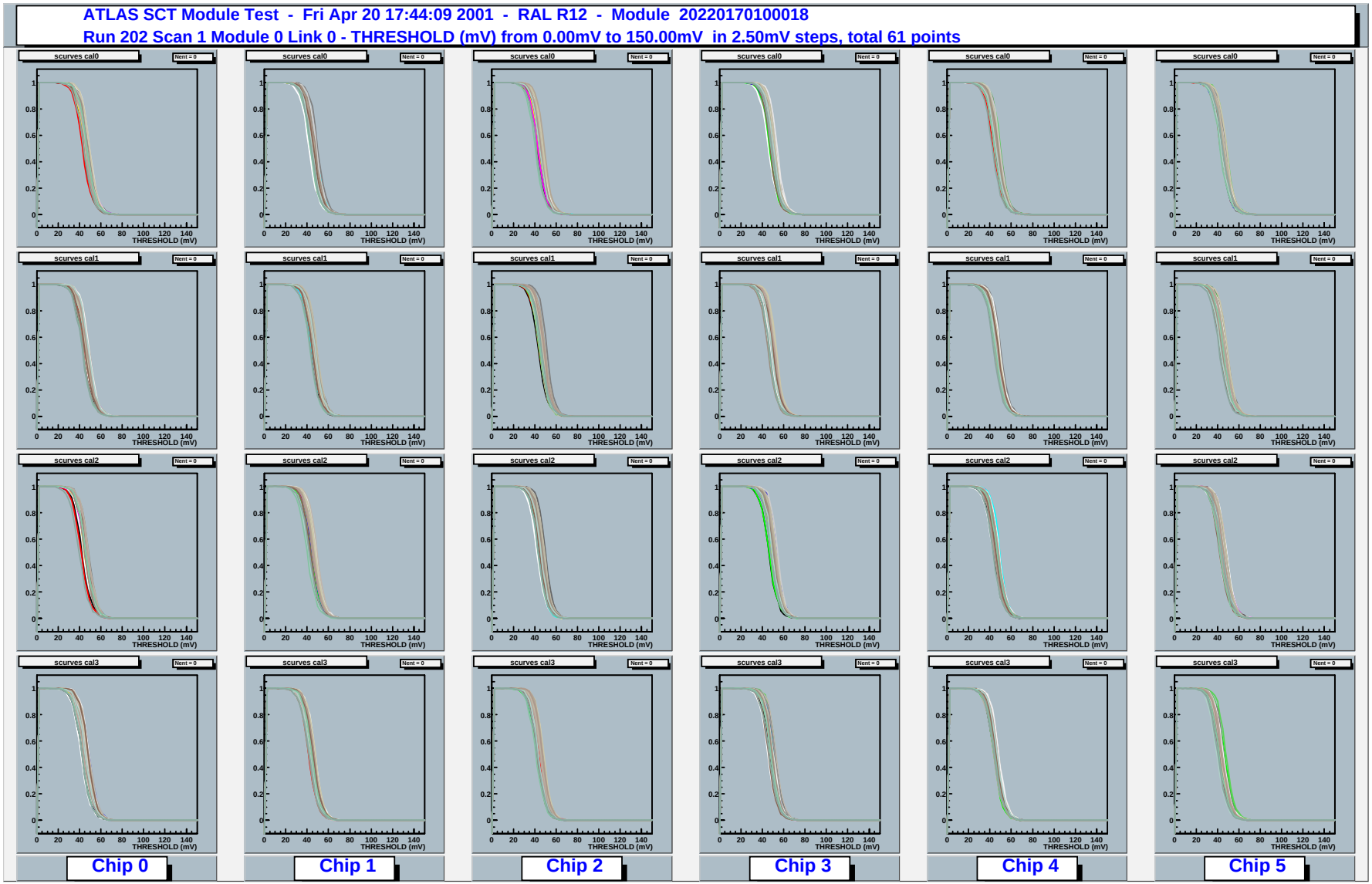

Figure 4: Curves of occupancy versus threshold superimposed for every readout channel of the first readout side of an ABCD3T-A module. Every fourth channel (32 in total) of each ASIC appears in each of the boxes.

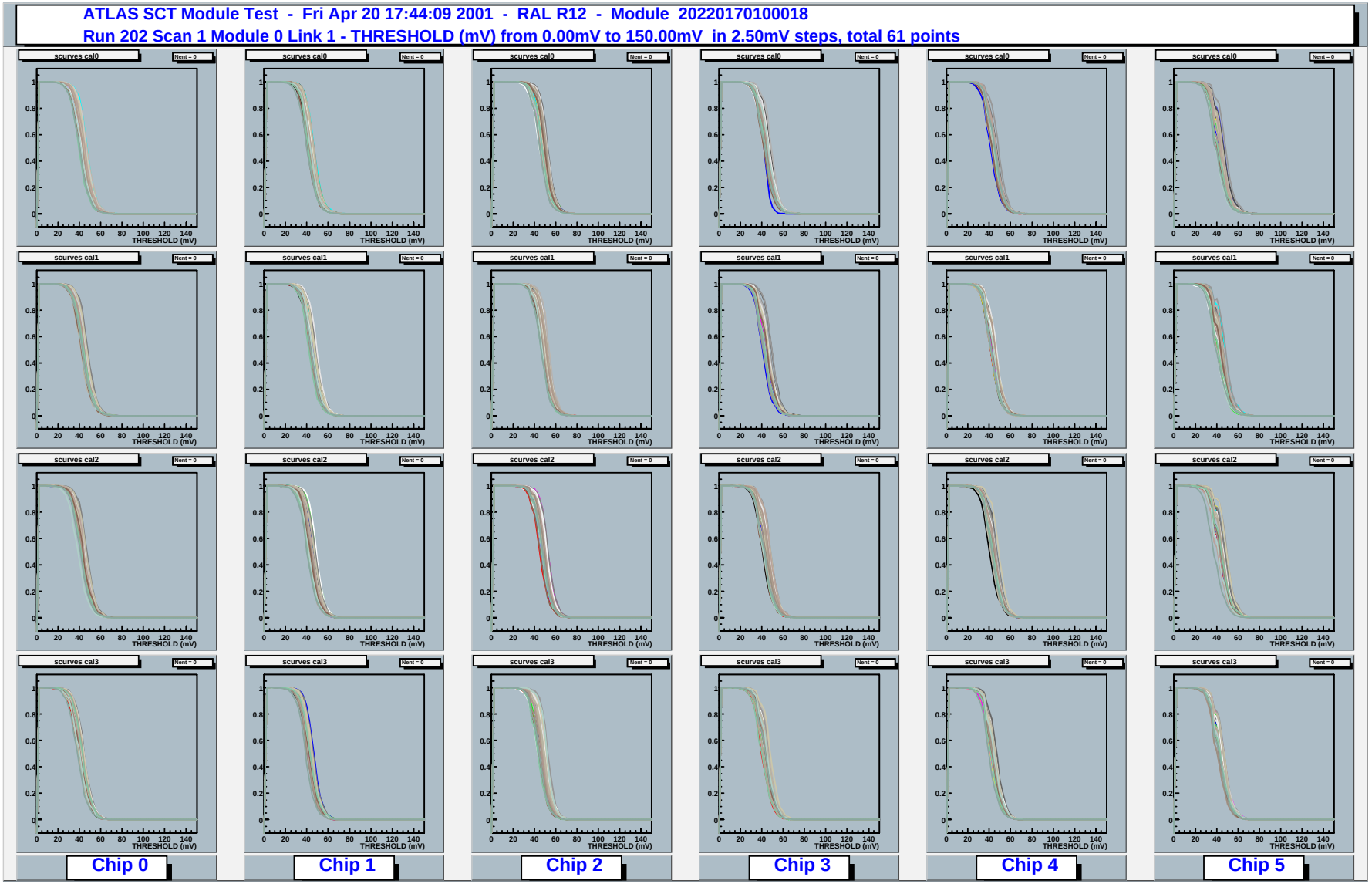

Figure 5: Curves of occupancy versus threshold superimposed for every readout channel of the second readout side of an ABCD3T-A module. Every fourth channel (32 in total) of each ASIC appears in each of the boxes.

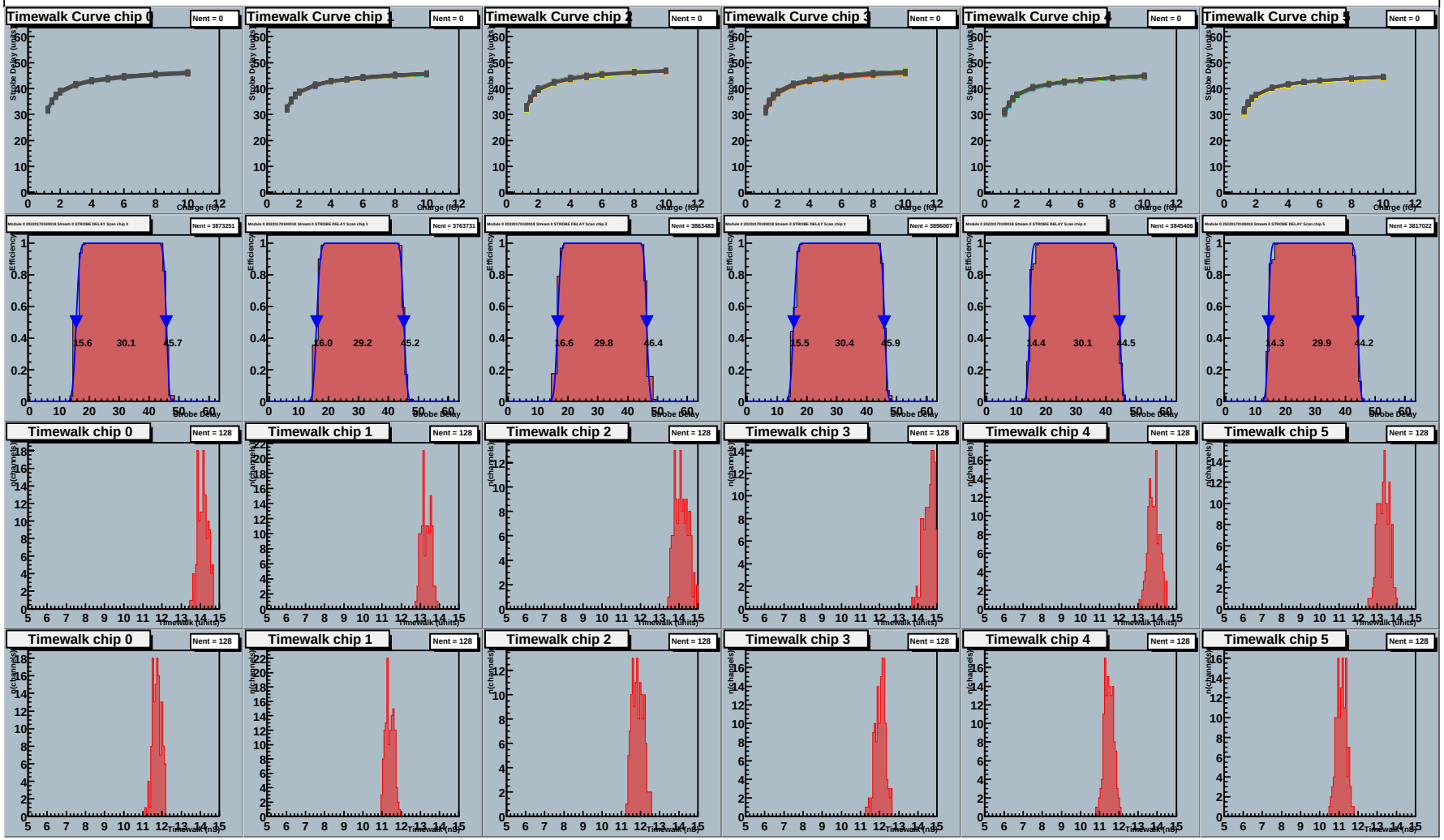

Figure 6: Timewalk curves for the first readout side of an ABCD3T-A module.

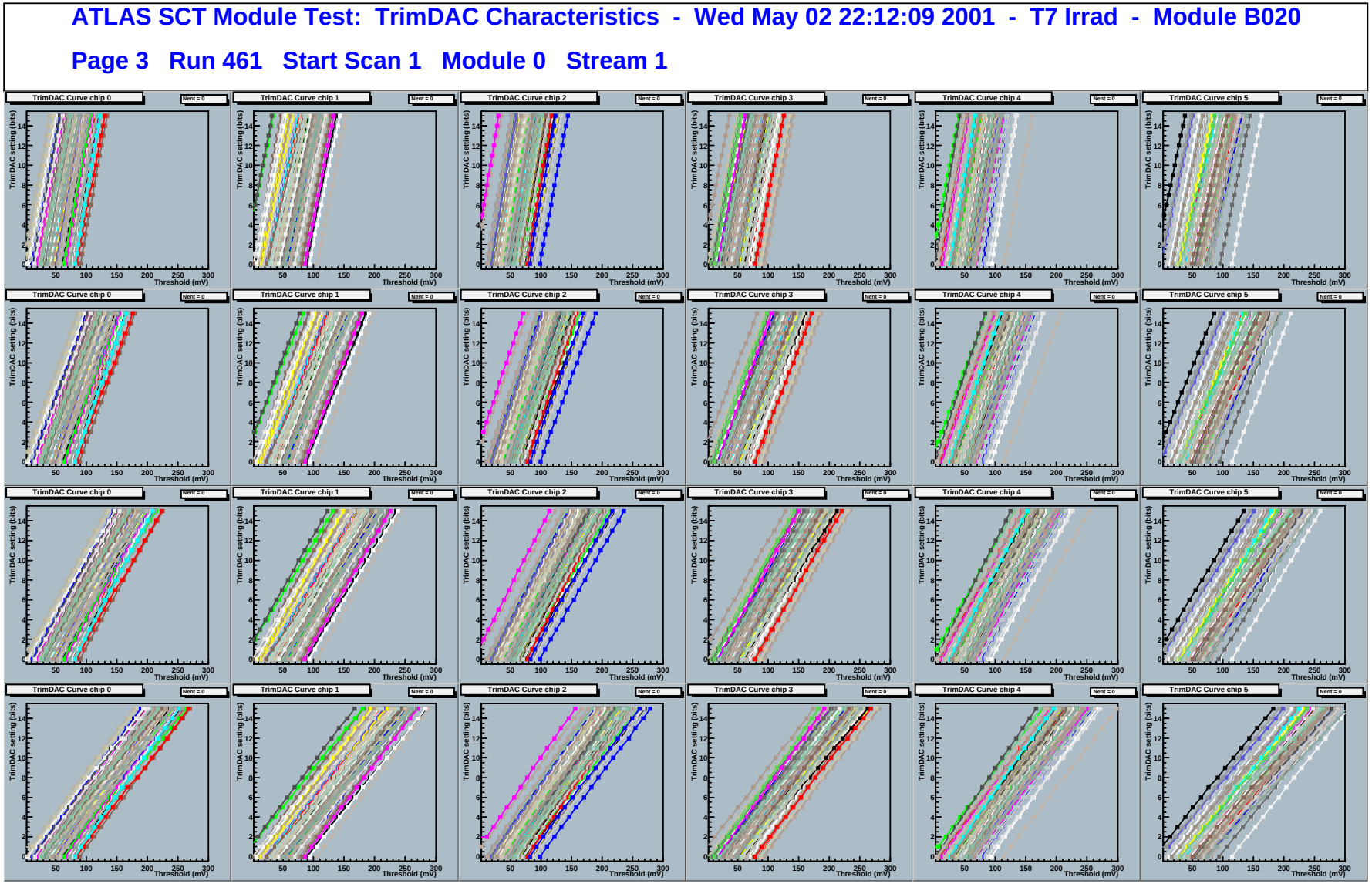

Figure 7: Trim DAC setting versus threshold for each of the 6 ASICs (horizontally) of the second readout side of module 20220170100020 after irradiation to $3x10^{14}$ pcm^{-2} for each of the 4 trim DAC ranges (vertically).

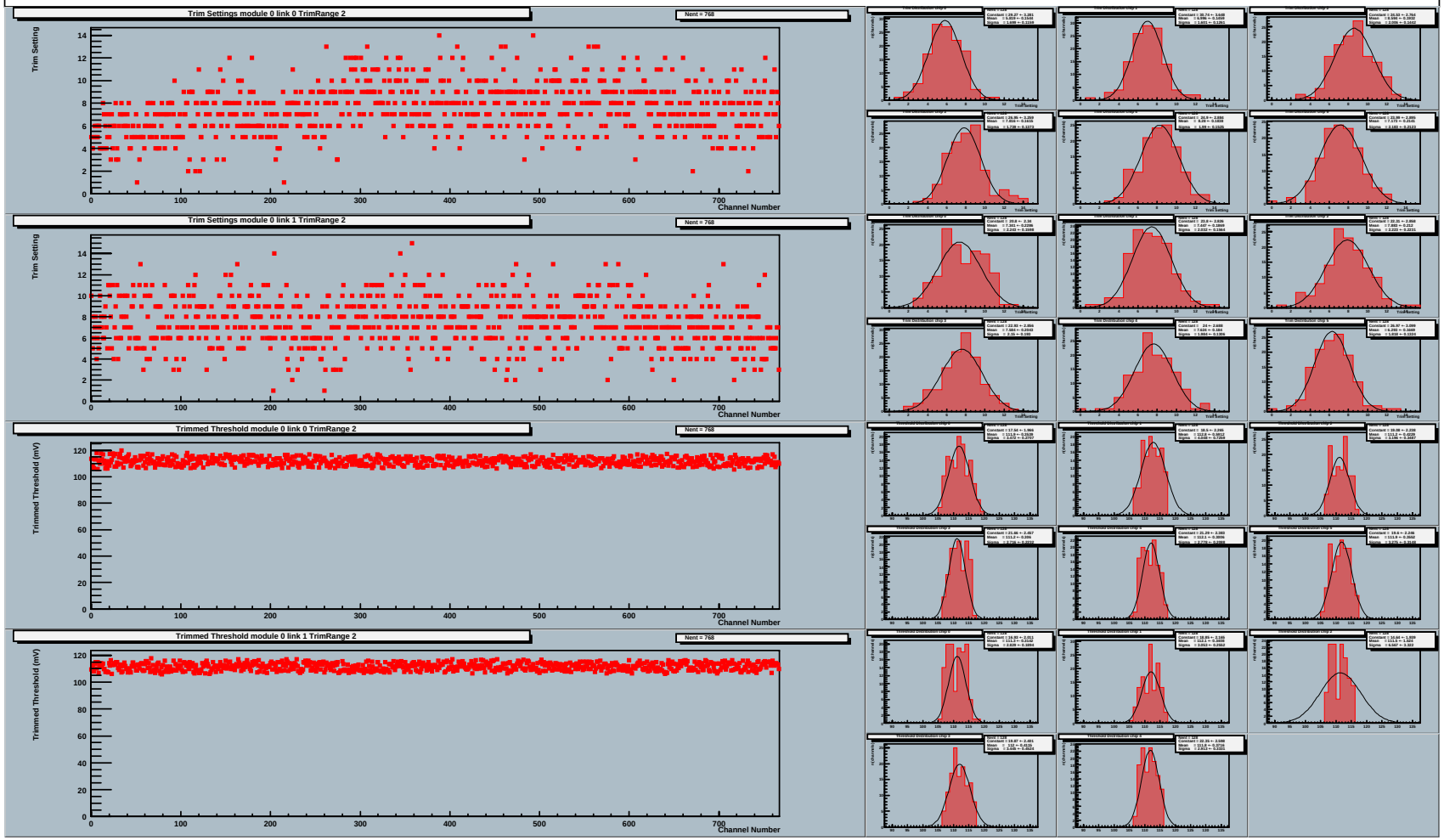

Figure 8: Trim DAC setting versus channel number (upper two rows) and trimmed threshold versus channel number (lower two rows) for module 20220170100020 after irradiation to $3x10^{14}$ pcm^{-2}. The right hand plots show the distribution of the variable for each ASIC on the second readout side of the module

5 MODULE TEST-BEAM RESULTS

The modules as indicated in Table 1 have been tested in the H8 beam at CERN in August 2000 and in the KEK test beam in December 2000. The CERN test beam has the advantage of high momentum particles, a 1.56T magnetic field and the possibility of rotating the angle of the face of the silicon with respect to the incident tracks over the ±20^{o} range relevant to barrel modules within ATLAS. However, only modules made with ABCD2T chips were available at the time of this test beam. The KEK test beam provides data from ABCD3T modules.

Both irradiated and non-irradiated modules have been measured in the beam tests. The modules are all kept cold, with the hybrids operating at about 0^{o}C. A beam telescope is used at both CERN and KEK to define the track positions at the module planes. SCT prototype power supplies are used, together with the MuSTARD readout system

Some principal results are briefly summarised in the following sections:

5.1 Charge Collection and Signal:Noise Ratio

The median charge of three modules, obtained from the 50% efficiency point in threshold scans, as a function of detector bias voltage from KEK data is shown in Figure 9.

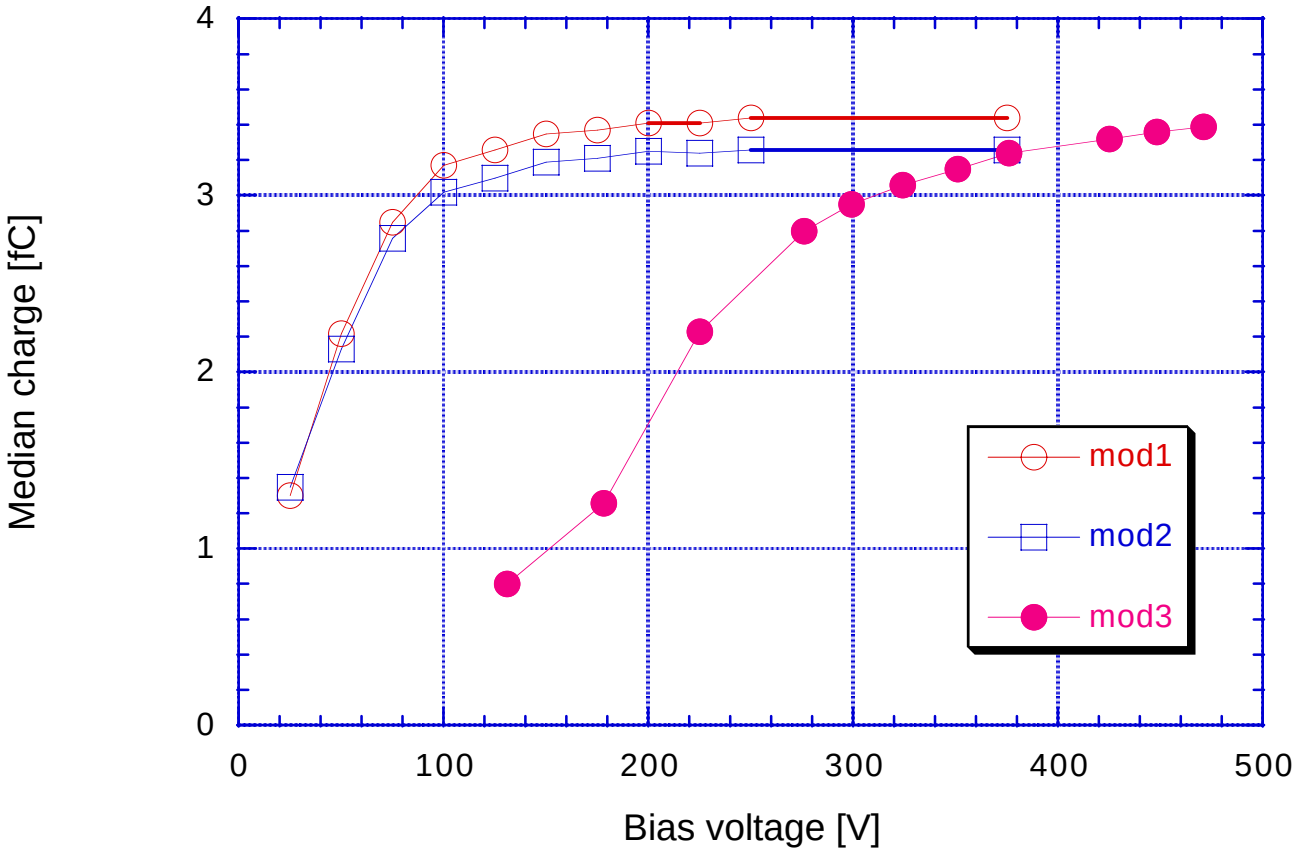

Figure 9: Median charge (fC) versus bias voltage for the ABCD3T modules 20220170100011, 22 and the irradiated module 20220170100003 (solid circles, mod3)).

The detectors of the two unirradiated modules have depletion voltages of ~80V, and are normally operated at ~150V bias. The irradiated module is operated at ~400V bias, at which point it is seen that the collected charge on a single strip is similar to that for unirradiated modules. This result has also been measured with our detectors readout by (unirradiated) analogue electronics in the laboratory during our detector QA procedures.

Any uncertainties in the performance of the calibration circuitry can be eliminated by looking at the signal:noise values of these modules as measured in the KEK test beam. This is shown, again as a function of bias voltage, in Figure 10. The signal:noise values discussed in section 4 above are to be seen.

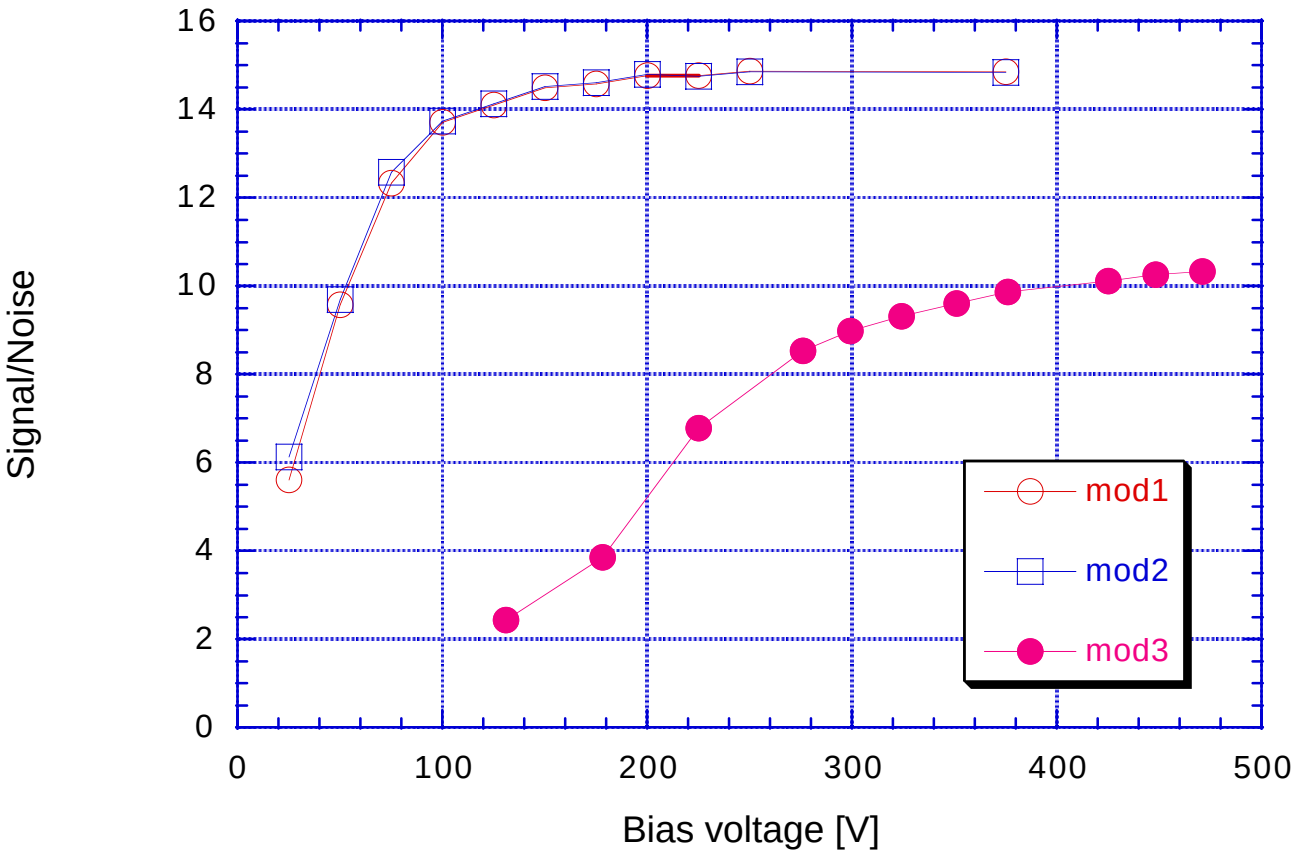

Figure 10: Signal:noise as a function of bias voltage for the same three modules as in Figure 9. Again, mod 3 is the irradiated module.

5.2 Efficiency at 1fC Threshold

The efficiency of the modules at the nominal operating threshold of the SCT is typically measured to be > 98% at the operational bias voltages over the full range of particle incident angles, with or without a magnetic field. This is illustrated by data from the CERN beam test. In Figure 11, the efficiency for an unirradiated module is shown as a function of angle, and in Figure 12 that of an irradiated module. (The maximum efficiency recorded is a function of tracking cuts, and plateau values in excess of 99% can be obtained).

These data give confidence that the modules will operate with high efficiency at 1fC threshold within the ATLAS environment.

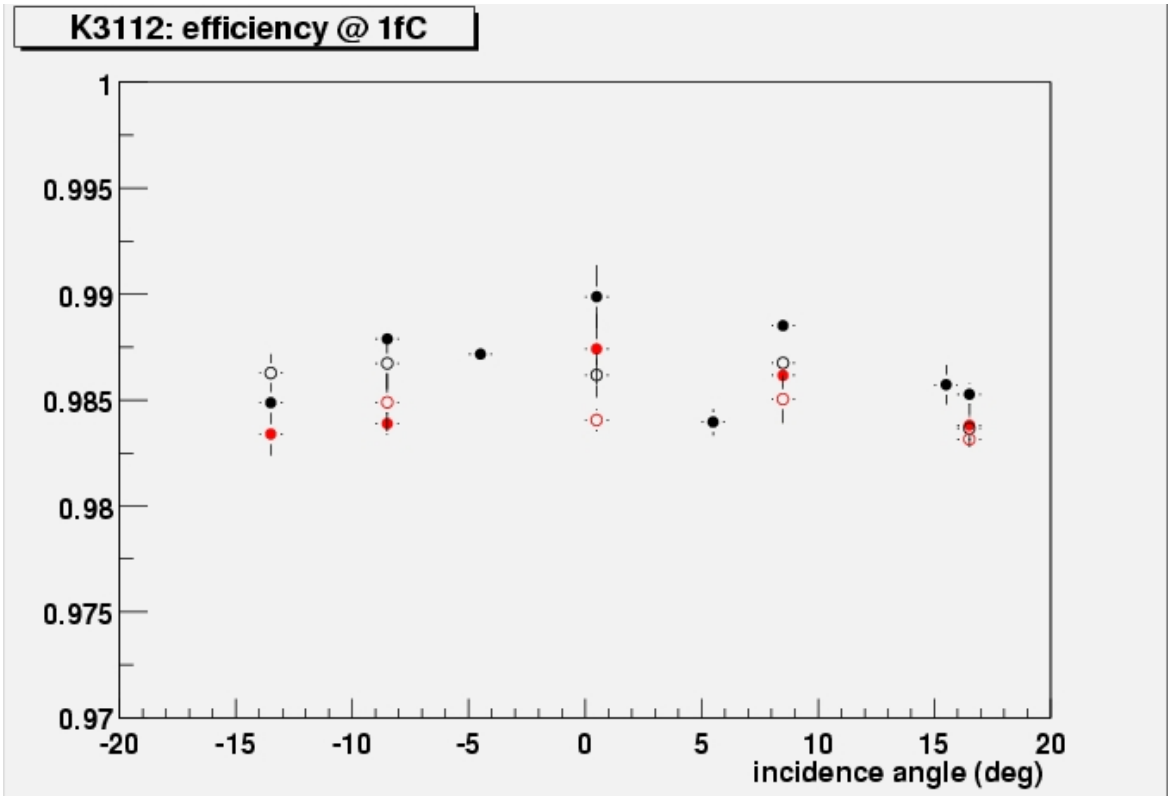

Figure 11: Measured efficiency of the unirradiated module K3112 at 1fC threshold as a function of the beam incident angle. The red symbols are with the magnetic filed of 1.56T, the black with zero field. The open circles are with a bias voltage of 120V, the full circles with 200V bias.

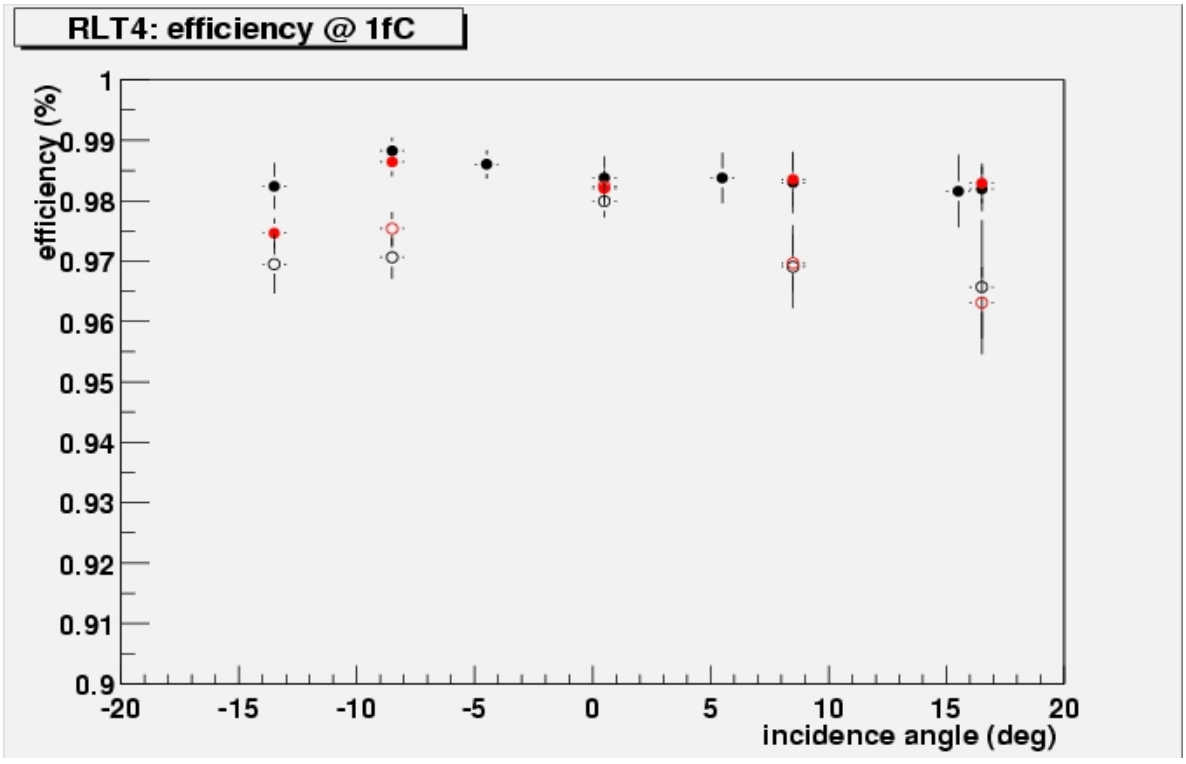

Figure 12: Measured efficiency of the fully irradiated module RLT4 at 1fC threshold as a function of the beam incident angle. The red symbols are with the magnetic filed of 1.56T, the black with zero field. The open circles are with a bias voltage of 300V, the full circles with 450V bias.

5.3 Resolution

The measured resolutions are consistent with the expectation of the 80μm binary strip pitch (ie 23μm). This is illustrated from the CERN beam test in Figure 13 for tracks at normal incidence, with the magnetic field on. The resolution for inclined tracks is slightly better because two strip clusters occur with greater frequency.

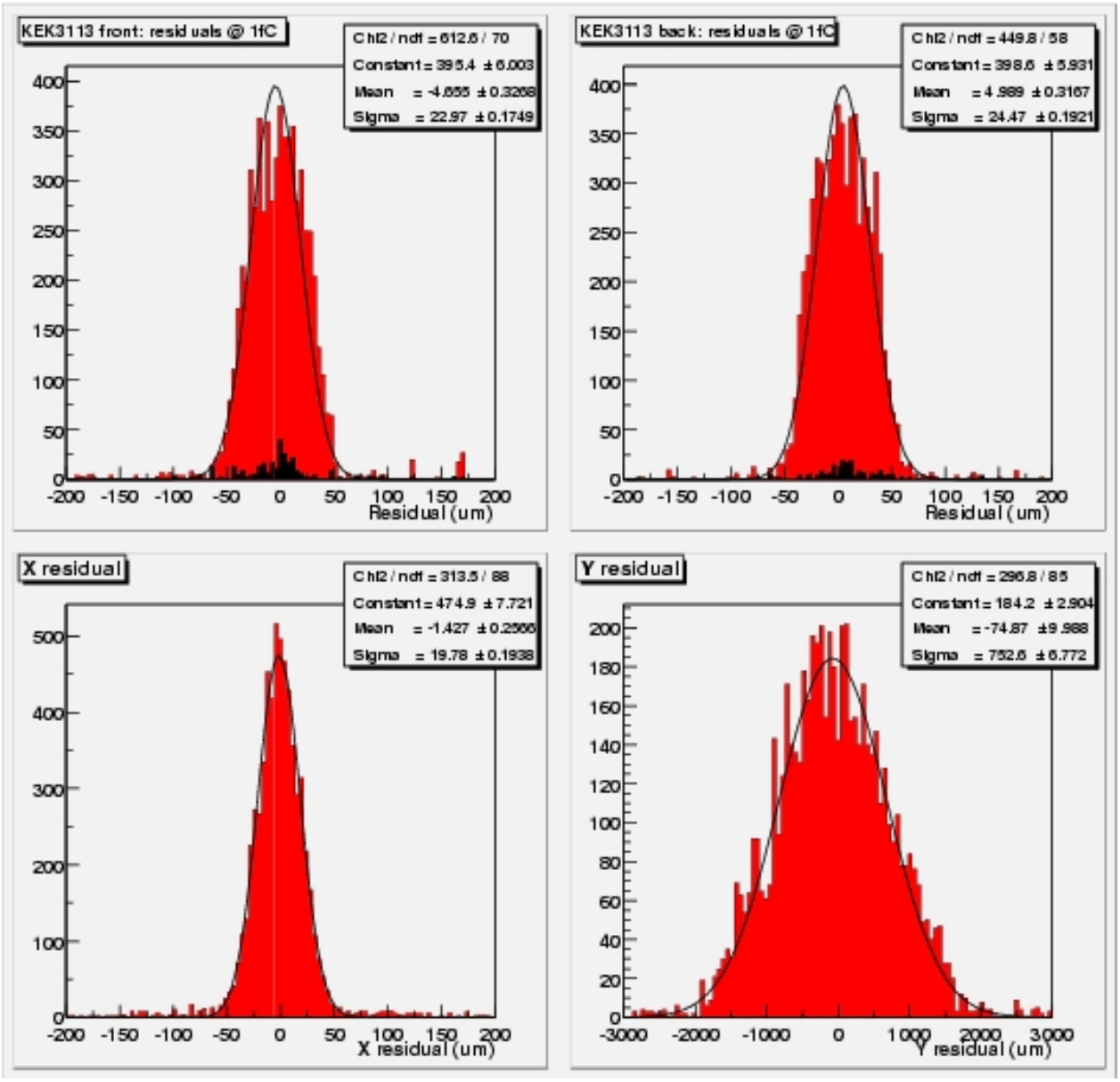

Figure 13: Reconstructed track residuals with the unirradiated module K3113. The top two plots show the u, v residuals of the two sides of the module (inclined at ±20mr), with the expected values of about 23 μm. The lower two plots show the reconstructed residuals in the x, y directions.

6 SYSTEM TEST AND FIRST RESULTS

6.1 General Description

The goal of the system test is to run as many modules as possible in a physical configuration which is as close as possible to the planned ATLAS SCT configuration, thereby testing the performance of the modules in such a system and comparing it to their stand-alone performance.

Modules are mounted on a sector of a Carbon-fibre-Corex-sandwich cylinder with dimensions very near to those of the innermost ATLAS SCT barrel. The sector can accommodate up to 48 modules, in four rows of 12.

Modules are powered and read out via prototype SCT barrel 'opto-harnesses', which transmit power to the modules, decode the optical clock and commands, transmit these signals electrically to the modules, and transform the data from the modules into optical signals for transfer to the readout electronics. Each opto-harness serves up to six modules, as in the final system.

The ASICs and opto-components are powered by the SCT prototype VME power supplies (SCTLVs); and the detectors are biased with the companion prototype high voltage units (SCTHVs).

The modules are read out using a CLOAC-SLOG-MuSTARD-OPTIF system, with the OPTIF[1] providing the electrical-optical interface. A further VME module is used to read module hybrid temperatures. The ROOT-based SCTDAQ software package is used, running on a Windows-NT PC which is connected to the VME crates via a National Instruments interface card.

Control and monitoring of all voltages and currents is currently carried out through the DAQ software, although a prototype DCS system is used to monitor environmental temperature and humidity.

All patch panels and power tapes used are true to the planned final ATLAS design, except for extra provisions on the patch panels to allow testing of various coupling schemes. The conventional cables used between PPB2 and the power supplies are 30 metres long The patch panel PP3 and the cables from PP3 to the power supplies, foreseen for the experiment, have not yet been simulated in the system test.

A schematic diagram of the system test can be seen in Figure 14 and photographs of the barrel sector can be seen in Figures 15 and 16.

6.2 Grounding and Shielding in the System Test

The system test bases its grounding and shielding scheme on the proposal outlined in *ATLAS SCT / Pixel Grounding and Shielding Note*[2]. The main elements as applied in the system test are described below, with any differences noted.

To control stray capacitance between the cooling pipe and the silicon detector backplane, shunt shields are placed between the modules and the cooling pipe. These shunt shields consist of copper on kapton; with the copper soldered to Analogue Ground on the 'dogleg' (the portion of the opto-harness to which the module is connected).

[1] http://s.home.cern.ch/s/sct/public/sctdaq/sctdaq.html

[2] http://scipp.ucsc.edu/groups/atlas/elect-doc/SCT_GND_SHIELD2.pdf

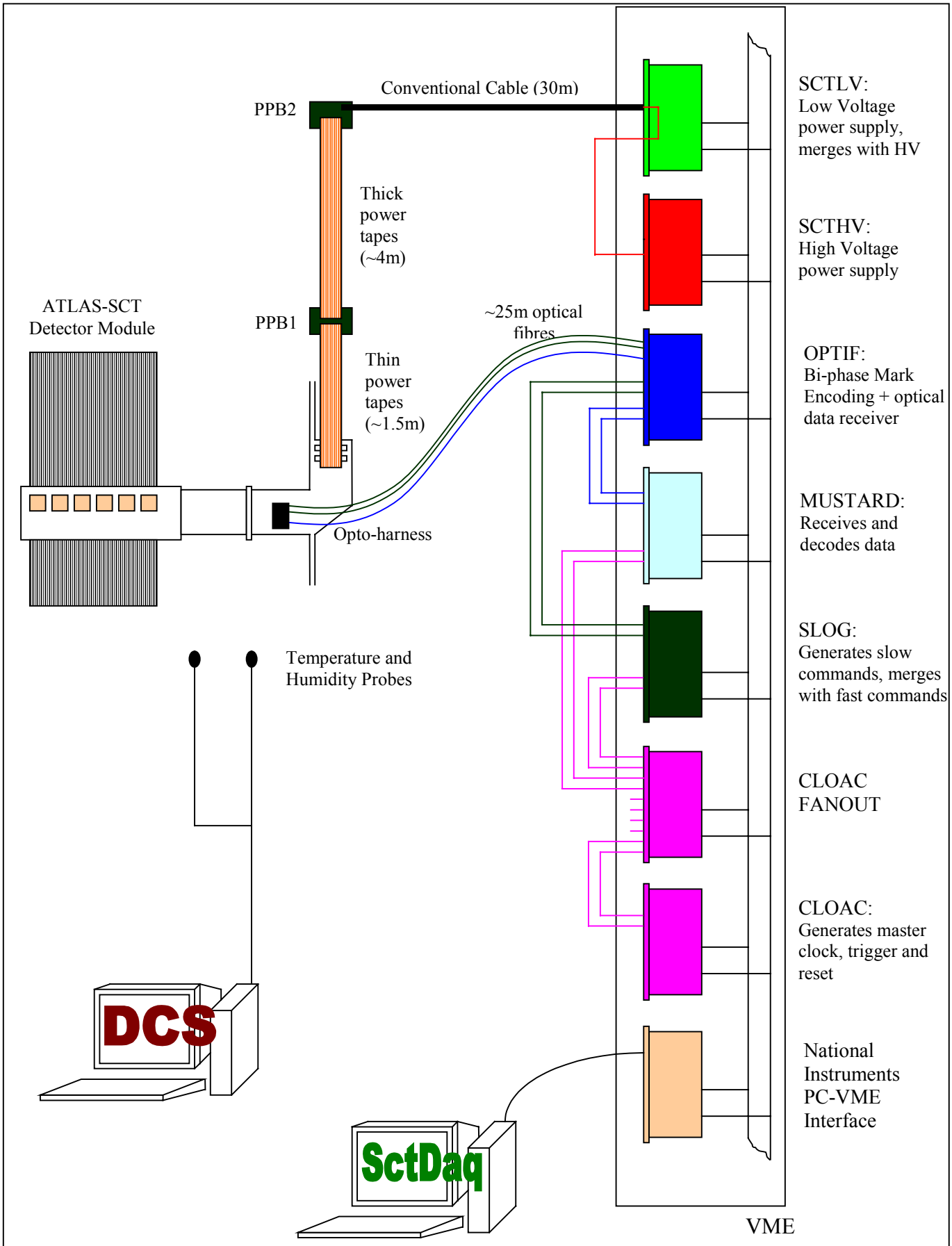

Figure 14: A schematic layout of the SCT barrel system test

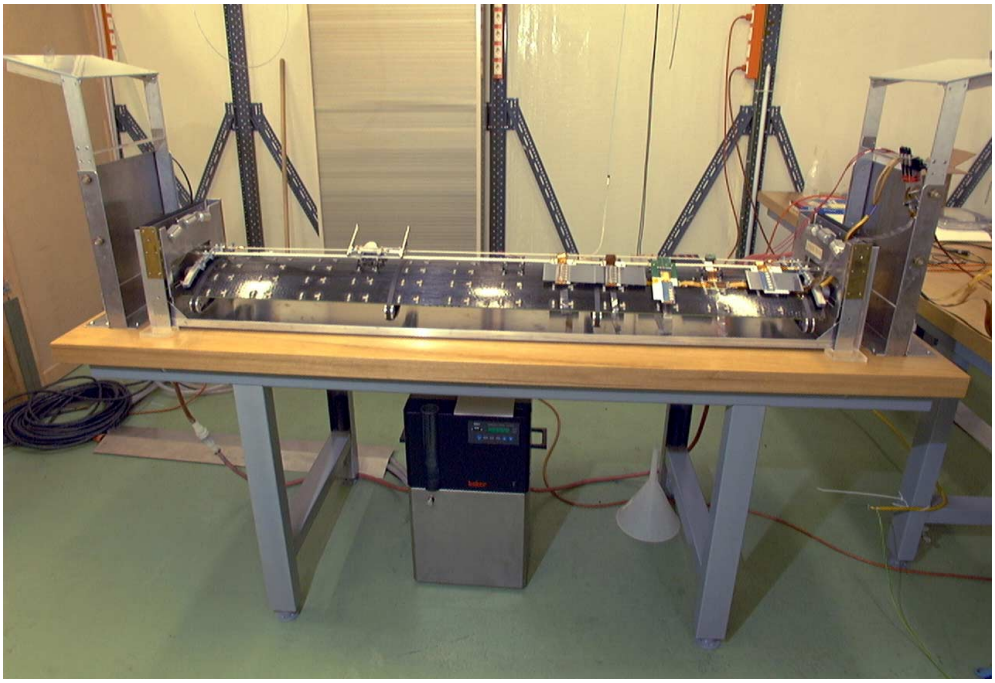

Figure 15: A photograph of the system test barrel carbon-fibre mounting structure

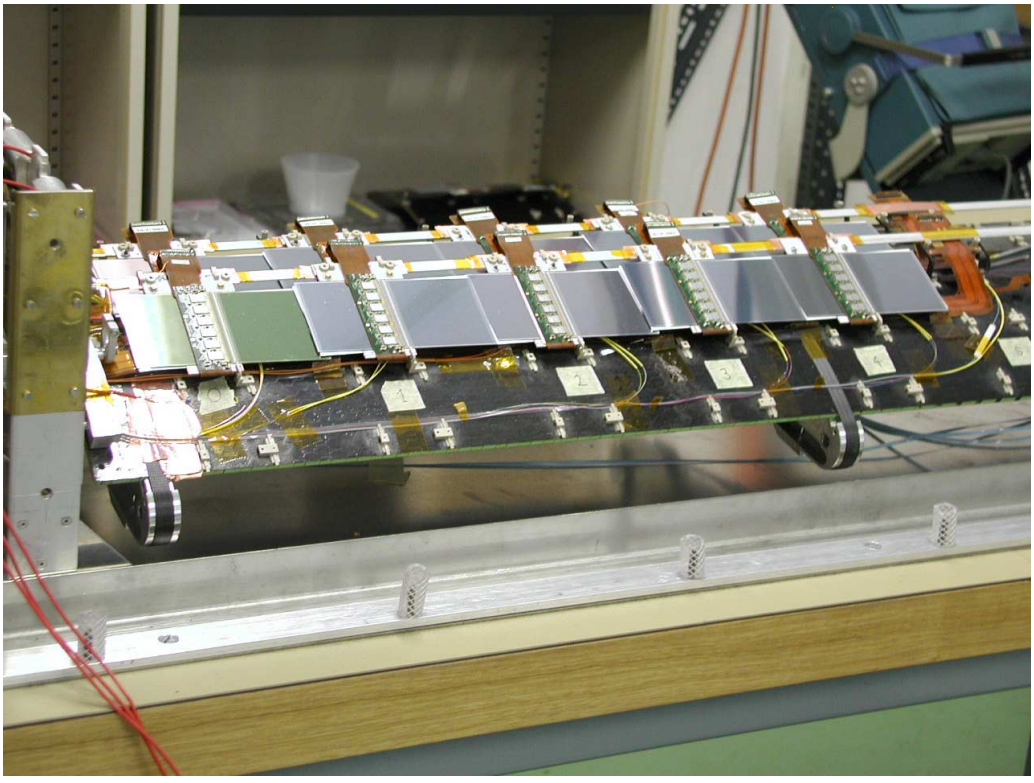

Figure 16: A photograph of barrel modules mounted on the carbon-fibre structure

The cooling pipes are connected together at both ends of the sector via an aluminium support bracket. This bracket is screwed onto the sector, providing electrical contact to the carbon fibre skin. Note that the cooling pipes are continuous, with no electrical break in the centre. The metalwork which supports the sector is also made of aluminium and is connected electrically to the sector by its contact with the carbon fibre skin. An aluminium cover (with square cross-section), used to provide a dry and light-tight atmosphere whilst running, is in electrical contact with the support structure. It should be noted that the cover is not electrically or geometrically similar to the planned ATLAS SCT thermal shield; a cover that will simulate the thermal shield is currently being produced.

Routing from the harness to PPB1, the six 'thin' power tapes from a harness are wrapped together with aluminium-on-kapton shielding which is DC-connected to the metalwork surrounding the sector. At PPB1, digital and analogue grounds are AC-connected (with 2.7 μF) to the cable shielding.

From PPB2 to PPB1, the system test is not very like the ATLAS SCT; there is no surrounding metal (e.g. heat spreader plates, cooling supply tubes) to connect to as is recommended in the note referenced above. For the 10-module tests reported below, one set of six 'thick' power tapes running from PPB1 to PPB2 were wrapped with aluminium-foil shielding which was connected to grounds at PPB1 in the same way as described above for the thin tapes; the other harness' thick tapes were not shielded.

Common-mode chokes are used between PPB2 and the conventional cables. These chokes are intended for use at PPB3 but as stated above PPB3 is not (yet) represented in the system test. Note that the conventional cable shield should be commoned through, but this is not yet implemented.

The low- and high-voltage power supplies have floating grounds.

An alternative grounding and shielding scheme, which involves DC connections between all metal in the system and DC connection of the module grounds to the cooling pipe, is working well in the SCT-endcap system test but remains to be tested in the barrel system test.

6.3 First Results from the Barrel System Test

When a module arrives at the system test, it is accompanied by the results from a standard characterisation as performed at the module building cluster. The first step in integrating the module into the system test is to repeat this standard characterisation on the 'electrical test bench' in the system test lab, to verify that the module has not suffered in transit. The electrical test bench is considerably simpler than the full system test as it bypasses the optical communication, and uses only very short power and signal cables. Therefore a module may be expected to give its best performance when running stand alone 'on the bench'.

Once the module is verified to be in good working order, it is mounted on the system test sector (with all grounding and shielding connections made), and the standard characterisation sequence is repeated, powering only that one module. This performance is compared to that on the bench and any differences are noted and investigated if possible. When this comparison is complete, the module is considered ready to be included in multi-module tests.

There are currently ten modules in the system test, as seen in Table 1. Eight of these are considered 'good' modules; the other two (20220170100004 and 9) are included on the sector to maximise the overlap of powered modules for these first results, until further modules are available. With the exception of module 20220170100008, all the modules showed approximately the same noise values (within about 100 ENC) when running alone on the sector as they did on the

bench. Module 0008 showed approximately 200 ENC more noise on the sector. This may be of significance, since this is the only module made with the ASICs attached to the hybrid via non-conducting glue. Conducting glue will be used for all ATLAS barrel modules.

A typical multi-module test which can be done is to measure the gain and noise with many modules running in parallel. This has been performed, using a three-point gain calculation, with the ten modules on the sector. For this test there were two harnesses on the left-hand half of the sector, mounted immediately adjacent to one another, with each harness holding five modules. From left to right on the front harness were Scand1, K3112, K3104, 0011 and K3103; and on the back harness were 0004, 0009, 0008, 0026 and 0022. The measured noise values of all ASICs on the modules, with all 10 modules in operation at a hybrid temperature of about 27^0C, are shown in Figure 17. With the exception of module 0008, as discussed above, the noise values lie in the anticipated range. The noise difference between this 10 module operation and that measured when a module is tested individually on the sector is shown in Figure 18 for each ASIC. The differences are seen to be rather small. The last ASIC (which is nearest the cooling pipe on the side of the module facing the sector) is somewhat noisier for the 10-module run for some of the modules. For module 0026 it should be noted that the high-voltage return line was broken and had to be repaired temporarily with a cable; the according influence on the noise behaviour is difficult to predict.

Detailed investigations are now in progress, and it is expected that further barrel modules will soon be added to the sector. The first results presented here are clearly encouraging.

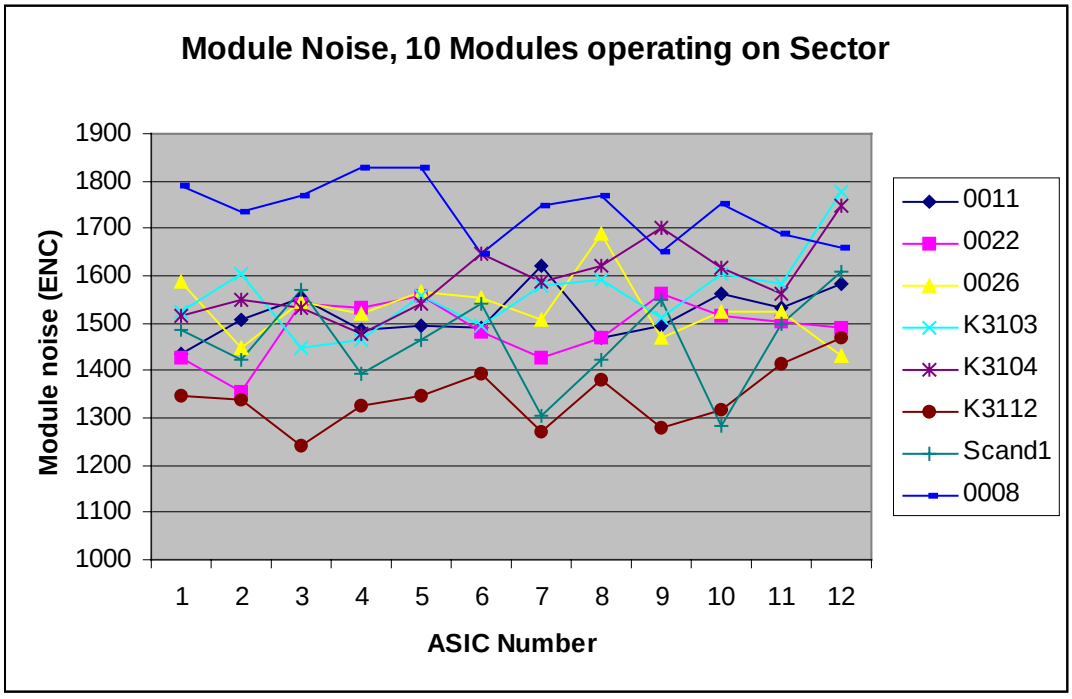

Figure 17: The measured module noise for each ASIC with 10 modules operating together on the barrel system test sector

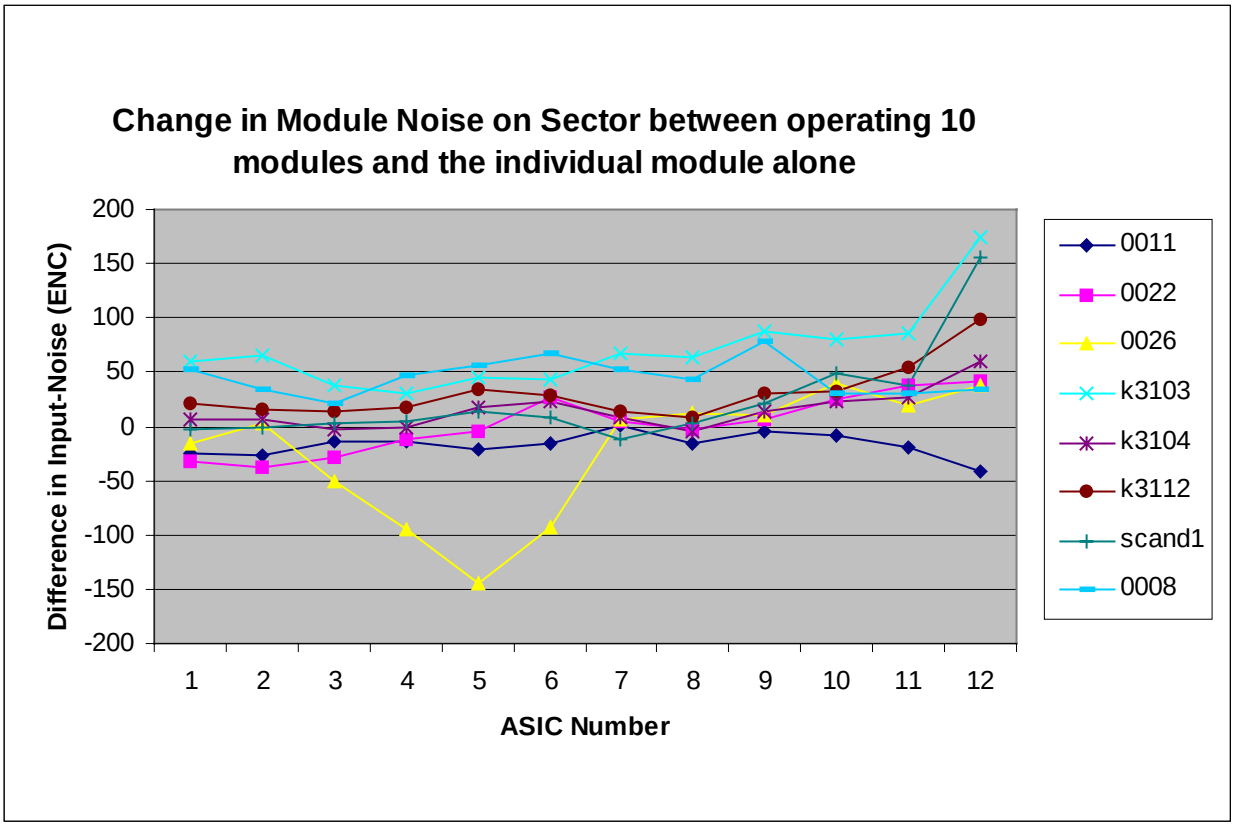

Figure 18: The change in the module noise on the sector between 10 module and individual module operation for each ASIC

7 SUMMARY

The SCT barrel modules satisfy the electrical performance goals of the ATLAS Inner Detector TDR, with the exception of a slightly higher final post-irradiation noise value. The modules operate in a stable fashion, with good efficiency and low noise occupancy at 1fC threshold. The first results from a collection of 10 modules running together in the SCT system test are encouraging.

The available data therefore indicate that the design of the barrel module, and all its components, adequately meet the electrical performance requirements of ATLAS.